

The Hebrew University of Jerusalem Israel, Faculty of Science

The School of Computer Science and Engineering,

Department of Applied Physics

Complex Optical
(Amplitude and Phase)
Device Characterization Tool

M.Sc. Thesis Submitted by

Yoram Palti

This work was done under the supervision of

Dr. Dan Marom

November 22, 2009

Abstract

Optical communications has experienced a rapid development during the last decade. More bandwidth can be acquired by decreasing the spacing of the optical channels or by increasing the data rate. Characterization of the optical components and active monitoring of the network calls for accurate measurement methods. The transfer function of optical components impacts the performance of communication systems. Analysis and accurate measurement of the transfer function is therefore essential in optimization of the performance of such systems.

Chromatic dispersion of optical fibers and frequency chirp of the laser transmitters set limits for the data rate and transmission distance. Measurements of dispersion have traditionally been performed using a Modulation Phase-Shift (MPS) method. When high RF modulation frequencies are applied to achieve high resolution an alias error could be introduced. In this thesis we introduce an apparatus for full complex-amplitude spectral characterization of optical components and fibers. Based on a modification of the MPS method, we introduce a frequency dither to the RF modulation drive, allowing us to detect small phase changes thus overcoming the limitations imposed by the conventional MPS method. Its salient feature is high sensitivity phase detection enabling the use of a low RF driving frequency as necessary for precise measurement of components exhibiting fine spectral features such as microresonators and slow light devices.

We analyze the modified MPS technique using the traditional small signal approximation and compare the results to a full analytic response of the MPS technique. The full analytic response is useful for optimization of the proposed technique. The characterization apparatus has been realized in our lab using commercially available optical and electrical components. We have characterized experimentally the signals passing in the apparatus. Care was taken to prevent higher RF tones (i.e. above 1st order) in the Mach-Zehnder Modulator (MZM) output field, which could interfere with the desired measurement. Moreover, care was taken to prevent RF leakages in the electronic circuitry, which could interfere with the measurement of weak signals. We demonstrate the operation of the modified MPS at two operating points, demodulating with either the same RF carrier or with a doubled one. We measured several component categories and fibers to demonstrate the measurement technique. Finally, we conclude with the advantages and disadvantages of the modified technique.

Keywords: Chromatic dispersion, group delay (GD) ripple, modulation phase-shift (MPS) method, optical variables measurement.

Acknowledgments

The research work for this thesis has been carried out in the Photonic Devices Group at the Applied Physics Department of The Hebrew University of Jerusalem Israel (HUJI) during the years 2006-2009.

First of all, I would like to thank my adviser Dr. Dan Marom for the research opportunities and for an opportunity to work in the laboratory. I am especially grateful for his valuable advice and continuous support in the past years. I would like to express my gratitude for introducing me to the field of optical communications

David Sinefeld has worked in several projects with me during these years providing invaluable help. I would also like to thank all the group mates. Asael Adler, Jonathan Dunayevsky, Yaron Glazer, Ami Mizrahi, Amitay Rudnick and Dror Shayovitz, for all their educational discussions.

Funding of this work was supported in part by the Peter Brojde Center for Innovative Engineering.

Last but not least, I would like to thank my family for supporting me through my academic years. Finally, I would like to thank my wife Polina for her loving, patience and support.

Contents

1 Dispersion of optical components	6
1.1 Example: Pulse propagation	7
2 Measurements methods for chromatic dispersion	11
2.1 Measuring dispersion using interferometric methods	11
2.2 Measuring dispersion using Time Of Flight (TOF) method	12
2.3 Measuring dispersion using Modulated Phase Shift (MPS) method	13
2.4 Measuring dispersion using Baseband AM response method	20
2.5 Modulation Phase Shift improvement on the accuracy	21
2.6 Chromatic dispersion measurement with Single Sideband method (SSB)	22
2.7 Chromatic dispersion measurement using Fixed Sideband Technique	24
2.8 Appendix: Jacobi-Anger expansion of amplitude modulation (AM)	25
3 Modulated Phase Shift method revisited	30
3.1 Simplified signal analysis	33
3.1.1 MPS with Audio	40
3.1.2 2nd order MPS with Audio	41
3.2 Appendix: MPS with audio accurate signal analysis Jacobi Anger expansion to AM and PM	44
4 Experimental realization of modified MPS	50
4.1 MPS with Audio apparatus	50
4.2 2nd order MPS with Audio apparatus	54
4.3 Appendix: Apparatus components characterization	57

5	Optical devices characterization results and discussion	61
5.1	MPS with Audio	61
5.1.1	Dispersion Compensating Fiber (DCF) modules	61
5.1.2	Arrayed Waveguide Planar Lightwave Circuit (AWG PLC) against reflective mirror	62
5.1.3	DWDM Demux	68
5.2	2nd order MPS with Audio	69
5.2.1	Dispersion Compensating Fiber (DCF) modules	69
5.2.2	Arrayed Waveguide Planar Lightwave Circuit (AWG PLC) against reflective mirror	70
5.2.3	DWDM Demux	73
6	Conclusions and future research	75
7	Appendix A: Modified MPS - photocurrent simplification	79
8	Appendix B: Extended model for conventional MPS	119

1 Dispersion of optical components

As of today optical communication systems are already deployed all over the world and are used to transmit digital data (meaning bits of '0' or '1'). Currently these systems are build up from many different building blocks (optical and electrical), while each building block may distort the transmitted signal. During transmission in the optical fibers for tens of kilometers the data may have losses which can be overcome by optical amplification. However the data might be distorted during transmission due to chromatic dispersion which might cause Inter Symbol Interference (ISI). In case of ISI the transmitted data bits broaden and overlap and upon detection the data will be lost. The current networks are built of transmitter and receiver stations, at each receiver station the data is being detected and transmitted till it reaches its destination. As the demand for higher bandwidth increases, the transmitted data is being modulated in higher frequencies and the allowed chromatic dispersion values decreases significantly. There are different approaches how to deal with chromatic dispersion. The simplest approach is to manage the chromatic dispersion across the transmitting path while maintaining a small dispersion in order to avoid accumulation of nonlinear phenomena in the the optical fibers. Another approach is to compensate the dispersion in the transmitter station using electronic predistortion and complex-value modulation. Another approach is to compensate the dispersion at the receiver station. In order to anticipate these distortions we need to know the complete behavior of each optical component used in the lightwave transmission system.

The linear characteristics of the optical component can be completely defined by using a complex transfer function, which can be written as $H(\omega) = B(\omega) \cdot e^{j\phi(\omega)}$ here ω is the optical angular frequency, $B(\omega)$ is the amplitude response and $\phi(\omega)$ is the phase response. The complex function can be calculated analytically or numerically.

Under the assumption of Linear Time-Invariant (LTI) system, group delay is a measure of the transit time of a signal through a Device Under Test (DUT). Group delay is calculated by differentiating the phase response of the DUT versus frequency. Another way to say this is that group delay is a measure of the slope of the phase response. The linear portion of the phase response is converted to a constant value (representing the average signal-transit time) and deviations from linear phase are transformed into deviations from constant group delay. The variations in group delay cause signal distortion. The group delay, τ_g , of the component is defined as a derivative of the phase response with respect to the angular frequency, ω , (the minus sign is due to the choice of the pulse propagating direction $\exp\{-j\omega_0 t\}$)

$$\tau_g = -\frac{d}{d\omega}\phi(\omega) \quad (1)$$

The 1st distortion to the signal is defined as the dispersion parameter, D , it is the derivative of the group delay with respect to wavelength

$$D = \frac{d}{d\lambda}\tau_g \quad (2)$$

The 2nd distortion to the signal is defined as the dispersion slope parameter with respect to wavelength, S , it is defined as $S = \frac{d}{d\lambda}D$. Usually the chromatic dispersion is sufficient in the case where we are far away from the zero dispersion wavelength. In close regime of the zero dispersion wavelength, the higher order dispersion term induces signal distortions which is defined as the dispersion slope. The dispersion slope effects short pulses such as Solitons.

The phase velocity of light is constant and independent of the wavelength in vacuum, while in materials it may vary with the wavelength. This phenomenon is commonly referred to as *dispersion*, in order to emphasize its wavelength-dependent nature it is sometimes referred as *chromatic dispersion*. In a prism, dispersion causes the angular separation of white light into spectral components of different wavelengths. The optical source in a high speed communication system is typically a single-line diode laser with very fine spectral width. Modulation, which is needed to transmit information along the laser light, increases the spectral width. Each wavelength (spectral) component of the signal travels at a slightly different speed due to dispersion, resulting in pulse broadening.

Chromatic dispersion in fiber results from the interplay of two effects - material dispersion and geometrical dispersion (a.k.a waveguide dispersion which can be found in a typical waveguide - single mode fibers). Material dispersion arises from changes in the refractive index as a function of wavelength, and the corresponding group velocity. Geometrical dispersion arises from reflections and interference effects inside the component. Waveguide dispersion arises from the wavelength dependent relationships of the group velocity to the core diameter and the difference in index between the core and the cladding. In single-mode fibers there is another component called second order Polarization Mode Dispersion (PMD) or differential group delay dispersion, which produces an effect which is identical to chromatic dispersion. The phenomenon arises from fiber PMD behavior details, second order PMD sets the ultimate limit to which a transmission path can be compensated for chromatic dispersion.

1.1 Example: Pulse propagation

In order to study pulse propagation in dispersive medium we need to consider the complex amplitude of the field envelope at a distance z inside the fiber $A(z, t)$, since each frequency component of the optical field travels at slightly different propagation constant. For this reason, it is useful to work in the spectral domain. The basic propagation equation governing pulse evolution inside a single-mode fiber known as the Nonlinear Schrödinger Equation (NLSE). Since the constant delay experienced by the optical signal does not affect the signal quality. It is often useful to work in a reference frame moving with the pulse [1]. The moving frame NLSE is:

$$\frac{\partial A}{\partial z'} + i\frac{\beta_2}{2}\frac{\partial^2 A}{\partial t'^2} - \frac{\beta_3}{6}\frac{\partial^3 A}{\partial t'^3} = i\gamma|A|^2 A - \frac{\alpha}{2} \quad (3)$$

where γ takes into account non linear effects occurring within the fiber due to Kerr effect, $|A|^2$ is the optical power, α represents the fiber loss (or possible gain whenever $\alpha \leq 0$) and $\beta_m = \left. \frac{\partial^m \beta}{\partial \omega^m} \right|_{\Omega_0}$ are the derivatives of the propagation constant β developed with a Taylor series around the optical frequency Ω_0 .

The propagation constant Taylor series development up to a third order

$$\beta(\omega - \omega_0) = \beta_0 + \beta_1(\omega - \omega_0) + \frac{\beta_2}{2}(\omega - \omega_0)^2 + \frac{\beta_3}{6}(\omega - \omega_0)^3 \quad (4)$$

$$\text{Group velocity } \frac{1}{v_g} = \left. \frac{\partial \beta}{\partial \omega} \right|_{\omega_0} \quad (5)$$

$$\text{Dispersion coefficient } D = \frac{d}{d\lambda} \left(\frac{1}{v_g} \right) = -\frac{2\pi c_0}{\lambda_0^2} \left. \frac{\partial^2 \beta}{\partial \omega^2} \right|_{\omega_0} \quad (6)$$

$$\text{Dispersion Slope } S = \left(\frac{2\pi c_0}{\lambda_0^2} \right)^2 \left. \frac{\partial^3 \beta}{\partial \omega^3} \right|_{\omega_0} \quad (7)$$

In order to see how group velocity dispersion (GVD) effects lightwave transmission systems , we can simplify the NLSE $\beta_3 \sim 0$ if the pulses are not shorter then 5psec, without nonlinear effects $\gamma = 0$ and assuming the losses are compensated periodically $\alpha = 0$. Dispersive effects are then governed by a simple linear equation:

$$\frac{\partial A}{\partial z'} + i \frac{\beta_2}{2} \frac{\partial^2 A}{\partial t'^2} = 0 \iff \frac{\partial A}{\partial z} + \beta_1 \frac{\partial A}{\partial t} + i \frac{\beta_2}{2} \frac{\partial^2 A}{\partial t^2} = 0 \quad (8)$$

This linear equation is similar to the paraxial wave equation governing diffraction of optical beams in free space in one transverse dimension [2]. The only difference is that the group velocity dispersion parameter β_2 can be positive or negative depending on whether the optical signal experiences normal ($\beta_2 > 0$) or anomalous ($\beta_2 < 0$) dispersion.

The incident pulse $A(0, t)$ and the transmitted pulse $A(z, t)$ may be regarded as the input and output of LTI system when neglecting γ . The signal can be propagated according to $\tilde{A}(z, \omega) = \tilde{A}(0, \omega) \cdot e^{j\beta(\omega)z}$ where $\tilde{A}(0, \omega)$ and $\tilde{A}(z, \omega)$ are the Fourier transform of $\tilde{A}(0, t)$ and $\tilde{A}(z, t)$ respectively and after propagating the signal is transformed back to the time domain. Suppose first that the complex envelope $A(0, t)$ is an unchirped Gaussian pulse with a pulse width 2τ at Full Width Half Maximum (FWHM)

$$A(0, t) = f(t)e^{j\omega_0 t} = \exp \left\{ -\frac{t^2}{2\tau^2} \right\} \exp \{j\omega_0 t\} \quad (9)$$

$$\tilde{A}(0, \omega) = \int_{-\infty}^{\infty} A(0, t)e^{-j\omega t} dt = \sqrt{2\pi}\tau \cdot \exp \left\{ -\frac{\tau^2(\omega - \omega_0)^2}{2} \right\} \quad (10)$$

$$\tilde{A}(z, \omega) = \tilde{A}(0, \omega) \cdot e^{j\beta_2 \cdot (\omega - \omega_0)^2 \cdot \frac{1}{2} z} \quad (11)$$

$$A(z, t) = \frac{1}{2\pi} \int_{-\infty}^{\infty} \tilde{A}(z, \omega) e^{j\omega t} d\omega =$$

$$A(z, t) = e^{j(\omega_0 t - \beta_0 z)} \frac{1}{\sqrt{1 + j \frac{\beta_2 z}{\tau^2}}} \exp \left\{ -\frac{(t - \frac{z}{v_g})^2}{2\tau^2 + 2 \frac{\beta_2^2 z^2}{\tau^2}} \left(1 - j \frac{\beta_2 z}{\tau^2} \right) \right\} \quad (12)$$

The Gaussian pulse width at the fiber output is broadened, after taking the intensity of the output field $|A(z, t)|^2$, the pulse width is $2\tau \sqrt{1 + \left(\frac{\beta_2 z}{\tau^2}\right)^2}$. We can see that the pulse broadens no matter the sign of β_2 .

Now we will examine the phase of the Gaussian broadened pulse

$$\phi(z, t) = \omega_0 t - \beta_0 z + \frac{(t - \frac{z}{v_g})^2}{2\tau^2 + 2 \frac{\beta_2^2 z^2}{\tau^2}} \frac{\beta_2 z}{\tau^2} \quad (13)$$

the time dependence of the phase $\phi(z, t)$ implies that the instantaneous frequency differs across the pulse from the central frequency ω_0 . The difference $\delta\omega$ is just the time derivative $\frac{\partial\phi}{\partial t}$ (a minus sign may appear due a different choice of the pulse propagating direction $\exp\{-j\omega_0 t\}$) and is given by

$$\delta\omega(z, t) = \frac{d\phi}{dt} = \omega_0 + \frac{2\beta_2 z}{\tau^2} \frac{(t - \frac{z}{v_g})}{2\tau^2 + 2 \frac{\beta_2^2 z^2}{\tau^2}} = \omega_0 + \frac{\beta_2 z}{\tau^2} \frac{(t - \frac{z}{v_g})}{\tau^2 + \frac{\beta_2^2 z^2}{\tau^2}} \quad (14)$$

from this last result we can see that the chirp of the signal depends linearly on the quadratic dispersion coefficient β_2 , and the propagation distance z . The term inside the brackets $t - \frac{z}{v_g}$ is actually the time shift (which can be eliminated in the moving time frame representation). This equation shows that the frequency changes linearly across the pulse, i.e., a fiber imposes linear frequency chirp on the pulse. The chirp $\delta\omega$ depends on the sign of β_2 . In the normal-dispersion regime ($\beta_2 > 0$), $\delta\omega$ is negative at the leading edge ($t < 0$) and increases linearly across the pulse; the opposite occurs in the anomalous-dispersion regime ($\beta_2 < 0$).

Dispersion induced pulse broadening can be understood by recalling that different frequency components of a pulse travel at slightly different speeds along the fiber because of *group velocity dispersion*. More specifically, red components travel faster than the blue components in the normal-dispersion regime ($\beta_2 > 0$), while the opposite occurs in the anomalous-dispersion regime ($\beta_2 < 0$). The pulse can maintain its width only if all spectral components arrive together. Any time delay in the arrival of different spectral components leads to pulse broadening.

We have now seen that quadratic changes in the phase correspond to linear frequency variations, for this reason such pulses are said to be linearly chirped. The spectrum of a chirped pulse and of an unchirped pulse are the same width. However, there is a spectral phase difference. This

can be seen for chirped Gaussian pulses with a pulse width 2τ at Full Width Half Maximum (FWHM) by substituting the incident pulse with the form

$$A(0, t) = f(t)e^{j\omega_0 t} = \exp\left\{-\left(1 + jC\right)\frac{t^2}{2\tau^2}\right\} \exp\{j\omega_0 t\} \quad (15)$$

where C is a chirp parameter governs the frequency chirp imposed on the pulse. By using the same LTI assumptions one finds that the instantaneous frequency increases linearly from the leading to the trailing edge (up-chirp) for $C > 0$ while the opposite occurs (down-chirp) for $C < 0$. It is common to refer to the chirp as positive or negative depending on whether C is positive or negative.

after performing Fourier transform to the chirped pulse

$$\tilde{A}(\omega - \omega_0) = \sqrt{\frac{2\pi\tau^2}{1 + jC}} \cdot \exp\left\{-\frac{\tau^2(\omega + \omega_0)^2}{2(1 + jC)}\right\} \quad (16)$$

the spectral FWHM is given by $\Delta\omega = \sqrt{(1 + C^2)}/\tau$ in the absence of frequency chirp ($C=0$) the spectral width is transform limited and satisfies the relation $\Delta\omega\tau = 1$. Such a pulse has the narrowest spectrum and is called *transform-limited*. The spectral width is enhanced by a factor of $\sqrt{1 + C^2}$ in the presence of linear chirp. One can find the analytical expression for the transmitted field using the inverse Fourier transform.

2 Measurements methods for chromatic dispersion

The dispersion of optical components has a significant effect on the performance of various optical systems. Analysis and accurate measurement of the dispersion is therefore essential in optimization of the performance of such systems. Measurements of chromatic dispersion can be performed by applying various techniques. They include applications low-coherence interferometry, various pulse delay measurements and phase-shift techniques. Traditionally the dispersion of an optical fiber has been an important characteristics to be measured. In the recent years when more components such as optical filters have been introduced it was necessary to accurately characterize them, especially the dispersion coefficient [3]. In particular, the development of the filters based on Fiber Bragg Gratings (FBG) permit for compensation of the dispersion of an optical fiber [4]. By applying FBG, the dispersion effects can be dramatically decreased in long-transmission systems. Accurate characterization of the dispersion of these filters has led to re-evaluation of the conventional methods to obtain reliable measurement results. There are three principal methods recognized by the International Telecommunications Union (ITU) for measuring chromatic dispersion: interferometric, phase-shift and time of flight [5]. The first two techniques are now commonly utilized for component characterization as well. All of the recognized methods are in fact indirect detection of the chromatic dispersion since the pulse broadening usually cannot be detected due to oscilloscope and detector rise time which can be hundred of picoseconds [6].

2.1 Measuring dispersion using interferometric methods

To obtain the group delay and the dispersion of the components, interferometric methods are applied to the components. The measurement setups are typically based on Michelson or Mach-Zehnder interferometers. Light from a broadband or wavelength tunable source is split in two paths. One path is coupled into the Device Under Test (DUT) and the other is a reference path. The light transversing the component is combined with light from the reference path and the resulting interferogram is detected see Fig. 1. From this interferogram it is possible to calculate both the amplitude and the phase response of the component by means of a Fourier transform. The main advantage is its very accurate resolution. The main disadvantage is group delay and dispersion of the component are differentiated from the phase of the interferogram which increases the noise. Another disadvantage is that interferometric methods are limited to the coherence length of the source usually a Diode Feedback Laser (DFB) has 100KHz-1MHz linewidth and the coherence length is approximately 300m-30m respectively. Meaning interferometric methods are applicable only for measurement of short length fibers.

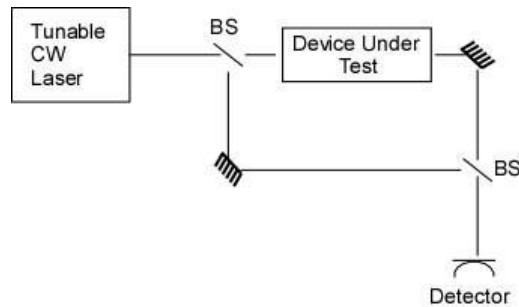


Figure 1: Schematic of Mach-Zehnder interferometer

$$I \propto \cos[\phi_{\text{Device Under Test}} - \phi_{\text{Reference}}] \quad (17)$$

Recently there have been a few reports of implementing interferometric methods in extracting the chromatic dispersion, while the results were with good agreement with the Phase Shift Method (which will be described in details in section 2.3) [7, 8, 9]. There is a commercial product made by Luna Technologies namely Optical Vector Analyzer based on the interferometer technique [10].

2.2 Measuring dispersion using Time Of Flight (TOF) method

The Time Of Flight (TOF) method was developed for long optical fiber samples. In this method the relative temporal delays is measured for pulses at different wavelengths. Due to its simplicity the TOF measurement method is an interesting application for the measurement of dispersion in already deployed fiber links. In optical fibers this method can be used to measure the variation of the group delay directly. “This can be done by determining the group delay in the fiber as a function of wavelength and taking the slope of the resulting curve. In order to avoid errors arising from the fact that the delay difference are small compared with the total delay, a pulse of fixed wavelength and delay can be injected together with a pulse or pulses of varying wavelength, to act as a reference time marker. Then the variation of delay with wavelength can be measured relative to this pulse avoiding the need to accurately measure the total transit time” [11]. Thus the relative group delay can be measured according to:

$$t_{TOF}(\Delta\lambda) = \frac{v_g}{L} \Rightarrow \tau_{GD} = t_{TOF}(\Delta\lambda_1) - t_{TOF}(\Delta\lambda_2) \quad (18)$$

where L is fiber length and v_g is the group velocity.

There are two approaches used to implement such a measurement . The first approach uses a fiber Raman laser source which utilize the nonlinear process of stimulated Raman scattering in a fiber

to generate additional wavelengths. Individual wavelengths which are injected to the tested fiber are selected by a monochromator. The second approach uses an array of semiconductor lasers which can be optically coupled into a test fiber and provide sufficient wavelengths to determine a five term Sellmeier equations which fit experimental delay measurements [12]. This method has a clear advantage the lack of a reference channel as long as the optical source has a stable wavelength and intensity for a time windows which will allow to complete the measurement. Furthermore this method allows for direct measurement of the group delay. Disadvantages of this method include enough fiber length in order that consecutive pulses must be distinguishable, a simple criteria in order to achieve this separation must be at least twice the FWHM of the input pulse width. Another disadvantage arises in case of amplitude and phase variation (when the phase distortion are more complex then quadratic) which will cause severe pulse distortion and the measurement meaningless. This method is limited to measurement of fibers only.

2.3 Measuring dispersion using Modulated Phase Shift (MPS) method

A basic measurement setup for the phase-shift method is outlined in Fig. 2. The light from a tunable laser source is intensity modulated with a sinusoidal signal. The modulation generates sidebands on both sides of the optical carrier. Each spectral component samples the DUT's different frequency components about the carrier frequency, and the interference or beating signal at a photodetector, due to the different response sampled by the sidebands can be used to extract the spectral phase [13]. The basic setup and variations of it using different light sources have been utilized for years. MPS was first used for measuring of narrow-band optical elements by Ryu and his colleagues [14]. Several commercially available dispersion measurement systems rely on this measurement principle from leading companies (like Agilent 86038B Photonics Dispersion and Loss Analyzer).

As seen in Fig. 2 an oscilloscope compares the phase of the ν_0 modulated signal passing in the DUT to a reference modulated signal [15]. Sometimes instead of an oscilloscope there is a network analyzer or a vector voltmeter which are used to compare phases between signals. Phase resolution is 0.1 or 0.01 degrees at best in the state of the art network analyzer.

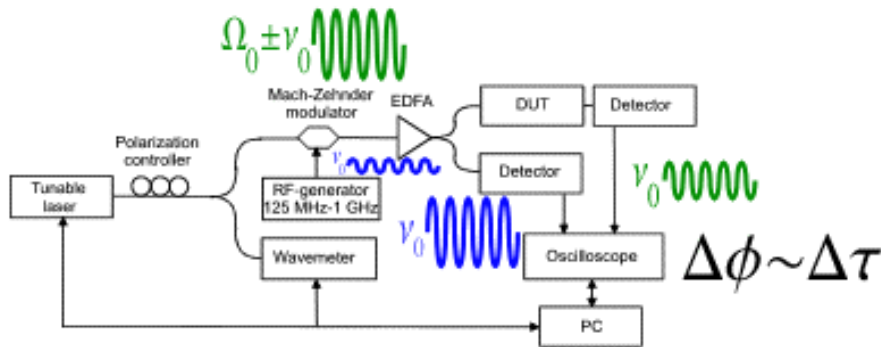


Figure 2: Experimental setup for group delay measurement using the MPS technique

Another simpler approach can be seen with an appropriate RF frequency mixer which will down convert the signal of interest to a DC term, instead of using RF measurement equipment see Fig. 3. We will treat it more rigorously in the following section.

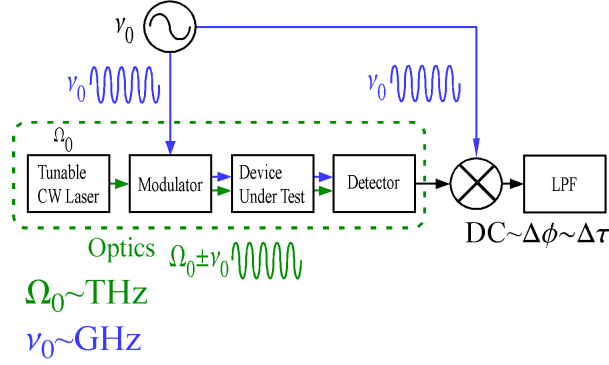


Figure 3: Schematic of MPS - down convert to DC

Optical path noted by the green dotted line, electrical path is noted by black arrows. DC output signal is proportional to the phase difference $\Delta\phi$ of the RF signal arriving from the detector and the reference RF signal. The group delay difference $\Delta\tau$ is proportional to the phase difference.

Conventional Modulated Phase Shift signal (MPS) analysis Signal processing analysis can help understand where the information is carried in the conventional MPS system. We utilize a continuous wave (CW) laser, $\sqrt{P_0}e^{j\Omega_0 t}$, where Ω_0 is the optical carrier frequency (\propto multi-THz range) and P_0 is the laser power. The laser is amplitude modulated by a RF signal (GHz range) applied to an external Mach-Zehnder Modulator (MZM). In this section we develop the RF amplitude modulation (AM) using small angle approximation. A full analytic expansion appears in the Appendix, employing Jacobi-Anger expansion to the harmonic phase. A MZM can be usually described as a 3-dB coupler that splits into 2 arms in which an induced Electro-Optic effect change the refraction index in order to make a phase change each arm independently see Fig. 4.

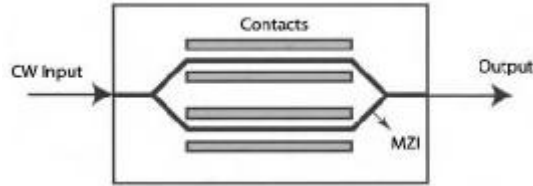


Figure 4: Schematic of $LiNbO_3$ modulator adopted from [16]

Using a transfer matrix of a 3-dB coupler there could be obtained the bar and cross arms of the interferometer output

$$\begin{pmatrix} A_b \\ A_c \end{pmatrix} = \frac{1}{2} \begin{pmatrix} 1 & j \\ j & 1 \end{pmatrix} \begin{pmatrix} e^{j\phi_1} & 0 \\ 0 & e^{j\phi_2} \end{pmatrix} \begin{pmatrix} 1 & j \\ j & 1 \end{pmatrix} \begin{pmatrix} A_{in} \\ 0 \end{pmatrix} \quad (19)$$

where A_{in} is the input amplitude and $\phi_j = \pi \frac{V_j}{V_\pi}$ is the phase shift in the j^{th} arm when a voltage V_j is applied across it ($j=1,2$) [16].

If we will take a simple MZM with one electrode arm, case in which $\phi_2 = 0$, then a phase shift will be induced only to the upper arm and the ports output will be as follows:

$$\text{bar port : } A_b = \frac{e^{j\phi_1} - 1}{2} \quad \text{cross port : } A_c = j \frac{e^{j\phi_1} + 1}{2} \quad (20)$$

With the assumption of Linear Time Invariant (LTI) system we can propagate the signal in the system. Using the convention (Engineering form) of the Fourier transform:

$$\tilde{U}(\omega) = \int_{-\infty}^{\infty} U(t) \cdot e^{-j\omega t} dt \quad (21)$$

$$U(t) = \frac{1}{2\pi} \int_{-\infty}^{\infty} \tilde{U}(\omega) \cdot e^{j\omega t} d\omega \quad (22)$$

In our model we use the most common MZM modulator commercially available, which is a single-arm-drive MZM (has only one arm under electric modulation field); or use one arm of a dual-drive modulator. This MZM has a combination of amplitude and phase modulation at its output [18]. We drive the MZM with a voltage signal which has DC and AC terms (the DC term could also be a constant phase delay between the ports), such that

$$RF = \pi \frac{V_b + V \sin(2\pi\nu_0 t + \theta)}{V_\pi} = \alpha + \beta \cdot \sin(\nu_0 t + \theta) \quad (23)$$

where V_b is the bias voltage, V is the modulation voltage, V_π is the voltage applied to achieve a π phase shift and ν_0 is the RF driving frequency (we omit the 2π constant in the harmonic on the right side of Eq. 23 for brevity). The signal is more conveniently parametrized by α and β .

First we look at the optical field arriving to the DUT after passing the MZM in the bar port

$$\begin{aligned} U(t) &= \frac{\sqrt{P_0}}{2} e^{j\Omega_0 t} \cdot \left(e^{j\alpha} e^{j\beta \cdot \sin(\nu_0 t)} - 1 \right) \approx \frac{\sqrt{P_0}}{2} e^{j\Omega_0 t} \cdot \left(e^{j\alpha} [1 + j\beta \cdot \sin(\nu_0 t)] - 1 \right) \\ &= \frac{\sqrt{P_0}}{2} e^{j\Omega_0 t} \cdot \left(e^{j\alpha} \cdot \left[1 + \frac{\beta}{2} \cdot (e^{j\nu_0 t} - e^{-j\nu_0 t}) \right] - 1 \right) \end{aligned} \quad (24)$$

under the approximation that the modulation depth is small $\beta \ll 1$ (i.e. $e^{jx} \approx 1 + jx + O(x^2)$)

$$U(t) = \frac{\sqrt{P_0}}{2} e^{j\Omega_0 t} e^{j\alpha} \cdot \left((1 - e^{-j\alpha}) + \frac{\beta}{2} \cdot (e^{j\nu_0 t} - e^{-j\nu_0 t}) \right) \quad (25)$$

(We can also derive an exact development for the MZM amplitude modulation of the optical carrier with the use of the identity of Jacobi-Anger:

$$e^{j \cdot A \cdot \sin(\omega_m t)} = \sum_{n=-\infty}^{\infty} J_n(A) \cdot e^{j \cdot n \cdot \omega_m t} \quad , \quad n \in \mathbb{N} \quad (26)$$

where $J_n(A)$ is the n-th j-Bessel function at A value. This demonstrates that there is an entire comb spectrum generated with power distribution dependent on A. The precise expression appears in the appendix to this chapter.)

After performing Fourier transform to the optical signal at the MZM output

$$\tilde{U}(\omega) = \int_{-\infty}^{\infty} U(t) \cdot e^{-j\omega t} dt = \frac{\sqrt{P_0}}{2} 2\pi e^{j\alpha} \left[(1 - e^{-j\alpha})\delta(\Omega_0 - \omega) + \frac{\beta}{2}\delta(\Omega_0 + \nu_0 - \omega) - \frac{\beta}{2}\delta(\Omega_0 - \nu_0 - \omega) \right] \quad (27)$$

This last expression shows three harmonics: the optical carrier Ω_0 , and the modulation sidetones $\Omega_0 \pm \nu_0$ see Fig. 5.

The DUT transfer function in the Fourier domain $H_{DUT}(\omega) = B(\omega) \cdot e^{j\phi(\omega)}$ where $B(\omega)$ represents the amplitude response and $\phi(\omega)$ represents the phase response as a function of frequency.

$$Y(\omega) = \tilde{U}(\omega) \cdot H_{DUT}(\omega) \quad (28)$$

$$Y(t) = \frac{1}{2\pi} \int_{-\infty}^{\infty} \tilde{U}(\omega) \cdot B(\omega) e^{j\phi(\omega)} \cdot e^{j\omega t} d\omega \quad (29)$$

$$Y(t) = \frac{\sqrt{P_0}}{2} e^{j\Omega_0 t} e^{j\alpha} \left[B(\Omega_0) e^{j\phi(\Omega_0)} + \frac{\beta}{2} \left[B(\Omega_0 + \nu_0) e^{j\phi(\Omega_0 + \nu_0) + j\nu_0 t} - B(\Omega_0 - \nu_0) e^{j\phi(\Omega_0 - \nu_0) - j\nu_0 t} \right] \right] \quad (30)$$

Since $\nu_0 \ll \Omega_0$, we shall make the following approximations:

1. the typical assumption is that the attenuation experienced by the three tones is identical.

$$\Rightarrow B(\Omega_0 \pm \nu_0) \simeq B(\Omega_0)$$

2. the phase is developed using Taylor series for the DUT response, assumption being that the phase can be expressed as a Taylor expansion about carrier frequency

$$\Rightarrow \phi(\Omega_0 \pm \nu_0) \cong \phi(\Omega_0) \pm \left. \frac{\partial \phi}{\partial \omega} \right|_{\Omega_0} \cdot \nu_0 + \frac{1}{2} \left. \frac{\partial^2 \phi}{\partial \omega^2} \right|_{\Omega_0} \cdot \nu_0^2 + \dots = \phi(\Omega_0) \pm \dot{\phi} \cdot \nu_0 + \ddot{\phi} \cdot \nu_0^2 + \dots$$

$$Y(t) = \frac{\sqrt{P_0}}{2} B(\Omega_0) e^{j\phi(\Omega_0)} e^{j\Omega_0 t} e^{j\alpha} \left[(1 - e^{-j\alpha}) + \frac{\beta}{2} \left[e^{j(\dot{\phi} \cdot \nu_0 + \frac{1}{2} \ddot{\phi} \cdot \nu_0^2) + j\nu_0 t} - e^{j(-\dot{\phi} \cdot \nu_0 + \frac{1}{2} \ddot{\phi} \cdot \nu_0^2) - j\nu_0 t} \right] \right] \quad (31)$$

$$Y(t) = \frac{\sqrt{P_0}}{2} B(\Omega_0) e^{j\phi(\Omega_0)} e^{j\Omega_0 t} e^{j\alpha} \left[(1 - e^{-j\alpha}) + \frac{\beta}{2} e^{j(\dot{\phi} \cdot \nu_0 + \frac{1}{2} \ddot{\phi} \cdot \nu_0^2) + j\nu_0 t} - \frac{\beta}{2} e^{j(-\dot{\phi} \cdot \nu_0 + \frac{1}{2} \ddot{\phi} \cdot \nu_0^2) - j\nu_0 t} \right] \quad (32)$$

The optical output of the MZM AM modulator can be seen in Fig. 5.

$$P(t) = Y(t) \cdot Y^*(t) = \frac{P_0}{4} B(\Omega_0)^2 \cdot \left[\underbrace{2(1 - \cos(\alpha)) + \frac{\beta^2}{2}}_{\text{dc response}} + \underbrace{+4\beta \sin\left(\frac{\alpha}{2}\right) \cos\left(\frac{\ddot{\phi} \nu_0^2}{2} + \frac{\alpha}{2}\right)}_{\text{amplitude of first harmonics } \nu_0} \cdot \underbrace{\sin\left(\nu_0(\dot{\phi} + t)\right)}_{\text{phase shift of first harmonics } \nu_0} - \underbrace{\frac{\beta^2}{2}}_{\text{amplitude of second harmonics } \nu_0} \cdot \underbrace{\cos\left(2\nu_0(\dot{\phi} + t)\right)}_{\text{phase shift of second harmonics } \nu_0} \right] \quad (33)$$

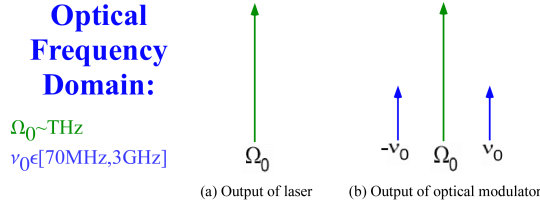


Figure 5: Schematic of MPS optical frequency domain signals

(a) optical output of laser: optical carrier Ω_0 . (b) optical output of optical modulator: optical carrier Ω_0 with two RF sidetones $\Omega_0 \pm \nu_0$. Each sidetone is separated from the optical carrier by the RF modulating frequency ν_0 .

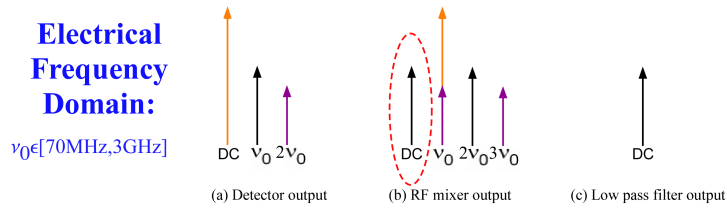


Figure 6: Schematic of MPS electrical frequency domain signals

(a) electrical output of detector beat term (DC, ν_0 and $2\nu_0$). (b) RF mixer output ν_0 signal shifted to DC and $2\nu_0$, DC signal shifted to ν_0 and $2\nu_0$ signal shifted to ν_0 and $3\nu_0$. (c) Low pass filter output filters all the harmonics above DC.

The generated photocurrent at the detector will have a DC beat term, an harmonic beat term between the sideband and the carrier and an harmonic beat term between the sidebands proportional to $\dot{\phi}$ see Fig. 6. Usually the case of small modulation is considered $\beta \ll 1$, then the corresponding AC term with the $2\nu_0$ harmonics can be neglected and our desired signal remains hidden in the ν_0 harmonics - $\sin((\nu_0(\dot{\phi} + t))$ [14]. The term being measured is the phase shift of the first harmonics ν_0 . This term can be demodulated by a RF mixer. The demodulated signal is passed through a low-pass filter, resulting in the signal proportional to: $\sin(\nu_0\dot{\phi})$. By sweeping the laser across the entire spectrum of interest, the first phase differential can be extracted for every central frequency Ω_0 . The chromatic dispersion term is a derivative of this function.

We should be aware of a possible fading of the modulated frequency current ν_0 due to the cosine term involving the dispersion $\ddot{\phi}$, moreover there is also another term which can cause signal fading, α , it is another degree of freedom which is related to the MZM bias voltage setting. However, we are interested in the measurement of the electrical phase shift and since this dispersion related term only introduces amplitude fading of the desired signal, so usually it is omitted when deriving the operation principle of the MPS technique. We need to emphasize that this amplitude fading is the basic principle behind the Baseband AM response which will be described later on.

The measurement itself is the electrical phase shift $\theta = 2\pi\nu_0\dot{\phi} = 2\pi\nu_0\tau_g$ which can be recovered from any electrical phase detector instrument. The minimum limit is the phase resolution limit of the instrument itself. Usually vector network analyzer and vector voltmeter have a resolution of 0.1 degrees, state of the art vector network analyzer can achieve a resolution of 0.01 degrees. The

maximum allowable measurable phase without ambiguity is $\theta = \pm\pi$. In case of a measurement beyond this limit there will be an alias error, and therefore a wrong measurement of the group delay. In practice, the wavelength is stepped or swept over a small wavelength interval and the corresponding change in the group delay $\Delta\tau_g$ [18] is calculated from the measured change in phase according to

$$\Delta\tau_g = \frac{\Delta\theta}{360} \frac{1}{\nu_0} \quad (34)$$

where $\Delta\theta$ is the phase change in degrees produced by a small wavelength step and ν_0 is the modulating frequency in Hz. We need to remember that the attribute called dispersion is defined by

$$D = \frac{\Delta\tau_g}{\Delta\lambda} \quad (35)$$

where $\Delta\tau_g$ is the change in group delay in seconds corresponding to a change in wavelength $\Delta\lambda$ in meters. We can combine this last two equations and find that

$$\Delta\theta = 360 \cdot D \cdot \nu_0 \cdot \Delta\lambda \quad (36)$$

this shows that the amount of phase change measured in response to a wavelength step is the product of device dispersion, modulation frequency and wavelength step.

From this result we can deduce the benefits and limitations of the MPS method. When the amount of spectral change is small, large RF frequencies are necessary in order to get meaningful signals. However, the approximation that the phase experienced by the sidebands varies linearly across a small bandwidth of $2\nu_0$ loses its validity. Also, the necessary RF components necessary for measurement become more challenging as the frequency ν_0 increases. At large spectral variations small RF frequencies are used, but at the expense of sensitivity [19].

For the technique to function properly, the sidetones must have the same amplitude, and the change in delay (or phase) must be accurately measured to obtain the dispersion. The measurement accuracy of the MPS method depends on the spacing of the modulation sidebands with respect to the actual group delay variations see Fig. 7. This is due to the fact that the measured group delay is essentially an average of the group delay at two wavelengths separated by twice the modulation frequency.

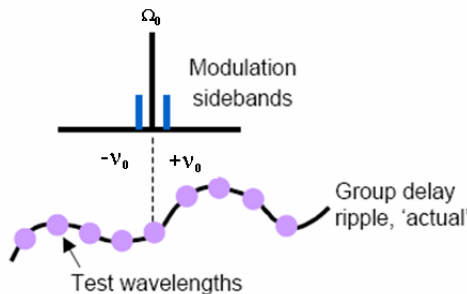


Figure 7: Modulation frequency selection for the measurement of group delay ripple (adopted from [18])

To achieve a high-resolution measurement of group delay ripple, the modulation frequency should be low enough that the modulation sidebands ride up and down the group delay ripple as a pair.

For components such as microresonators and fiber Bragg grating in which the group delay fluctuation is large in the bandwidth of the optical signal, higher spectral resolution is required [19]. Resolution of fine group delay ripple is improved by reducing the modulation frequency, but at the expense of sensitivity. In devices which have relatively small change in group delay sensitivity improvement will be reached by increasing the modulation frequency. Ultimately, the device under test features will determine the desired modulation frequency.

There have suggested several improvements to the MPS method all of which will be described in details later. One technique is based on the amplitude fading due to *dispersion · length* product which causes the two intensity sidebands to be in counter phase thereby producing a zero in the amplitude of the ν_0 signal [20]. Another technique utilized complex modulation to excite only a single sideband (SSB) and used the beat term at the fundamental frequency ν_0 [21]. Another technique utilized two measurements at different frequencies ν_1 and ν_2 , using the MPS method [22]. Scaling the two measurements by weighting functions improved the MPS group delay measurement beyond the limit normally imposed by the phase noise of the measurement system. Another technique which uses a fixed sideband and a moving sideband to measure the group delay (phase change) due to the moving sideband [23]. Another technique using two single-sideband tones [24].

2.4 Measuring dispersion using Baseband AM response method

Chromatic dispersion changes the relative phase of sidebands of modulated signals. In case of a simple intensity modulation chromatic dispersion can convert amplitude modulation (AM) to frequency modulation (FM). The term being measured is the amplitude of the first harmonics ν_0 which can be used in order to measure the chromatic dispersion coefficient at the operating wavelength with high resolution. The high resolution is achieved due to a characteristic shape of the Baseband AM response. The concept of these measurement is rather simple: a tunable laser with narrow spectral width is tuned to the wavelength at which dispersion is to be measured. The light is intensity modulated by a lithium niobate MZM modulator. As the RF modulated frequency is swept, the Baseband AM response exhibits a series of nulls [20]. This measurement is done in the frequency domain using a standard lightwave component analyzer.

The nulls occurs whenever the *dispersion · length* product causes the two intensity sidebands to be in counter phase thereby producing a zero in the amplitude of the signal from the photodiode at the RF modulated frequency (see Fig. 8). The null frequencies ν_0 in GHz are predicted by

$$\nu_0 = \sqrt{\frac{500 \cdot c \cdot (1 + 2N)}{D \cdot L \cdot \lambda_0^2}} \quad (37)$$

where $N = 0, 1, 2, \dots$ is the index of the null, c is the speed of light in vacuum in m/sec, D is the chromatic dispersion coefficient in psec/nm-km, L is the fiber length in km, λ_0 is the wavelength in nm. This method is most applicable to measurement of relatively large values of dispersion, that is, well away from the zero dispersion wavelength [13].

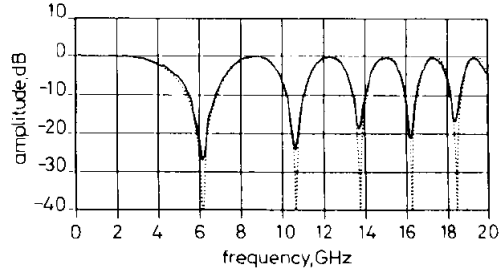


Figure 8: Frequency transfer function of 95.814km SMF (Results adopted from [20])
line measured transfer function, dotted line calculated transfer function.

This phenomena has crucial impact on optical millimeter-wave systems in which the mm-wave signal suffers from power severe power degradation. Therefore it was stated that simple intensity modulation format is not suited for transmitting a mm-wave signal modulating an optical carrier in the 1550nm wavelength [25]. Furthermore this measurement technique can also be used to check effects of linear chirped fiber Bragg gratings and their dispersion compensation properties [26].

2.5 Modulation Phase Shift improvement on the accuracy

There is a filtering limitation inherent in the standard MPS method. The filtering limitation occurs because the optical phase is effectively sampled at two points separated by twice the modulation frequency. This distortion can be described by taking the Fourier transform $T(s)$ of the measured group delay $\tau_{GD}(\Omega_0)$ where Ω_0 is the optical frequency.

$$T(s) \equiv F[\tau_{GD}(\Omega_0)] \quad (38)$$

The Fourier transform $T(s)$ describes the magnitude of the group delay ripple components as a function of s , the inverse of the ripple period in optical frequency [22]. The MPS method filters the ripple components in the Fourier domain according to the "sinc" transfer function, MPS instrument function, given by [19]

$$H_1(s) = \text{sinc} \left(\frac{\pi s}{s_1} \right) \quad (39)$$

where the parameter s is related to the ripple period p by the relationship $s = \frac{1}{p}$, the parameter s_1 is related to the RF modulation frequency ν_1 by the relationship $s_1 = \frac{1}{2\nu_1}$. The filtering function $H_1(s)$. for large group delay ripple ($s \ll s_1$), attenuation by filtering is minimal, but as the ripple period decreases and approaches $1/2\nu_0$ ($s \sim s_1$) these ripple components are completely suppressed. For a ripple periods less than $1/2\nu_0$ ($s > s_1$) there can be a 180° phase reversal. This inverting effect can increase the distortion in the group delay measurement since

these components are subtracted when they should be added. Using standard signal processing concepts, this filtering distortion can be removed using deconvolution by dividing the measured data with the known filtering transfer function in the Fourier domain

$$\tau_{GD}(\Omega_0) = F^{-1} \left[\frac{T_1(s)}{H_1(s)} \right] \quad (40)$$

this simple solution diverges in the cases where the denominator goes to zero. In order to avoid post processing which have been described by Genty and his colleagues [15] this problem can be resolved by performing two measurements using two different frequencies of RF modulation (ν_1, ν_2), so that there exists no ripple period for which both transfer functions become zero at the same time see Fig. 9. By an averaged weighting of the two measured responses, the effect of the filtering can be eliminated

$$\tau_{GD}(\Omega_0) = F^{-1} \left[\frac{H_1(s)}{H_1^2(s) + H_2^2(s)} T_1(s) + \frac{H_2(s)}{H_1^2(s) + H_2^2(s)} T_2(s) \right] \quad (41)$$

The resulting summation would yield the original pre-filtered signal while avoiding zeroes in the denominator.

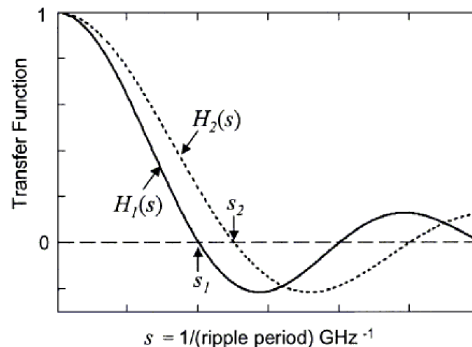


Figure 9: Transfer functions showing the filtering process inherent to the MPS method of two different RF modulation frequencies adopted from [22]

2.6 Chromatic dispersion measurement with Single Sideband method (SSB)

The SSB technique avoids amplitude fading of the desired signal as can be seen in the Baseband AM response method. It has been previously demonstrated that in intensity modulation schemes, used for fiber-radio systems, dispersion effects can be reduced by the elimination of one sideband to produce an optical single sideband (SSB). Using a dual electrode MZM modulator to produce optical SSB, while carefully selecting the working points of the electrodes and applying small modulation depth [27]. It was also demonstrated that optical filtering can achieve Optical SSB transmission [28]. A demonstration of this complex modulation applied to characterize fiber

gratings with high resolution, where it was also suggested that this technique can be applicable to any optical device [29].

The basic principle of the SSB technique is outlined in Fig. 10. An optical signal of frequency Ω_0 is SSB modulated at RF frequency ν_0 . Assuming only a SSB is generated, the time domain electric field, $e_{SSB}^{in}(t)$ at the device input, can be written as

$$e_{SSB}^{in}(t) = A(\nu_0)e^{j\Omega_0 t} + C(\nu_0)e^{j(\Omega_0 \pm \nu_0)t} \quad (42)$$

where $A(\nu_0)$ and $C(\nu_0)$ represent the complex amplitude of the optical carrier at Ω_0 and the upper sideband at $\Omega_0 + \nu_0$, representing suppression of the lower sideband ($\Omega_0 - \nu_0$). Likewise in the lower sideband at $\Omega_0 - \nu_0$, representing suppression of the upper sideband ($\Omega_0 + \nu_0$). Notice that A and C depend on the RF response of the modulator and are thus function of ν_0 .

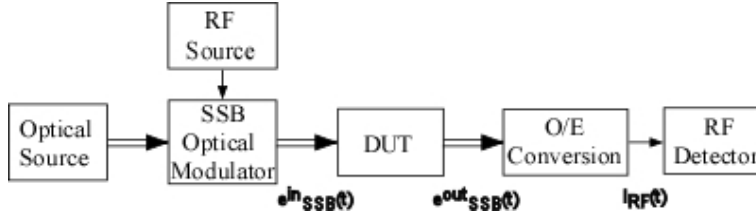


Figure 10: Schematic of chromatic dispersion measurement using SSB optical modulator

The time domain electric field, $e_{SSB}^{out}(t)$, at the device output can be written as

$$e_{SSB}^{out}(t) = A(\nu_0)B(\Omega_0)e^{j\Omega_0 t + j\Phi(\Omega_0)} + C(\nu_0)B(\Omega_0 \pm \nu_0)e^{j(\Omega_0 \pm \nu_0)t} e^{j\Phi(\Omega_0 \pm \nu_0)} \quad (43)$$

The beat note of the photodetector current $\propto [e_{SSB}^{out}(t)]^2$, where '+' sign represents upper sideband and '-' sign represents lower sideband, is given by

$$I_{RF}(t) = kB(\Omega_0)B(\Omega_0 \pm \nu_0) \cdot \cos[\pm\nu_0 t + \Phi(\Omega_0 \pm \nu_0) - \Phi(\Omega_0)] \quad (44)$$

where k is a constant. Thus if the frequency ν_0 of the RF source is swept while the optical frequency Ω_0 is kept fixed, the photo-current will map both the optical amplitude $B(\Omega_0 \pm \nu_0)$ and the optical phase $\Phi(\Omega_0 \pm \nu_0)$ responses of the device. The suppressed sideband could be chosen by means of changing the quadrature point of the MZM. In Roman et al. publication from 1998 they have achieved a 13dB optical sideband suppression in between the RF frequencies of 2-18GHz.

Another SSB technique was suggested by Madsen which measures chromatic and polarization mode dispersion using phase-sensitive sideband detection for each sideband individually [21]. It is based on decomposing the fiber or DUT phase response into the sum of an even and

odd function, as any mathematical function can be described. The sidebands are not required to have the same amplitude as they are required in the MPS method. A single modulation frequency yields relative delay and quadratic dispersion. It is also claimed that doing the same measurement on orthogonal polarizations Polarization Mode Dispersion (PMD) information is obtained.

2.7 Chromatic dispersion measurement using Fixed Sideband Technique

A variation of the standard MPS method that requires no hardware change of the conventional MPS instead it is a new concept of the measurement itself. The basic principle behind this method is to adjust the modulation frequency and the optical carrier wavelength simultaneously so that one of the two sidebands remains at the same fixed wavelength while the other sideband scans part of the measurement wavelength range see Fig. 11 [23].

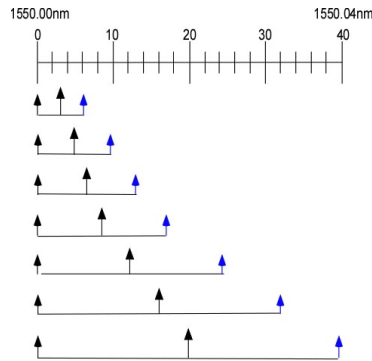


Figure 11: Schematic of chromatic dispersion measurement using fixed sideband technique

Since the measured phase is dependent on the position of the two sidebands and one of the sidebands remains fixed, the measured change in phase is due to the moving sideband. It is suggested that in this approach the modulation frequency remains at high frequencies in the GHz range while wavelength resolution is determined by the moving sideband. The limitation of this technique lies in the accuracy of the placement of the carrier. So theoretically given an optical source with sub-picometer wavelength resolution this technique has a potential of yielding sub picosecond and sub picometer resolution simultaneously. The sub picosecond is due to inherit limitation in the MPS method in which the measured phase, $\phi = 2\pi\tau\nu_0 = 360 \cdot \tau \cdot \nu_0$, with given a typical phase resolution accuracy of 0.05 degrees yields a resolution of $2.8psec @ \nu_0 = 50MHz$ compared to $0.07psec @ \nu_0 = 2GHz$.

There is also a limitation on the RF frequency which controls the moving sideband, as we have seen in the Baseband AM technique there is a series of nulls depending on the dispersion-length product. So there need to be caution with the modulation frequency and dispersion combination which will cause fading of the amplitude intensity and make the measurement meaningless.

2.8 Appendix: Jacobi-Anger expansion of amplitude modulation (AM)

We will examine the LTI signal analysis of the MPS in the most general case. In case we drive the upper arm with a voltage signal which has a DC component and an AC term (there could also be a constant phase delay between the ports) we have omitted 2π factor in the right side of Eq. 45 for brevity, we can return it in the end of the analysis

$$RF = \pi \frac{V_b + V \sin(2\pi\nu_0 t)}{V_\pi} \triangleq \alpha + \beta \cdot \sin(\nu_0 t) \quad (45)$$

where V_b is the bias voltage, V is the modulation voltage, V_π is the voltage applied to achieve a π phase shift and ν_0 is the RF driving frequency. The signal is more conveniently parametrized by α and β .

First we look at the optical field arriving to the DUT after passing the MZM in the bar port with the use of Jacobi-Anger identity. This demonstrates that there is an entire comb spectrum generated with distributed powers dependent on $J_n(\beta)$, n -th order Bessel function of the first kind evaluated at β .

$$U(t) = \frac{\sqrt{P_0}}{2} \cdot e^{j\Omega_0 t} \cdot \left(e^{j\alpha} \cdot e^{j\beta \cdot \sin(\nu_0 t)} - 1 \right) = \frac{\sqrt{P_0}}{2} \cdot e^{j\Omega_0 t} \cdot \left(e^{j\alpha} \cdot \sum_{n=-\infty}^{\infty} J_n(\beta) \cdot e^{j \cdot n \cdot \nu_0 t} - 1 \right), n \in \mathbb{N} \quad (46)$$

Using standard assumptions about constant spectral amplitude and spectral phase expansion by a Taylor series.

$$Y(t) = \frac{\sqrt{P_0}}{2} \cdot B(\Omega_0) \cdot e^{j\phi(\Omega_0)} e^{j\Omega_0 t} \cdot \left[e^{j\alpha} \cdot \sum_{n=-\infty}^{\infty} J_n(\beta) \cdot e^{j(n\nu_0\phi + \frac{n^2\nu_0^2\ddot{\phi}}{2})} \cdot e^{jn\nu_0 t} - 1 \right] \quad (47)$$

i.e., each harmonic term is scaled and acquires spectral phase.

The expression of the photocurrent

$$\begin{aligned} P(t) &= Y(t) \cdot Y^*(t) = \frac{P_0}{4} \cdot B(\Omega_0)^2 \cdot \left[e^{j\alpha} \cdot \sum_{n=-\infty}^{\infty} J_n(\beta) \cdot e^{j(n\nu_0\phi + \frac{n^2\nu_0^2\ddot{\phi}}{2})} \cdot e^{jn\nu_0 t} - 1 \right] \\ &\cdot \left[e^{-j\alpha} \cdot \sum_{m=-\infty}^{\infty} J_m(\beta) \cdot e^{-j(m\nu_0\phi + \frac{m^2\nu_0^2\ddot{\phi}}{2})} \cdot e^{-jm\nu_0 t} - 1 \right] \\ &= \frac{P_0}{4} \cdot B(\Omega_0)^2 \cdot \left\{ \sum_{n=-\infty}^{\infty} \sum_{m=-\infty}^{\infty} J_n(\beta) J_m(\beta) \cdot e^{j(\phi(n-m)\nu_0 + \frac{\ddot{\phi}(n^2-m^2)\nu_0^2}{2})} \cdot e^{j(n-m)\nu_0 t} \right. \\ &\left. - e^{j\alpha} \cdot \sum_{n=-\infty}^{\infty} J_n(\beta) \cdot e^{j(n\nu_0\phi + \frac{n^2\nu_0^2\ddot{\phi}}{2})} \cdot e^{jn\nu_0 t} \right. \\ &\left. - e^{-j\alpha} \cdot \sum_{m=-\infty}^{\infty} J_m(\beta) \cdot e^{-j(m\nu_0\phi + \frac{m^2\nu_0^2\ddot{\phi}}{2})} \cdot e^{-jm\nu_0 t} \right\} \end{aligned}$$

$$\left. -e^{-j\alpha} \cdot \sum_{m=-\infty}^{\infty} J_m(\beta) \cdot e^{-j(m\nu_0\dot{\phi} + \frac{m^2\nu_0^2\ddot{\phi}}{2})} \cdot e^{-jm\nu_0 t} + 1 \right\} \quad (48)$$

in order to emphasize the harmonics we define an index change $k = n - m \Rightarrow m = n - k$

$$n^2 - m^2 = (n - m)(n + m) = k \cdot (2n - k)$$

also for the stand alone harmonics we can substitute $n, m = k$

$$\begin{aligned} P(t) = \frac{P_0}{4} \cdot B(\Omega_0)^2 \cdot & \left\{ \sum_{n=-\infty}^{\infty} \sum_{k=-\infty}^{\infty} J_n(\beta) J_{n-k}(\beta) \cdot e^{jk\nu_0(\dot{\phi}+t)} \cdot e^{j\frac{\ddot{\phi}k(2n-k)\nu_0^2}{2}} \right. \\ & - e^{j\alpha} \cdot \sum_{k=-\infty}^{\infty} J_k(\beta) \cdot e^{jk\nu_0(\dot{\phi}+t)} \cdot e^{j\frac{k^2\nu_0^2\ddot{\phi}}{2}} \\ & \left. - e^{-j\alpha} \cdot \sum_{k=-\infty}^{\infty} J_k(\beta) \cdot e^{-jk\nu_0(\dot{\phi}+t)} \cdot e^{-j\frac{k^2\nu_0^2\ddot{\phi}}{2}} + 1 \right\} \quad (49) \end{aligned}$$

We can split each infinite sum into two equal weight terms, in the second term we change the index from positive to negative sign, i.e. $k \rightarrow -k$. Due to the symmetric and anti-symmetric characteristic of the Bessel J-th functions the photocurrent can be represented in the equivalent form

$$\begin{aligned} P(t) = \frac{P_0}{4} \cdot B(\Omega_0)^2 \cdot & \left\{ \sum_{n=-\infty}^{\infty} \sum_{k=-\infty}^{\infty} J_n(\beta) J_{n-k}(\beta) \cdot \left[\begin{array}{l} \cos(k\nu_0(\dot{\phi}+t)) \cos\left(\frac{\ddot{\phi}}{2}k(2n-k)\nu_0^2\right) \\ -\sin(k\nu_0(\dot{\phi}+t)) \sin\left(\frac{\ddot{\phi}}{2}k(2n-k)\nu_0^2\right) \end{array} \right]_k \right. \\ & \left. - 2 \sum_{k=-\infty}^{\infty} J_k(\beta) \cdot \left[\begin{array}{l} \cos(k\nu_0(\dot{\phi}+t)) \cos\left(\alpha + \frac{\ddot{\phi}}{2}k^2\nu_0^2\right) \\ -\sin(k\nu_0(\dot{\phi}+t)) \sin\left(\alpha + \frac{\ddot{\phi}}{2}k^2\nu_0^2\right) \end{array} \right]_k + 1 \right\} \quad (50) \end{aligned}$$

where $\left[\begin{array}{c} \dots \\ \dots \end{array} \right]_k$ formalizm formalism is introduced to denote that top element is chosen if k is even and bottom if k is odd.

Lets look at DC response ($k=0$):

$$\tilde{P}_0 = \frac{P_0}{4} \cdot B(\Omega_0)^2 \cdot \underbrace{\left[\sum_{n=-\infty}^{\infty} J_n(\beta)^2 - 2J_0(\beta) \cdot \cos(\alpha) + 1 \right]}_{\text{dc response}}$$

Response at first harmonic ($k = \pm 1$):

$$\begin{aligned} \tilde{P}_1 = \frac{P_0}{4} \cdot B(\Omega_0)^2 \cdot & \left\{ 4J_1(\beta) \sin[\nu_0(\dot{\phi}+t)] \sin\left[\frac{\ddot{\phi}}{2}\nu_0^2 + \alpha\right] \right. \\ & \left. - 2 \sum_{n=-\infty}^{\infty} J_n(\beta) J_{n-1}(\beta) \sin[\nu_0(\dot{\phi}+t)] \sin\left[\frac{\ddot{\phi}}{2}(2n-1)\nu_0^2\right] \right\} \end{aligned}$$

Response at first harmonic ($k = \pm 2$):

$$\tilde{P}_2 = \frac{P_0}{4} \cdot B(\Omega_0)^2 \cdot \left\{ 2 \sum_{n=-\infty}^{\infty} J_n(\beta) J_{n-2}(\beta) \cos \left[2\nu_0(\dot{\phi} + t) \right] \cos \left[\ddot{\phi}(2n-2)\nu_0^2 \right] \right. \\ \left. - 4J_2(\beta) \cos \left[2\nu_0(\dot{\phi} + t) \right] \cos \left[\ddot{\phi}2\nu_0^2 + \alpha \right] \right\}$$

Now we will gather all the contributions to dc response, first and second harmonics ν_0 while considering the lower index cases contributions $n \in [-4, 4]$ $k \in [-1, 1]$

$$P(t) = \frac{P_0}{4} B(\Omega_0)^2 \cdot \left[\underbrace{J_0(\beta)^2 + 2J_1(\beta)^2 + 2J_2(\beta)^2 - 2J_0(\beta)\cos(\alpha) + 1}_{\text{dc response}} \right. \\ \left. + \underbrace{\left[4J_1(\beta) \left\{ \sin \left[\frac{\nu_0^2 \ddot{\phi}}{2} + \alpha \right] - J_0(\beta) \sin \left[\frac{\nu_0^2 \ddot{\phi}}{2} \right] \right\} - 4J_1(\beta)J_2(\beta) \sin \left[\frac{3\nu_0^2 \ddot{\phi}}{2} \right] - 4J_2(\beta)J_3(\beta) \sin \left[\frac{3\nu_0^2 \ddot{\phi}}{2} \right] \right]}_{\text{amplitude of first harmonics } \nu_0} \cdot \underbrace{\sin[\nu_0(\dot{\phi} + t)]}_{\text{phase shift of first harmonics } \nu_0} \right. \\ \left. + \underbrace{\left[4J_2(\beta) \left\{ J_0(\beta) \cos \left[\frac{4\nu_0^2 \ddot{\phi}}{2} \right] - \cos \left[\frac{4\nu_0^2 \ddot{\phi}}{2} + \alpha \right] \right\} - 2J_1(\beta)^2 + 4J_1(\beta)J_3(\beta) \cos \left[\frac{8\nu_0^2 \ddot{\phi}}{2} \right] + \right.}_{\text{amplitude of second harmonics } \nu_0} \right. \\ \left. \underbrace{\left[4J_2(\beta)J_4(\beta) \cos \left[\frac{12\nu_0^2 \ddot{\phi}}{2} \right] \right]}_{\text{amplitude of second harmonics } \nu_0} \cdot \underbrace{\cos[2\nu_0(\dot{\phi} + t)]}_{\text{phase shift of second harmonics } \nu_0} \right] \quad (51)$$

We should note that increasing β , arises a broader spectrum of ν_0 harmonics which need to be taken into account in this summation. Thus affecting the amplitude of first ν_0 harmonic terms and effect the dc response contributions i.e. $2 \sum_{n=3}^{\infty} J_n(\beta)^2$.

Now we can return the 2π constant to the analysis of the photocurrent ($\nu_0 \rightarrow 2\pi\nu_0$).

Each of the amplitude responses needs to be carefully estimated depending on the RF modulating frequency ν_0 . In order to see whether they could be neglected or needed to be taken into account. If we will consider the case that the RF modulating frequency is far away from the RF fading dip typically found in the AM Baseband method. Then we could estimate the following expressions as following $\sin \left[\frac{m\nu_0^2 \ddot{\phi}}{2} \right] \sim 0$ and $\cos \left[\frac{m\nu_0^2 \ddot{\phi}}{2} \right] \sim 1$.

We can rewrite this last expression according to the following identity of cosine and sine functions

$$\cos[\alpha \pm \beta] = [\cos \alpha \cos \beta \mp \sin \alpha \sin \beta]$$

$$\sin[\alpha \pm \beta] = [\sin \alpha \cos \beta \pm \cos \alpha \sin \beta]$$

Finally, under the assumption about the driving RF frequency is far from RF fading dip

$$\begin{aligned}
P(t) = & \frac{P_0}{4} B(\Omega_0)^2 \cdot \left[\underbrace{J_0(\beta)^2 + 2J_1(\beta)^2 + 2J_2(\beta)^2 - 2J_0(\beta)\cos(\alpha) + 1}_{\text{dc response}} \right. \\
& + \underbrace{4J_1(\beta)\sin[\alpha]}_{\text{amplitude of first harmonics } \nu_0} \cdot \underbrace{\sin[\nu_0(\dot{\phi} + t)]}_{\text{phase shift of first harmonics } \nu_0} \\
& \left. + \underbrace{[4J_2(\beta)\{J_0(\beta) - \cos[\alpha]\} - 2J_1(\beta)^2 + 4J_1(\beta)J_3(\beta) + 4J_2(\beta)J_4(\beta)]}_{\text{amplitude of second harmonics } \nu_0} \cdot \underbrace{\cos[2\nu_0(\dot{\phi} + t)]}_{\text{phase shift of second harmonics } \nu_0} \right] \quad (52)
\end{aligned}$$

In order to examine the validation of the small signal approximation, we need to check the J.A. expansion under the approximation that the RF modulation index is small, i.e. $\beta \ll 1$. The Bessel function approximation for small values of x is $J_n(x) \underset{x \rightarrow 0}{\sim} \frac{1}{2^n \cdot n!} x^n$. Up to the 4th order the Bessel functions approximations are $J_0(x) \sim 1$, $J_1(x) \sim \frac{x}{2}$, $J_2(x) \sim \frac{x^2}{8}$, $J_3(x) \sim \frac{x^3}{48}$, $J_4(x) \sim \frac{x^4}{384}$. Therefore we can rewrite the photocurrent

$$\begin{aligned}
P(t) = & \frac{P_0}{4} B(\Omega_0)^2 \cdot \left[\underbrace{1 + 2 \cdot \left(\frac{\beta}{2}\right)^2 + 2 \cdot \left(\frac{\beta^2}{8}\right)^2 - 2 \cdot \cos(\alpha) + 1}_{\text{dc response}} \right. \\
& + \underbrace{4 \cdot \frac{\beta}{2} \cdot \sin[\alpha]}_{\text{amplitude of first harmonics } \nu_0} \cdot \underbrace{\sin[\nu_0(\dot{\phi} + t)]}_{\text{phase shift of first harmonics } \nu_0} \\
& \left. + \underbrace{\left[4 \cdot \frac{\beta^2}{8} \cdot \{1 - \cos[\alpha]\} - 2 \cdot \left(\frac{\beta}{2}\right)^2 + 4 \cdot \frac{\beta}{2} \cdot \frac{\beta^3}{48} + 4 \cdot \frac{\beta^2}{8} \cdot \frac{\beta^4}{384} \right]}_{\text{amplitude of second harmonics } \nu_0} \cdot \underbrace{\cos[2\nu_0(\dot{\phi} + t)]}_{\text{phase shift of second harmonics } \nu_0} \right] \quad (53)
\end{aligned}$$

we will keep all the β power up to the 2nd order, hence

$$\begin{aligned}
P(t) = & \frac{P_0}{4} B(\Omega_0)^2 \cdot \left[\underbrace{2[1 - \cos(\alpha)] + \frac{\beta^2}{2}}_{\text{dc response}} + \underbrace{2 \cdot \beta \cdot \sin[\alpha]}_{\text{amplitude of first harmonics } \nu_0} \cdot \underbrace{\sin[\nu_0(\dot{\phi} + t)]}_{\text{phase shift of first harmonics } \nu_0} \right. \\
& \left. - \underbrace{\frac{\beta^2}{2} \cdot \cos[\alpha]}_{\text{amplitude of second harmonics } \nu_0} \cdot \underbrace{\cos[2\nu_0(\dot{\phi} + t)]}_{\text{phase shift of second harmonics } \nu_0} \right] \quad (54)
\end{aligned}$$

Now we will rearrange the photocurrent expression of the small signal approximation (this is Eq. 33 again), in order to notice the difference in between these expressions.

$$\begin{aligned}
P(t) = \frac{P_0}{4} B(\Omega_0)^2 \cdot & \left[\underbrace{2(1 - \cos(\alpha)) + \frac{\beta^2}{2}}_{\text{dc response}} + \underbrace{4\beta \sin\left(\frac{\alpha}{2}\right) \cos\left(\frac{\ddot{\phi}\nu_0^2}{2} + \frac{\alpha}{2}\right)}_{\text{amplitude of first harmonics } \nu_0} \cdot \underbrace{\sin\left(\nu_0(\dot{\phi} + t)\right)}_{\text{phase shift of first harmonics } \nu_0} \right. \\
& \left. - \underbrace{\frac{\beta^2}{2}}_{\text{amplitude of second harmonics } \nu_0} \cdot \underbrace{\cos\left(2\nu_0(\dot{\phi} + t)\right)}_{\text{phase shift of second harmonics } \nu_0} \right] \quad (55)
\end{aligned}$$

standard assumption the driving RF frequency is far from RF fading dip ($\frac{\nu_0^2 \ddot{\phi}}{2} \ll 1$). We can rewrite the photocurrent of the small signal approximation after trigonometric manipulation

$$\begin{aligned}
P(t) = \frac{P_0}{4} B(\Omega_0)^2 \cdot & \left[\underbrace{2(1 - \cos(\alpha)) + \frac{\beta^2}{2}}_{\text{dc response}} + \underbrace{2\beta \sin(\alpha)}_{\text{amplitude of first harmonics } \nu_0} \cdot \underbrace{\sin\left(\nu_0(\dot{\phi} + t)\right)}_{\text{phase shift of first harmonics } \nu_0} \right. \\
& \left. - \underbrace{\frac{\beta^2}{2}}_{\text{amplitude of second harmonics } \nu_0} \cdot \underbrace{\cos\left(2\nu_0(\dot{\phi} + t)\right)}_{\text{phase shift of second harmonics } \nu_0} \right] \quad (56)
\end{aligned}$$

From comparison of the J.A expansion and the small signal expansion there is a small correction in the amplitude of the 2nd harmonics $2\nu_0$ depending on the chosen working point of the MZM modulator, i.e. factor of $\cos(\alpha)$.

3 Modulated Phase Shift method revisited

Our apparatus expands on the well known Modulation Phase Shift (MPS) measurement technique by introducing an additional slow frequency component whose variations are tracked with a Lock-In Amplifier (LIA). The apparatus combines *optical frequencies* Ω_0 (THz) to be measured, with *RF frequencies* ν_0 (MHz-GHz) for differential optical phase accumulation, and *audio frequencies* f_0 (KHz) for feedback tracking and data extraction with the use of the LIA. The apparatus is depicted in Fig. 12.

In our approach we directly measure the Group Delay (GD) as in the standard MPS technique, as a function of optical wavelength by laser stepping over a desired wavelength range. In contrast to the MPS technique, we measure the RF phase accumulation with an harmonic term oscillatory at an audio frequency, instead of comparing phases of either RF frequency or down converting to DC. The measured phase term still depends on the phase delay experienced by the RF tones. The introduction of a lock-in amplifier to the apparatus enables us to extract the audio frequency with high resolution in comparison with RF phase comparator; in comparison with DC measurements we avoid $1/f$ noise. Furthermore, we avoid the 2π phase ambiguity while measuring phase by a feedback loop. Its simplicity should make it a viable alternative to competing commercial products, while improving on their performance by the use of clever signal processing techniques.

As we can see in the apparatus shown in Fig. 12 there are two possibilities for the RF demodulation signal ν_0 or $2\nu_0$ (the $2\nu_0$ demodulation option is marked in purple). The RF demodulation signal frequency depending on the presence of a RF x2 frequency doubler in the processing circuit.

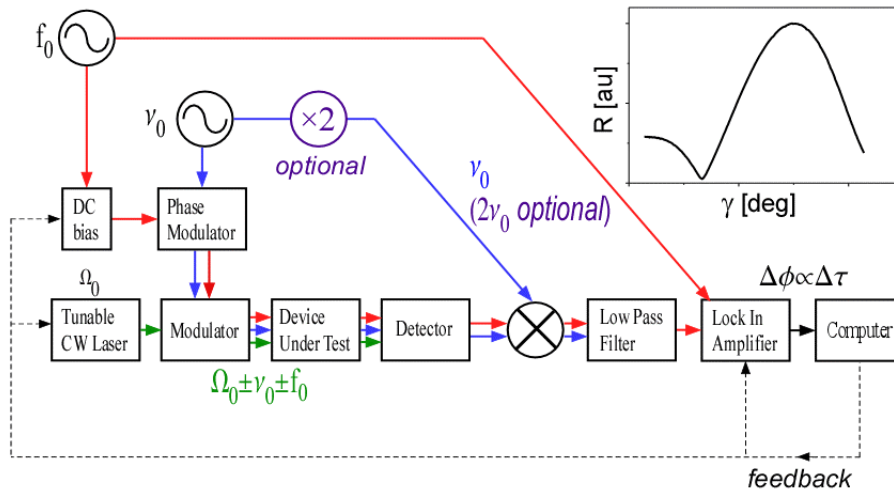


Figure 12: Schematic of revised MPS method, introducing audio dither to the RF drive, RF x2 frequency doubler (optional) and Lock In Amplifier. Inset: measured audio signal component as function of DC bias phase.

The RF signal driving the optical modulator is first phase modulated by the low frequency signal see Fig. 13. Signal analysis of the system (see section 3.1 small signal analysis; see appendix for full analysis) demonstrates that this phase information is preserved in the E/O/E conversion (through the optical modulator see Fig. 14), in transport (through the DUT), and upon detection

of the beat term see Fig. 15(a). The E/O conversion actually multiplies the optical field which have sampled the DUT with its complex conjugate. The contribution to the DC beat term arises from each optical tone multiplied by its complex conjugate tone. The contribution to the ν_0 beat term arises from beating in between the optical carrier and each of the RF sidetones, this actually combines two different phasors and averages them. While the contribution to the $2\nu_0$ beat term arises from the beating in between the two RF sidetones. Therefore the beat term contains a few arguments: DC and harmonic terms ($\nu_0, 2\nu_0$, etc). Since the information is preserved in each of the harmonic terms we can choose to demodulate it with either ν_0 harmonic or $2\nu_0$ harmonic. From here the case of ν_0 harmonics demodulation will be referred as *MPS with Audio* see Fig. 15(b), and the case of $2\nu_0$ harmonics demodulation will be referred as *2nd order MPS with Audio* see Fig. 15(d).

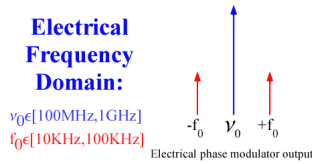


Figure 13: Schematic of electrical phase modulator output
RF carrier frequency ν_0 surrounded with a slow harmonic frequency component $\pm f_0$.

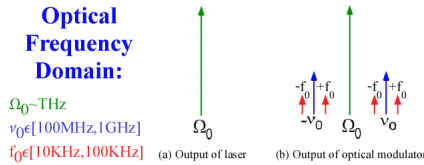


Figure 14: Schematic of 2nd order MPS with Audio optical signal
(a) laser optical output (b) optical modulator output: each of the RF sidetones $\pm\nu_0$ is surrounded with the audio frequency component $\pm f_0$.

As in conventional MPS in *MPS with Audio*, we choose to extract the measured phase from the ν_0 frequency which carries the slow phase information. Beat term now proportional to $\cos[\nu_0(t + \dot{\phi}) + \gamma] \cdot \sin([f(\dot{\phi} + t)])$, where $\gamma + \psi \cdot \sin(f_0 t)$ is the slow phase modulation, ψ is the modulation depth, γ is our controllable phase bias (shown in Fig. 12), and f_0 is the low frequency signal. This beat term is subsequently demodulated and fed to the LIA together with the reference f_0 signal. The LIA then tracks the oscillatory signal component f_0 , which is given by: $\sin[\nu_0 \dot{\phi} + \gamma] \cdot \sin([f(\dot{\phi} + t)])$. The introduction of a LIA allows us to obtain very high accuracy in measuring the amplitude and phase of the signal. The sine function, is ambiguous for extracting its argument; hence we continuously null the amplitude by a feedback loop on the DC bias γ (see inset in Fig. 12 showing amplitude as function of γ , with amplitude null at unique bias angle). Control circuits operate best when locking onto a null point, and the oscillatory signal provides a remainder signal for identification. This also prevents the ambiguity due to phase wrap. In practice, the laser wavelength is stepped a small wavelength interval, and the DC bias is swept to null the audio tone component, from which GD is extracted. The GD is recorded at every optical carrier frequency, and can be used to find the distortions by

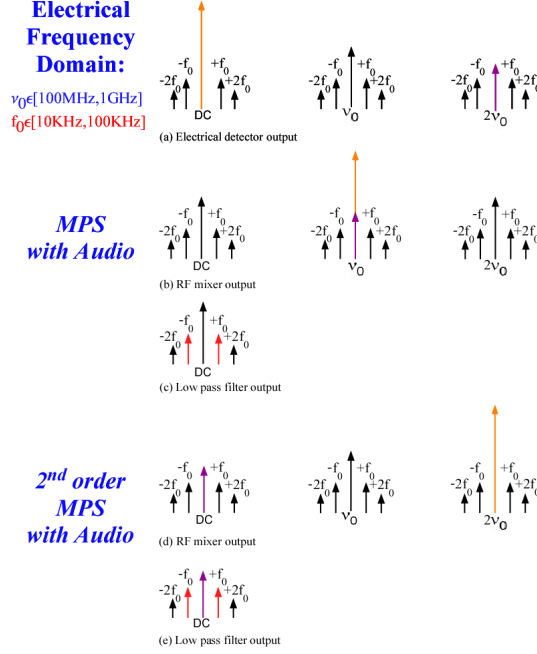


Figure 15: Schematic of modified MPS electrical signal processing (a) optical detector electrical output (b) MPS with Audio RF mixer output (down converting with ν_0 demodulation) (c) MPS with Audio low pass filter output (d) 2nd order MPS with Audio RF mixer output (down converting with $2\nu_0$ demodulation) (e) 2nd order MPS with Audio low pass filter output.

differentiation of the sampled function.

In contrast to conventional MPS, in *2nd order MPS with Audio*, we choose to extract the measured phase from the $2\nu_0$ frequency (avoiding RF fading problems) which carries the slow phase information, which has been doubled in magnitude, not frequency. Beat term now proportional to $\sin[2\nu_0(t + \dot{\phi}) + 2\gamma] \cdot \sin([f(\dot{\phi} + t)]$, where $\gamma + \psi \cdot \sin(f_0 t)$ is the slow phase modulation, ψ is the modulation depth, γ is our controllable phase bias (shown in Fig. 12), and f_0 is the low frequency signal. This beat term is subsequently demodulated and fed to the LIA together with the reference f_0 signal. The LIA then tracks the oscillatory signal component f_0 , which is given by: $\cos[2\nu_0\dot{\phi} + 2\gamma] \cdot \sin([f(\dot{\phi} + t)]$, while the amplitude dependence in between MPS with Audio and 2nd order MPS with Audio has been doubled in magnitude, not frequency. The cosine function, is also ambiguous for extracting its argument; hence we continuously null the amplitude by a feedback loop on the DC bias γ (see inset in 12 showing amplitude as function of γ , with amplitude null at unique bias angle). This again prevents the ambiguity due to phase wrap.

Several parameters can be optimized for each measurement: The frequency offset ν_0 , which should be fine for accurate measurements of rapidly varying devices [30], the RF phase offset γ to set either the sine or cosine function at an appropriate bias point (in order to avoid the phase measurement ambiguity problem), the modulation depth ψ , and the bias point of the MZM modulator, to control power transfer to tones. The phase modulation slow oscillator signal can also include a DC term δ (not shown in figure) together with the oscillatory component $\tilde{\theta} = \psi \cdot \sin(f_0 t + \delta)$, as a less sensitive measurement to the GD, due to the slow varying frequency f_0 which is several scales beneath the RF driving frequency, which can be used to eliminate the phase wrap.

Our MPS measurement technique (see 12) can measure phase (and directly GD) unambiguously within $(0, \pi)$ (and analogously, within $(0, 1/[4\nu_0])$ GD for 2nd order MPS with Audio or $(0, 1/[2\nu_0])$ in the case of MPS with Audio), and not within $(-\pi, \pi)$ as we demodulate with an in-band mixer (losing the quadrature information). Phase measurement ambiguity is avoided, provided $\Delta\lambda$ small enough, when the condition $\Delta\lambda < 1/(4\nu_0 D)$ is satisfied ($\Delta\lambda < 1/(2\nu_0 D)$) in the case of MPS with Audio). Satisfying the condition ensures that two consecutive measurements will fall in the range of $(0, \pi)$, which avoids phase wrap errors in between two measurements. Furthermore, in case of a measurement near the ambiguity region (i.e. phase measurement near 0 or π), the measured phase can be shifted using an appropriate phase offset γ . By continuously tracking the GD as the laser is stepped, the uncertainty due to the cosinoidal (sinusoidal) mapping of the output interference is also eliminated.

The LIA will lock to the oscillatory component $\sin(f_0 t + \delta)$ and extract its amplitude, while sweeping the fixed phase bias γ (through a feedback loop) in order to locate the fixed phase bias minima point γ_{min} . We have chosen to work around a minima point rather than maxima point from a few reasons. The maxima point location is harder to find, than a minima point location, through a control circuit approach. Furthermore the maxima environment is relatively slowly changing while the minima point changes rapidly. Moreover next to the minima environment we will have higher dynamic range due to the introduction of the LIA which can detect very weak signals (from 1 Volt down to 1 nVolt). The difference in between the two demodulation options is the amplitude dependence of the oscillatory component $\sin([f(t + \dot{\phi}) + \delta])$. We will now regard these two optional demodulation signals noting the differences in between them. The amplitude dependence in between MPS with Audio and 2nd order MPS with Audio has been doubled in magnitude, not frequency. While the sine term in MPS with Audio has changed from a sine term to a cosine term in the 2nd order MPS with Audio.

$$\left. \begin{array}{l} \text{MPS with Audio: } \sin(\nu_0 \dot{\phi} + \gamma) \\ \text{2nd order MPS with Audio: } \cos(2\nu_0 \dot{\phi} + 2\gamma) \end{array} \right\} \cdot \underbrace{\sin[f_0(t + \dot{\phi}) + \delta]}_{\text{LIA will lock to this term}} \quad (57)$$

In the following simplified signal analysis subsections we will present the calculations and approximations supporting this simple and most meaningful result.

3.1 Simplified signal analysis

In this section we will present the signal analysis that demonstrates this phase information is preserved in the E/O conversion (through the optical modulator), in transport (through the DUT), and upon detection of the beat term. The MPS with Audio and 2nd order MPS with Audio signal analysis is the same up to the E/O conversion. However the RF demodulation signal analysis varies in between them, so we will present subsections supporting each separate signal processing scheme.

Our technique involves the use of a modulated subcarrier signal added to the optical carrier frequency at the phase modulator. When this signal is propagated through dispersive media, or Device Under Test (DUT), the dispersion induces a relative optical phase delay between the

subcarrier sidebands. This effect is well known and is responsible for the fading experienced in double sideband subcarrier signals when direct detection is employed. Signal processing analysis can help us understand where the information is carried in our system.

We utilize a continuous wave (CW) laser, $\sqrt{P_0}e^{j\Omega_0 t}$, where Ω_0 is the optical carrier frequency (multi-THz range) and P_0 is the laser power. The laser is amplitude modulated by a RF signal (GHz range) applied to an external MZM, where the driving voltage signal is further phase modulated by a low frequency signal (KHz range). In this section we develop the RF amplitude modulation (AM) and audio phase modulation (PM) using small angle approximations. A full analytic expansion appears in the Appendix, employing Jacobi-Anger expansions to the harmonic phases.

In our model we use the most common MZM modulator commercially available, which is a single-arm-drive MZM (has only one arm under electric modulation field); or use one arm of a dual-drive modulator. This MZM has a combination of amplitude and phase modulation at its output [17]. We drive the MZM with a voltage signal which has DC and AC terms (the DC term could also be a constant phase delay between the ports), such that

$$RF = \pi \frac{V_b + V \sin(2\pi\nu_0 t + \theta)}{V_\pi} = \alpha + \beta \cdot \sin(\nu_0 t + \theta) \quad (58)$$

where V_b is the bias voltage, V is the modulation voltage, V_π is the voltage applied to achieve a π phase shift and ν_0 is the RF driving frequency (we omit the 2π constant in the harmonic on the right side of Eq. 58 for brevity). The signal is more conveniently parametrized by α and β .

The RF signal driving the optical modulator is phase modulated by the low frequency signal

$$\theta = \gamma + \psi \sin(f_0 t + \delta) \quad (59)$$

where γ is the DC bias phase at RF frequency, ψ is the audio modulation depth, f_0 is the low (audio) frequency signal and δ is the DC phase offset at low (audio) frequency.

First we look at the optical field arriving to the DUT after passing the MZM in the bar port under the approximation that the RF modulation depth is small $\beta \ll 1$ (i.e. $e^{jx} \approx 1 + jx$)

$$\begin{aligned} U(t) &= \frac{\sqrt{P_0}}{2} e^{j\Omega_0 t} \cdot (e^{j[\alpha + \beta \cdot \sin(\nu_0 t + \theta)]} - 1) \approx \frac{\sqrt{P_0}}{2} e^{j\Omega_0 t} \cdot (e^{j\alpha} [1 + j\beta \cdot \sin(\nu_0 t + \theta)] - 1) \\ &= \frac{\sqrt{P_0}}{2} e^{j\Omega_0 t} \cdot \left(e^{j\alpha} \cdot \left[1 + \frac{\beta}{2} \cdot (e^{j\nu_0 t + j\theta} - e^{-j\nu_0 t - j\theta}) \right] - 1 \right) \end{aligned} \quad (60)$$

substituting θ of Eq. (59)

$$U(t) = \frac{\sqrt{P_0}}{2} e^{j\Omega_0 t} e^{j\alpha} \left((1 - e^{-j\alpha}) + \frac{\beta}{2} \left(e^{j(\nu_0 t + \gamma + \psi \sin(f_0 t + \delta))} - e^{-j(\nu_0 t + \gamma + \psi \sin(f_0 t + \delta))} \right) \right) \quad (61)$$

under the approximation that the PM modulation depth is also small $\psi \ll 1$, we will simplify the expressions of $e^{\pm j[\gamma + \psi \sin(2\pi f_0 t + \delta)]}$

$$\begin{aligned}
e^{j[\gamma + \psi \sin(2\pi f_0 t + \delta)]} &= e^{j\gamma} \left[1 + \frac{\psi}{2} (e^{j(2\pi f_0 t + \delta)} - e^{-j(2\pi f_0 t + \delta)}) \right] \\
e^{-j[\gamma + \psi \sin(2\pi f_0 t + \delta)]} &= e^{-j\gamma} \left[1 - \frac{\psi}{2} (e^{j(2\pi f_0 t + \delta)} - e^{-j(2\pi f_0 t + \delta)}) \right] \\
U(t) &= \frac{\sqrt{P_0}}{2} e^{j\Omega_0 t} e^{j\alpha} \left((1 - e^{-j\alpha}) + \frac{\beta}{2} e^{j\nu_0 t} e^{j\gamma} \left[1 + \frac{\psi}{2} (e^{j(2\pi f_0 t + \delta)} - e^{-j(2\pi f_0 t + \delta)}) \right] \right. \\
&\quad \left. - \frac{\beta}{2} e^{-j\nu_0 t} e^{-j\gamma} \left[1 - \frac{\psi}{2} (e^{j(2\pi f_0 t + \delta)} - e^{-j(2\pi f_0 t + \delta)}) \right] \right) \tag{62}
\end{aligned}$$

This last expression defines seven harmonics: optical carrier Ω_0 and six modulation sidetones at $\Omega_0 \pm \nu_0 \pm f_0$ (see Fig. 14(b)).

the optical field at the DUT output

$$\begin{aligned}
Y(t) &= \frac{\sqrt{P_0}}{2} e^{j\alpha} \left[(1 - e^{-j\alpha}) B(\Omega_0) e^{j\phi(\Omega_0)} e^{j\Omega_0 t} + \frac{\beta}{2} e^{j\gamma} B(\Omega_0 + \nu_0) e^{j\phi(\Omega_0 + \nu_0)} e^{j(\Omega_0 + \nu_0)t} \right. \\
&\quad + \frac{\beta\psi}{4} e^{j(\gamma + \delta)} B(\Omega_0 + \nu_0 + f_0) e^{j\phi(\Omega_0 + \nu_0 + f_0)} e^{j(\Omega_0 + \nu_0 + f_0)t} - \frac{\beta\psi}{4} e^{j(\gamma - \delta)} B(\Omega_0 + \nu_0 - f_0) \\
&\quad \cdot e^{j\phi(\Omega_0 + \nu_0 - f_0)} e^{j(\Omega_0 + \nu_0 - f_0)t} - \frac{\beta}{2} e^{-j\gamma} B(\Omega_0 - \nu_0) e^{j\phi(\Omega_0 - \nu_0)} e^{j(\Omega_0 - \nu_0)t} \\
&\quad + \frac{\beta\psi}{4} e^{-j(\gamma - \delta)} B(\Omega_0 - \nu_0 + f_0) e^{j\phi(\Omega_0 - \nu_0 + f_0)} e^{j(\Omega_0 - \nu_0 + f_0)t} \\
&\quad \left. - \frac{\beta\psi}{4} e^{-j(\gamma + \delta)} B(\Omega_0 - \nu_0 - f_0) e^{j\phi(\Omega_0 - \nu_0 - f_0)} e^{j(\Omega_0 - \nu_0 - f_0)t} \right] \tag{63}
\end{aligned}$$

The typical assumption is that the attenuation experienced by the seven tones is identical. The phase is developed using Taylor series for the DUT response, assumption being that the phase can be expressed as a Taylor expansion about carrier frequency

$$\begin{aligned}
Y(t) &= \frac{\sqrt{P_0}}{2} B(\Omega_0) e^{j\alpha} e^{j\phi(\Omega_0)} e^{j\Omega_0 t} \left[(1 - e^{-j\alpha}) + \frac{\beta}{2} e^{j\gamma} e^{j\frac{\nu_0^2}{2} \ddot{\phi}} e^{j\nu_0(\dot{\phi} + t)} \right. \\
&\quad + \frac{\beta\psi}{4} e^{j(\gamma + \delta)} e^{j\frac{(\nu_0 + f_0)^2}{2} \ddot{\phi}} e^{j(\nu_0 + f_0)(\dot{\phi} + t)} - \frac{\beta\psi}{4} e^{j(\gamma - \delta)} e^{j\frac{(\nu_0 - f_0)^2}{2} \ddot{\phi}} e^{j(\nu_0 - f_0)(\dot{\phi} + t)} \\
&\quad - \frac{\beta}{2} e^{-j\gamma} e^{j\frac{(-\nu_0)^2}{2} \ddot{\phi}} e^{-j\nu_0(\dot{\phi} + t)} + \frac{\beta\psi}{4} e^{-j(\gamma - \delta)} e^{j\frac{(-\nu_0 + f_0)^2}{2} \ddot{\phi}} e^{-j(\nu_0 - f_0)(\dot{\phi} + t)} \\
&\quad \left. - \frac{\beta\psi}{4} e^{-j(\gamma + \delta)} e^{j\frac{(-\nu_0 - f_0)^2}{2} \ddot{\phi}} e^{-j(\nu_0 + f_0)(\dot{\phi} + t)} \right] \tag{64}
\end{aligned}$$

For simplicity we may represent the optical field with harmonics functions

$$Y(t) = \frac{\sqrt{P_0}}{2} B(\Omega_0) e^{j\alpha} e^{j\phi(\Omega_0)} e^{j\Omega_0 t} \left[(1 - e^{-j\alpha}) + \frac{\beta}{2} e^{j\frac{\nu_0^2}{2} \ddot{\phi}} \cdot 2j \cdot \sin[\nu_0(\dot{\phi} + t) + \gamma] \right]$$

$$\begin{aligned}
& + \frac{\beta\psi}{4} e^{j\frac{(\nu_0+f_0)^2}{2}\ddot{\phi}} \cdot 2j \cdot \sin[(\nu_0 + f_0)(\dot{\phi} + t) + \gamma + \delta] \\
& + \frac{\beta\psi}{4} e^{j\frac{(\nu_0-f_0)^2}{2}\ddot{\phi}} \cdot (-2j) \cdot \sin[(\nu_0 - f_0)(\dot{\phi} + t) + \gamma - \delta] \Big] \\
& = \frac{\sqrt{P_0}}{2} B(\Omega_0) e^{j\alpha} e^{j\phi(\Omega_0)} e^{j\Omega_0 t} \left[(1 - e^{-j\alpha}) + j\beta e^{j\frac{\nu_0^2}{2}\ddot{\phi}} \sin[\nu_0(\dot{\phi} + t) + \gamma] \right. \\
& \quad \left. + j\frac{\beta\psi}{2} e^{j\frac{(\nu_0+f_0)^2}{2}\ddot{\phi}} \sin[(\nu_0 + f_0)(\dot{\phi} + t) + \gamma + \delta] - j\frac{\beta\psi}{2} e^{j\frac{(\nu_0-f_0)^2}{2}\ddot{\phi}} \sin[(\nu_0 - f_0)(\dot{\phi} + t) + \gamma - \delta] \right] \tag{65}
\end{aligned}$$

Before finding the photocurrent we utilize the following identity

$$\sin \alpha \cdot \sin \beta = \frac{1}{2} [\cos(\alpha - \beta) - \cos(\alpha + \beta)]$$

The photocurrent expression

$$\begin{aligned}
P(t) & = Y(t) \cdot Y^*(t) = \frac{P_0}{4} B(\Omega_0)^2 \cdot \left[(1 - e^{-j\alpha})(1 - e^{j\alpha}) + j\beta e^{j\frac{\nu_0^2}{2}\ddot{\phi}} \sin[\nu_0(\dot{\phi} + t) + \gamma] \right. \\
& + j\frac{\beta\psi}{2} e^{j\frac{(\nu_0+f_0)^2}{2}\ddot{\phi}} \sin[(\nu_0 + f_0)(\dot{\phi} + t) + \gamma + \delta] - j\frac{\beta\psi}{2} e^{j\frac{(\nu_0-f_0)^2}{2}\ddot{\phi}} \sin[(\nu_0 - f_0)(\dot{\phi} + t) + \gamma - \delta] \\
& - j\beta e^{-j\frac{\nu_0^2}{2}\ddot{\phi}} \sin[\nu_0(\dot{\phi} + t) + \gamma] - j\frac{\beta\psi}{2} e^{-j\frac{(\nu_0-f_0)^2}{2}\ddot{\phi}} \sin[(\nu_0 + f_0)(\dot{\phi} + t) + \gamma + \delta] \\
& + j\frac{\beta\psi}{2} e^{-j\frac{(\nu_0+f_0)^2}{2}\ddot{\phi}} \sin[(\nu_0 - f_0)(\dot{\phi} + t) + \gamma - \delta] - j\beta e^{j(\alpha + \frac{\nu_0^2}{2}\ddot{\phi})} \sin[\nu_0(\dot{\phi} + t) + \gamma] \\
& - j\frac{\beta\psi}{2} e^{j(\alpha + \frac{(\nu_0+f_0)^2}{2}\ddot{\phi})} \sin[(\nu_0 + f_0)(\dot{\phi} + t) + \gamma + \delta] + j\frac{\beta\psi}{2} e^{j(\alpha + \frac{(\nu_0-f_0)^2}{2}\ddot{\phi})} \sin[(\nu_0 - f_0)(\dot{\phi} + t) + \gamma - \delta] \\
& + j\beta e^{-j(\alpha + \frac{\nu_0^2}{2}\ddot{\phi})} \sin[\nu_0(\dot{\phi} + t) + \gamma] + j\frac{\beta\psi}{2} e^{-j(\alpha + \frac{(\nu_0-f_0)^2}{2}\ddot{\phi})} \sin[(\nu_0 + f_0)(\dot{\phi} + t) + \gamma + \delta] \\
& - j\frac{\beta\psi}{2} e^{-j(\alpha + \frac{(\nu_0+f_0)^2}{2}\ddot{\phi})} \sin[(\nu_0 - f_0)(\dot{\phi} + t) + \gamma - \delta] \\
& + \frac{\beta^2}{2} - \frac{\beta^2}{2} \cos[2\nu_0(\dot{\phi} + t) + 2\gamma] \\
& + \frac{\beta^2\psi}{4} e^{-j\frac{(2\nu_0 f_0 + f_0^2)}{2}\ddot{\phi}} \left[\cos[-f_0(\dot{\phi} + t) - \delta] - \cos[(2\nu_0 + f_0)(\dot{\phi} + t) + 2\gamma + \delta] \right] \\
& - \frac{\beta^2\psi}{4} e^{-j\frac{(-2\nu_0 f_0 + f_0^2)}{2}\ddot{\phi}} \left[\cos[f_0(\dot{\phi} + t) + \delta] - \cos[(2\nu_0 - f_0)(\dot{\phi} + t) + 2\gamma - \delta] \right] \\
& + \frac{\beta^2\psi}{4} e^{j\frac{(2\nu_0 f_0 + f_0^2)}{2}\ddot{\phi}} \left[\cos[f_0(\dot{\phi} + t) + \delta] - \cos[(2\nu_0 + f_0)(\dot{\phi} + t) + 2\gamma + \delta] \right] \\
& + \frac{\beta^2\psi^2}{8} - \frac{\beta^2\psi^2}{8} \cos[(2\nu_0 + 2f_0)(\dot{\phi} + t) + 2\gamma + 2\delta] \\
& - \frac{\beta^2\psi^2}{8} e^{j\frac{4\nu_0 f_0}{2}\ddot{\phi}} \left[\cos[2f_0(\dot{\phi} + t) + 2\delta] - \cos[2\nu_0(\dot{\phi} + t) + 2\gamma] \right] \\
& - \frac{\beta^2\psi}{4} e^{j\frac{(-2\nu_0 f_0 + f_0^2)}{2}\ddot{\phi}} \left[\cos[-f_0(\dot{\phi} + t) - \delta] - \cos[(2\nu_0 - f_0)(\dot{\phi} + t) + 2\gamma - \delta] \right] \\
& - \frac{\beta^2\psi^2}{8} e^{j\frac{4\nu_0 f_0}{2}\ddot{\phi}} \left[\cos[-2f_0(\dot{\phi} + t) - 2\delta] - \cos[2\nu_0(\dot{\phi} + t) + 2\gamma] \right]
\end{aligned}$$

$$+ \frac{\beta^2 \psi^2}{8} - \frac{\beta^2 \psi^2}{8} \cos[(2\nu_0 - 2f_0)(\dot{\phi} + t) + 2\gamma - 2\delta] \quad (66)$$

remembering that cosine is an even function $\cos(-x) = \cos(x)$

$$\begin{aligned} P(t) = & \frac{E_0}{4} B(\Omega_0)^2 \cdot \left[2 - 2\cos(\alpha) + j\beta \cdot j \sin\left[\frac{\nu_0^2}{2}\ddot{\phi}\right] \sin[\nu_0(\dot{\phi} + t) + \gamma] \right. \\ & + j\frac{\beta\psi}{2} \cdot 2j \cdot \sin\left[\frac{(\nu_0+f_0)^2}{2}\ddot{\phi}\right] \sin[(\nu_0 + f_0)(\dot{\phi} + t) + \gamma + \delta] + j\frac{\beta\psi}{2} \cdot (-2j) \cdot \sin\left[\frac{(\nu_0-f_0)^2}{2}\ddot{\phi}\right] \sin[(\nu_0 - f_0)(\dot{\phi} + t) + \gamma - \delta] \\ & + j\beta \cdot (-2j) \cdot \sin\left[\alpha + \frac{\nu_0^2}{2}\ddot{\phi}\right] \sin[\nu_0(\dot{\phi} + t) + \gamma] \\ & + j\frac{\beta\psi}{2} \cdot (-2j) \cdot \sin\left[\alpha + \frac{(\nu_0+f_0)^2}{2}\ddot{\phi}\right] \sin[(\nu_0 + f_0)(\dot{\phi} + t) + \gamma + \delta] + j\frac{\beta\psi}{2} \cdot 2j \cdot \sin\left[\alpha + \frac{(\nu_0-f_0)^2}{2}\ddot{\phi}\right] \sin[(\nu_0 - f_0)(\dot{\phi} + t) + \gamma - \delta] \\ & + \frac{\beta^2}{2} + \frac{\beta^2 \psi^2}{4} \\ & + \frac{\beta^2 \psi}{4} \cdot \left(2 \cos\left[\frac{2\nu_0 f_0 + f_0^2}{2}\ddot{\phi}\right] - 2 \cos\left[\frac{-2\nu_0 f_0 + f_0^2}{2}\ddot{\phi}\right] \right) \cos[f_0(\dot{\phi} + t) + \delta] \\ & - \frac{\beta^2 \psi^2}{8} \cdot 2 \cos\left[\frac{4\nu_0 f_0}{2}\ddot{\phi}\right] \cos[2f_0(\dot{\phi} + t) + 2\delta] \\ & - \frac{\beta^2 \psi^2}{8} \cdot \cos[(2\nu_0 - 2f_0)(\dot{\phi} + t) + 2\gamma - 2\delta] \\ & + \frac{\beta^2 \psi}{4} \cdot 2 \cos\left[\frac{-2\nu_0 f_0 + f_0^2}{2}\ddot{\phi}\right] \cos[(2\nu_0 - f_0)(\dot{\phi} + t) + 2\gamma - \delta] \\ & + \left\{ -\frac{\beta^2}{2} + \frac{\beta^2 \psi^2}{8} \cdot 2 \cos\left[\frac{4\nu_0 f_0}{2}\ddot{\phi}\right] \right\} \cos[2\nu_0(\dot{\phi} + t) + 2\gamma] \\ & - \frac{\beta^2 \psi}{4} \cdot 2 \cos\left[\frac{2\nu_0 f_0 + f_0^2}{2}\ddot{\phi}\right] \cos[(2\nu_0 + f_0)(\dot{\phi} + t) + 2\gamma + \delta] \\ & \left. - \frac{\beta^2 \psi^2}{8} \cdot \cos[(2\nu_0 + 2f_0)(\dot{\phi} + t) + 2\gamma + 2\delta] \right] \quad (67) \end{aligned}$$

now we can use the following trigonometric identities to simplify somewhat the photocurrent

$$\cos \alpha - \cos \beta = -2 \sin\left(\frac{\alpha+\beta}{2}\right) \sin\left(\frac{\alpha-\beta}{2}\right)$$

$$\sin \alpha - \sin \beta = 2 \cos\left(\frac{\alpha+\beta}{2}\right) \sin\left(\frac{\alpha-\beta}{2}\right)$$

$$\begin{aligned} P(t) = & \frac{E_0}{4} B(\Omega_0)^2 \cdot \left[2(1 - \cos(\alpha)) + \frac{\beta^2}{2} + \frac{\beta^2 \psi^2}{4} \right. \\ & - 2\beta\psi \cos\left[\frac{\alpha}{2} + \frac{(\nu_0-f_0)^2}{2}\ddot{\phi}\right] \sin\left[\frac{\alpha}{2}\right] \sin[(\nu_0 - f_0)(\dot{\phi} + t) + \gamma - \delta] \\ & + 4\beta \cos\left[\frac{\alpha}{2} + \frac{\nu_0^2}{2}\ddot{\phi}\right] \sin\left[\frac{\alpha}{2}\right] \sin[\nu_0(\dot{\phi} + t) + \gamma] \\ & + 2\beta\psi \cos\left[\frac{\alpha}{2} + \frac{(\nu_0+f_0)^2}{2}\ddot{\phi}\right] \sin\left[\frac{\alpha}{2}\right] \sin[(\nu_0 + f_0)(\dot{\phi} + t) + \gamma + \delta] \\ & \left. - \beta^2 \psi \sin\left[\frac{f_0^2}{2}\ddot{\phi}\right] \sin\left[\frac{2\nu_0 f_0}{2}\ddot{\phi}\right] \cos[f_0(\dot{\phi} + t) + \delta] \right] \end{aligned}$$

$$\begin{aligned}
& -\frac{\beta^2\psi^2}{4} \cos\left[\frac{4\nu_0 f_0}{2}\ddot{\phi}\right] \cos[2f_0(\dot{\phi} + t) + 2\delta] \\
& -\frac{\beta^2\psi^2}{8} \cos[(2\nu_0 - 2f_0)(\dot{\phi} + t) + 2\gamma - 2\delta] \\
& +\frac{\beta^2\psi}{2} \cos\left[\frac{-2\nu_0 f_0 + f_0^2}{2}\ddot{\phi}\right] \cos[(2\nu_0 - f_0)(\dot{\phi} + t) + 2\gamma - \delta] \\
& + \left\{ \frac{\beta^2\psi^2}{4} \cos\left[\frac{4\nu_0 f_0}{2}\ddot{\phi}\right] - \frac{\beta^2}{2} \right\} \cos[2\nu_0(\dot{\phi} + t) + 2\gamma] \\
& -\frac{\beta^2\psi}{2} \cos\left[\frac{2\nu_0 f_0 + f_0^2}{2}\ddot{\phi}\right] \cos[(2\nu_0 + f_0)(\dot{\phi} + t) + 2\gamma + \delta] \\
& \quad \left. -\frac{\beta^2\psi^2}{8} \cdot \cos[(2\nu_0 + 2f_0)(\dot{\phi} + t) + 2\gamma + 2\delta] \right] \tag{68}
\end{aligned}$$

It is worth recalling that $\ddot{\phi}$ is linked to CD by the relationship $\ddot{\phi} = -D\lambda^2/(2\pi c)$ where D is the chromatic dispersion (typically expressed in psec/nm), λ is the wavelength in nm and c is the vacuum speed of light in m/sec. We can simplify the photocurrent expression since $f_0 \ll \nu_0$, when the RF frequency is far away from RF dip, e.g. $\cos[\frac{4\nu_0 f_0}{2}\ddot{\phi}] \sim 1, \sin[\frac{2\nu_0 f_0}{2}\ddot{\phi}] \sim 0, \cos[\frac{f_0^2}{2}\ddot{\phi}] \sim 1, \sin[\frac{f_0^2}{2}\ddot{\phi}] \sim 0$. Also by examining the amplitude dependencies according to the following identities of cosine and sine functions

$$\cos[\alpha \pm \beta] = [\cos \alpha \cos \beta \mp \sin \alpha \sin \beta]$$

$$\sin[\alpha \pm \beta] = [\sin \alpha \cos \beta \pm \cos \alpha \sin \beta]$$

$$\cos\left[\frac{\alpha}{2} + \frac{(\nu_0 \pm f_0)^2}{2}\ddot{\phi}\right] = \cos\left[\frac{\alpha}{2} + \frac{\nu_0^2}{2}\ddot{\phi}\right] \cos\left[\frac{\pm 2\nu_0 f_0 + f_0^2}{2}\ddot{\phi}\right] - \sin\left[\frac{\alpha}{2} + \frac{\nu_0^2}{2}\ddot{\phi}\right] \sin\left[\frac{\pm 2\nu_0 f_0 + f_0^2}{2}\ddot{\phi}\right] =$$

$$= \cos\left[\frac{\alpha}{2} + \frac{\nu_0^2}{2}\ddot{\phi}\right] \left(\underbrace{\cos\left[\frac{\pm 2\nu_0 f_0}{2}\ddot{\phi}\right]}_1 \underbrace{\cos\left[\frac{f_0^2}{2}\ddot{\phi}\right]}_1 - \underbrace{\sin\left[\frac{\pm 2\nu_0 f_0}{2}\ddot{\phi}\right]}_{-0} \underbrace{\sin\left[\frac{f_0^2}{2}\ddot{\phi}\right]}_0 \right)$$

$$- \sin\left[\frac{\alpha}{2} + \frac{\nu_0^2}{2}\ddot{\phi}\right] \left(\underbrace{\sin\left[\frac{\pm 2\nu_0 f_0}{2}\ddot{\phi}\right]}_0 \underbrace{\cos\left[\frac{f_0^2}{2}\ddot{\phi}\right]}_1 - \underbrace{\cos\left[\frac{\pm 2\nu_0 f_0}{2}\ddot{\phi}\right]}_1 \underbrace{\sin\left[\frac{f_0^2}{2}\ddot{\phi}\right]}_0 \right) =$$

$$= \cos\left[\frac{\alpha}{2} + \frac{\nu_0^2}{2}\ddot{\phi}\right]$$

$$\cos\left[\frac{\pm 2\nu_0 f_0 + f_0^2}{2}\ddot{\phi}\right] = \cos\left[\frac{\pm 2\nu_0 f_0}{2}\ddot{\phi}\right] \cos\left[\frac{f_0^2}{2}\ddot{\phi}\right] - \sin\left[\frac{\pm 2\nu_0 f_0}{2}\ddot{\phi}\right] \underbrace{\sin\left[\frac{f_0^2}{2}\ddot{\phi}\right]}_{\substack{0 \text{ far from RF fading} \\ 0}} = \cos[\pm\nu_0 f_0 \ddot{\phi}] \cos\left[\frac{f_0^2}{2}\ddot{\phi}\right] \sim$$

1

Therefore

$$P(t) = \frac{P_0}{4} B(\Omega_0)^2 \cdot \left[2(1 - \cos(\alpha)) + \frac{\beta^2}{2} + \frac{\beta^2\psi^2}{4} \right]$$

$$-2\beta\psi \cos\left[\frac{\alpha}{2} + \frac{\nu_0^2}{2}\ddot{\phi}\right] \sin\left[\frac{\alpha}{2}\right] \sin[(\nu_0 - f_0)(\dot{\phi} + t) + \gamma - \delta]$$

$$+4\beta \cos\left[\frac{\alpha}{2} + \frac{\nu_0^2}{2}\ddot{\phi}\right] \sin\left[\frac{\alpha}{2}\right] \sin[\nu_0(\dot{\phi} + t) + \gamma]$$

$$\begin{aligned}
& +2\beta\psi \cos\left[\frac{\alpha}{2} + \frac{\nu_0^2}{2}\ddot{\phi}\right] \sin\left[\frac{\alpha}{2}\right] \sin[(\nu_0 + f_0)(\dot{\phi} + t) + \gamma + \delta] \\
& -\frac{\beta^2\psi^2}{4} \cos[2f_0(\dot{\phi} + t) + 2\delta] \\
& -\frac{\beta^2\psi^2}{8} \cos[(2\nu_0 - 2f_0)(\dot{\phi} + t) + 2\gamma - 2\delta] \\
& +\frac{\beta^2\psi}{2} \cos[(2\nu_0 - f_0)(\dot{\phi} + t) + 2\gamma - \delta] \\
& +\left\{\frac{\beta^2\psi^2}{4} - \frac{\beta^2}{2}\right\} \cos[2\nu_0(\dot{\phi} + t) + 2\gamma] \\
& -\frac{\beta^2\psi}{2} \cos[(2\nu_0 + f_0)(\dot{\phi} + t) + 2\gamma + \delta] \\
& \quad \left. -\frac{\beta^2\psi^2}{8} \cdot \cos[(2\nu_0 + 2f_0)(\dot{\phi} + t) + 2\gamma + 2\delta]\right] \tag{69}
\end{aligned}$$

Now we can use the following trigonometric identities

$$\sin \alpha - \sin \beta = 2 \cos \left[\frac{\alpha + \beta}{2} \right] \sin \left[\frac{\alpha - \beta}{2} \right]$$

$$\cos \alpha + \cos \beta = 2 \cos \left(\frac{\alpha + \beta}{2} \right) \cos \left(\frac{\alpha - \beta}{2} \right)$$

$$\cos \alpha - \cos \beta = -2 \sin \left(\frac{\alpha + \beta}{2} \right) \sin \left(\frac{\alpha - \beta}{2} \right)$$

We can then find that the photocurrent expression is simplified

$$\begin{aligned}
P(t) &= \frac{P_0}{4} B(\Omega_0)^2 \cdot \left[2(1 - \cos(\alpha)) + \frac{\beta^2}{2} + \frac{\beta^2\psi^2}{4} \right. \\
& -\frac{\beta^2\psi^2}{4} \cos[2f_0(\dot{\phi} + t) + 2\delta] \\
& +4\beta \sin\left[\frac{\alpha}{2}\right] \cos\left[\frac{\alpha}{2} + \frac{\nu_0^2}{2}\ddot{\phi}\right] \left\{ \psi \cos[\nu_0(\dot{\phi} + t) + \gamma] \sin[f_0(\dot{\phi} + t) + \delta] + \sin[\nu_0(\dot{\phi} + t) + \gamma] \right\} \\
& -\frac{\beta^2\psi^2}{4} \cdot \cos[2\nu_0(\dot{\phi} + t) + 2\gamma] \cos[2f_0(\dot{\phi} + t) + 2\delta] + \beta^2\psi \sin[2\nu_0(\dot{\phi} + t) + 2\gamma] \sin[f_0(\dot{\phi} + t) + \delta] \\
& \quad \left. + \left\{ \frac{\beta^2\psi^2}{4} - \frac{\beta^2}{2} \right\} \cos[2\nu_0(\dot{\phi} + t) + 2\gamma] \right] \tag{70}
\end{aligned}$$

As we can see signal analysis of the system indeed demonstrates that this phase information is preserved in the E/O conversion (through the optical modulator), in transport (through the DUT), and upon detection of the beat term. The beat term contains a few arguments: DC and harmonic terms (ν_0 , $2\nu_0$). Since the phase information is preserved in the harmonic terms we can choose to demodulate it with either ν_0 harmonic or $2\nu_0$ harmonic.

When realizing the suggested signal processing scheme, we have to consider the RF Mixer RF to IF leakage (assuming it is the same as LO to IF leakage 30 dB typical). Moreover there is also a LO to RF leakage of typically 35 dB - taking in mind that the LO port contains only a pure RF harmonic without any audio tones around it. In case they will leak they might limit the minimum audio signal we can achieve when changing the DC bias phase, γ , e.g. the slow frequency signal component $\cos[2f_0(\dot{\phi} + t) + 2\delta]$. Therefore we choose to lock to the slow frequency component $\sin[f_0(\dot{\phi} + t) + \delta]$.

3.1.1 MPS with Audio

First when applying the MPS with Audio method we need to consider the fact that we are biasing the optical modulator at the midpoint in order to maximize the ν_0 at the photodetector output, $\alpha = \frac{\pi}{2} \frac{V_c}{V_\pi} = \frac{\pi}{2}$. The photocurrent is multiplied with a local oscillator signal oscillating at the ν_0 frequency, $LO(t) = \sin[\nu_0 t]$ (not regarding any constant electrical group delay that our electrical circuit may have). Using the following identities

$$\cos \alpha \cdot \sin \beta = \frac{1}{2} [\sin(\alpha + \beta) - \sin(\alpha - \beta)]$$

$$\sin \alpha \cdot \sin \beta = \frac{1}{2} [\cos(\alpha - \beta) - \cos(\alpha + \beta)]$$

$$\begin{aligned} M(t) = & \frac{P_0}{4} B(\Omega_0)^2 \cdot \left[\left(2(1 - \cos(\alpha)) + \frac{\beta^2}{2} + \frac{\beta^2 \psi^2}{4} \right) \sin[\nu_0 t] \right. \\ & - \frac{\beta^2 \psi^2}{8} \left(\sin[\nu_0 t + 2f_0(\dot{\phi} + t) + 2\delta] - \sin[2f_0(\dot{\phi} + t) - \nu_0 t + 2\delta] \right) \\ & + 4\beta \sin\left[\frac{\alpha}{2}\right] \cos\left[\frac{\alpha}{2} + \frac{\nu_0^2}{2} \ddot{\phi}\right] \left\{ \frac{\psi}{2} \left[\sin[2\nu_0 t + \nu_0 \dot{\phi} + \gamma] - \sin[\nu_0 \dot{\phi} + \gamma] \right] \sin[f_0(\dot{\phi} + t) + \delta] \right. \\ & \left. + \frac{1}{2} \left[\cos[\nu_0 \dot{\phi} + \gamma] - \cos[2\nu_0 t + \nu_0 \dot{\phi} + \gamma] \right] \right\} \\ & - \frac{\beta^2 \psi^2}{8} \left(\sin[2\nu_0 \dot{\phi} + 3\nu_0 t + 2\gamma] - \sin[2\nu_0 \dot{\phi} + \nu_0 t + 2\gamma] \right) \cos[2f_0(\dot{\phi} + t) + 2\delta] \\ & + \frac{\beta^2 \psi}{2} \left(\cos[2\nu_0 \dot{\phi} + \nu_0 t + 2\gamma] - \cos[2\nu_0 \dot{\phi} + 3\nu_0 t + 2\gamma] \right) \sin[f_0(\dot{\phi} + t) + \delta] \\ & \left. + \left\{ \frac{\beta^2 \psi^2}{8} - \frac{\beta^2}{4} \right\} \left(\sin[2\nu_0 \dot{\phi} + 3\nu_0 t + 2\gamma] - \sin[2\nu_0 \dot{\phi} + \nu_0 t + 2\gamma] \right) \right] \end{aligned} \quad (71)$$

at the mixer output we have connected a Low Pass Filter (LPF). Meaning that every ν_0 , $2\nu_0$ harmonic terms will be extinguished by the LPF. Therefore we remain with the following expression

$$V(t) = -\frac{P_0}{2} B(\Omega_0)^2 \sin\left[\frac{\alpha}{2}\right] \cos\left[\frac{\alpha}{2} + \frac{\nu_0^2}{2} \ddot{\phi}\right] \beta \left(\underbrace{\psi \sin[\nu_0 \dot{\phi} + \gamma] \sin[f_0(\dot{\phi} + t) + \delta]}_{\text{the LIA may lock onto this expression}} - \cos[\nu_0 \dot{\phi} + \gamma] \right) \quad (72)$$

According to this LPF output indeed we are able to control the amplitude of the f_0 tone with the aid of dc bias phase, γ , while holding the audio dc bias as constant δ . Of course the DC contribution found in the 2nd expression will be eliminated in the LIA circuits.

Once more there are three possible working points to choose γ :

1. maximize the f_0 tone signal, $\nu_0 \dot{\phi} + \gamma = \frac{\pi}{2}$.
2. work at half maximum of the f_0 tone signal, $\nu_0 \dot{\phi} + \gamma = \frac{\pi}{4}$.
3. eliminate the f_0 tone signal, $\nu_0 \dot{\phi} + \gamma = 0$.

Conclusions:

1. The LIA will lock to the oscillating term $\sin[f_0(\dot{\phi} + t) + \delta]$, with the reference term of $\sin[f_0 t + \delta]$.
2. Group delay is measured at the nulling of a sine term with oscillating frequency f_0 , i.e. $\nu_0 \dot{\phi} + \gamma = 0$.

The measurement itself is the electrical phase shift $\Theta = 2\pi\nu_0\dot{\phi} + \gamma = 2\pi\nu_0\tau_g + \gamma$ which can be recovered from any electrical phase detector instrument locked to the slow oscillating term f_0 which is present in θ . The minimum limit is the phase resolution limit of the instrument itself, and the maximum allowable measurable phase without ambiguity is $\Theta \in [0, \pi]$. In case of a measurement beyond this limit there will be an alias error, and therefore a wrong measurement of the group delay (without applying a RF phase offset γ). However, we can set the RF phase offset γ at an appropriate bias point and therefore we can avoid the ambiguity problem typically found in phase measurements. Thus keeping the interference point always at the null point, which sets the phase bias directly proportional to the measured optical phase. In practice, the wavelength is stepped a small wavelength interval and the corresponding change in the group delay $\Delta\tau_g$ is calculated from the measured change in phase according to

$$\Delta\tau_g = \frac{\Delta\Theta}{360} \frac{1}{\nu_0} \quad (73)$$

where $\Delta\Theta$ is the phase change in degrees produced by a small wavelength step and ν_0 is the modulating frequency in Hz. We need to remember that the attribute called dispersion is defined by

$$D = \frac{\Delta\tau_g}{\Delta\lambda} \quad (74)$$

where $\Delta\tau_g$ is the change in group delay in seconds corresponding to a change in wavelength $\Delta\lambda$ in meters. We can combine this last two equations and find that

$$\Delta\theta_{MPS \text{ with Audio}} = 360 \cdot D \cdot \nu_0 \cdot \Delta\lambda \quad (75)$$

this shows that the amount of phase change measured in response to a wavelength step is the product of device dispersion, the modulation frequency and wavelength step as in the conventional MPS (see Eq. 36).

3.1.2 2nd order MPS with Audio

First when applying the 2nd order MPS with Audio method we need to consider the fact that we are biasing the optical modulator at the minimum point in order to maximize the $2\nu_0$ at the photodetector output, $\alpha = \pi \frac{V_\pi}{V_\pi} = \pi$. The photocurrent is multiplied with a local oscillator

signal oscillating at the $2\nu_0$ frequency, $LO(t) = \sin[2\nu_0 t]$ (not regarding any constant electrical group delay that our electrical circuit may have).

$$\begin{aligned}
M(t) = & \frac{P_0}{4} B(\Omega_0)^2 \cdot \left[\left(2(1 - \cos(\alpha)) + \frac{\beta^2}{2} + \frac{\beta^2 \psi^2}{4} \right) \sin[2\nu_0 t] \right. \\
& - \frac{\beta^2 \psi^2}{8} \left(\sin[2\nu_0 t + 2f_0(\dot{\phi} + t) + 2\delta] - \sin[2f_0(\dot{\phi} + t) - 2\nu_0 t + 2\delta] \right) \\
& + 4\beta \sin\left[\frac{\alpha}{2}\right] \cos\left[\frac{\alpha}{2} + \frac{\nu_0^2}{2} \dot{\phi}\right] \left\{ \frac{\psi}{2} \left[\sin[3\nu_0 t + \nu_0 \dot{\phi} + \gamma] + \sin[\nu_0 t - \nu_0 \dot{\phi} - \gamma] \right] \sin[f_0(\dot{\phi} + t) + \delta] \right. \\
& \left. + \frac{1}{2} \left[\cos[\nu_0 t - \nu_0 \dot{\phi} - \gamma] - \cos[3\nu_0 t + \nu_0 \dot{\phi} + \gamma] \right] \right\} \\
& - \frac{\beta^2 \psi^2}{8} \left(\sin[2\nu_0 \dot{\phi} + 4\nu_0 t + 2\gamma] - \sin[2\nu_0 \dot{\phi} + 2\gamma] \right) \cos[2f_0(\dot{\phi} + t) + 2\delta] \\
& + \frac{\beta^2 \psi}{2} \left(\cos[2\nu_0 \dot{\phi} + 2\gamma] - \cos[2\nu_0 \dot{\phi} + 4\nu_0 t + 2\gamma] \right) \sin[f_0(\dot{\phi} + t) + \delta] \\
& \left. + \left\{ \frac{\beta^2 \psi^2}{8} - \frac{\beta^2}{4} \right\} \left(\sin[2\nu_0 \dot{\phi} + 4\nu_0 t + 2\gamma] - \sin[2\nu_0 \dot{\phi} + 2\gamma] \right) \right] \quad (76)
\end{aligned}$$

at the mixer output we have connected a Low Pass Filter (LPF). Meaning that every ν_0 , $2\nu_0$ harmonic terms will be extincted by the LPF. Therefor we remain with the following expression

$$\begin{aligned}
V(t) = & \frac{P_0}{4} B(\Omega_0)^2 \left[\left\{ \frac{\beta^2}{4} - \frac{\beta^2 \psi^2}{8} \right\} \sin[2\nu_0 \dot{\phi} + 2\gamma] + \underbrace{\frac{\beta^2 \psi}{2} \cos[2\nu_0 \dot{\phi} + 2\gamma] \sin[f_0(\dot{\phi} + t) + \delta]}_{\text{the LIA may lock onto this expresion}} \right. \\
& \left. + \frac{\beta^2 \psi^2}{8} \sin[2\nu_0 \dot{\phi} + 2\gamma] \cos[2f_0(\dot{\phi} + t) + 2\delta] \right] \quad (77)
\end{aligned}$$

This LPF output expression contains dc, f_0 and $2f_0$ harmonics with amplitude dependence on group delay, with a $\frac{\pi}{2}$ phase in between them. The LIA will lock onto the $\sin[f_0(\dot{\phi} + t) + \delta]$ harmonic term. According to this LPF output indeed we are able to control the amplitude of the f_0 tone with the aid of dc bias phase, γ , while holding the audio dc bias as constant δ . Of course the DC contribution found in the 2nd expression will be eliminated in the LIA circuits.

As in MPS with Audio case there are 3 possible working points to choose γ . However, the GD dependence is inside a cosine instead of a sine term:

1. maximize the f_0 tone signal, $2\nu_0 \dot{\phi} + 2\gamma = 0$.
2. work at half maximum of the f_0 tone signal, $2\nu_0 \dot{\phi} + 2\gamma = \frac{\pi}{4}$.
3. eliminate the f_0 tone signal, $2\nu_0 \dot{\phi} + 2\gamma = \frac{\pi}{2}$.

Conclusions:

1. The LIA will lock to the oscillating term $\sin[f_0(\dot{\phi} + t) + \delta]$, with the reference term of $\sin[f_0 t + \delta]$.

2. Group delay is measured at the nulling of a cosine term oscillating with frequency f_0 , i.e. $2\nu_0\dot{\phi} + 2\gamma = \frac{\pi}{2}$.

The measurement itself is the electrical phase shift $\Theta = 2\pi 2\nu_0\dot{\phi} + 2\gamma = 2\pi 2\nu_0\tau_g + 2\gamma$ which can be recovered from any electrical phase detector instrument locked to the slow oscillating term f_0 which is present in θ . The minimum limit is the phase resolution limit of the instrument itself, and the maximum allowable measurable phase without ambiguity is $\Theta \in [0, \pi]$. In case of a measurement beyond this limit there will be an alias error, and therefore a wrong measurement of the group delay (without applying a RF phase offset γ). However, we can set the RF phase offset γ at an appropriate bias point and therefore we can avoid the ambiguity problem typically found in phase measurements. Thus keeping the interference point always at the null point, which sets the phase bias directly proportional to the measured optical phase. In practice, the wavelength is stepped a small wavelength interval and the corresponding change in the group delay $\Delta\tau_g$ is calculated from the measured change in phase according to

$$\Delta\tau_g = \frac{\Delta\Theta}{360} \frac{1}{2\nu_0} \quad (78)$$

where $\Delta\Theta$ is the phase change in degrees produced by a small wavelength step and ν_0 is the modulating frequency in Hz. We need to remember that the attribute called dispersion is defined by

$$D = \frac{\Delta\tau_g}{\Delta\lambda} \quad (79)$$

where $\Delta\tau_g$ is the change in group delay in seconds corresponding to a change in wavelength $\Delta\lambda$ in meters. We can combine this last two equations and find that

$$\Delta\theta_{2nd\ order\ MPS\ with\ Audio} = 360 \cdot D \cdot 2\nu_0 \cdot \Delta\lambda \quad (80)$$

this shows that the amount of phase change measured in response to a wavelength step is the product of device dispersion, twice the modulation frequency and wavelength step. Quite similar to the conventional MPS, where the amount of measured phase change (see Eq. 36) in response to a wavelength step is the product of device dispersion, the modulation frequency and wavelength step

3.2 Appendix: MPS with audio accurate signal analysis Jacobi Anger expansion to AM and PM

In this appendix we develop the RF AM modulation in the optical field expression according to Jacobi-Anger expansion to the harmonic phase term. As is well known an entire comb of RF harmonics around the optical carrier will appear; the power distribution to these tones depends on the modulation strength. The higher harmonics might introduce undesired signal contributions to the component we are interested in measuring. We first expand the RF modulation, assuming phase θ is constant (or slowly varying) and then expand the audio variation, PM modulation, according to a second Jacobi-Anger expansion to the audio harmonic phase term.

In case we drive the upper arm with a voltage signal which have a DC component and an AC term (there could also be a constant phase delay between the ports) we have omitted 2π factor in the right side of Eq. 81 for brevity, we can return it in the end of the analysis

$$RF = \pi \frac{V_b + V \sin(2\pi\nu_0 t + \theta)}{V_\pi} \triangleq \alpha + \beta \cdot \sin(\nu_0 t + \theta) \quad (81)$$

where V_b is the bias voltage, V is the modulation voltage, V_π is the voltage applied to achieve a π phase shift and ν_0 is the RF driving frequency. The signal is more conveniently parametrized by α and β .

$$\begin{aligned} U(t) &= \frac{\sqrt{P_0}}{2} e^{j\Omega_0 t} \cdot [e^{j[\alpha + \beta \cdot \sin(\nu_0 t + \theta)]} - 1] = \frac{\sqrt{P_0}}{2} e^{j\Omega_0 t} [e^{j\alpha} e^{j\beta \sin(\nu_0 t + \theta)} - 1] \\ &= \frac{\sqrt{P_0}}{2} e^{j\Omega_0 t} \left[e^{j\alpha} \sum_{m=-\infty}^{\infty} J_m(\beta) e^{jm(\nu_0 t + \theta)} - 1 \right] \end{aligned} \quad (82)$$

where Ω_0 is the optical carrier frequency, ν_0 is the RF modulation frequency, P_0 is the laser intensity, α is the MZM bias point, β is the MZM RF modulation depth, J_m is the Bessel J function of order m and θ is the RF phase delay.

The RF signal driving the optical modulator is phase modulated by the low frequency signal

$$\theta = \gamma + \psi \sin(f_0 t + \delta) \quad (83)$$

where γ is the DC bias phase, ψ is the audio modulation depth, f_0 is the low (audio) frequency signal and δ is the DC phase offset at low (audio) frequency.

$$U(t) = \frac{\sqrt{P_0}}{2} e^{j\Omega_0 t} \left[e^{j\alpha} \sum_{m=-\infty}^{\infty} J_m(\beta) e^{jm(\nu_0 t + \gamma + \psi \sin(f_0 t + \delta))} - 1 \right] \quad (84)$$

$$U(t) = \frac{\sqrt{P_0}}{2} e^{j\Omega_0 t} \left[e^{j\alpha} \sum_{m=-\infty}^{\infty} J_m(\beta) e^{jm(\nu_0 t + \gamma)} e^{jm\psi \sin(f_0 t + \delta)} - 1 \right] \quad (85)$$

We will use the J.A expression for the PM signal at the slow frequency component f_0

$$U(t) = \frac{\sqrt{P_0}}{2} e^{j\Omega_0 t} \left[e^{j\alpha} \sum_{m=-\infty}^{\infty} J_m(\beta) e^{jm(\nu_0 t + \gamma)} \sum_{n=-\infty}^{\infty} J_n(m\psi) e^{jn(f_0 t + \delta)} - 1 \right] \quad (86)$$

we will rearrange this optical field expression at the MZM output

$$U(t) = \frac{\sqrt{P_0}}{2} e^{j\Omega_0 t} \left[e^{j\alpha} \sum_{m=-\infty}^{\infty} \sum_{n=-\infty}^{\infty} J_m(\beta) J_n(m\psi) e^{j[(m\nu_0 + n f_0)t + m\gamma + n\delta]} - 1 \right] \quad (87)$$

inserting the optical carrier frequency to the infinite sums in order to see the complete optical spectrum

$$U(t) = \frac{\sqrt{P_0}}{2} \left[e^{j\alpha} \sum_{m=-\infty}^{\infty} \sum_{n=-\infty}^{\infty} J_m(\beta) J_n(m\psi) e^{j[(\Omega_0 + m\nu_0 + n f_0)t + m\gamma + n\delta]} - e^{j\Omega_0 t} \right] \quad (88)$$

Remark in this expression we indeed see an entire comb of slow frequency $n f_0$ around RF a comb of RF frequency $m\nu_0$. Under the assumptions of LTI system we can propagate the signal in the system using the convention of the Fourier transform.

$$Y(t) = \frac{\sqrt{P_0}}{2} \left[e^{j\alpha} \sum_{m,n=-\infty}^{\infty} J_m(\beta) J_n(m\psi) e^{j(m\gamma + n\delta)} B(\Omega_0 + m\nu_0 + n f_0) e^{j\phi(\Omega_0 + m\nu_0 + n f_0)} e^{j(\Omega_0 + m\nu_0 + n f_0)t} - B(\Omega_0) e^{j\Omega_0 t} e^{j\phi(\Omega_0)} \right] \quad (89)$$

Since, $n f_0 \ll m\nu_0 \ll \Omega_0$, we shall make the following approximations:

1. the typical assumption is that the attenuation experienced by all the tones is identical.

$$\Rightarrow B(\Omega_0 + m\nu_0 + n f_0) \simeq B(\Omega_0)$$

2. the phase is developed using Taylor series for the DUT response, assumption being that the phase can be expressed as a Taylor expansion about carrier frequency

$$\Rightarrow \phi(\Omega_0 + m\nu_0 + n f_0) \cong \phi(\Omega_0) + \left. \frac{\partial \phi}{\partial \omega} \right|_{\Omega_0} (m\nu_0 + n f_0) + \frac{1}{2} \left. \frac{\partial^2 \phi}{\partial \omega^2} \right|_{\Omega_0} (m\nu_0 + n f_0)^2 + \dots$$

$$= \phi(\Omega_0) + \dot{\phi}(m\nu_0 + n f_0) + \frac{1}{2} \ddot{\phi}(m\nu_0 + n f_0)^2 + \dots$$

$$Y(t) = \frac{\sqrt{P_0}}{2} \left[e^{j\alpha} \sum_{m,n=-\infty}^{\infty} J_m(\beta) J_n(m\psi) e^{j(m\gamma + n\delta)} B(\Omega_0) e^{j[\phi(\Omega_0) + \dot{\phi}(m\nu_0 + n f_0) + \frac{1}{2} \ddot{\phi}(m\nu_0 + n f_0)^2]} \right].$$

$$\cdot e^{j(\Omega_0+m\nu_0+n f_0)t} - B(\Omega_0)e^{j\Omega_0 t} e^{j\phi(\Omega_0)} \Big] \quad (90)$$

rearranging and gathering common expressions in the optical field at the DUT output

$$Y(t) = \frac{\sqrt{P_0}}{2} e^{j\Omega_0 t} e^{j\phi(\Omega)} e^{j\alpha} B(\Omega_0) \left[\sum_{m,n=-\infty}^{\infty} J_m(\beta) J_n(m\psi) e^{j(m\gamma+n\delta)} e^{j\frac{1}{2}\ddot{\phi}(m\nu_0+n f_0)^2} e^{j(m\nu_0+n f_0)(\dot{\phi}+t)} \right. \\ \left. - e^{-j\alpha} \right] \quad (91)$$

$$Y^*(t) = \frac{\sqrt{P_0}}{2} e^{-j\Omega_0 t} e^{-j\phi(\Omega)} e^{-j\alpha} B(\Omega_0) \left[\sum_{m,n=-\infty}^{\infty} J_m(\beta) J_n(m\psi) e^{-j(m\gamma+n\delta)} e^{-j\frac{1}{2}\ddot{\phi}(m\nu_0+n f_0)^2} e^{-j(m\nu_0+n f_0)(\dot{\phi}+t)} \right. \\ \left. - e^{j\alpha} \right] \quad (92)$$

changing of indexes $m \rightarrow p$, $n \rightarrow q$ when multiplying the combs.

A few minor calculations

$$j\frac{1}{2}\ddot{\phi} \left[(m\nu_0 + n f_0)^2 - (p\nu_0 + q f_0)^2 \right] = j\frac{1}{2}\ddot{\phi} \left[m^2\nu_0^2 + 2mn\nu_0 f_0 + n^2 f_0^2 - p^2\nu_0^2 - 2pq\nu_0 f_0 - q^2 f_0^2 \right] = \\ = j\frac{1}{2}\ddot{\phi} \left[(m^2 - p^2)\nu_0^2 + 2(mn - pq)\nu_0 f_0 + (n^2 - q^2)f_0^2 \right].$$

From the received field we find an expression for the optical power reaching a detector (being proportional to generated photocurrent):

$$P(t) = Y(t) \cdot Y^*(t) = \frac{P_0}{4} B(\Omega_0)^2 \cdot \left[1 + \right. \\ \left. - e^{-j\alpha} \sum_{m,n=-\infty}^{\infty} J_m(\beta) J_n(m\psi) e^{-j(m\gamma+n\delta)} e^{-j\frac{1}{2}\ddot{\phi}(m\nu_0+n f_0)^2} e^{-j(m\nu_0+n f_0)(\dot{\phi}+t)} + \right. \\ \left. - e^{j\alpha} \sum_{m,n=-\infty}^{\infty} J_m(\beta) J_n(m\psi) e^{j(m\gamma+n\delta)} e^{j\frac{1}{2}\ddot{\phi}(m\nu_0+n f_0)^2} e^{j(m\nu_0+n f_0)(\dot{\phi}+t)} + \right. \\ \left. + \sum_{\substack{m,n,p,q \\ =-\infty}}^{\infty} J_m(\beta) J_n(m\psi) J_p(\beta) J_q(p\psi) e^{j[(m-p)\gamma+(n-q)\delta]} e^{j[(m-p)\nu_0+(n-q)f_0](\dot{\phi}+t)} \right. \\ \left. \cdot e^{j\frac{1}{2}\ddot{\phi}[(m^2-p^2)\nu_0^2+2(mn-pq)\nu_0 f_0+(n^2-q^2)f_0^2]} \right] \quad (93)$$

In order to emphasize the harmonic terms we can perform an index change $k=m-p$, $l=n-q$. After manipulating the infinite sum terms (using tricks as index shifts and sign changes see Appendix A) and using the symmetric and anti-symmetric characteristic of the Bessel J functions, the photocurrent can be represented in the equivalent form

$$P(t) = \frac{P_0}{4} \cdot B(\Omega_0)^2 \cdot \left\{ 1 - \sum_{k,n=-\infty}^{\infty} 2 \cdot J_k(\beta) J_n(k\beta) \cdot \left[\begin{array}{c} \cos \left((k\nu_0 + n f_0)(\dot{\phi} + t) + k\gamma + n\delta \right) \\ - \sin \left((k\nu_0 + n f_0)(\dot{\phi} + t) + k\gamma + n\delta \right) \end{array} \right]_k \right\}$$

$$\begin{aligned}
& \left[\begin{array}{c} \cos \left(\alpha + \frac{\ddot{\phi}}{2}(k\nu_0 + nf_0)^2 \right) \\ \sin \left(\alpha + \frac{\ddot{\phi}}{2}(k\nu_0 + nf_0)^2 \right) \end{array} \right]_k + \sum_{m,n,k,l=-\infty}^{\infty} J_m(\beta) J_{m+k}(\beta) J_n(m\psi) J_{n+l}([m+k]\psi) \cdot \\
& \left[\begin{array}{c} \cos \left((k\nu_0 + lf_0)(\dot{\phi} + t) + k\gamma + l\delta \right) \\ -\sin \left((k\nu_0 + lf_0)(\dot{\phi} + t) + k\gamma + l\delta \right) \end{array} \right]_k \cdot \\
& \left. \left[\begin{array}{c} \cos \left(\frac{\ddot{\phi}}{2} \{ k(2m+k)\nu_0^2 + 2(nk+l(m+k))\nu_0 f_0 + l(2n+l)f_0^2 \} \right) \\ \sin \left(\frac{\ddot{\phi}}{2} \{ k(2m+k)\nu_0^2 + 2(nk+l(m+k))\nu_0 f_0 + l(2n+l)f_0^2 \} \right) \end{array} \right]_k \right\} \quad (94)
\end{aligned}$$

where $\left[\begin{array}{c} \dots \\ \dots \end{array} \right]_k$ formalism is introduced to denote that top element is chosen if k is even and bottom if k is odd.

Now we can return the 2π constant to to the generated photocurrent expression.

The photocurrent can be demodulated using local oscillator at $\sin(q\nu_0 t)$ to find the response of the system about DC (i.e. $q=1$ MPS with Audio and $q=2$ 2nd order MPS with Audio). We collect the contributions about DC according to an ideal mixer (using $k = \pm q$). We then collect the contributions at frequency f_0 (using $l = \pm 1$). During this selection process, summation of four index terms reduces to two indices (referred to as bi-term), while the summation of the two index term reduces to a single term (now single term). The photocurrent can be simplified since the RF fading term primarily contributes from the term $\frac{\ddot{\phi}}{2}k(2m+k)\nu_0^2$ [20], since $f_0 \ll \nu_0$, we can perform the following assumption $\ddot{\phi}((nk+l(m+k))\nu_0 f_0) \ll 1$ moreover $\frac{\ddot{\phi}}{2}l(2n+l)f_0^2 \lll 1$ can be entirely neglected. The signal used by the LIA for extraction of the GD in the case of MPS with Audio is:

$$V(t) = -\frac{P_0}{2} B(\Omega_0)^2 \sin(\nu_0 \dot{\phi} + \gamma) \cdot \sin(f_0(\dot{\phi} + t) + \delta).$$

$$\left\{ \cdot \sum_{m,n,k,l=-\infty}^{\infty} J_m(\beta) J_{m+1}(\beta) J_n(m\psi) J'_n([m+1]\psi) \cdot \sin \left(\frac{\ddot{\phi}}{2}(2m+1)\nu_0^2 \right) + 2J_1(\beta) J_1(\psi) \sin \left(\alpha + \frac{\ddot{\phi}}{2}\nu_0^2 \right) \right\} \quad (95)$$

and for the 2nd order MPS with Audio is

$$V(t) = \frac{P_0}{2} B(\Omega_0)^2 \sin(2\nu_0 \dot{\phi} + 2\gamma) \cdot \sin(f_0(\dot{\phi} + t) + \delta).$$

$$\left\{ \cdot \sum_{m,n,k,l=-\infty}^{\infty} J_m(\beta) J_{m+2}(\beta) J_n(m\psi) J'_n([m+2]\psi) \cdot \cos \left(\ddot{\phi}(2m+2)\nu_0^2 \right) - 2J_2(\beta) J_1(2\psi) \cos \left(\alpha + \ddot{\phi}2\nu_0^2 \right) \right\} \quad (96)$$

Usually the desired RF driving frequency is chosen to satisfy the requirement of $\ddot{\phi}\nu_0^2 \lll 1$, therefore avoiding signal extinction due to RF fading. Upon closer observation of these terms we can simplify these results.

In the case of MPS with Audio, the main contribution to the signal arises from the second term in the parenthesis of Eq. (95), $2J_1(\beta)J_1(\psi)\sin(\alpha)$, which originates from the beat between the +/-1st tones and the center carrier. As in standard MPS, the MZM bias point should be chosen to satisfy $\alpha = \pi/2$, thus working in the linear response regime of the MZM when the condition $\beta, \psi \ll 1$ is fulfilled.

In the case of 2nd order MPS with Audio, the main contribution to the signal arises from the bi-term (double infinite sum term in the brackets of Eq. (96), $J_m(\beta)J_{m+2}(\beta)J_n(m\psi)J'_n([m+2]\psi)$). The most prominent beat tone arises from the beat tone between the +1 and -1 sidetones, $J_{-1}(\beta)J_1(\beta)$. The remaining contributions are undesired, e.g. beat tone in between the optical carrier and the 2nd sidetone $J_0(\beta)J_2(\beta)$. If the MZM bias point is chosen to satisfy $\alpha = \pi/2$, then the single term will disappear entirely, however the bi-term contribution remains present.

Therefore optimization of the modulation depths β and ψ and the MZM bias point α is required, in order to maximize the desired signal. In the case of MPS with Audio, setting both of the modulation depths $\beta, \psi = 1.841$. In the case of 2nd order MPS with Audio, we require maximum power transfer to the 1st sidetones, while desiring minimum power transfer to the 2nd undesired sidetones. However, when setting the MZM bias point α at an appropriate bias point, we can cancel the single term and bi-term contributions of the response at $J_2(\beta)$ (i.e. $m=0, n=0$ and $m=-2, n = \pm 1$). Upon fulfillment of the condition

$$-2J_2(\beta)J_1(2\psi) \left[J_0(\beta)\cos\left(\ddot{\phi}2\nu_0^2\right) + \cos\left(\alpha + \ddot{\phi}2\nu_0^2\right) \right] = 0 \quad (97)$$

we can simplify Eq. (97), in case we have negligible RF fading $\ddot{\phi}\nu_0^2 \ll 1$. Therefore, setting $\alpha = \arccos[-J_0(\beta)]$, will eliminate the $J_0(\beta)J_2(\beta)$ contribution. A 20dB difference in between the desired and undesired contributions, is achieved by setting the RF modulation depths $\beta = 0.341$, the audio modulation depth $\psi = 0.921$.

In confirmation of our analysis (Jacobi-Anger and small signal), we can demonstrate that the full analytic derivation converges to the small signal analysis performed in section 2 by assuming $\beta, \psi \ll 1$, and expanding the Bessel J-th function of the first kind using the small value approximation, 2nd order at most. Then we can conclude that the full analysis mixer output, which is described in Eq. (95) and (96), converges to the small signal analysis mixer output, which is described by Eqs. (72) and (77).

Note that standard MPS technique (without audio) can also be derived from Eq. (94), by setting the condition $\psi = 0$. Thus $n=0$ and $l=0$, since $J_n(0) = 0$ except for $n=0$ and $J_0(0) = 1$. Then the photocurrent can be demodulated using $\sin(\nu_0 t)$ to find the response of the system at DC. We collect the contributions at DC according to an ideal mixer (using $k = \pm 1$), obtaining:

$$\begin{aligned} V(t) &= \frac{P_0}{4} B(\Omega_0)^2 \cos\left(\nu_0 \dot{\phi} + \gamma\right) \cdot \left\{ 2J_1(\beta) \sin\left(\alpha + \frac{\ddot{\phi}}{2}\nu_0^2\right) - \frac{1}{2} \sum_{m, n, l = -\infty}^{\infty} J_m(\beta) \right. \\ &\quad \left. J_{m+1}(\beta) \sin\left(\frac{\ddot{\phi}}{2}(2m+1)\nu_0^2\right) + 2J_{m-1}(\beta) \sin\left(\frac{\ddot{\phi}}{2}(2m-1)\nu_0^2\right) \right\} \\ &\approx \frac{P_0}{4} B(\Omega_0)^2 \beta \cdot \sin\left(\alpha + \frac{\ddot{\phi}}{2}\nu_0^2\right) \cdot \cos\left(\nu_0 \dot{\phi} + \gamma\right) \end{aligned} \quad (98)$$

where the approximation made is of small modulation depths, hence $\beta \ll 1$.

Notice that the standard MPS result in Eq. (98) has a RF $\pi/2$ phase shift for the null point in comparison with MPS with Audio result in Eq. (95). We confirmed this result experimentally, as shown in Fig. 16. We further see that standard MPS signal nulling point at DC is not a well-defined value, while the slow varying frequency f_0 demonstrates signal nulling at a unique angle. We exploit the LIA high sensitivity and large dynamic range in measurement of the amplitude of frequency component f_0 , allowing us to detect small phase changes at low ν_0 , thus overcoming the limitations imposed by the conventional MPS method. Measurement at the frequency component f_0 avoids the broad band $1/f$ noise of DC measurement.

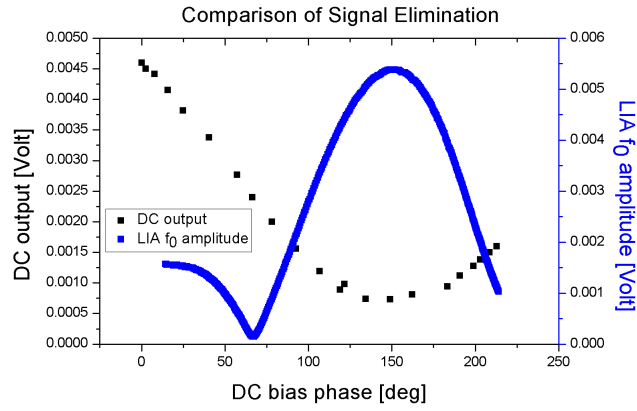


Figure 16: Comparison of signal nulling measurements using DC and f_0 frequency Vs. RF phase delay.

4 Experimental realization of modified MPS

In both of our experimental apparatus we have chosen the RF carrier frequency 400 MHz in order to achieve ultra fine resolution. In case there will be a need to change the RF carrier frequency there will be a need to characterize the RF Phase Modulator (RF PM) at that specific frequency. In the appendix to this chapter the reader may find that the RF PM circuit has a different characteristic s-shape of the DC bias phase versus applied DC bias voltage. In order to resolve rapidly changing group delay we have in our lab three RF phase modulators in the following RF frequency range: 100-150 MHz, 366-446 MHz and 700-1000 MHz.

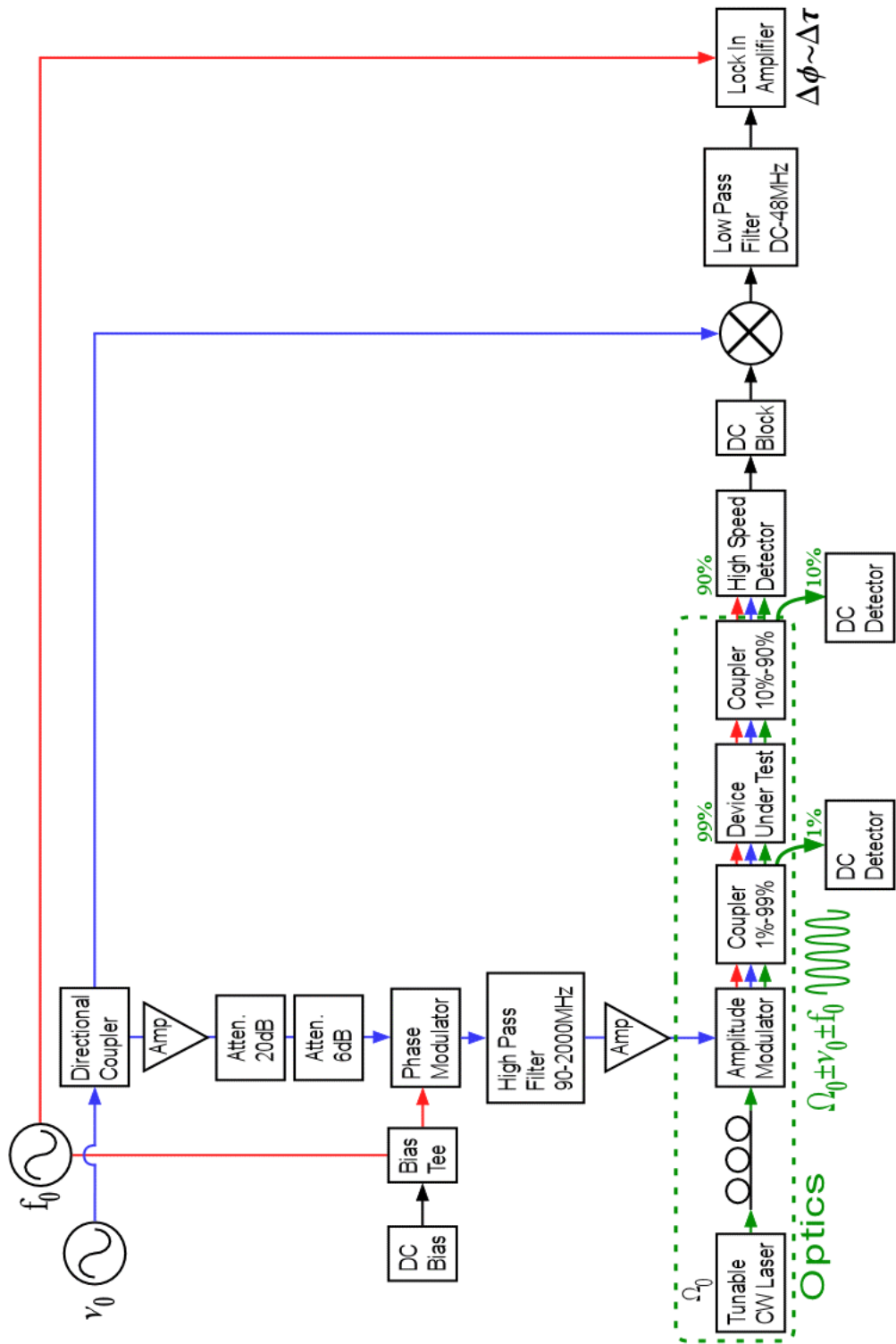
4.1 MPS with Audio apparatus

In order to address conventional MPS disadvantages there are two major conceptual changes in our scheme. The first is an introduction of RF PM in order to introduce a slow frequency component f_0 into the optical signal. The second is the introduction of the LIA which will lock upon the slow frequency component in order to avoid $1/f$ noise and solving limitations in rapidly changing group delay. Furthermore we can achieve a measurement resolution improvement. Our MPS with Audio apparatus complete circuit used with the RF frequency range of 366-446 MHz is depicted in Fig. 17.

The instruments appearing in this scheme are as following: slow (audio) frequency source and DC bias controls (Stanford Research Systems SR850 DSP Lock-In Amplifier), RF frequency source (Agilent 8341B Synthesizer Sweeper 10MHz-20GHz), tunable CW laser (Agilent 8164A Light-wave measurement system; 81640A), DC detectors (Agilent 81525A High power InGaAs optical heads with electrical bandwidth below 1 KHz), high speed detector (New Focus 1544-LF 12GHz Amplified Photoreceiver), and LIA (Stanford Research Systems SR850 DSP Lock-In Amplifier). The optical components are as following: manual polarization controller (Fiber Control FPC-2 Manual Polarization Controller), optical couplers (JDSU AC0199-A3 Optical Coupler 1%-99% & JDSU AC1900-A18-G3W Optical Coupler 10%-90%) and optical amplitude modulator (JDSU 10020427 10 GHz amplitude modulator). The electrical components are as following: bias tee (Picosecond Pulse Labs 5541A 80KHz-26GHz), low noise amplifiers (MiniCircuits ZX60-33LN Low Noise Amplifier 50-3000 MHz), fixed attenuators (MiniCircuits VAT-20 20 dB attenuator & VAT-6 6 dB attenuator), RF phase shifter (MiniCircuits JSPHS-446 Narrow band phase shifter 366-446 MHz), high pass filter (MiniCircuits SHP-100 High pass filter 90-2000 MHz), low pass filter (MiniCircuits SLP-50 Low pass filter DC-48 MHz), DC block (Picosecond Pulse Labs 5502C 20KHz-14GHz) and RF mixer (MiniCircuits ZFM-150).

Our experimental setup is comprised of a few electronic filters and a directional coupler which are used to filter unwanted signals which might interfere in the electronic signal processing. We have encountered a presence of audio signals even when we were blocking the optical path of the DUT. The physical source for this audio signals is impedance mismatch which causes reflection of signals in the electronic circuit. Therefore we have been interested in investigating these signals sources. At first we have used a simple RF broadband (DC-18GHz) 6 dB power divider which is consisted of a network of 3 equivalent resistors of 16.7Ω see Fig. 18(a) (Picosecond Pulse Labs 5330A 6 dB Power divider). The experimental setup use to characterize this reflections is depicted in Fig. 19. We have found out that of the RF PM have shown us that both of

the RF port input and output there exhibit a leakage of the slow frequency component f_0 see Fig. 20(a) around DC signal. Further investigation of our RF Phase Modulator (PM) revealed reflection our RF, ν_0 , phase modulated signal back to the power divider, shown in Fig. 20(b) around $\nu_0 = 400MHz$ signal, passing through to the Local Oscillator (LO) port of the RF mixer. In order to decrease this reflections we are using a directional coupler 5-2000MHz while using it's coupling port to feed the RF PM see Fig. 18(b). Therefore for all of our designated phase modulators we are using a high pass filter in the frequency range of 90-2000MHz in order to filter this slow frequency component from arriving to the optical domain, which after detection can leak from the RF port of the RF mixer to the IF port and interfering with our desired signal.



Modulation Phase Shift (MPS) with Audio complete circuit

Figure 17: Schematic of MPS with Audio complete circuit

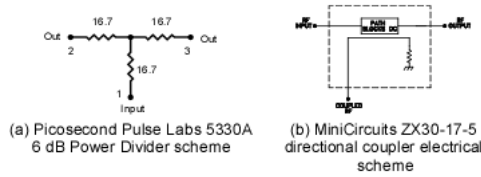


Figure 18: Schematic of (a) 6dB power divider, (b) directional coupler scheme.

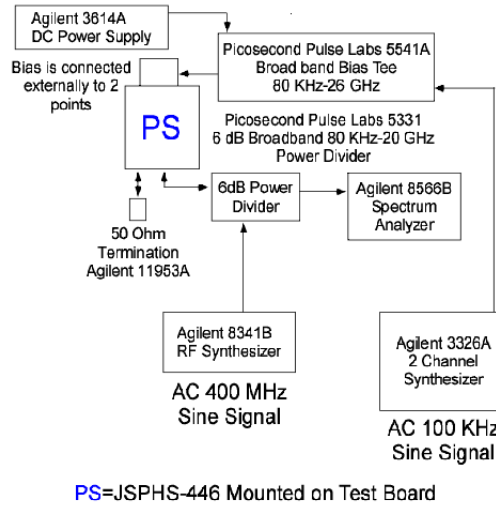


Figure 19: Schematic of phase modulator audio leakage experiment

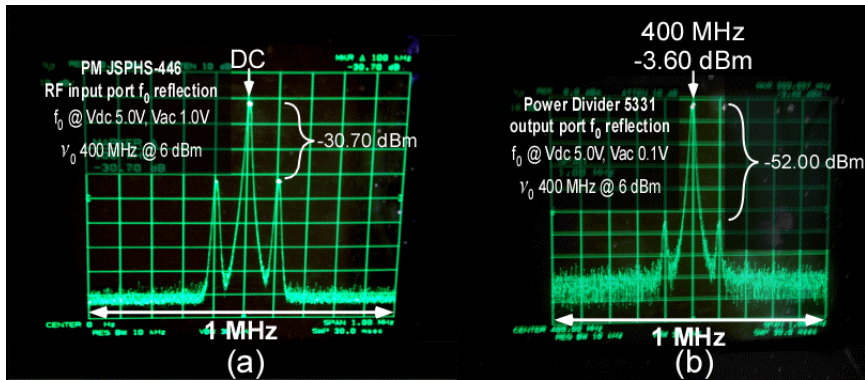


Figure 20: RF electrical spectrum demonstrating audio leakage

A bias tee is used to supply a DC+AC signal to both of the RF PM bias ports. A low noise amplifier and a fixed attenuator are used to adjust the power level to a maximum level 0 dBm at the PM RF input port. A DC block, frequency bandwidth of 20KHz-14GHz, since the high speed detector detector output currently available to us in the lab needs to be connected to a DC block. A low pass filter DC-48 MHz is used to filter the unwanted signals at the RF mixer output, also to avoid strong signals from arriving to the LIA input and distributing it's circuits.

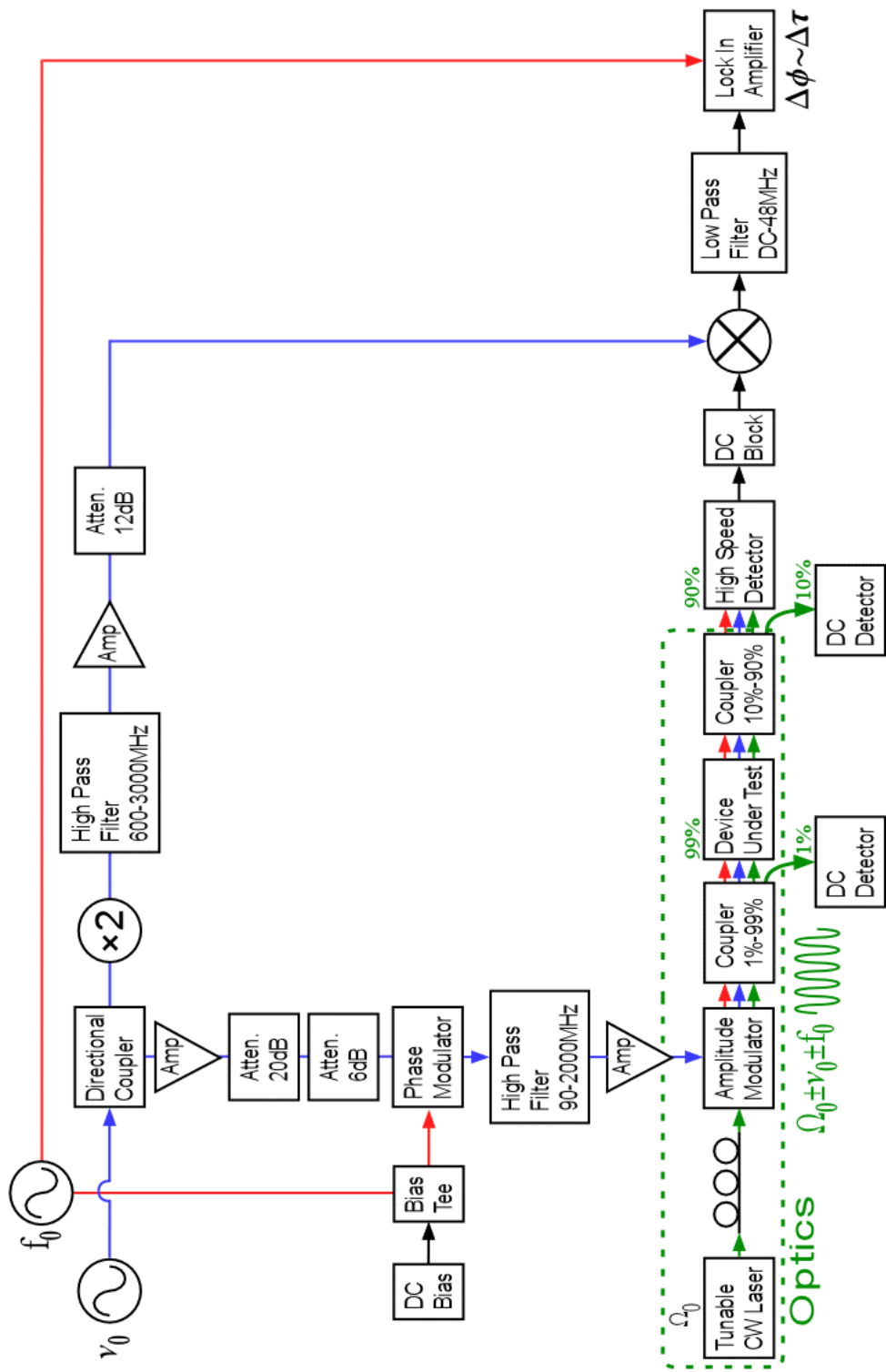
Upon changing of the RF PM there is also a necessity to change the fixed attenuators in order to set the optimal RF power level at 0 dBm at the PM RF input and +10 dBm Local Oscillator (LO) at the LO port of the RF mixer.

4.2 2nd order MPS with Audio apparatus

In order to address conventional MPS disadvantages there are three major conceptual changes in our scheme. The first is an introduction of RF Phase Modulator (PM) in order to introduce a slow frequency component f_0 into the optical signal. The second is the introduction of the LIA which will lock upon the slow frequency component in order to avoid $1/f$ noise and solving limitations in rapidly changing group delay. The third is the introduction of the RF X2 frequency multiplier which will demodulate the $2\nu_0$ harmonics. Furthermore we can achieve a measurement resolution improvement. Our 2nd order MPS with Audio apparatus complete circuit used with the RF frequency range of 366-446 MHz is depicted in Fig. 21.

The instruments appearing in this scheme are as following: slow frequency source and DC bias controls (Stanford Research Systems SR850 DSP Lock-In Amplifier), RF frequency source (Agilent 8341B Synthesizer Sweeper 10MHz-20GHz), tunable CW laser (Agilent 8164A Lightwave measurement system; 81640A), DC detectors (Agilent 81525A High power InGaAs optical heads with electrical bandwidth below 1 KHz), high speed detector (New Focus 1544-LF 12GHz Amplified Photoreceiver), and LIA (Stanford Research Systems SR850 DSP Lock-In Amplifier). The optical components are as following: manual polarization controller (Fiber Control FPC-2 Manual Polarization Controller), optical couplers (JDSU AC0199-A3 Optical Coupler 1%-99% & JDSU AC1900-A18-G3W Optical Coupler 10%-90%) and optical amplitude modulator (JDSU 10020427 10 GHz amplitude modulator). The electrical components are as following: bias tee (Picosecond Pulse Labs 5541A 80KHz-26GHz), low noise amplifiers (MiniCircuits ZX60-33LN Low Noise Amplifier 50-3000 MHz), fixed attenuators (MiniCircuits VAT-6 6 dB, VAT-12 12 dB & VAT-20 20 dB attenuators), RF phase shifter (Minicircuits JSPHS-446 Narrow band phase shifter 366-446 MHz), high pass filters (Minicircuits SHP-100 High pass filter 90-2000 MHz & SHP-600 High pass filter 600-3000MHz), low pass filter (MiniCircuits SLP-50 Low pass filter DC-48 MHz), DC block (Picosecond Pulse Labs 5502C 20KHz-14GHz), x2 frequency multiplier (MiniCircuits FK-3000 x2 Frequency multiplier 70-1500MHz) and RF mixer (MiniCircuits ZFM-150).

Our experimental setup is comprised of a few electronic filters and a directional coupler which are used to filter unwanted signals which might interfere in the electronic signal processing. As described in the previous section, the physical source for this audio signals is impedance mismatch which causes reflection of signals in the electronic circuit. In order to decrease this reflections we are using a directional coupler 5-2000MHz while using it's coupling port to feed the RF PM. Further investigation of the RF PM have shown us that both of the RF port input and output there exhibit a leakage of the slow frequency component f_0 around DC signal. Therefore for all of our designated phase modulators we are using a high pass filter in the frequency range of 90-2000MHz in order to filter this slow frequency component from arriving to the optical domain, which after detection can leak from the RF port of the RF mixer to the IF port and interfering with our desired signal. A bias tee is used to supply a DC+AC signal to both of the RF PM bias ports. A low noise amplifier and a fixed attenuator are used to adjust the power level to 0 dBm at the PM RF input port.



2nd order Modulation Phase Shift (MPS) with Audio complete circuit

Figure 21: Schematic of 2nd order MPS with Audio complete circuit

The x2 frequency multiplier, input range 70-1500 MHz, is connected to the output port of the directional coupler. Since the frequency multiplier is a nonlinear device several harmonics are

created at the component output (1st, 2nd, 3rd and 4th ν_0 harmonics). Since we are interested only in the 2nd harmonics we are using a high pass filter 600-3000MHz which decreases the 1st harmonics at approximately 30 dB. Without the use of the high pass filter all of these harmonics are multiplying our photocurrent, which has DC, ν_0 and $2\nu_0$ terms, thus contributing a non desired term (photocurrent ν_0 term) to our desired signal at the IF port of the RF mixer. A low noise amplifier and a fixed attenuator are used to adjust the power level to +10 dBm at the RF mixer LO port.

Upon changing of the RF PM there is also a necessity to change the high pass filter accordingly, which is located at the frequency multiplier output and used to lower the 1st harmonics output of the frequency multiplier, in order to get a better dynamic range between the 1st and 2nd harmonics output of the frequency multiplier. Of course there will also need to be a change of the fixed attenuators in order to set the optimal RF power at 0 dBm at the PM input and +10 dBm Local Oscillator (LO) at the LO port of the RF mixer.

A DC block, frequency bandwidth of 20Khz-14GHz, since the high speed detector detector output currently available to us in the lab needs to be connected to a DC block. A low pass filter DC-48 MHz is used to filter the unwanted signals at the RF mixer output, also to avoid strong signals from arriving to the LIA input and distributing it's circuits.

In Fig. 22 we can see how the signal is passing in our apparatus. I have inserted pictures of the RF power spectrum in order to demonstrate that. We have an entire controllable comb of slow frequency component $f_0 = 100$ KHz around the RF modulation frequency $\nu_0 = 400$ MHz. We can see that the Local Oscillator (LO) signal at the RF mixer LO port is clean from any speckles due to all the additional filtering elements in the circuit. After detection we can see the all the beating signals, an entire comb of slow frequency component $f_0 = 100$ KHz around the RF frequency $\nu_0 = 400$ MHz and around $2x$ RF frequency $2\nu_0 = 800$ MHz. At the RF mixer IF port we can see that our slow varying component exist and has been preserved in our apparatus!

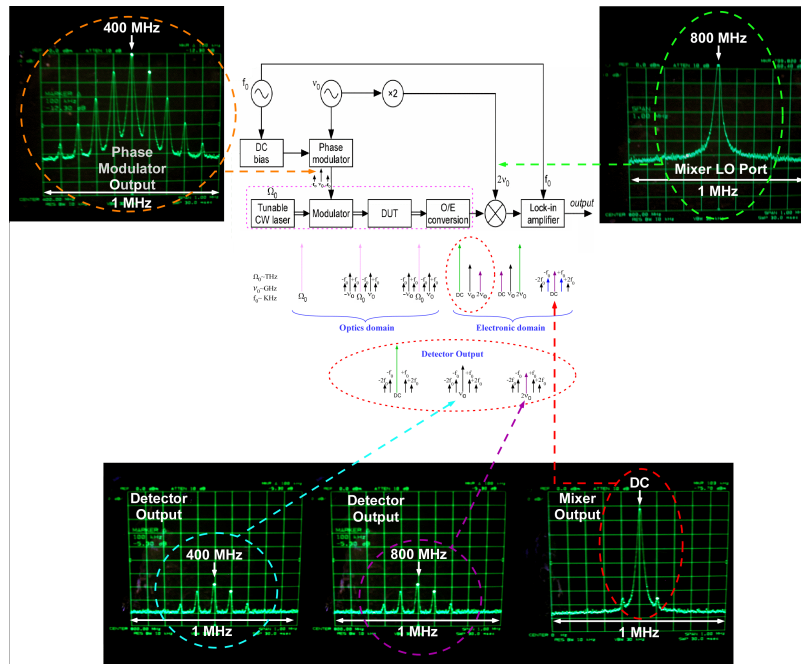


Figure 22: Schematic of 2nd order MPS with Audio - low frequency signal preserved in our apparatus

4.3 Appendix: Apparatus components characterization

Since the RF x2 frequency multiplier is a nonlinear device it contains in its output not only the desired 2nd harmonics, but also the 1st, 3rd, and 4th harmonics. We are interested only in the 2nd harmonics. Therefore we have used the RF Spectrum Analyzer to read the frequency multiplier output in order to characterize the behavior of the frequency multiplier see Fig. 23. We have found the behavior of the multiplier to be dependent on the input power arriving to the frequency multiplier see Fig. 24. The most efficient working point for our apparatus demands that the 2nd harmonics will be the strongest as possible, while the 1st harmonics will be lowest as possible. In the 2nd order MPS with Audio apparatus a high pass filter is connected at the frequency multiplier output in order to attenuate the 1st harmonics by additional 30dB. Since the desired demodulation at the photodiode output is of the $2\nu_0$ beat term, while the ν_0 beat term might contribute to unwanted signal.



Figure 23: Schematic of x2 frequency doubler power sweep characterization

FK-3000 x2 Frequency Multiplier Characterization @ $\nu_0=400\text{MHz}$

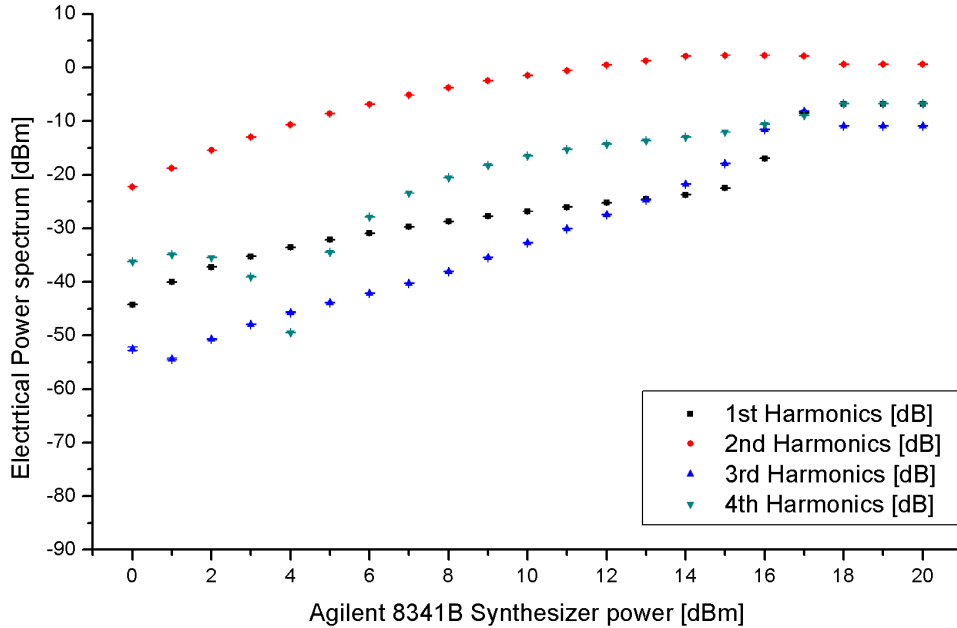


Figure 24: x2 Frequency doubler characterization

In order to demonstrate the influence High Pass Filter (HPF) we have measured its RF spectrum at the HPF connected to the x2 frequency multiplier output. We will summarize the results in Tab. 1.

x2 Frequency multiplier harmonics	without HPF [dBm]	with HPF [dBm]
1st	-25.25±0.05	-61.00±0.05
2nd	0.45±0.05	0.05±0.05
3rd	-27.45±0.05	-29.35±0.05
4th	-14.35±0.05	-15.25±0.05

Table 1: x2 Frequency doubler harmonic output comparison without\with HPF

Every passive component we have used in our apparatus has been measured for Insertion Loss (IL) according to the following simple setup utilizing a broadband source as a white light source see Fig. 25. In order to measure IL before connecting the passive DUT we have measured the power that goes through our patch cord fibers which we will be using to connect to the DUT. After wards we connect the DUT with these patch cords and subtract from the measured spectra the patch cords spectra thus obtaining our DUT IL. In order to characterize the optical couplers splitting ratio (in percentage) we have measured how much power is transmitted to each port. Then each port was divided by the total output power in order to obtain the DUT splitting ratio in percentage.



Figure 25: Schematic of optical passive components characterization setup

The RF phase versus applied DC bias was obtained using an oscilloscope A/D converter, and the phase shifts were extracted in Matlab from the parameter fitting of a sine function to the sampled data of both the reference channel (RF directional coupler output) and the RF phase shifter output channel.

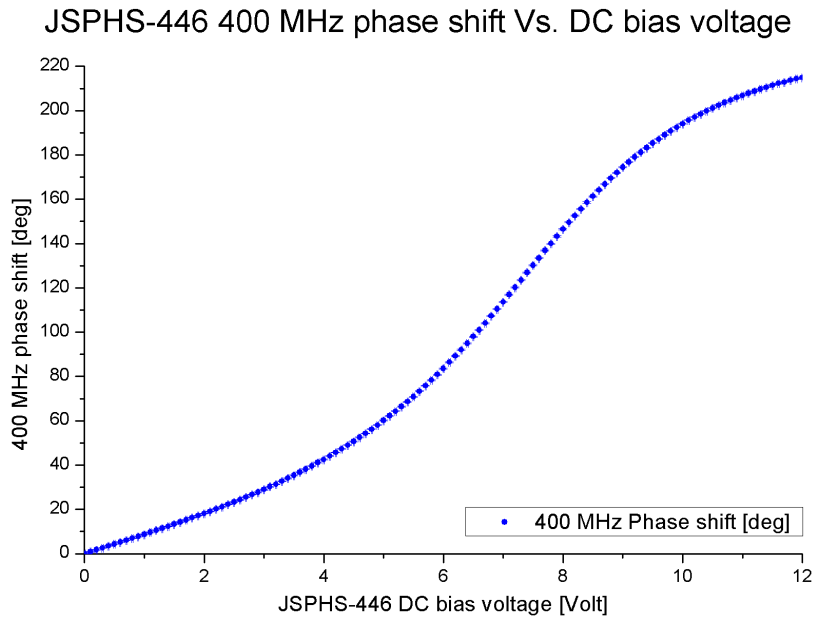


Figure 26: RF phase modulator 400 MHz phase shift Vs. DC bias characterization

Each RF carrier frequency demonstrates a different characteristic s-shape this is why performing

RF frequency sweep changes the relative phase shift . The RF PM circuit does not create second harmonics of the RF carrier.

The PM circuit allows us to control of the audio comb around the RF carrier. In order to demonstrate this behavior I have attached here are 2 power spectrum pictures in Fig. 27 of the PM output at 2 different audio AC Voltages 0.5 Volt and 1.2 Volt.

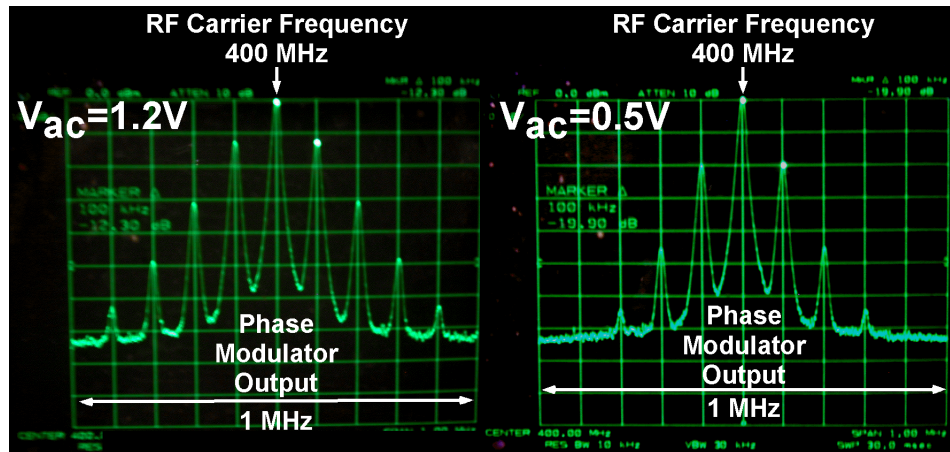


Figure 27: Controllable audio comb demonstration

The RF carrier passes a little of his energy to the audio comb as can be seen from these graphs, we can see that the audio comb different harmonics arises as the audio AC voltage increases see Fig. 29. We can also notice the saturation of the comb as expected from theory (Jacobi-Anger expansion).

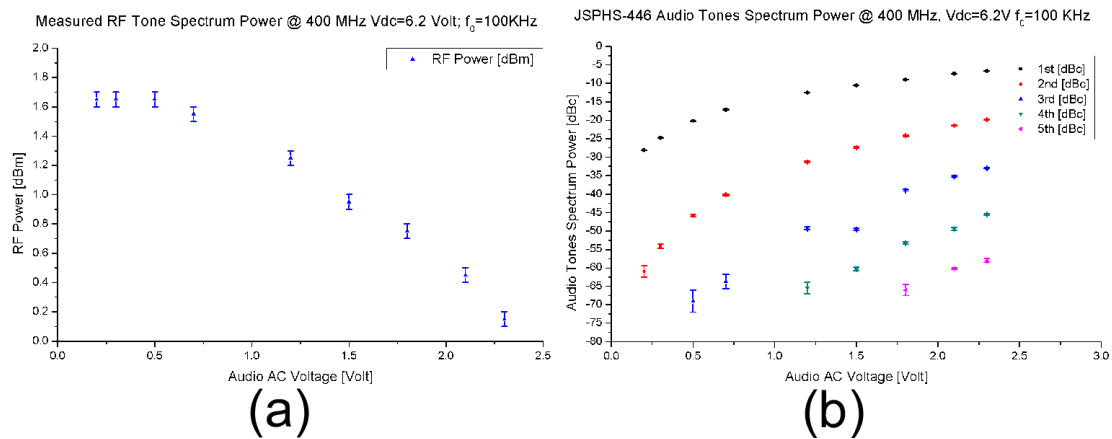


Figure 28: PM output - RF carrier and audio tones power Vs. audio AC voltage

(a) measured RF carrier 400 MHz power while sweeping audio AC voltage (b) measured audio tone harmonics relative to the RF carrier 400 MHz while sweeping audio AC voltage. Notice that the audio tone comb gains more harmonics as the audio AC voltage is increased, moreover there is also a saturation in this increased sidetones power.

We can see that the RF mixer has a linear dynamic range of about 80 dB see Fig. 29. Moreover we have a conversion loss of about 5dB see Fig. 30. The RF mixer LO-RF isolation for LO power +10dBm @ 400 MHz RF carrier is 39.05 ± 0.05 dB. The LO-IF isolation for LO power

+10dBm @ Rf carrier 400 MHz is 36.05 ± 0.05 dB. The RF mixer LO-RF isolation for LO power +10dBm @ 800 MHz RF carrier is 39.05 ± 0.05 dB. The LO-IF isolation for LO power +10dBm @ Rf carrier 800 MHz is 29.35 ± 0.05 dB.

ZFM-150 RF Mixer Characterization @ IF 100 KHz Vs. RF Power Sweep

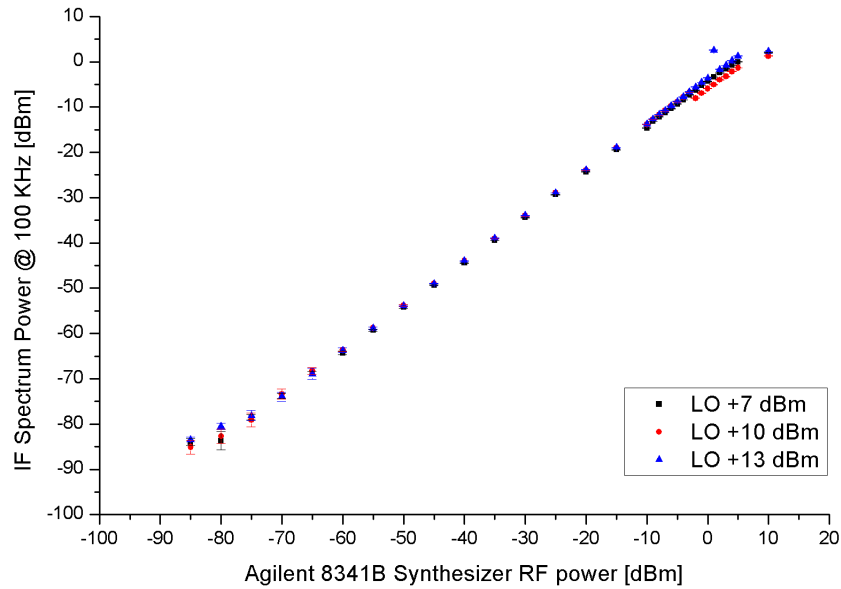


Figure 29: RF mixer characterization IF 100 KHz

ZFM-150 RF Mixer Conversion Loss Characterization

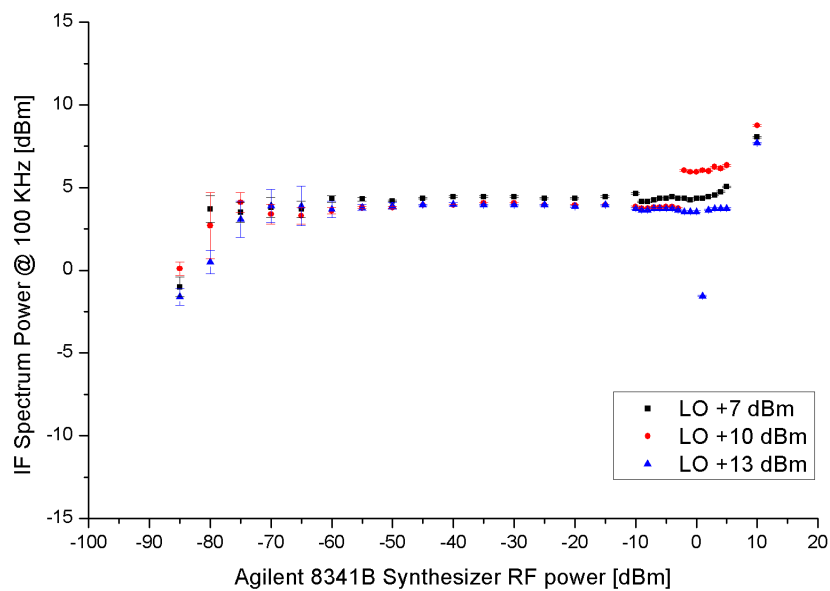


Figure 30: RF Mixer conversion loss characterization

The conversion loss defined as the output power difference at the IF port relative to the summation of the RF and LO ports power.

5 Optical devices characterization results and discussion

The characterization apparatus has been realized in our lab using commercially available optical and electrical components. We set $\nu_0 = 400\text{MHz}$, demonstrating the high sensitivity extraction even at such low RF driving frequency. Due to resolution limit of the Optical Spectrum Analyzer (OSA) in such low RF driving frequency we cannot use optical spectrum analysis method directly to measure the MZM output field power spectrum [31]. Care was taken to prevent higher RF tones (i.e. above 1st order) in the MZM output field, which could interfere with the desired measurement. f_0 is set to 50KHz , matching the bandwidth of our LIA (SRS model 850). The chosen LIA conveniently provides both DC bias controls and the slow varying (audio) signal which has been inserted into the optical domain and processed using standard electronic circuits. Care was taken to prevent RF leakages in the electronic circuitry, which could interfere with the measurement of weak signals. The apparatus was used for characterization of dispersion compensating devices and optical components.

We measured several component categories and fibers to demonstrate the measurement technique. At each wavelength step, the GD term is extracted. All the presented data points obtained using the apparatus are without data averaging, smoothing or processing. In essence, the LIA provides a degree of averaging through its integration time. Currently the measurement time for a single optical carrier step takes relatively long time due to GPIB bus limits on signaling and data transfer (each RF phase bias sweep and data transfer takes ~ 7 sec). Future commercialization of the apparatus can reduce the measurement time dramatically by introducing custom electronics.

5.1 MPS with Audio

5.1.1 Dispersion Compensating Fiber (DCF) modules

Measurements of Dispersion Compensating Fiber (DCF) modules are depicted in Fig. 31. The DCF exhibit nearly flat amplitude response and a nearly linear relation of GD vs. λ (almost constant CD). After unwrapping the GD data points and curve fitting to a 2nd degree polynomial, the dispersion and dispersion slope are extracted in Fig. 32. In Fig. 31 the left DCF module demonstrated CD of -298.21 ps/nm with dispersion slope of -2.55 ps/nm², while the right DCF module demonstrated CD of -1346.5 ps/nm with dispersion slope of -1.97 ps/nm². These results are obtained from measurements spanning 5 nm only. The long fiber length of the DCF modules ($\sim 1.1\text{km}$) prevented us from conducting comparative measurements using the interferometer technique, due to coherence length limitations.

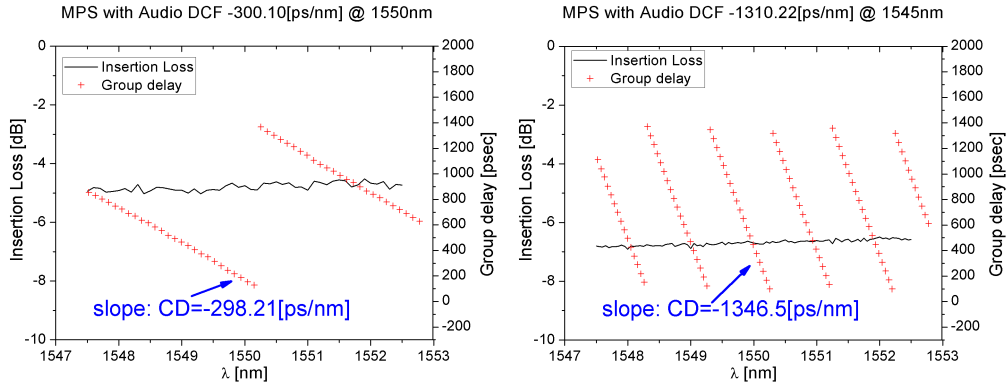


Figure 31: Dispersion Compensating Fiber (DCF) modules MPS with Audio measurements

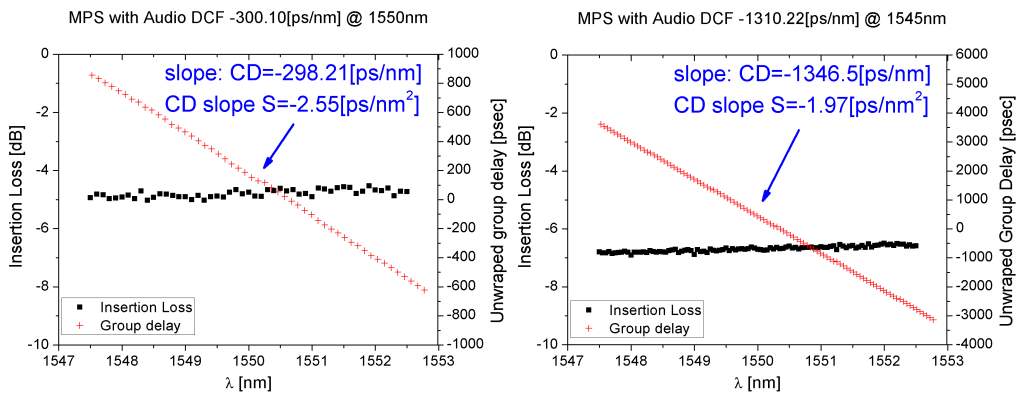


Figure 32: Dispersion Compensating Fiber (DCF) modules MPS with Audio unwrapping group delay

5.1.2 Arrayed Waveguide Planar Lightwave Circuit (AWG PLC) against reflective mirror

Example of high resolution optical component measurement is depicted in Fig. 34, in this case a custom Arrayed Waveguide Grating with 100GHz Free Spectral Range (FSR) Planar Lightwave Circuit (AWG PLC) against reflective mirror (see reference [32, 33] for device illustration and abbreviation). CD of -564 ps/nm are extracted from the group delay measured slope. The f_0 audio AC voltage was set to 0.3Volt and the laser intensity was set to maximum. The apparatus was connected to the AWG PLC through a circulator. Input port (port 1) was connected to MPS with audio, port 2 was connected to the AWG PLC and the output port (port 3) was connected to the 2nd optical coupler of MPS with audio apparatus see Fig. 33.

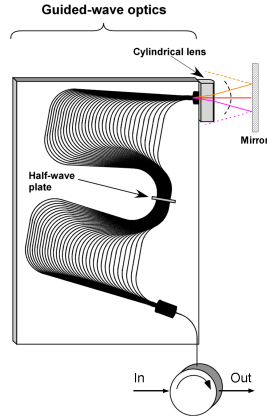


Figure 33: 100 GHz FSR AWG against reflective mirror experimental setup

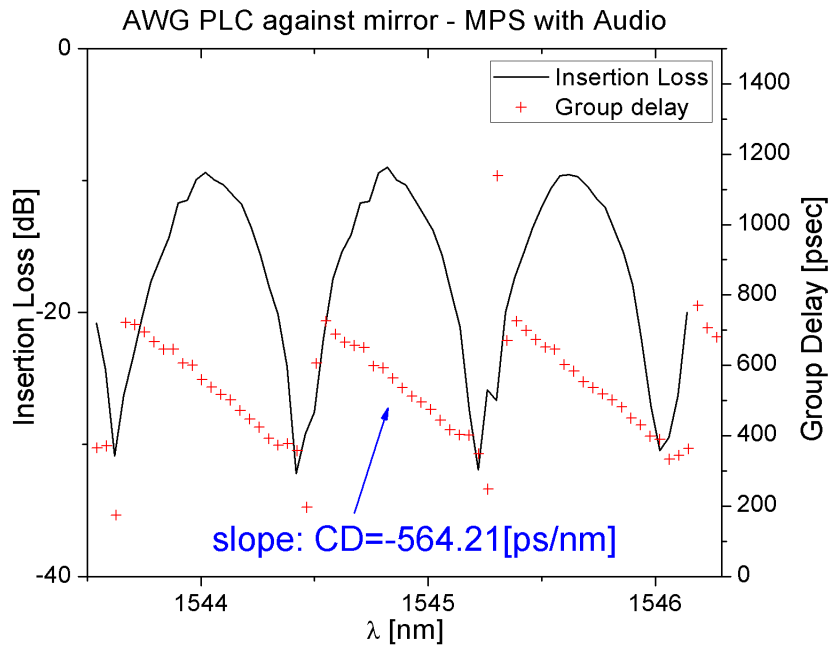


Figure 34: MPS with Audio 100 GHz FSR AWG against reflective mirror measurement.

In order to evaluate the apparatus dynamic range, IL tolerance, we have made an additional experiment in which the f_0 audio ac voltage was set to be constant through this sweep to 1.929 Volt and the laser intensity was swept, since all of the optical signals are predominated by the optical carrier power level see Fig. 35. Comparison of the extracted chromatic dispersion values are listed in Tab. 2. As we can see from the chromatic dispersion extraction using linear fitting to the group delay values the optical carrier IL tolerance is 16.38 dB (the minimum output power of the laser relative to the maximum optical power in this wavelength range) see Fig. 36.

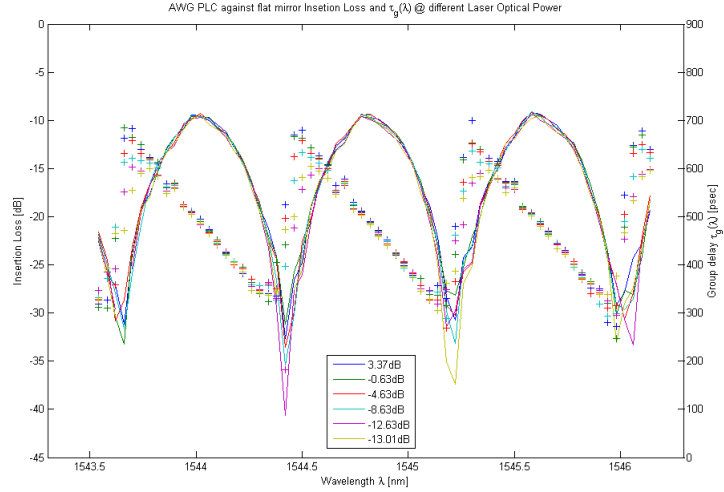


Figure 35: AWG PLC against mirror insetion loss and group delay comparison versus laser optical power

laser attenuation of 16.38dB does not affect the extraction of the group delay, therefore we can estimate that the MPS with Audio apparatus have at least 26dB tolerance to DUT IL.

Laser optical power [dBm]	Chromatic dispersion [ps/nm]
3.37	-517.13
-0.63	-514.64
-4.63	-533.48
-8.63	-510.52
-12.63	-504.40
-13.01	-511.81

Table 2: AWG PLC against mirror chromatic dispersion versus laser optical power

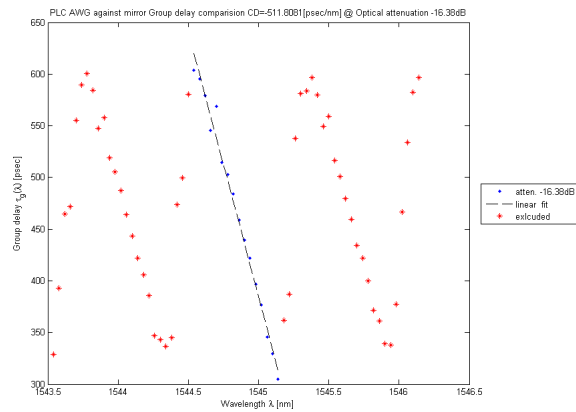


Figure 36: Group delay linear fitting optical power attenuated 16.38dB

From this group delay linear fittings we can see a chromatic dispersion value of -511.81 [psec/nm] at the lowest optical carrier power level. According to the theoretical value this PLC should exhibit a chromatic dispersion of 530 [psec/nm]. Thus we have measured a relatively close value to the theoretical value with an error of 18.19 [psec/nm] (3.43% error from the theoretical value).

This error might be caused from a chromatic dispersion in the circulator, or perhaps from the low coupling efficiency of the mirror (10 dB IL on the center wavelength) and the insertion loss curvature induced by the radius of the cylindrical lens at the AWG PLC output. This insertion loss curvature may contribute to a summing of two phasors which are not equal in there power spectrum power and therefore one of the phasors will dominate in the MPS with Audio apparatus.

We set another experiment in order to check the MPS with Audio technique tolerance to insertion loss. We have inserted a tunable attenuator at the circulator input port in order to emulate insertion tolerance of the signals see Fig. 35, same experimental setup see Fig. 33. The f_0 audio AC voltage was held constant 1.5Volt through the laser optical power sweep. Chromatic dispersion extraction from linear fitting to the group delay is given as an example see Fig. 39. The extracted chromatic dispersion values from the group delay linear fittings are summarized in Tab. 3.

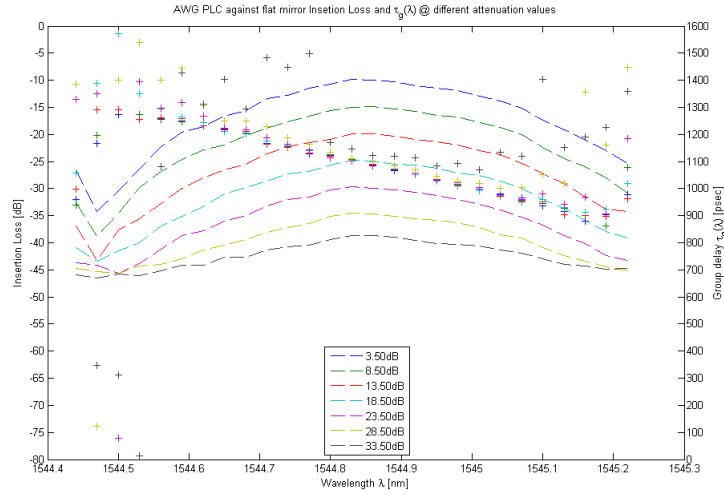


Figure 37: AWG PLC against mirror insertion loss and group delay comparison versus tunable attenuation

group delay values up to IL of 23.5dB appear to be the same, while another increase in the IL give a noisy measurement of the group delay.

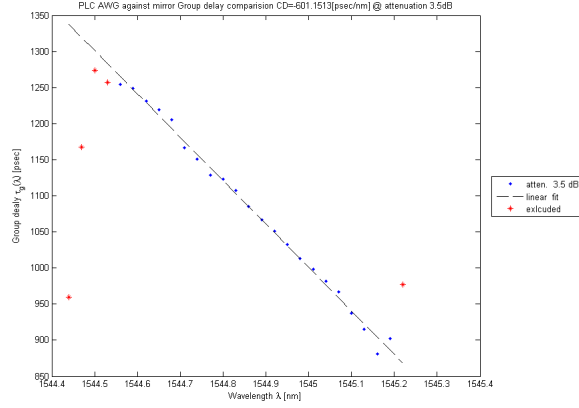


Figure 38: Group delay linear fitting attenuation value 3.5dB

Tunable attenuation [dB]	Chromatic dispersion [ps/nm]
3.5	-601.15
8.5	-599.16
13.5	-594.94
18.5	-617.90
23.5	-642.02
28.5	-675.26
33.5	-434.53

Table 3: AWG PLC against mirror with tunable attenuator chromatic dispersion comparison

In order to estimate the MPS with Audio optical dynamic range of the system we can define an error range of 5%. Therefore if will consider the smallest attenuation (3.5dB) as a reliable measurement then five percent error (30 ps/nm) means that our optical dynamic range is at 18.5dB, since the best coupling in between the AWG PLC and the mirror is 10 dB.

Since we have an electrical controllable RF phase modulated comb, which is transmitted to an optical signal comb we can try and increase the dynamic range of the apparatus from the electrical power spectrum. Therefore we have measured the same experimental setup while maintaining a constant optical power of 3.37dBm, while sweeping the f_0 audio AC voltage (see Fig. 39 on the following page).

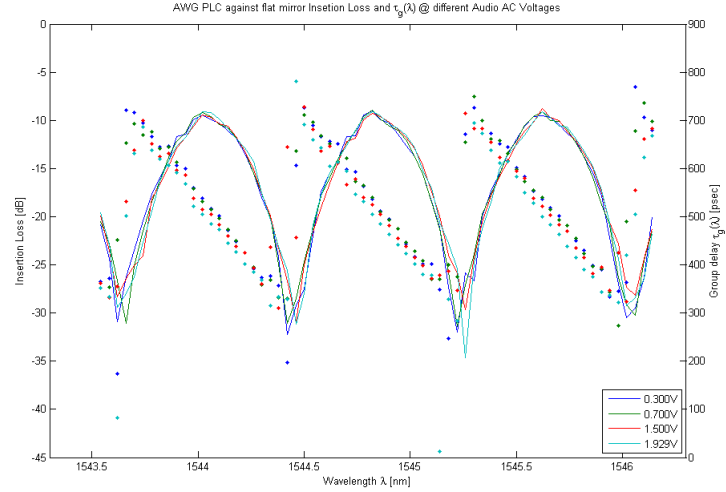


Figure 39: AWG PLC against mirror Insetion Loss and group delay while sweeping f_0 audio AC Voltage

Chromatic dispersion extraction from linear fitting to the group delay is given as an example in Fig. 40. The extracted chromatic dispersion values from the group delay linear fittings are summarized in Tab. 4.

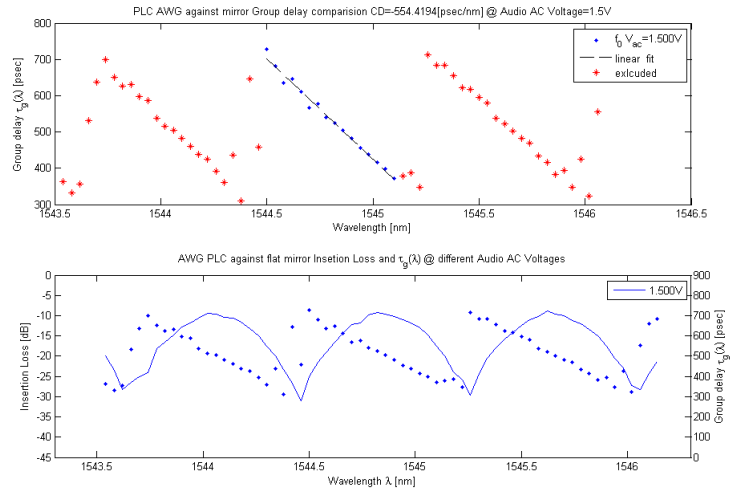


Figure 40: AWG PLC against mirror group delay linear fitting: f_0 audio AC Voltage 1.5Volt

f_0 audio AC voltage [Volt]	Chromatic dispersion [ps/nm]
0.300	-564.21
0.700	-552.09
1.500	-554.42
1.929	-540.70

Table 4: AWG PLC against mirror chromatic dispersion versus f_0 audio AC voltage comparison

In conclusion the MPS with Audio apparatus has an optical dynamic range of 28.5dB or equivalently 2.8% error in chromatic dispersion extraction. Moreover in another set of measurements

(see Tab. 4) while holding the optical power as constant and changing the audio AC voltages values thus increasing the optical comb sampling the DUT spectra, for f_o audio AC voltage 1.5Volt we have measured a value of -554.42 [psec/nm] (11.45% error from this measured value in the dynamic range limit of the MPS with Audio apparatus) . We need to mention that we have also measured the group delay of the tunable attenuator (attenuation values of 3.5,13.5,23.5dB; in the defined optical dynamic range of the MPS with Audio apparatus). In a separate measurement we didn't find any contribution to group delay or chromatic dispersion values in the measured wavelength sweep range. This measured value is not far from the theoretical value of 530 [psec/nm] (16.6% error from the theoretical value). As it is known that this AWG PLC has Polarization Dependent λ (PDL) of 2dB. It is also possible that in these measurement the PDL and PDL was worse (since I have measured a polarization dependence of 6-8dB at the DC output detector, while changing the polarization with polarization controller at the circulator input port).

Furthermore, in another set of measurements (see Tab. 4 on the previous page) while holding the optical power as constant and changing the audio AC voltages values thus increasing the optical comb sampling the DUT spectra, for f_o audio AC voltage 1.929Volt we have measured a value of -540.70 [psec/nm]. This measured value is not far from the theoretical value of 530 [psec/nm] (2% error from the theoretical value).

5.1.3 DWDM Demux

A final example of an optical component is a DWDM 20 channels 200 GHz spacing demux (Fig. 41). The MPS with Audio results are compared with a LUNA Optical Vector Analyzer (LUNA OVA model CTe), which is based on interferometer technique [10]. We have preformed characterization of ETEK Dynamics C-band 20 channels DWDM Demux (model no. DWDM2YM3CRV01) with the MPS with Audio technique using audio tone oscillating voltage ($V_{ac} = 1.2$ Volt). In order to cover all the DWDM demux spectra we have decided to measure 3 channels: 1, 13 and 20. The Insertion Loss (IL) characterization and the chromatic dispersion agree in between the two techniques. Results at low IL compare well, whereas the phase estimates for the LUNA becomes unreliable at high IL values. Even the LUNA OVA measurement was acquired 200 samples it was still needed to play with the DSP capabilities of the LUNA in order to remove the noise from its measurements by narrowing the filter bandwidth in order to cut high frequency components which translates to oscillations that can be demonstrated in channel 20. When performing a better filtering of this noise the chromatic dispersion behavior is seen clearer (see channels 1 and channel 13).

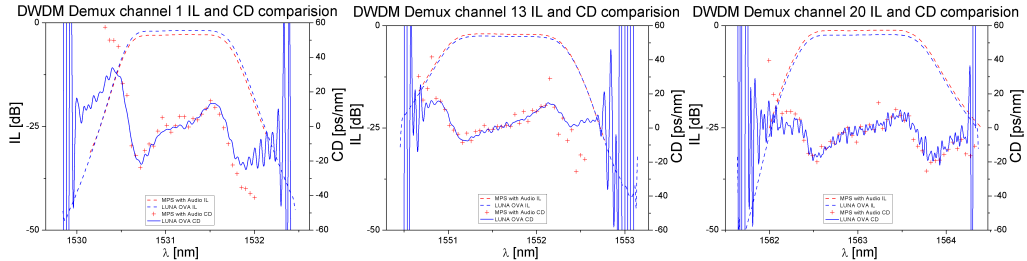


Figure 41: DWDM Demux MPS with Audio & LUNA OVA insertion loss and chromatic dispersion comparison

The MPS with Audio technique has an electrical RF PM controllable comb which is been transported through the DUT optical spectra. As the audio oscillating voltage increased there is a slight drift in measuring the group delay absolute value see Fig. 43 left side. However when calculating the local group delay slope we can see that all these drifts are filtered out and that there is a good agreement no matter the chosen audio tone oscillating voltage see Fig. 43 right side.

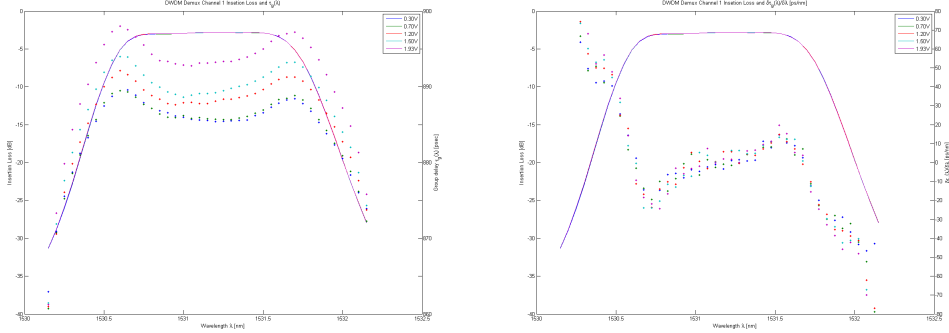


Figure 42: DWDM Demux channel 1 - MPS with Audio insertion loss, group delay and chromatic dispersion comparison Vs. f_0 audio AC Voltage

5.2 2nd order MPS with Audio

5.2.1 Dispersion Compensating Fiber (DCF) modules

Measurements of Dispersion Compensating Fiber (DCF) modules are depicted in Fig. 44. The DCF exhibit nearly flat amplitude response and a nearly linear relation of GD vs. λ (almost constant CD). After unwrapping the GD data points and curve fitting to a 2nd degree polynomial, the dispersion and dispersion slope are extracted in Fig. 45. In Fig. 44 the left DCF module demonstrated CD of -299.42 ps/nm with dispersion slope of -4.5 ps/nm², while the right DCF module demonstrated CD of -1344.6 ps/nm with dispersion slope of -2.4 ps/nm². These results are obtained from measurements spanning 5 nm only. The long fiber length of the DCF modules (~ 1.1 km) prevented us from conducting comparative measurements using the interferometer technique, due to coherence length limitations.

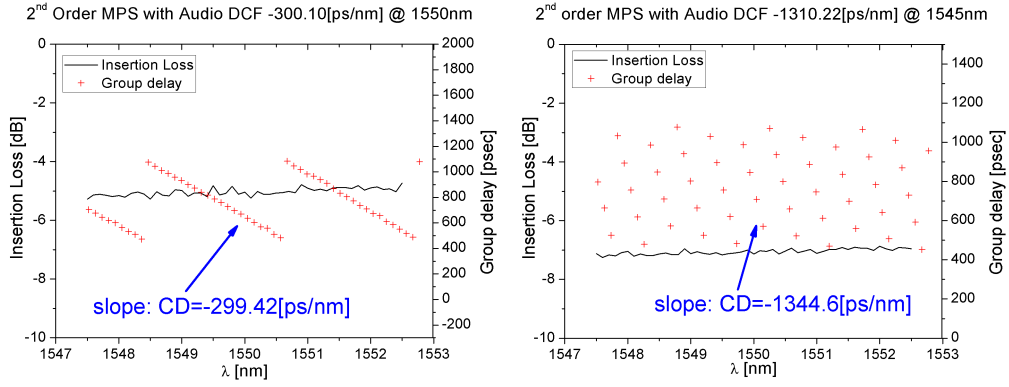


Figure 43: Dispersion Compensating Fiber (DCF) modules 2nd Order MPS with Audio measurements

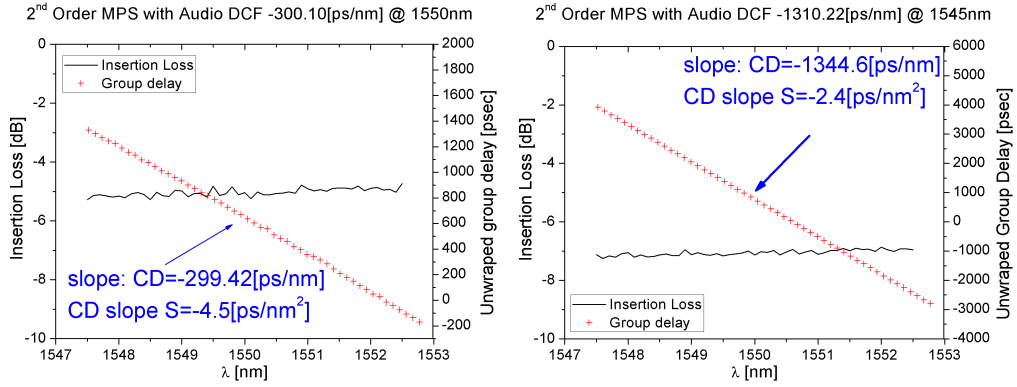


Figure 44: Dispersion Compensating Fiber (DCF) modules 2nd Order MPS with Audio unwrapping group delay

5.2.2 Arrayed Waveguide Planar Lightwave Circuit (AWG PLC) against reflective mirror

Example of high resolution optical component measurement is depicted in Fig. 5.2.2, in this case a custom Arrayed Waveguide Grating with 100GHz Free Spectral Range (FSR) Planar Lightwave Circuit (AWG PLC) against reflective mirror (see reference [32, 33] for device illustration and abbreviation). CD of -566 ps/nm are extracted from the group delay measured slope. The f_0 audio AC voltage was set to 0.3Volt and the laser intensity was set to maximum.

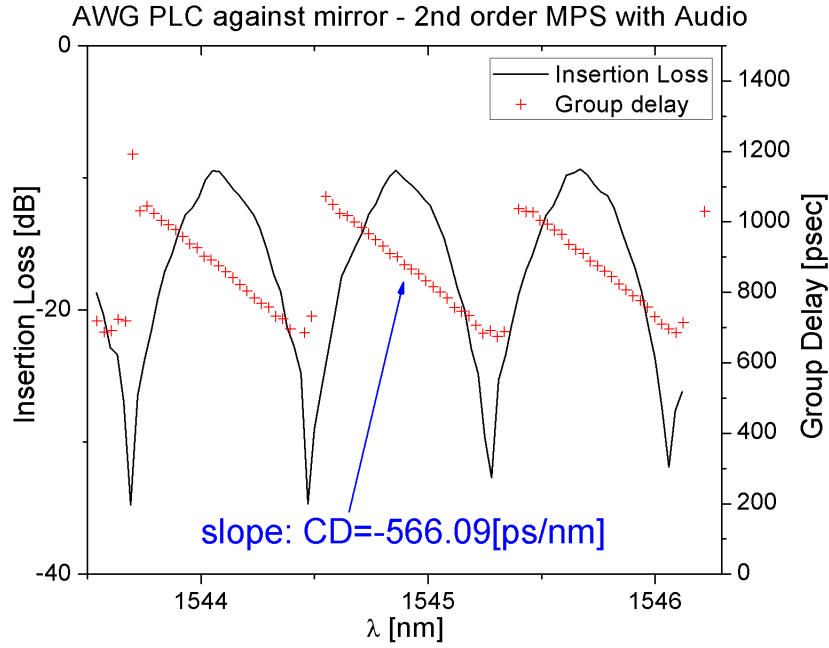


Figure 45: 2nd Order MPS with Audio 100 GHz FSR AWG against reflective mirror measurement.

We have repeated the experiment of AWG PLC against mirror see experiment on Fig. 34 on page 63. I have applied the current 2nd order MPS with Audio apparatus using the RF broadband amplifier and setting the optical bias point at maximum transfer regime of the optical AM modulator ($V_{\text{bias}}=3.0\text{Volt}$), the f_0 audio AC voltage was set to 1.929Volt. As can be seen in Fig. 46 as the laser output power is decreased a curvature of the group delay starts to arise at attenuation level of 12.00dB (optical power -8.63dBm). Linear group delay fitting are given as an example in Fig. 47. The extracted chromatic dispersion values are summarized in Tab. 5.

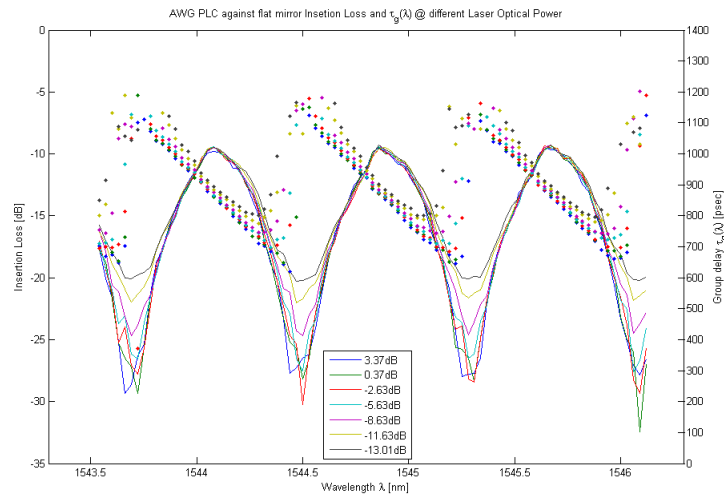


Figure 46: AWG PLC against mirror insertion loss and group delay comparison versus laser optical power

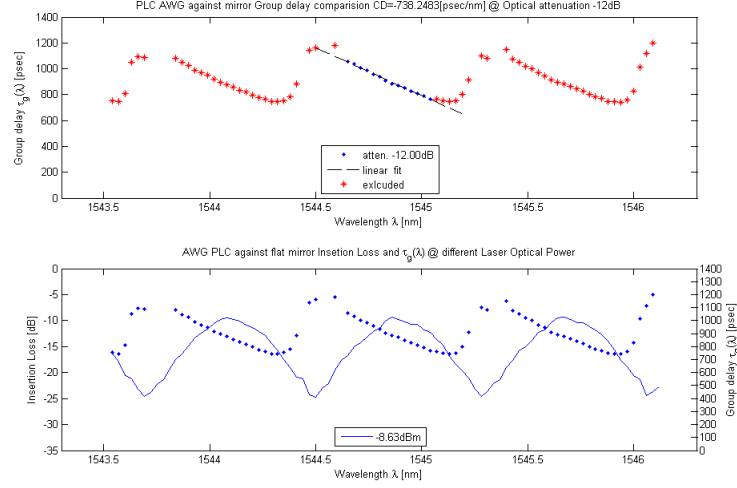


Figure 47: Group delay linear fitting optical power attenuated 12.00dB

Laser optical power [dBm]	Chromatic dispersion [ps/nm]
3.37	-680.92
0.37	-684.61
-2.63	-699.87
-5.63	-704.04
-8.63	-738.25
-11.63	-840.83
-13.01	-838.10

Table 5: AWG PLC against mirror chromatic dispersion versus laser optical power

From this group delay linear fittings we can see a chromatic dispersion value of -680 [psec/nm] at the highest optical carrier power level, in agreement with the f_0 audio AC Voltage sweep measured results (see Tab. 6 on the following page), $f_0 V_{ac} = 1.929\text{Volt} -682.37$ [psec/nm]. According to the theoretical value this PLC should exhibit a chromatic dispersion of 530 [psec/nm]. Thus we have measured a discrepancy in the chromatic dispersion value. Once more this measured value is far from the theoretical value of 530 [psec/nm]. It is known that this AWG PLC has Polarization Dependent λ (PD λ) of 2dB.

We have measured the same experimental setup while maintaining a constant optical power of 3.37dBm, while sweeping the f_0 audio AC voltage see results in Fig. 48. The extracted chromatic dispersion values from the group delay linear fittings are summarized in Tab. 6.

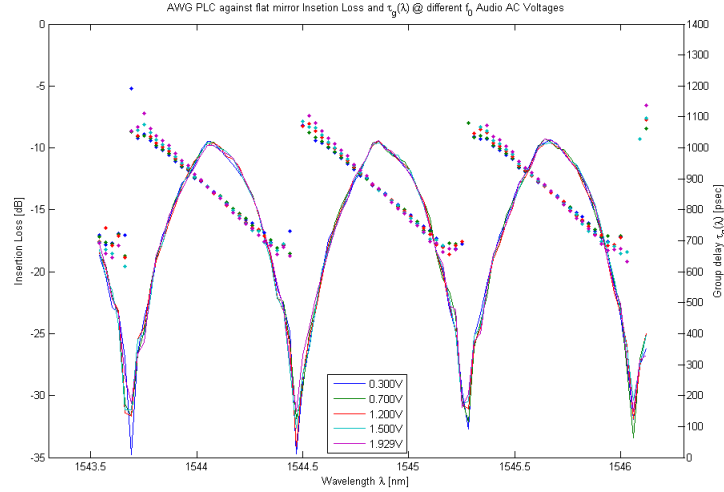


Figure 48: AWG PLC against mirror Insetion Loss and Group Delay versus f_0 audio AC Voltage

f_0 audio AC voltage [Volt]	Chromatic dispersion [ps/nm]
0.300	-566.09
0.7000	-579.61
1.200	-621.37
1.500	-630.74
1.929	-682.37

Table 6: AWG PLC against mirror chromatic dispersion versus f_0 audio AC voltage comparison

In order to estimate the 2nd order MPS with Audio optical dynamic range of the system we can define an error range of 5%. Therefore if we will consider the smallest attenuation (0.0dB) as a reliable measurement then five percent error (34 ps/nm) means that our optical dynamic range is at -5.63dBm (10 dB attenuation). Since the largest coupling in between the AWG PLC and the mirror is 10 dB as can be seen in the insetion loss curves in Fig. 46 on page 71.

In conclusion the 2nd order MPS with Audio apparatus has an optical dynamic range of 20.0dB or equivalently 3.2% error in chromatic dispersion extraction.

5.2.3 DWDM Demux

A final example of an optical component is a DWDM 20 channels 200 GHz spacing demux (Fig. 49). The MPS with Audio results are compared with a LUNA Optical Vector Analyzer (LUNA OVA model CTe), which is based on interferometer technique [10]. We have preformed characterization of ETEK Dynamics C-band 20 channels DWDM Demux (model no. DWDM2YM3CRV01) with the MPS with Audio technique using audio tone oscillating voltage ($V_{ac} = 1.2\text{Volt}$). In order to cover all the DWDM demux spectra we have decided to measure 3 channels: 1, 13 and 20. The Insetion Loss (IL) characterization and the chromatic dispersion agree in between the two techniques. Results at low IL compare well, whereas the phase estimates for the LUNA becomes unreliable at high IL values. 2nd order MPS demonstrates less noisy measurements in comparison with the LUNA.

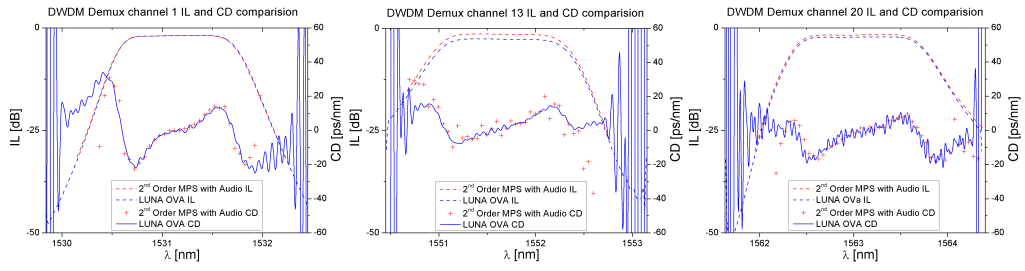


Figure 49: DWDM Demux 2nd order MPS with Audio & LUNA OVA insertion loss and chromatic dispersion comparison

The 2nd Order MPS with Audio technique has an electrical RF PM controllable comb which is been transported through the DUT optical spectra. As the audio oscillating voltage increased there is a slight drift in measuring the group delay absolute value see Fig. 51 left side. However when calculating the local group delay slope we can see that all these drifts are filtered out and that there is a good agreement no matter the chosen audio tone oscillating voltage see Fig. 51 right side.

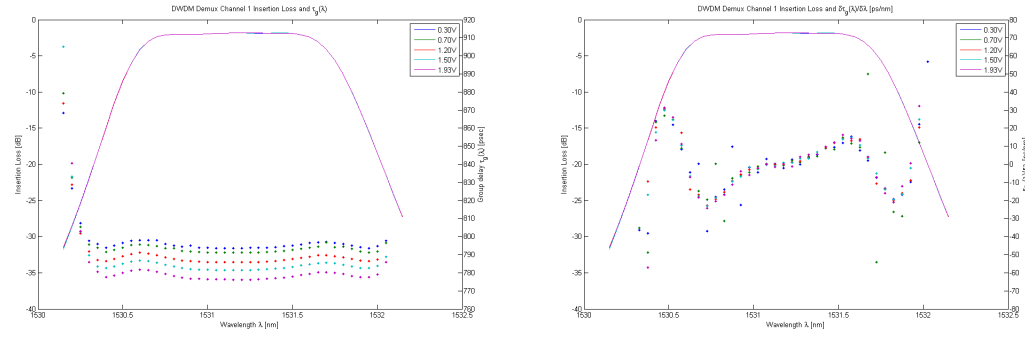


Figure 50: DWDM Demux channel 1 - 2nd Order MPS with Audio insertion loss, group delay and chromatic dispersion comparison

6 Conclusions and future research

We introduce a frequency dither of the RF modulation drive which drives the MZM, using a PM modulation at low (audio) frequency. Signal analysis of the system demonstrates that the audio phase information is preserved in the E/O/E conversion. In contrast to the MPS technique, we measure the RF phase accumulation with an harmonic term oscillatory at the audio frequency, instead of comparing phases of RF frequency. The measured phase term still depends on the phase delay experienced by the RF tones. We presented a full analytic response of the modified MPS technique, and compared it to the traditional small signal approximation. We performed optimization of the modulation depths and the MZM bias point in order to maximize the desired signal contribution, while suppressing the undesired contributions (see Appendix 3.2). The 2nd order MPS technique does not suffer from RF fading at all, since we extract the GD from the symmetric beat tone of the +1 and -1 sidetones, at a cost of lower signal amplitude in comparison with standard MPS.

Our approach exploits the high sensitivity and large dynamic range of a LIA to extract the low (audio) frequency amplitude. The RF frequency is used to sample the GD, while the audio frequency is used for the LIA measurement. Thus, enabling the use of a low RF driving frequency as necessary for precise measurement of components exhibiting fine spectral features such as microresonators and slow light devices.

Moreover, an elegant solution to the ambiguity problem typically found in phase measurements is suggested, with the help of the RF phase offset. We demonstrated that modifying the MPS technique by introducing the audio secondary modulation and using the LIA improves the GD measurement resolution in case of devices with fine spectral resolution. Also the apparatus can measure fine structure as well as long devices, as it isn't limited by coherence length. A comparison summarizing the differences in between MPS with Audio and 2nd order MPS with Audio in Tab. 7.

	MPS with Audio	2nd order MPS with Audio
Signal suffer from RF fading	Yes	No
Demodulation frequency	ν_0	$2\nu_0$
Electrical phase change	$360 \cdot D \cdot \nu_0 \cdot \Delta\lambda_0$	$360 \cdot D \cdot 2\nu_0 \cdot \Delta\lambda$
GD measurement without ambiguity	$(0, 1/[2\nu_0])$	$(0, 1/[4\nu_0])$

Table 7: Comparison table in between MPS with Audio and 2nd order MPS with Audio

In conclusion, the modified MPS technique was investigated and was successfully demonstrated in measurement of several component categories and fibers. The future work with the apparatus noise analysis of the apparatus can be conducted with HCN gas cell, which can be used as a known physical reference [34]. A polarization controller can be added to the apparatus as part of an all parameter station, to extract DUT's polarization dependencies. In order to avoid electrode charging and reduce drift in the measurement, the MZM can be driven with a slow varying AC signal instead of the DC signal (i.e. frequency component lower than the sweep rate of the RF phase shift DC bias).

References

- [1] Chapter 3, "Lightwave Technology Telecommunication Systems", G. P. Agrawal, John Wiley & Sons, 2005.
- [2] Section 8.6, "Principles of Optics", 7th ed., M. Born and E. Wolf, Cambridge University Press, New York, 1999.
- [3] G. Nykolak, G. Lenz, B. J. Eggleton, T. A. Strasser, "Impact of fiber grating dispersion on WDM system performance," OFC '98, Tech. Dig., vol. 2, pp. 4, TuA3, 1998.
- [4] Chapter 7, "Optical Fiber Telecommunication IIIA", I. P. Kaminov and T. L. Koch, Academic Press, pp. 162-195, 1997.
- [5] ITU: International Telecommunications Union, Recommendation G.650.
- [6] H. R. D. Sunak, "Single-mode fiber measurements," IEEE Trans. On Instru. and Meas., vol. 37, no. 4, 1988.
- [7] K. S. Abedin, M. Hyodo and N. Onodera, "Measurement of the chromatic dispersion of an optical fiber by use of a Sagnac interferometer employing asymmetric modulation," Optics Letters, vol. 25, no. 5, pp. 299-301, 2000.
- [8] M. Li and H. Li, "Chromatic dispersion measurement for multichannel FBG based on a novel asymmetrical Sagnac loop interferometer," IEEE Photonics Technology Letters, vol. 19, no. 20, pp. 1601-1603, 2007.
- [9] J. Y. Lee and D. Y. Kim, "Versatile chromatic dispersion measurement of a single mode fiber using spectral white light interferometry," Optics Express, vol. 14, no. 24, pp. 11608-11615, 2006.
- [10] D. K. Gifford, B. J. Soller, M. S. Wolfe, and M. E. Froggatt, "Optical vector network analyzer for single-scan measurements of loss, group delay, and polarization mode dispersion," Applied Optics, vol. 44, no. 34, pp. 7287-7286, 2006.
- [11] B. Luther-Davies, D. N. Payne and W. A. Gambling, "Evaluation of material dispersion in low loss phosphosilicate core optical fibres", Optics Communications, vol. 13, no. 1, pp. 84-88, 1975.
- [12] L. G. Cohen, "Comparison of single-mode fiber dispersion measurement techniques," J. of Lightwave Technology, vol. LT-3, no. 5, pp. 958-966, 1985.
- [13] Dennis Derickson, "Fiber optic test and measurement", Chapter 12, Englewood Cliffs, NJ: Prentice-Hall PTR, 1998.
- [14] S. Ryu, Y. Horiuchi and K. Mochizuki, "Novel chromatic dispersion measurement method over continuous gigahertz tuning range," J. of Lightwave Technology, vol. 7, no. 8, pp. 1177-1180, 1989.
- [15] G. Genty, T. Niemi, and H. Ludvigsen, "New method to improve the accuracy of group-delay measurements using the phase-shift technique," Optics Communications, vol. 204, pp. 119-126, 2002.

- [16] Chapter 2, "Lightwave Technology Telecommunication Systems", G. P. Agrawal, John Wiley & Sons, 2005.
- [17] F. Koyama and K. Iga, "Frequency chirping in external modulators," *J. of Lightwave Technology*, vol 6, no. 1, pp. 87-93, 1988
- [18] P. Hernday, "Measuring the group delay characteristics of narrow-band devices by the modulation phase shift method," *App. Eng. White Paper Agilent*, 2002.
- [19] T. Niemi, M. Uusimaa and H. Ludvigsen, "Limitations of the phase shift method in measuring dense group delay ripple in fiber Bragg grating," *IEEE Photonics Technology Letters*, vol.13, no.12, p.1334-1336, 2001.
- [20] B. Christensen, J. Mark G. Jacobsen and E. Bodtker, "Simple dispersion measurement technique with high resolution," *Electronics Letters*, vol. 29, no. 1, pp. 132-132, 1993.
- [21] C. K. Madsen, "Chromatic and polarization mode dispersion measurement technique using phase-sensitive sideband detection", *Optical Fiber Communication Conference (OFC) 2001*, MO6-1, 2001.
- [22] R. Fortenberry, W. V. Sorin and P. Hernday, "Improvement of group delay measurement accuracy using a two-frequency modulation phase-shift method," *IEEE Photonics Technology Letters*, vol 15, no. 5, pp.736-738, 2003.
- [23] R. M. Fortenberry, "Enhanced wavelength resolution chromatic dispersion measurements using fixed sideband technique", *Conf. on Optical Fiber Communication, OSA Technical Digest Series (Optical Society of America)*, Washington DC, TuG8, pp. 107-109, 2000.
- [24] J. H. Lee, Y. Noboru, T. Tsuritani, and T. Otani, "Link Performance Monitoring Technique for Measuring Residual Chromatic Dispersion of Optical Links," *IEEE Photonics Technology Letters*, vol. 20, no. 21, pp. 1751-1753, 2008.
- [25] H. Schmuck, "Comparison of optical millimetre-wave system concepts with regard to chromatic dispersion", *Electronics Letters*, vol. 31, no. 21, pp. 1848-1849, 1995.
- [26] J. Marti, J. M. Fuster and R. I. Laming, "Experimental reduction of chromatic dispersion effects in lightwave microwave/millimeter-wave transmissions using tapered linearly chirped fibre gratings," *Electronics Letters*, vol. 33, no. 13, pp. 1170-1171, 1997.
- [27] G. H. Smith, D. Novak and Z. Ahmed, "Technique for optical SSB generation to overcome dispersion penalties in fibre-radio systems," *Electronics Letters*, vol. 33, no. 1, pp 74-75, 1997.
- [28] K. Yonenaga and N. Takachio, "A fiber chromatic dispersion compensation technique with an optical SSB transmission in optical homodyne detection systems," *IEEE Photonics Technology Letters*, vol. 5, no. 8, pp. 949-951, 1993.
- [29] J. E. Roman, M. Y. Frankel and R. D. Esman, "Spectral characterization of fiber gratings with high resolution," *Optics Letters*, vol. 23, no. 12, pp 939-941, 1998.
- [30] T. Niemi, G. Genty and H. Ludvigsen, "Group-delay measurements using the phase-shift method: improvement on the accuracy," *Proc. 27th Eur. Conf. on Opt. Comm. (ECOC'01 Amsterdam)*, 2001.

- [31] Y. Shi, L. Yan and A. E. Wilner, "High-speed electrooptic modulator characterization using optical spectrum analysis," *J. Lightwave Technology*, vol. 21, no. 10, pp. 2358-2367, 2003.
- [32] D. Sinefeld and D. M. Marom, "Colorless photonic spectral processor using hybrid guided-wave/free-space optics arrangement and LCoS modulator," in *Optical Fiber Communication Conference, OSA Technical Digest (CD)* (Optical Society of America, 2009), paper OThB4.
- [33] D. M. Marom, C. R. Doerr, M. A. Cappuzzo, E. Y. Chen, A. Wong-Foy, L. T. Gomez, and S. Chandrasekhar, "Compact colorless tunable dispersion compensator with 1000-ps/nm tuning range for 40-Gb/s data rates," *J. Lightwave Technology*, vol. 24, no. 1, pp. 237-241, 2006.
- [34] T. Dennis and P. A. Williams, "Achieving high absolute accuracy for group-delay measurements using the modulation phase-shift technique," *J. Lightwave Technology*, vol. 23, no. 11, pp. 3748-3754, 2005.

7 Appendix A: Modified MPS - photocurrent simplification

We recall the expression for the optical power reaching a detector (being proportional to generated photocurrent):

$$\begin{aligned}
P(t) &= Y(t) \cdot Y^*(t) = \frac{E_0}{4} B(\Omega_0)^2 \cdot \left[1 + \right. \\
&- e^{-j\alpha} \sum_{m,n=-\infty}^{\infty} J_m(\beta) J_n(m\psi) e^{-j(m\gamma+n\delta)} e^{-j\frac{1}{2}\ddot{\phi}(m\nu_0+n f_0)^2} e^{-j(m\nu_0+n f_0)(\dot{\phi}+t)} + \\
&- e^{j\alpha} \sum_{m,n=-\infty}^{\infty} J_m(\beta) J_n(m\psi) e^{j(m\gamma+n\delta)} e^{j\frac{1}{2}\ddot{\phi}(m\nu_0+n f_0)^2} e^{j(m\nu_0+n f_0)(\dot{\phi}+t)} + \\
&+ \sum_{\substack{m,n,p,q \\ =-\infty}}^{\infty} J_m(\beta) J_n(m\psi) J_p(\beta) J_q(p\psi) e^{j[(m-p)\gamma+(n-q)\delta]} e^{j[(m-p)\nu_0+(n-q)f_0](\dot{\phi}+t)} \\
&\left. \cdot e^{j\frac{1}{2}\ddot{\phi}[(m^2-p^2)\nu_0^2+2(mn-pq)\nu_0 f_0+(n^2-q^2)f_0^2]} \right].
\end{aligned}$$

In order to deal with the two infinite sum terms we will use the following approach, taking each infinite sum to 2 sums while substituting a variable with its minus variable on one of the infinite sums.

$$\begin{aligned}
&- e^{-j\alpha} \sum_{k,n=-\infty}^{\infty} J_k(\beta) J_n(k\psi) e^{-j[k(\nu_0(\dot{\phi}+t)+\gamma)]} \cdot e^{-j\frac{1}{2}\ddot{\phi}(k\nu_0+n f_0)^2} \cdot e^{-j[n(f_0(\dot{\phi}+t)+\delta)]} \\
&- e^{j\alpha} \sum_{k,n=-\infty}^{\infty} J_k(\beta) J_n(k\psi) e^{j[k(\nu_0(\dot{\phi}+t)+\gamma)]} \cdot e^{j\frac{1}{2}\ddot{\phi}(k\nu_0+n f_0)^2} \cdot e^{j[n(f_0(\dot{\phi}+t)+\delta)]} \\
&= -\frac{1}{2} e^{-j\alpha} \sum_{k,n=-\infty}^{\infty} J_k(\beta) J_n(k\psi) e^{-j[k(\nu_0(\dot{\phi}+t)+\gamma)]} \cdot e^{-j\frac{1}{2}\ddot{\phi}(k\nu_0+n f_0)^2} \cdot e^{-j[n(f_0(\dot{\phi}+t)+\delta)]} \\
&- \frac{1}{2} e^{-j\alpha} \sum_{k,n=-\infty}^{\infty} J_{-k}(\beta) J_n(-k\psi) e^{-j[-k(\nu_0(\dot{\phi}+t)+\gamma)]} \cdot e^{-j\frac{1}{2}\ddot{\phi}(-k\nu_0+n f_0)^2} \cdot e^{-j[n(f_0(\dot{\phi}+t)+\delta)]} \\
&- \frac{1}{2} e^{j\alpha} \sum_{k,n=-\infty}^{\infty} J_k(\beta) J_n(k\psi) e^{j[k(\nu_0(\dot{\phi}+t)+\gamma)]} \cdot e^{j\frac{1}{2}\ddot{\phi}(k\nu_0+n f_0)^2} \cdot e^{j[n(f_0(\dot{\phi}+t)+\delta)]} \\
&- \frac{1}{2} e^{j\alpha} \sum_{k,n=-\infty}^{\infty} J_{-k}(\beta) J_n(-k\psi) e^{j[-k(\nu_0(\dot{\phi}+t)+\gamma)]} \cdot e^{j\frac{1}{2}\ddot{\phi}(-k\nu_0+n f_0)^2} \cdot e^{j[n(f_0(\dot{\phi}+t)+\delta)]} \\
&= -\frac{1}{4} e^{-j\alpha} \sum_{k,n=-\infty}^{\infty} J_k(\beta) J_n(k\psi) e^{-j[k(\nu_0(\dot{\phi}+t)+\gamma)]} \cdot e^{-j\frac{1}{2}\ddot{\phi}(k\nu_0+n f_0)^2} \cdot e^{-j[n(f_0(\dot{\phi}+t)+\delta)]} \\
&- \frac{1}{4} e^{-j\alpha} \sum_{k,n=-\infty}^{\infty} J_k(\beta) J_{-n}(k\psi) e^{-j[k(\nu_0(\dot{\phi}+t)+\gamma)]} \cdot e^{-j\frac{1}{2}\ddot{\phi}(k\nu_0-n f_0)^2} \cdot e^{j[n(f_0(\dot{\phi}+t)+\delta)]} \\
&- \frac{1}{4} e^{-j\alpha} \sum_{k,n=-\infty}^{\infty} J_{-k}(\beta) J_n(-k\psi) e^{j[k(\nu_0(\dot{\phi}+t)+\gamma)]} \cdot e^{-j\frac{1}{2}\ddot{\phi}(-k\nu_0+n f_0)^2} \cdot e^{-j[n(f_0(\dot{\phi}+t)+\delta)]} \\
&- \frac{1}{4} e^{-j\alpha} \sum_{k,n=-\infty}^{\infty} J_{-k}(\beta) J_{-n}(-k\psi) e^{j[k(\nu_0(\dot{\phi}+t)+\gamma)]} \cdot e^{-j\frac{1}{2}\ddot{\phi}(-k\nu_0-n f_0)^2} \cdot e^{j[n(f_0(\dot{\phi}+t)+\delta)]} \\
&- \frac{1}{4} e^{j\alpha} \sum_{k,n=-\infty}^{\infty} J_k(\beta) J_n(k\psi) e^{j[k(\nu_0(\dot{\phi}+t)+\gamma)]} \cdot e^{j\frac{1}{2}\ddot{\phi}(k\nu_0+n f_0)^2} \cdot e^{j[n(f_0(\dot{\phi}+t)+\delta)]}
\end{aligned}$$

$$\begin{aligned}
& -\frac{1}{4}e^{j\alpha} \sum_{k,n=-\infty}^{\infty} J_k(\beta)J_{-n}(k\psi)e^{j[k(\nu_0(\dot{\phi}+t)+\gamma)]} \cdot e^{j\frac{1}{2}\ddot{\phi}(k\nu_0-nf_0)^2} \cdot e^{-j[n(f_0(\dot{\phi}+t)+\delta)]} \\
& -\frac{1}{4}e^{j\alpha} \sum_{k,n=-\infty}^{\infty} J_{-k}(\beta)J_n(-k\psi)e^{-j[k(\nu_0(\dot{\phi}+t)+\gamma)]} \cdot e^{j\frac{1}{2}\ddot{\phi}(-k\nu_0+nf_0)^2} \cdot e^{j[n(f_0(\dot{\phi}+t)+\delta)]} \\
& -\frac{1}{4}e^{j\alpha} \sum_{k,n=-\infty}^{\infty} J_{-k}(\beta)J_{-n}(-k\psi)e^{-j[k(\nu_0(\dot{\phi}+t)+\gamma)]} \cdot e^{j\frac{1}{2}\ddot{\phi}(-k\nu_0-nf_0)^2} \cdot e^{-j[n(f_0(\dot{\phi}+t)+\delta)]}
\end{aligned}$$

Using $J_{-n}(x) = (-1)^n \cdot J_n(x)$ and $J_n(-x) = (-1)^n \cdot J_n(x)$

$$\begin{aligned}
& = -\frac{1}{4}e^{-j\alpha} \sum_{k,n=-\infty}^{\infty} J_k(\beta)J_n(k\psi)e^{-j[k(\nu_0(\dot{\phi}+t)+\gamma)]} \cdot e^{-j\frac{1}{2}\ddot{\phi}(k\nu_0+nf_0)^2} \cdot e^{-j[n(f_0(\dot{\phi}+t)+\delta)]} \\
& -\frac{1}{4}e^{-j\alpha} \sum_{k,n=-\infty}^{\infty} (-1)^n J_k(\beta)J_n(k\psi)e^{-j[k(\nu_0(\dot{\phi}+t)+\gamma)]} \cdot e^{-j\frac{1}{2}\ddot{\phi}(k\nu_0-nf_0)^2} \cdot e^{j[n(f_0(\dot{\phi}+t)+\delta)]} \\
& -\frac{1}{4}e^{-j\alpha} \sum_{k,n=-\infty}^{\infty} (-1)^{k+n} J_k(\beta)J_n(k\psi)e^{j[k(\nu_0(\dot{\phi}+t)+\gamma)]} \cdot e^{-j\frac{1}{2}\ddot{\phi}(k\nu_0-nf_0)^2} \cdot e^{-j[n(f_0(\dot{\phi}+t)+\delta)]} \\
& -\frac{1}{4}e^{-j\alpha} \sum_{k,n=-\infty}^{\infty} (-1)^{2n+k} J_k(\beta)J_n(k\psi)e^{j[k(\nu_0(\dot{\phi}+t)+\gamma)]} \cdot e^{-j\frac{1}{2}\ddot{\phi}(k\nu_0+nf_0)^2} \cdot e^{j[n(f_0(\dot{\phi}+t)+\delta)]} \\
& -\frac{1}{4}e^{j\alpha} \sum_{k,n=-\infty}^{\infty} J_k(\beta)J_n(k\psi)e^{j[k(\nu_0(\dot{\phi}+t)+\gamma)]} \cdot e^{j\frac{1}{2}\ddot{\phi}(k\nu_0+nf_0)^2} \cdot e^{j[n(f_0(\dot{\phi}+t)+\delta)]} \\
& -\frac{1}{4}e^{j\alpha} \sum_{k,n=-\infty}^{\infty} (-1)^n J_k(\beta)J_n(k\psi)e^{j[k(\nu_0(\dot{\phi}+t)+\gamma)]} \cdot e^{j\frac{1}{2}\ddot{\phi}(k\nu_0-nf_0)^2} \cdot e^{-j[n(f_0(\dot{\phi}+t)+\delta)]} \\
& -\frac{1}{4}e^{j\alpha} \sum_{k,n=-\infty}^{\infty} (-1)^{k+n} J_k(\beta)J_n(k\psi)e^{-j[k(\nu_0(\dot{\phi}+t)+\gamma)]} \cdot e^{j\frac{1}{2}\ddot{\phi}(k\nu_0-nf_0)^2} \cdot e^{j[n(f_0(\dot{\phi}+t)+\delta)]} \\
& -\frac{1}{4}e^{j\alpha} \sum_{k,n=-\infty}^{\infty} (-1)^{2n+k} J_k(\beta)J_n(k\psi)e^{-j[k(\nu_0(\dot{\phi}+t)+\gamma)]} \cdot e^{j\frac{1}{2}\ddot{\phi}(k\nu_0+nf_0)^2} \cdot e^{-j[n(f_0(\dot{\phi}+t)+\delta)]}
\end{aligned}$$

Now we can rearrange the expression, with the same terms of optical bias point and RF fading due to dispersion.

$$\begin{aligned}
& = -\frac{1}{4}e^{-j\alpha} \sum_{k,n=-\infty}^{\infty} J_k(\beta)J_n(k\psi)e^{-j[k(\nu_0(\dot{\phi}+t)+\gamma)]} \cdot e^{-j\frac{1}{2}\ddot{\phi}(k\nu_0+nf_0)^2} \cdot e^{-j[n(f_0(\dot{\phi}+t)+\delta)]} \\
& -\frac{1}{4}e^{-j\alpha} \sum_{k,n=-\infty}^{\infty} (-1)^{2n+k} J_k(\beta)J_n(k\psi)e^{j[k(\nu_0(\dot{\phi}+t)+\gamma)]} \cdot e^{-j\frac{1}{2}\ddot{\phi}(k\nu_0+nf_0)^2} \cdot e^{j[n(f_0(\dot{\phi}+t)+\delta)]} \\
& -\frac{1}{4}e^{-j\alpha} \sum_{k,n=-\infty}^{\infty} (-1)^n J_k(\beta)J_n(k\psi)e^{-j[k(\nu_0(\dot{\phi}+t)+\gamma)]} \cdot e^{-j\frac{1}{2}\ddot{\phi}(k\nu_0-nf_0)^2} \cdot e^{j[n(f_0(\dot{\phi}+t)+\delta)]} \\
& -\frac{1}{4}e^{-j\alpha} \sum_{k,n=-\infty}^{\infty} (-1)^{k+n} J_k(\beta)J_n(k\psi)e^{j[k(\nu_0(\dot{\phi}+t)+\gamma)]} \cdot e^{-j\frac{1}{2}\ddot{\phi}(k\nu_0-nf_0)^2} \cdot e^{-j[n(f_0(\dot{\phi}+t)+\delta)]} \\
& -\frac{1}{4}e^{j\alpha} \sum_{k,n=-\infty}^{\infty} J_k(\beta)J_n(k\psi)e^{j[k(\nu_0(\dot{\phi}+t)+\gamma)]} \cdot e^{j\frac{1}{2}\ddot{\phi}(k\nu_0+nf_0)^2} \cdot e^{j[n(f_0(\dot{\phi}+t)+\delta)]} \\
& -\frac{1}{4}e^{j\alpha} \sum_{k,n=-\infty}^{\infty} (-1)^{2n+k} J_k(\beta)J_n(k\psi)e^{-j[k(\nu_0(\dot{\phi}+t)+\gamma)]} \cdot e^{j\frac{1}{2}\ddot{\phi}(k\nu_0+nf_0)^2} \cdot e^{-j[n(f_0(\dot{\phi}+t)+\delta)]} \\
& -\frac{1}{4}e^{j\alpha} \sum_{k,n=-\infty}^{\infty} (-1)^n J_k(\beta)J_n(k\psi)e^{j[k(\nu_0(\dot{\phi}+t)+\gamma)]} \cdot e^{j\frac{1}{2}\ddot{\phi}(k\nu_0-nf_0)^2} \cdot e^{-j[n(f_0(\dot{\phi}+t)+\delta)]}
\end{aligned}$$

$$-\frac{1}{4}e^{j\alpha} \sum_{k,n=-\infty}^{\infty} (-1)^{k+n} J_k(\beta) J_n(k\psi) e^{-j[k(\nu_0(\dot{\phi}+t)+\gamma)]} \cdot e^{j\frac{1}{2}\ddot{\phi}(k\nu_0-nf_0)^2} \cdot e^{j[n(f_0(\dot{\phi}+t)+\delta)]}$$

Making this expression simpler

$$\begin{aligned} &= -\frac{1}{4}e^{-j\alpha} \sum_{k,n=-\infty}^{\infty} J_k(\beta) J_n(k\psi) \cdot e^{-j\frac{1}{2}\ddot{\phi}(k\nu_0+nf_0)^2} \cdot [e^{-j[k(\nu_0(\dot{\phi}+t)+\gamma)]} \cdot e^{-j[n(f_0(\dot{\phi}+t)+\delta)]} \\ &+ (-1)^{2n+k} e^{j[k(\nu_0(\dot{\phi}+t)+\gamma)]} \cdot e^{j[n(f_0(\dot{\phi}+t)+\delta)]}] \\ &-\frac{1}{4}e^{-j\alpha} \sum_{k,n=-\infty}^{\infty} J_k(\beta) J_n(k\psi) \cdot e^{-j\frac{1}{2}\ddot{\phi}(k\nu_0-nf_0)^2} \cdot [(-1)^n e^{-j[k(\nu_0(\dot{\phi}+t)+\gamma)]} \cdot e^{j[n(f_0(\dot{\phi}+t)+\delta)]} \\ &+ (-1)^{n+k} e^{j[k(\nu_0(\dot{\phi}+t)+\gamma)]} \cdot e^{-j[n(f_0(\dot{\phi}+t)+\delta)]}] \\ &-\frac{1}{4}e^{j\alpha} \sum_{k,n=-\infty}^{\infty} J_k(\beta) J_n(k\psi) \cdot e^{j\frac{1}{2}\ddot{\phi}(k\nu_0+nf_0)^2} \cdot [e^{j[k(\nu_0(\dot{\phi}+t)+\gamma)]} \cdot e^{j[n(f_0(\dot{\phi}+t)+\delta)]} \\ &+ (-1)^{2n+k} e^{-j[k(\nu_0(\dot{\phi}+t)+\gamma)]} \cdot e^{-j[n(f_0(\dot{\phi}+t)+\delta)]}] \\ &-\frac{1}{4}e^{j\alpha} \sum_{k,n=-\infty}^{\infty} J_k(\beta) J_n(k\psi) \cdot e^{j\frac{1}{2}\ddot{\phi}(k\nu_0-nf_0)^2} \cdot [(-1)^{n+k} e^{-j[k(\nu_0(\dot{\phi}+t)+\gamma)]} \cdot e^{j[n(f_0(\dot{\phi}+t)+\delta)]} \\ &+ (-1)^n e^{j[k(\nu_0(\dot{\phi}+t)+\gamma)]} \cdot e^{-j[n(f_0(\dot{\phi}+t)+\delta)]}] \end{aligned}$$

we need to distinguish in between the following cases

$$(-1)^{2n+k} = \begin{cases} 1 & k \text{ even} \\ -1 & k \text{ odd} \end{cases}$$

$$(-1)^n = \begin{cases} 1 & n \text{ even} \\ -1 & n \text{ odd} \end{cases}$$

$$(-1)^{n+k} = \begin{cases} 1 & n \text{ even, } k \text{ even} \\ -1 & n \text{ odd, } k \text{ odd} \\ -1 & n \text{ odd, } k \text{ even} \\ 1 & n \text{ even, } k \text{ odd} \end{cases} \text{ or } \begin{cases} n \text{ odd, } k \text{ odd} \\ n \text{ even, } k \text{ odd} \end{cases}$$

k even, n even case

$$\begin{aligned}
&= -\frac{1}{4}e^{-j\alpha} \sum_{k,n=-\infty}^{\infty} J_k(\beta)J_n(k\psi) \cdot e^{-j\frac{1}{2}\ddot{\phi}(k\nu_0+nf_0)^2} \cdot [e^{-j[k(\nu_0(\dot{\phi}+t)+\gamma)]} \cdot e^{-j[n(f_0(\dot{\phi}+t)+\delta)]} \\
&\quad + e^{j[k(\nu_0(\dot{\phi}+t)+\gamma)]} \cdot e^{j[n(f_0(\dot{\phi}+t)+\delta)]}] \\
&-\frac{1}{4}e^{-j\alpha} \sum_{k,n=-\infty}^{\infty} J_k(\beta)J_n(k\psi) \cdot e^{-j\frac{1}{2}\ddot{\phi}(k\nu_0-nf_0)^2} \cdot [e^{-j[k(\nu_0(\dot{\phi}+t)+\gamma)]} \cdot e^{j[n(f_0(\dot{\phi}+t)+\delta)]} \\
&\quad + e^{j[k(\nu_0(\dot{\phi}+t)+\gamma)]} \cdot e^{-j[n(f_0(\dot{\phi}+t)+\delta)]}] \\
&-\frac{1}{4}e^{j\alpha} \sum_{k,n=-\infty}^{\infty} J_k(\beta)J_n(k\psi) \cdot e^{j\frac{1}{2}\ddot{\phi}(k\nu_0+nf_0)^2} \cdot [e^{j[k(\nu_0(\dot{\phi}+t)+\gamma)]} \cdot e^{j[n(f_0(\dot{\phi}+t)+\delta)]} \\
&\quad + e^{-j[k(\nu_0(\dot{\phi}+t)+\gamma)]} \cdot e^{-j[n(f_0(\dot{\phi}+t)+\delta)]}] \\
&-\frac{1}{4}e^{j\alpha} \sum_{k,n=-\infty}^{\infty} J_k(\beta)J_n(k\psi) \cdot e^{j\frac{1}{2}\ddot{\phi}(k\nu_0-nf_0)^2} \cdot [e^{-j[k(\nu_0(\dot{\phi}+t)+\gamma)]} \cdot e^{j[n(f_0(\dot{\phi}+t)+\delta)]} \\
&\quad + e^{j[k(\nu_0(\dot{\phi}+t)+\gamma)]} \cdot e^{-j[n(f_0(\dot{\phi}+t)+\delta)]}] \\
&= -\frac{1}{2}e^{-j\alpha} \sum_{k,n=-\infty}^{\infty} J_k(\beta)J_n(k\psi) \cdot e^{-j\frac{1}{2}\ddot{\phi}(k\nu_0+nf_0)^2} \cdot \cos[(k\nu_0+nf_0)(\dot{\phi}+t)+k\gamma+n\delta] \\
&\quad -\frac{1}{2}e^{-j\alpha} \sum_{k,n=-\infty}^{\infty} J_k(\beta)J_n(k\psi) \cdot e^{-j\frac{1}{2}\ddot{\phi}(k\nu_0-nf_0)^2} \cdot \cos[(k\nu_0-nf_0)(\dot{\phi}+t)+k\gamma-n\delta] \\
&\quad -\frac{1}{2}e^{j\alpha} \sum_{k,n=-\infty}^{\infty} J_k(\beta)J_n(k\psi) \cdot e^{j\frac{1}{2}\ddot{\phi}(k\nu_0+nf_0)^2} \cdot \cos[(k\nu_0+nf_0)(\dot{\phi}+t)+k\gamma+n\delta] \\
&\quad -\frac{1}{2}e^{j\alpha} \sum_{k,n=-\infty}^{\infty} J_k(\beta)J_n(k\psi) \cdot e^{j\frac{1}{2}\ddot{\phi}(k\nu_0-nf_0)^2} \cdot \cos[(k\nu_0-nf_0)(\dot{\phi}+t)+k\gamma-n\delta] \\
&= -\frac{1}{2} \sum_{k,n=-\infty}^{\infty} J_k(\beta)J_n(k\psi) \cdot \cos[(k\nu_0+nf_0)(\dot{\phi}+t)+k\gamma+n\delta] \\
&\quad \cdot [e^{j[\alpha+\frac{1}{2}\ddot{\phi}(k\nu_0+nf_0)^2]} + e^{-j[\alpha+\frac{1}{2}\ddot{\phi}(k\nu_0+nf_0)^2]}] \\
&\quad -\frac{1}{2} \sum_{k,n=-\infty}^{\infty} J_k(\beta)J_n(k\psi) \cdot \cos[(k\nu_0-nf_0)(\dot{\phi}+t)+k\gamma-n\delta] \\
&\quad \cdot [e^{j[\alpha+\frac{1}{2}\ddot{\phi}(k\nu_0-nf_0)^2]} + e^{-j[\alpha+\frac{1}{2}\ddot{\phi}(k\nu_0-nf_0)^2]}] \\
&= - \sum_{k,n=-\infty}^{\infty} J_k(\beta)J_n(k\psi) \cdot \cos[(k\nu_0+nf_0)(\dot{\phi}+t)+k\gamma+n\delta] \\
&\quad \cdot \cos[\alpha+\frac{1}{2}\ddot{\phi}(k\nu_0+nf_0)^2] \\
&\quad - \sum_{k,n=-\infty}^{\infty} J_k(\beta)J_n(k\psi) \cdot \cos[(k\nu_0-nf_0)(\dot{\phi}+t)+k\gamma-n\delta] \\
&\quad \cdot \cos[\alpha+\frac{1}{2}\ddot{\phi}(k\nu_0-nf_0)^2]
\end{aligned}$$

substituting n=-n

$$= - \sum_{k,n=-\infty}^{\infty} J_k(\beta)J_n(k\psi) \cdot \cos[(k\nu_0+nf_0)(\dot{\phi}+t)+k\gamma+n\delta]$$

$$\begin{aligned} & \cdot \cos[\alpha + \frac{1}{2}\ddot{\phi}(k\nu_0 + nf_0)^2] \\ & - \sum_{k,n=-\infty}^{\infty} J_k(\beta)J_{-n}(k\psi) \cdot \cos[(k\nu_0 + nf_0)(\dot{\phi} + t) + k\gamma + n\delta] \end{aligned}$$

$$\cdot \cos[\alpha + \frac{1}{2}\ddot{\phi}(k\nu_0 + nf_0)^2]$$

since n even

$$= -2 \cdot \sum_{k,n=-\infty}^{\infty} J_k(\beta)J_n(k\psi) \cdot \cos[(k\nu_0 + nf_0)(\dot{\phi} + t) + k\gamma + n\delta]$$

$$\cdot \cos[\alpha + \frac{1}{2}\ddot{\phi}(k\nu_0 + nf_0)^2].$$

k even, n odd case

$$= -\frac{1}{4}e^{-j\alpha} \sum_{k,n=-\infty}^{\infty} J_k(\beta)J_n(k\psi) \cdot e^{-j\frac{1}{2}\ddot{\phi}(k\nu_0 + nf_0)^2} \cdot [e^{-j[k(\nu_0(\dot{\phi}+t)+\gamma)]} \cdot e^{-j[n(f_0(\dot{\phi}+t)+\delta)]}$$

$$+ e^{j[k(\nu_0(\dot{\phi}+t)+\gamma)]} \cdot e^{j[n(f_0(\dot{\phi}+t)+\delta)]}]$$

$$- \frac{1}{4}e^{-j\alpha} \sum_{k,n=-\infty}^{\infty} J_k(\beta)J_n(k\psi) \cdot e^{-j\frac{1}{2}\ddot{\phi}(k\nu_0 - nf_0)^2} \cdot [-e^{-j[k(\nu_0(\dot{\phi}+t)+\gamma)]} \cdot e^{j[n(f_0(\dot{\phi}+t)+\delta)]}$$

$$- e^{j[k(\nu_0(\dot{\phi}+t)+\gamma)]} \cdot e^{-j[n(f_0(\dot{\phi}+t)+\delta)]}]$$

$$- \frac{1}{4}e^{j\alpha} \sum_{k,n=-\infty}^{\infty} J_k(\beta)J_n(k\psi) \cdot e^{j\frac{1}{2}\ddot{\phi}(k\nu_0 + nf_0)^2} \cdot [e^{j[k(\nu_0(\dot{\phi}+t)+\gamma)]} \cdot e^{j[n(f_0(\dot{\phi}+t)+\delta)]}$$

$$+ e^{-j[k(\nu_0(\dot{\phi}+t)+\gamma)]} \cdot e^{-j[n(f_0(\dot{\phi}+t)+\delta)]}]$$

$$- \frac{1}{4}e^{j\alpha} \sum_{k,n=-\infty}^{\infty} J_k(\beta)J_n(k\psi) \cdot e^{j\frac{1}{2}\ddot{\phi}(k\nu_0 - nf_0)^2} \cdot [-e^{-j[k(\nu_0(\dot{\phi}+t)+\gamma)]} \cdot e^{j[n(f_0(\dot{\phi}+t)+\delta)]}$$

$$- e^{j[k(\nu_0(\dot{\phi}+t)+\gamma)]} \cdot e^{-j[n(f_0(\dot{\phi}+t)+\delta)]}]$$

$$= -\frac{1}{2}e^{-j\alpha} \sum_{k,n=-\infty}^{\infty} J_k(\beta)J_n(k\psi) \cdot e^{-j\frac{1}{2}\ddot{\phi}(k\nu_0 + nf_0)^2} \cdot \cos[(k\nu_0 + nf_0)(\dot{\phi} + t) + k\gamma + n\delta]$$

$$+ \frac{1}{2}e^{-j\alpha} \sum_{k,n=-\infty}^{\infty} J_k(\beta)J_n(k\psi) \cdot e^{-j\frac{1}{2}\ddot{\phi}(k\nu_0 - nf_0)^2} \cdot \cos[(k\nu_0 - nf_0)(\dot{\phi} + t) + k\gamma - n\delta]$$

$$- \frac{1}{2}e^{j\alpha} \sum_{k,n=-\infty}^{\infty} J_k(\beta)J_n(k\psi) \cdot e^{j\frac{1}{2}\ddot{\phi}(k\nu_0 + nf_0)^2} \cdot \cos[(k\nu_0 + nf_0)(\dot{\phi} + t) + k\gamma + n\delta]$$

$$+ \frac{1}{2}e^{j\alpha} \sum_{k,n=-\infty}^{\infty} J_k(\beta)J_n(k\psi) \cdot e^{j\frac{1}{2}\ddot{\phi}(k\nu_0 - nf_0)^2} \cdot \cos[(k\nu_0 - nf_0)(\dot{\phi} + t) + k\gamma - n\delta]$$

$$= -\frac{1}{2} \sum_{k,n=-\infty}^{\infty} J_k(\beta)J_n(k\psi) \cdot \cos[(k\nu_0 + nf_0)(\dot{\phi} + t) + k\gamma + n\delta]$$

$$\cdot [e^{j[\alpha + \frac{1}{2}\ddot{\phi}(k\nu_0 + nf_0)^2]} + e^{-[\alpha + j\frac{1}{2}\ddot{\phi}(k\nu_0 + nf_0)^2]}]$$

$$+ \frac{1}{2} \sum_{k,n=-\infty}^{\infty} J_k(\beta)J_n(k\psi) \cdot \cos[(k\nu_0 - nf_0)(\dot{\phi} + t) + k\gamma - n\delta]$$

$$\cdot [e^{j[\alpha + j\frac{1}{2}\ddot{\phi}(k\nu_0 - nf_0)^2]} + e^{-j[\alpha + j\frac{1}{2}\ddot{\phi}(k\nu_0 - nf_0)^2]}]$$

$$\begin{aligned}
&= - \sum_{k,n=-\infty}^{\infty} J_k(\beta) J_n(k\psi) \cdot \cos[(k\nu_0 + nf_0)(\dot{\phi} + t) + k\gamma + n\delta] \\
&\cdot \cos[\alpha + \frac{1}{2}\ddot{\phi}(k\nu_0 + nf_0)^2] \\
&+ \sum_{k,n=-\infty}^{\infty} J_k(\beta) J_n(k\psi) \cdot \cos[(k\nu_0 - nf_0)(\dot{\phi} + t) + k\gamma - n\delta] \\
&\cdot \cos[\alpha + j\frac{1}{2}\ddot{\phi}(k\nu_0 - nf_0)^2]
\end{aligned}$$

substituting n=-n

$$\begin{aligned}
&= - \sum_{k,n=-\infty}^{\infty} J_k(\beta) J_n(k\psi) \cdot \cos[(k\nu_0 + nf_0)(\dot{\phi} + t) + k\gamma + n\delta] \\
&\cdot \cos[\alpha + \frac{1}{2}\ddot{\phi}(k\nu_0 + nf_0)^2] \\
&+ \sum_{k,n=-\infty}^{\infty} J_k(\beta) J_{-n}(k\psi) \cdot \cos[(k\nu_0 + nf_0)(\dot{\phi} + t) + k\gamma + n\delta] \\
&\cdot \cos[\alpha + j\frac{1}{2}\ddot{\phi}(k\nu_0 + nf_0)^2]
\end{aligned}$$

since n odd

$$\begin{aligned}
&= -2 \cdot \sum_{k,n=-\infty}^{\infty} J_k(\beta) J_n(k\psi) \cdot \cos[(k\nu_0 + nf_0)(\dot{\phi} + t) + k\gamma + n\delta] \\
&\cdot \cos[\alpha + \frac{1}{2}\ddot{\phi}(k\nu_0 + nf_0)^2]
\end{aligned}$$

identical to previous case.

k odd, n even case

$$\begin{aligned}
&= -\frac{1}{4}e^{-j\alpha} \sum_{k,n=-\infty}^{\infty} J_k(\beta) J_n(k\psi) \cdot e^{-j\frac{1}{2}\ddot{\phi}(k\nu_0+nf_0)^2} \cdot [e^{-j[k(\nu_0(\dot{\phi}+t)+\gamma)]} \cdot e^{-j[n(f_0(\dot{\phi}+t)+\delta)]} \\
&- e^{j[k(\nu_0(\dot{\phi}+t)+\gamma)]} \cdot e^{j[n(f_0(\dot{\phi}+t)+\delta)]}] \\
&-\frac{1}{4}e^{-j\alpha} \sum_{k,n=-\infty}^{\infty} J_k(\beta) J_n(k\psi) \cdot e^{-j\frac{1}{2}\ddot{\phi}(k\nu_0-nf_0)^2} \cdot [e^{-j[k(\nu_0(\dot{\phi}+t)+\gamma)]} \cdot e^{j[n(f_0(\dot{\phi}+t)+\delta)]} \\
&- e^{j[k(\nu_0(\dot{\phi}+t)+\gamma)]} \cdot e^{-j[n(f_0(\dot{\phi}+t)+\delta)]}] \\
&-\frac{1}{4}e^{j\alpha} \sum_{k,n=-\infty}^{\infty} J_k(\beta) J_n(k\psi) \cdot e^{j\frac{1}{2}\ddot{\phi}(k\nu_0+nf_0)^2} \cdot [e^{j[k(\nu_0(\dot{\phi}+t)+\gamma)]} \cdot e^{j[n(f_0(\dot{\phi}+t)+\delta)]} \\
&- e^{-j[k(\nu_0(\dot{\phi}+t)+\gamma)]} \cdot e^{-j[n(f_0(\dot{\phi}+t)+\delta)]}] \\
&-\frac{1}{4}e^{j\alpha} \sum_{k,n=-\infty}^{\infty} J_k(\beta) J_n(k\psi) \cdot e^{j\frac{1}{2}\ddot{\phi}(k\nu_0-nf_0)^2} \cdot [-e^{-j[k(\nu_0(\dot{\phi}+t)+\gamma)]} \cdot e^{j[n(f_0(\dot{\phi}+t)+\delta)]} \\
&+ e^{j[k(\nu_0(\dot{\phi}+t)+\gamma)]} \cdot e^{-j[n(f_0(\dot{\phi}+t)+\delta)]}] \\
&= \frac{j}{2}e^{-j\alpha} \sum_{k,n=-\infty}^{\infty} J_k(\beta) J_n(k\psi) \cdot e^{-j\frac{1}{2}\ddot{\phi}(k\nu_0+nf_0)^2} \cdot \sin[(k\nu_0 + nf_0)(\dot{\phi} + t) + k\gamma + n\delta] \\
&+ \frac{j}{2}e^{-j\alpha} \sum_{k,n=-\infty}^{\infty} J_k(\beta) J_n(k\psi) \cdot e^{-j\frac{1}{2}\ddot{\phi}(k\nu_0-nf_0)^2} \cdot \sin[(k\nu_0 - nf_0)(\dot{\phi} + t) + k\gamma - n\delta]
\end{aligned}$$

$$\begin{aligned}
& -\frac{j}{2}e^{j\alpha} \sum_{k,n=-\infty}^{\infty} J_k(\beta)J_n(k\psi) \cdot e^{j\frac{1}{2}\ddot{\phi}(k\nu_0+nf_0)^2} \cdot \sin[(k\nu_0+nf_0)(\dot{\phi}+t)+k\gamma+n\delta] \\
& -\frac{j}{2}e^{j\alpha} \sum_{k,n=-\infty}^{\infty} J_k(\beta)J_n(k\psi) \cdot e^{j\frac{1}{2}\ddot{\phi}(k\nu_0-nf_0)^2} \cdot \sin[(k\nu_0-nf_0)(\dot{\phi}+t)+k\gamma-n\delta] \\
& = -\frac{j}{2} \sum_{k,n=-\infty}^{\infty} J_k(\beta)J_n(k\psi) \cdot \sin[(k\nu_0+nf_0)(\dot{\phi}+t)+k\gamma+n\delta] \\
& \cdot [e^{j[\alpha+\frac{1}{2}\ddot{\phi}(k\nu_0+nf_0)^2]} - e^{-j[\alpha+\frac{1}{2}\ddot{\phi}(k\nu_0+nf_0)^2]}] \\
& -\frac{j}{2} \sum_{k,n=-\infty}^{\infty} J_k(\beta)J_n(k\psi) \cdot \sin[(k\nu_0-nf_0)(\dot{\phi}+t)+k\gamma-n\delta] \\
& [e^{j[\alpha+\frac{1}{2}\ddot{\phi}(k\nu_0-nf_0)^2]} - e^{-j[\alpha+\frac{1}{2}\ddot{\phi}(k\nu_0-nf_0)^2]}] \\
& = \sum_{k,n=-\infty}^{\infty} J_k(\beta)J_n(k\psi) \cdot \sin[(k\nu_0+nf_0)(\dot{\phi}+t)+k\gamma+n\delta] \\
& \cdot \sin[\alpha + \frac{1}{2}\ddot{\phi}(k\nu_0+nf_0)^2] \\
& + \sum_{k,n=-\infty}^{\infty} J_k(\beta)J_n(k\psi) \cdot \sin[(k\nu_0-nf_0)(\dot{\phi}+t)+k\gamma-n\delta] \\
& \cdot \sin[\alpha + \frac{1}{2}\ddot{\phi}(k\nu_0-nf_0)^2]
\end{aligned}$$

substitute n=-n

$$\begin{aligned}
& = \sum_{k,n=-\infty}^{\infty} J_k(\beta)J_n(k\psi) \cdot \sin[(k\nu_0+nf_0)(\dot{\phi}+t)+k\gamma+n\delta] \\
& \cdot \sin[\alpha + \frac{1}{2}\ddot{\phi}(k\nu_0+nf_0)^2] \\
& + \sum_{k,n=-\infty}^{\infty} J_k(\beta)J_{-n}(k\psi) \cdot \sin[(k\nu_0+nf_0)(\dot{\phi}+t)+k\gamma+n\delta] \\
& \cdot \sin[\alpha + \frac{1}{2}\ddot{\phi}(k\nu_0+nf_0)^2]
\end{aligned}$$

since n even

$$\begin{aligned}
& = 2 \cdot \sum_{k,n=-\infty}^{\infty} J_k(\beta)J_n(k\psi) \cdot \sin[(k\nu_0+nf_0)(\dot{\phi}+t)+k\gamma+n\delta] \\
& \cdot \sin[\alpha + \frac{1}{2}\ddot{\phi}(k\nu_0+nf_0)^2].
\end{aligned}$$

k odd, n odd case

$$\begin{aligned}
& = -\frac{1}{4}e^{-j\alpha} \sum_{k,n=-\infty}^{\infty} J_k(\beta)J_n(k\psi) \cdot e^{-j\frac{1}{2}\ddot{\phi}(k\nu_0+nf_0)^2} \cdot [e^{-j[k(\nu_0(\dot{\phi}+t)+\gamma)]} \cdot e^{-j[n(f_0(\dot{\phi}+t)+\delta)]} \\
& - e^{j[k(\nu_0(\dot{\phi}+t)+\gamma)]} \cdot e^{j[n(f_0(\dot{\phi}+t)+\delta)]}] \\
& -\frac{1}{4}e^{-j\alpha} \sum_{k,n=-\infty}^{\infty} J_k(\beta)J_n(k\psi) \cdot e^{-j\frac{1}{2}\ddot{\phi}(k\nu_0-nf_0)^2} \cdot [-e^{-j[k(\nu_0(\dot{\phi}+t)+\gamma)]} \cdot e^{j[n(f_0(\dot{\phi}+t)+\delta)]} \\
& + e^{j[k(\nu_0(\dot{\phi}+t)+\gamma)]} \cdot e^{-j[n(f_0(\dot{\phi}+t)+\delta)]}]
\end{aligned}$$

$$\begin{aligned}
& -\frac{1}{4}e^{j\alpha} \sum_{k,n=-\infty}^{\infty} J_k(\beta)J_n(k\psi) \cdot e^{j\frac{1}{2}\ddot{\phi}(k\nu_0+n f_0)^2} \cdot [e^{j[k(\nu_0(\dot{\phi}+t)+\gamma)]} \cdot e^{j[n(f_0(\dot{\phi}+t)+\delta)]} \\
& -e^{-j[k(\nu_0(\dot{\phi}+t)+\gamma)]} \cdot e^{-j[n(f_0(\dot{\phi}+t)+\delta)]}] \\
& -\frac{1}{4}e^{j\alpha} \sum_{k,n=-\infty}^{\infty} J_k(\beta)J_n(k\psi) \cdot e^{j\frac{1}{2}\ddot{\phi}(k\nu_0-n f_0)^2} \cdot [e^{-j[k(\nu_0(\dot{\phi}+t)+\gamma)]} \cdot e^{j[n(f_0(\dot{\phi}+t)+\delta)]} \\
& -e^{j[k(\nu_0(\dot{\phi}+t)+\gamma)]} \cdot e^{-j[n(f_0(\dot{\phi}+t)+\delta)]}] \\
& = \frac{j}{2}e^{-j\alpha} \sum_{k,n=-\infty}^{\infty} J_k(\beta)J_n(k\psi) \cdot e^{-j\frac{1}{2}\ddot{\phi}(k\nu_0+n f_0)^2} \cdot \sin[(k\nu_0+n f_0)(\dot{\phi}+t)+k\gamma+n\delta] \\
& -\frac{j}{2}e^{-j\alpha} \sum_{k,n=-\infty}^{\infty} J_k(\beta)J_n(k\psi) \cdot e^{-j\frac{1}{2}\ddot{\phi}(k\nu_0-n f_0)^2} \cdot \sin[(k\nu_0-n f_0)(\dot{\phi}+t)+k\gamma-n\delta] \\
& -\frac{j}{2}e^{j\alpha} \sum_{k,n=-\infty}^{\infty} J_k(\beta)J_n(k\psi) \cdot e^{j\frac{1}{2}\ddot{\phi}(k\nu_0+n f_0)^2} \cdot \sin[(k\nu_0+n f_0)(\dot{\phi}+t)+k\gamma+n\delta] \\
& +\frac{j}{2}e^{j\alpha} \sum_{k,n=-\infty}^{\infty} J_k(\beta)J_n(k\psi) \cdot e^{j\frac{1}{2}\ddot{\phi}(k\nu_0-n f_0)^2} \cdot \sin[(k\nu_0-n f_0)(\dot{\phi}+t)+k\gamma-n\delta] \\
& = -\frac{j}{2} \sum_{k,n=-\infty}^{\infty} J_k(\beta)J_n(k\psi) \cdot \sin[(k\nu_0+n f_0)(\dot{\phi}+t)+k\gamma+n\delta] \\
& \cdot [e^{j[\alpha+\frac{1}{2}\ddot{\phi}(k\nu_0+n f_0)^2]} - e^{-j[\alpha+\frac{1}{2}\ddot{\phi}(k\nu_0+n f_0)^2]}] \\
& -\frac{j}{2} \sum_{k,n=-\infty}^{\infty} J_k(\beta)J_n(k\psi) \cdot \sin[(k\nu_0-n f_0)(\dot{\phi}+t)+k\gamma-n\delta] \\
& \cdot [e^{-j[\alpha+\frac{1}{2}\ddot{\phi}(k\nu_0-n f_0)^2]} - e^{j[\alpha+\frac{1}{2}\ddot{\phi}(k\nu_0-n f_0)^2]}] \\
& = \sum_{k,n=-\infty}^{\infty} J_k(\beta)J_n(k\psi) \cdot \sin[(k\nu_0+n f_0)(\dot{\phi}+t)+k\gamma+n\delta] \\
& \cdot \sin[\alpha+\frac{1}{2}\ddot{\phi}(k\nu_0+n f_0)^2] \\
& - \sum_{k,n=-\infty}^{\infty} J_k(\beta)J_n(k\psi) \cdot \sin[(k\nu_0-n f_0)(\dot{\phi}+t)+k\gamma-n\delta] \\
& \cdot \sin[\alpha+\frac{1}{2}\ddot{\phi}(k\nu_0-n f_0)^2] \\
& \text{substitute } n=-n \\
& = \sum_{k,n=-\infty}^{\infty} J_k(\beta)J_n(k\psi) \cdot \sin[(k\nu_0+n f_0)(\dot{\phi}+t)+k\gamma+n\delta] \\
& \cdot \sin[\alpha+\frac{1}{2}\ddot{\phi}(k\nu_0+n f_0)^2] \\
& - \sum_{k,n=-\infty}^{\infty} J_k(\beta)J_{-n}(k\psi) \cdot \sin[(k\nu_0+n f_0)(\dot{\phi}+t)+k\gamma+n\delta] \\
& \cdot \sin[\alpha+\frac{1}{2}\ddot{\phi}(k\nu_0+n f_0)^2] \\
& \text{since } n \text{ odd} \\
& = 2 \cdot \sum_{k,n=-\infty}^{\infty} J_k(\beta)J_n(k\psi) \cdot \sin[(k\nu_0+n f_0)(\dot{\phi}+t)+k\gamma+n\delta]
\end{aligned}$$

$$\cdot \sin[\alpha + \frac{1}{2}\ddot{\phi}(k\nu_0 + nf_0)^2]$$

same as previous case.

Finally we can summarize this calculations by noting that the expression:

$$-e^{-j\alpha} \sum_{k,n=-\infty}^{\infty} J_k(\beta)J_n(k\psi)e^{-j[k(\nu_0(\dot{\phi}+t)+\gamma)]} \cdot e^{-j\frac{1}{2}\ddot{\phi}(k\nu_0+nf_0)^2} \cdot e^{-j[n(f_0(\dot{\phi}+t)+\delta)]}$$

$$-e^{j\alpha} \sum_{k,n=-\infty}^{\infty} J_k(\beta)J_n(k\psi)e^{j[k(\nu_0(\dot{\phi}+t)+\gamma)]} \cdot e^{j\frac{1}{2}\ddot{\phi}(k\nu_0+nf_0)^2} \cdot e^{j[n(f_0(\dot{\phi}+t)+\delta)]}$$

is independent of n , and can be represented in the equivalent form

$$= 2 \sum_{k,n=-\infty}^{\infty} J_k(\beta)J_n(k\psi) \cdot \left[\begin{array}{c} -\cos[\alpha + \frac{1}{2}\ddot{\phi}(k\nu_0 + nf_0)^2] \cdot \cos[(k\nu_0 + nf_0)(\dot{\phi} + t) + k\gamma + n\delta] \\ \sin[\alpha + \frac{1}{2}\ddot{\phi}(k\nu_0 + nf_0)^2] \cdot \sin[(k\nu_0 + nf_0)(\dot{\phi} + t) + k\gamma + n\delta] \end{array} \right]_k$$

where $\left[\begin{array}{c} \dots \\ \dots \end{array} \right]_k$ formalizm formalizm is introduced to denote that top element is chosen if k is even and bottom if k is odd.

We will apply the same approach to the four infinite sum terms

$$\sum_{\substack{m,n,k,l \\ =-\infty}}^{\infty} J_m(\beta)J_n(m\psi)J_{m-k}(\beta)J_{n-l}([m-k]\psi) \cdot e^{j[k\gamma+l\delta]} \cdot e^{j[k\nu_0+lf_0](\dot{\phi}+t)}$$

$$\cdot e^{j\frac{1}{2}\ddot{\phi}[k(2m-k)\nu_0^2+2[nk+l(m-k)]\nu_0f_0+l(2n-l)f_0^2]}$$

$$= \frac{1}{2} \sum_{\substack{m,n,k,l \\ =-\infty}}^{\infty} J_m(\beta)J_n(m\psi)J_{m-k}(\beta)J_{n-l}([m-k]\psi) \cdot e^{j[k\gamma+l\delta]} \cdot e^{j[k\nu_0+lf_0](\dot{\phi}+t)}$$

$$\cdot e^{j\frac{1}{2}\ddot{\phi}[k(2m-k)\nu_0^2+2[nk+l(m-k)]\nu_0f_0+l(2n-l)f_0^2]}$$

$$+ \frac{1}{2} \sum_{\substack{m,n,k,l \\ =-\infty}}^{\infty} J_{-m}(\beta)J_n(-m\psi)J_{-m-k}(\beta)J_{n-l}([-m-k]\psi) \cdot e^{j[k\gamma+l\delta]} \cdot e^{j[k\nu_0+lf_0](\dot{\phi}+t)}$$

$$\cdot e^{j\frac{1}{2}\ddot{\phi}[k(-2m-k)\nu_0^2+2[nk+l(-m-k)]\nu_0f_0+l(2n-l)f_0^2]}$$

$$= \frac{1}{4} \sum_{\substack{m,n,k,l \\ =-\infty}}^{\infty} J_m(\beta)J_n(m\psi)J_{m-k}(\beta)J_{n-l}([m-k]\psi) \cdot e^{j[k\gamma+l\delta]} \cdot e^{j[k\nu_0+lf_0](\dot{\phi}+t)}$$

$$\cdot e^{j\frac{1}{2}\ddot{\phi}[k(2m-k)\nu_0^2+2[nk+l(m-k)]\nu_0f_0+l(2n-l)f_0^2]}$$

$$+ \frac{1}{4} \sum_{\substack{m,n,k,l \\ =-\infty}}^{\infty} J_m(\beta)J_n(m\psi)J_{m-k}(\beta)J_{n-l}([m-k]\psi) \cdot e^{j[k\gamma+l\delta]} \cdot e^{j[k\nu_0+lf_0](\dot{\phi}+t)}$$

$$\cdot e^{j\frac{1}{2}\ddot{\phi}[k(2m-k)\nu_0^2+2[-nk+l(m-k)]\nu_0f_0+l(-2n-l)f_0^2]}$$

$$+ \frac{1}{4} \sum_{\substack{m,n,k,l \\ =-\infty}}^{\infty} J_{-m}(\beta)J_n(-m\psi)J_{-m-k}(\beta)J_{n-l}([-m-k]\psi) \cdot e^{j[k\gamma+l\delta]} \cdot e^{j[k\nu_0+lf_0](\dot{\phi}+t)}$$

$$\begin{aligned}
& \cdot e^{j\frac{1}{2}\ddot{\phi}[k(-2m-k)\nu_0^2+2[nk+l(-m-k)]\nu_0f_0+l(2n-l)f_0^2]} \\
& + \frac{1}{4} \sum_{\substack{m,n,k,l \\ =-\infty}}^{\infty} J_{-m}(\beta)J_{-n}(-m\psi)J_{-m-k}(\beta)J_{-n-l}([-m-k]\psi) \cdot e^{j[k\gamma+l\delta]} \cdot e^{j[k\nu_0+lf_0](\dot{\phi}+t)} \\
& \cdot e^{j\frac{1}{2}\ddot{\phi}[k(-2m-k)\nu_0^2+2[-nk+l(-m-k)]\nu_0f_0+l(-2n-l)f_0^2]} \\
& = \frac{1}{8} \sum_{\substack{m,n,k,l \\ =-\infty}}^{\infty} J_m(\beta)J_n(m\psi)J_{m-k}(\beta)J_{n-l}([m-k]\psi) \cdot e^{j[k\gamma+l\delta]} \cdot e^{j[k\nu_0+lf_0](\dot{\phi}+t)} \\
& \cdot e^{j\frac{1}{2}\ddot{\phi}[k(2m-k)\nu_0^2+2[nk+l(m-k)]\nu_0f_0+l(2n-l)f_0^2]} \\
& + \frac{1}{8} \sum_{\substack{m,n,k,l \\ =-\infty}}^{\infty} J_m(\beta)J_n(m\psi)J_{m+k}(\beta)J_{n-l}([m+k]\psi) \cdot e^{j[-k\gamma+l\delta]} \cdot e^{j[-k\nu_0+lf_0](\dot{\phi}+t)} \\
& \cdot e^{j\frac{1}{2}\ddot{\phi}[-k(2m+k)\nu_0^2+2[-nk+l(m+k)]\nu_0f_0+l(2n-l)f_0^2]} \\
& + \frac{1}{8} \sum_{\substack{m,n,k,l \\ =-\infty}}^{\infty} J_m(\beta)J_{-n}(m\psi)J_{m-k}(\beta)J_{-n-l}([m-k]\psi) \cdot e^{j[k\gamma+l\delta]} \cdot e^{j[k\nu_0+lf_0](\dot{\phi}+t)} \\
& \cdot e^{j\frac{1}{2}\ddot{\phi}[k(2m-k)\nu_0^2+2[-nk+l(m-k)]\nu_0f_0+l(-2n-l)f_0^2]} \\
& + \frac{1}{8} \sum_{\substack{m,n,k,l \\ =-\infty}}^{\infty} J_m(\beta)J_{-n}(m\psi)J_{m+k}(\beta)J_{-n-l}([m+k]\psi) \cdot e^{j[-k\gamma+l\delta]} \cdot e^{j[-k\nu_0+lf_0](\dot{\phi}+t)} \\
& \cdot e^{j\frac{1}{2}\ddot{\phi}[-k(2m+k)\nu_0^2+2[nk+l(m+k)]\nu_0f_0+l(-2n-l)f_0^2]} \\
& + \frac{1}{8} \sum_{\substack{m,n,k,l \\ =-\infty}}^{\infty} J_{-m}(\beta)J_n(-m\psi)J_{-m-k}(\beta)J_{-n-l}([-m-k]\psi) \cdot e^{j[k\gamma+l\delta]} \cdot e^{j[k\nu_0+lf_0](\dot{\phi}+t)} \\
& \cdot e^{j\frac{1}{2}\ddot{\phi}[k(-2m-k)\nu_0^2+2[nk+l(-m-k)]\nu_0f_0+l(2n-l)f_0^2]} \\
& + \frac{1}{8} \sum_{\substack{m,n,k,l \\ =-\infty}}^{\infty} J_{-m}(\beta)J_n(-m\psi)J_{-m+k}(\beta)J_{-n-l}([-m+k]\psi) \cdot e^{j[-k\gamma+l\delta]} \cdot e^{j[-k\nu_0+lf_0](\dot{\phi}+t)} \\
& \cdot e^{j\frac{1}{2}\ddot{\phi}[-k(-2m+k)\nu_0^2+2[-nk+l(-m+k)]\nu_0f_0+l(2n-l)f_0^2]} \\
& + \frac{1}{8} \sum_{\substack{m,n,k,l \\ =-\infty}}^{\infty} J_{-m}(\beta)J_{-n}(-m\psi)J_{-m-k}(\beta)J_{-n-l}([-m-k]\psi) \cdot e^{j[k\gamma+l\delta]} \cdot e^{j[k\nu_0+lf_0](\dot{\phi}+t)} \\
& \cdot e^{j\frac{1}{2}\ddot{\phi}[k(-2m-k)\nu_0^2+2[-nk+l(-m-k)]\nu_0f_0+l(-2n-l)f_0^2]} \\
& + \frac{1}{8} \sum_{\substack{m,n,k,l \\ =-\infty}}^{\infty} J_{-m}(\beta)J_{-n}(-m\psi)J_{-m+k}(\beta)J_{-n-l}([-m+k]\psi) \cdot e^{j[-k\gamma+l\delta]} \cdot e^{j[-k\nu_0+lf_0](\dot{\phi}+t)} \\
& \cdot e^{j\frac{1}{2}\ddot{\phi}[-k(-2m+k)\nu_0^2+2[nk+l(-m+k)]\nu_0f_0+l(-2n-l)f_0^2]} \\
& = \frac{1}{16} \sum_{\substack{m,n,k,l \\ =-\infty}}^{\infty} J_m(\beta)J_n(m\psi)J_{m-k}(\beta)J_{n-l}([m-k]\psi) \cdot e^{j[k\gamma+l\delta]} \cdot e^{j[k\nu_0+lf_0](\dot{\phi}+t)} \\
& \cdot e^{j\frac{1}{2}\ddot{\phi}[k(2m-k)\nu_0^2+2[nk+l(m-k)]\nu_0f_0+l(2n-l)f_0^2]}
\end{aligned}$$

$$\begin{aligned}
& + \frac{1}{16} \sum_{\substack{m,n,k,l \\ =-\infty}}^{\infty} J_m(\beta) J_n(m\psi) J_{m-k}(\beta) J_{n+l}([m-k]\psi) \cdot e^{j[k\gamma-l\delta]} \cdot e^{j[k\nu_0-lf_0](\phi+t)} \\
& \cdot e^{j\frac{1}{2}\phi[k(2m-k)\nu_0^2+2[nk-l(m-k)]\nu_0f_0-l(2n+l)f_0^2]} \\
& + \frac{1}{16} \sum_{\substack{m,n,k,l \\ =-\infty}}^{\infty} J_m(\beta) J_n(m\psi) J_{m+k}(\beta) J_{n-l}([m+k]\psi) \cdot e^{j[-k\gamma+l\delta]} \cdot e^{j[-k\nu_0+lf_0](\phi+t)} \\
& \cdot e^{j\frac{1}{2}\phi[-k(2m+k)\nu_0^2+2[-nk+l(m+k)]\nu_0f_0+l(2n-l)f_0^2]} \\
& + \frac{1}{16} \sum_{\substack{m,n,k,l \\ =-\infty}}^{\infty} J_m(\beta) J_n(m\psi) J_{m+k}(\beta) J_{n+l}([m+k]\psi) \cdot e^{j[-k\gamma-l\delta]} \cdot e^{j[-k\nu_0-lf_0](\phi+t)} \\
& \cdot e^{j\frac{1}{2}\phi[-k(2m+k)\nu_0^2+2[-nk-l(m+k)]\nu_0f_0-l(2n+l)f_0^2]} \\
& + \frac{1}{16} \sum_{\substack{m,n,k,l \\ =-\infty}}^{\infty} J_m(\beta) J_{-n}(m\psi) J_{m-k}(\beta) J_{-n-l}([m-k]\psi) \cdot e^{j[k\gamma+l\delta]} \cdot e^{j[k\nu_0+lf_0](\phi+t)} \\
& \cdot e^{j\frac{1}{2}\phi[k(2m-k)\nu_0^2+2[-nk+l(m-k)]\nu_0f_0+l(-2n-l)f_0^2]} \\
& + \frac{1}{16} \sum_{\substack{m,n,k,l \\ =-\infty}}^{\infty} J_m(\beta) J_{-n}(m\psi) J_{m-k}(\beta) J_{-n+l}([m-k]\psi) \cdot e^{j[k\gamma-l\delta]} \cdot e^{j[k\nu_0-lf_0](\phi+t)} \\
& \cdot e^{j\frac{1}{2}\phi[k(2m-k)\nu_0^2+2[-nk-l(m-k)]\nu_0f_0-l(-2n+l)f_0^2]} \\
& + \frac{1}{16} \sum_{\substack{m,n,k,l \\ =-\infty}}^{\infty} J_m(\beta) J_{-n}(m\psi) J_{m+k}(\beta) J_{-n-l}([m+k]\psi) \cdot e^{j[-k\gamma+l\delta]} \cdot e^{j[-k\nu_0+lf_0](\phi+t)} \\
& \cdot e^{j\frac{1}{2}\phi[-k(2m+k)\nu_0^2+2[nk+l(m+k)]\nu_0f_0+l(-2n-l)f_0^2]} \\
& + \frac{1}{16} \sum_{\substack{m,n,k,l \\ =-\infty}}^{\infty} J_m(\beta) J_{-n}(m\psi) J_{m+k}(\beta) J_{-n+l}([m+k]\psi) \cdot e^{j[-k\gamma-l\delta]} \cdot e^{j[-k\nu_0-lf_0](\phi+t)} \\
& \cdot e^{j\frac{1}{2}\phi[-k(2m+k)\nu_0^2+2[nk-l(m+k)]\nu_0f_0-l(-2n+l)f_0^2]} \\
& + \frac{1}{16} \sum_{\substack{m,n,k,l \\ =-\infty}}^{\infty} J_{-m}(\beta) J_n(-m\psi) J_{-m-k}(\beta) J_{n-l}([-m-k]\psi) \cdot e^{j[k\gamma+l\delta]} \cdot e^{j[k\nu_0+lf_0](\phi+t)} \\
& \cdot e^{j\frac{1}{2}\phi[k(-2m-k)\nu_0^2+2[nk+l(-m-k)]\nu_0f_0+l(2n-l)f_0^2]} \\
& + \frac{1}{16} \sum_{\substack{m,n,k,l \\ =-\infty}}^{\infty} J_{-m}(\beta) J_n(-m\psi) J_{-m-k}(\beta) J_{n+l}([-m-k]\psi) \cdot e^{j[k\gamma-l\delta]} \cdot e^{j[k\nu_0-lf_0](\phi+t)} \\
& \cdot e^{j\frac{1}{2}\phi[k(-2m-k)\nu_0^2+2[nk-l(-m-k)]\nu_0f_0-l(2n+l)f_0^2]} \\
& + \frac{1}{16} \sum_{\substack{m,n,k,l \\ =-\infty}}^{\infty} J_{-m}(\beta) J_n(-m\psi) J_{-m+k}(\beta) J_{n-l}([-m+k]\psi) \cdot e^{j[-k\gamma+l\delta]} \cdot e^{j[-k\nu_0+lf_0](\phi+t)} \\
& \cdot e^{j\frac{1}{2}\phi[-k(-2m+k)\nu_0^2+2[-nk+l(-m+k)]\nu_0f_0+l(2n-l)f_0^2]} \\
& + \frac{1}{16} \sum_{\substack{m,n,k,l \\ =-\infty}}^{\infty} J_{-m}(\beta) J_n(-m\psi) J_{-m+k}(\beta) J_{n+l}([-m+k]\psi) \cdot e^{j[-k\gamma-l\delta]} \cdot e^{j[-k\nu_0-lf_0](\phi+t)} \\
& \cdot e^{j\frac{1}{2}\phi[-k(-2m+k)\nu_0^2+2[-nk+l(-m+k)]\nu_0f_0+l(2n+l)f_0^2]}
\end{aligned}$$

$$\begin{aligned}
& \cdot e^{j\frac{1}{2}\ddot{\phi}[-k(-2m+k)\nu_0^2+2[-nk-l(-m+k)]\nu_0f_0-l(2n+l)f_0^2]} \\
& + \frac{1}{16} \sum_{\substack{m,n,k,l \\ =-\infty}}^{\infty} J_{-m}(\beta)J_{-n}(-m\psi)J_{-m-k}(\beta)J_{-n-l}([-m-k]\psi) \cdot e^{j[k\gamma+l\delta]} \cdot e^{j[k\nu_0+l f_0](\dot{\phi}+t)} \\
& \cdot e^{j\frac{1}{2}\ddot{\phi}[k(-2m-k)\nu_0^2+2[-nk+l(-m-k)]\nu_0f_0+l(-2n-l)f_0^2]} \\
& + \frac{1}{16} \sum_{\substack{m,n,k,l \\ =-\infty}}^{\infty} J_{-m}(\beta)J_{-n}(-m\psi)J_{-m-k}(\beta)J_{-n+l}([-m-k]\psi) \cdot e^{j[k\gamma-l\delta]} \cdot e^{j[k\nu_0-l f_0](\dot{\phi}+t)} \\
& \cdot e^{j\frac{1}{2}\ddot{\phi}[k(-2m-k)\nu_0^2+2[-nk-l(-m-k)]\nu_0f_0-l(-2n+l)f_0^2]} \\
& + \frac{1}{16} \sum_{\substack{m,n,k,l \\ =-\infty}}^{\infty} J_{-m}(\beta)J_{-n}(-m\psi)J_{-m+k}(\beta)J_{-n-l}([-m+k]\psi) \cdot e^{j[-k\gamma+l\delta]} \cdot e^{j[-k\nu_0+l f_0](\dot{\phi}+t)} \\
& \cdot e^{j\frac{1}{2}\ddot{\phi}[-k(-2m+k)\nu_0^2+2[nk+l(-m+k)]\nu_0f_0+l(-2n-l)f_0^2]} \\
& + \frac{1}{16} \sum_{\substack{m,n,k,l \\ =-\infty}}^{\infty} J_{-m}(\beta)J_{-n}(-m\psi)J_{-m+k}(\beta)J_{-n+l}([-m+k]\psi) \cdot e^{j[-k\gamma-l\delta]} \cdot e^{j[-k\nu_0-l f_0](\dot{\phi}+t)} \\
& \cdot e^{j\frac{1}{2}\ddot{\phi}[-k(-2m+k)\nu_0^2+2[nk-l(-m+k)]\nu_0f_0-l(-2n+l)f_0^2]}
\end{aligned}$$

Using $J_{-n}(x) = (-1)^n \cdot J_n(x)$ and $J_n(-x) = (-1)^n \cdot J_n(x)$

$$\begin{aligned}
& = \frac{1}{16} \sum_{\substack{m,n,k,l \\ =-\infty}}^{\infty} J_m(\beta)J_n(m\psi)J_{m-k}(\beta)J_{n-l}([m-k]\psi) \cdot e^{j[k\gamma+l\delta]} \cdot e^{j[k\nu_0+l f_0](\dot{\phi}+t)} \\
& \cdot e^{j\frac{1}{2}\ddot{\phi}[k(2m-k)\nu_0^2+2[nk+l(m-k)]\nu_0f_0+l(2n-l)f_0^2]} \\
& + \frac{1}{16} \sum_{\substack{m,n,k,l \\ =-\infty}}^{\infty} J_m(\beta)J_n(m\psi)J_{m-k}(\beta)J_{n+l}([m-k]\psi) \cdot e^{j[k\gamma-l\delta]} \cdot e^{j[k\nu_0-l f_0](\dot{\phi}+t)} \\
& \cdot e^{j\frac{1}{2}\ddot{\phi}[k(2m-k)\nu_0^2+2[nk-l(m-k)]\nu_0f_0-l(2n+l)f_0^2]} \\
& + \frac{1}{16} \sum_{\substack{m,n,k,l \\ =-\infty}}^{\infty} J_m(\beta)J_n(m\psi)J_{m+k}(\beta)J_{n-l}([m+k]\psi) \cdot e^{j[-k\gamma+l\delta]} \cdot e^{j[-k\nu_0+l f_0](\dot{\phi}+t)} \\
& \cdot e^{j\frac{1}{2}\ddot{\phi}[-k(2m+k)\nu_0^2+2[-nk+l(m+k)]\nu_0f_0+l(2n-l)f_0^2]} \\
& + \frac{1}{16} \sum_{\substack{m,n,k,l \\ =-\infty}}^{\infty} J_m(\beta)J_n(m\psi)J_{m+k}(\beta)J_{n+l}([m+k]\psi) \cdot e^{j[-k\gamma-l\delta]} \cdot e^{j[-k\nu_0-l f_0](\dot{\phi}+t)} \\
& \cdot e^{j\frac{1}{2}\ddot{\phi}[-k(2m+k)\nu_0^2+2[-nk-l(m+k)]\nu_0f_0-l(2n+l)f_0^2]} \\
& + \frac{1}{16} \sum_{\substack{m,n,k,l \\ =-\infty}}^{\infty} J_m(\beta)J_n(m\psi)J_{m-k}(\beta)J_{n+l}([m-k]\psi) \cdot e^{j[k\gamma+l\delta]} \cdot e^{j[k\nu_0+l f_0](\dot{\phi}+t)} \\
& \cdot (-1)^{2n+l} \cdot e^{j\frac{1}{2}\ddot{\phi}[k(2m-k)\nu_0^2+2[-nk+l(m-k)]\nu_0f_0+l(-2n-l)f_0^2]} \\
& + \frac{1}{16} \sum_{\substack{m,n,k,l \\ =-\infty}}^{\infty} J_m(\beta)J_n(m\psi)J_{m-k}(\beta)J_{n-l}([m-k]\psi) \cdot e^{j[k\gamma-l\delta]} \cdot e^{j[k\nu_0-l f_0](\dot{\phi}+t)} \\
& \cdot (-1)^{2n-l} \cdot e^{j\frac{1}{2}\ddot{\phi}[k(2m-k)\nu_0^2+2[-nk-l(m-k)]\nu_0f_0-l(-2n+l)f_0^2]}
\end{aligned}$$

$$\begin{aligned}
& + \frac{1}{16} \sum_{\substack{m,n,k,l \\ =-\infty \\ =-\infty}}^{\infty} J_m(\beta) J_n(m\psi) J_{m+k}(\beta) J_{n+l}([m+k]\psi) \cdot e^{j[-k\gamma+l\delta]} \cdot e^{j[-k\nu_0+lf_0](\phi+t)} \\
& \cdot (-1)^{2n+l} \cdot e^{j\frac{1}{2}\ddot{\phi}[-k(2m+k)\nu_0^2+2[nk+l(m+k)]\nu_0f_0+l(-2n-l)f_0^2]} \\
& + \frac{1}{16} \sum_{\substack{m,n,k,l \\ =-\infty \\ =-\infty}}^{\infty} J_m(\beta) J_n(m\psi) J_{m+k}(\beta) J_{n-l}([m+k]\psi) \cdot e^{j[-k\gamma-l\delta]} \cdot e^{j[-k\nu_0-lf_0](\phi+t)} \\
& \cdot (-1)^{2n-l} \cdot e^{j\frac{1}{2}\ddot{\phi}[-k(2m+k)\nu_0^2+2[nk-l(m+k)]\nu_0f_0-l(-2n+l)f_0^2]} \\
& + \frac{1}{16} \sum_{\substack{m,n,k,l \\ =-\infty \\ =-\infty}}^{\infty} J_m(\beta) J_n(m\psi) J_{m+k}(\beta) J_{n-l}([m+k]\psi) \cdot e^{j[k\gamma+l\delta]} \cdot e^{j[k\nu_0+lf_0](\phi+t)} \\
& \cdot (-1)^{2m+k+2n-l} \cdot e^{j\frac{1}{2}\ddot{\phi}[k(-2m-k)\nu_0^2+2[nk+l(-m-k)]\nu_0f_0+l(2n-l)f_0^2]} \\
& + \frac{1}{16} \sum_{\substack{m,n,k,l \\ =-\infty \\ =-\infty}}^{\infty} J_m(\beta) J_n(m\psi) J_{m+k}(\beta) J_{n+l}([m+k]\psi) \cdot e^{j[k\gamma-l\delta]} \cdot e^{j[k\nu_0-lf_0](\phi+t)} \\
& \cdot (-1)^{2m+k+2n+l} \cdot e^{j\frac{1}{2}\ddot{\phi}[k(-2m-k)\nu_0^2+2[nk-l(-m-k)]\nu_0f_0-l(2n+l)f_0^2]} \\
& + \frac{1}{16} \sum_{\substack{m,n,k,l \\ =-\infty \\ =-\infty}}^{\infty} J_m(\beta) J_n(m\psi) J_{m-k}(\beta) J_{n-l}([m-k]\psi) \cdot e^{j[-k\gamma+l\delta]} \cdot e^{j[-k\nu_0+lf_0](\phi+t)} \\
& \cdot (-1)^{2m-k+2n-l} \cdot e^{j\frac{1}{2}\ddot{\phi}[-k(-2m+k)\nu_0^2+2[-nk+l(-m+k)]\nu_0f_0+l(2n-l)f_0^2]} \\
& + \frac{1}{16} \sum_{\substack{m,n,k,l \\ =-\infty \\ =-\infty}}^{\infty} J_m(\beta) J_n(m\psi) J_{m-k}(\beta) J_{n+l}([m-k]\psi) \cdot e^{j[-k\gamma-l\delta]} \cdot e^{j[-k\nu_0-lf_0](\phi+t)} \\
& \cdot (-1)^{2m-k+2n+l} \cdot e^{j\frac{1}{2}\ddot{\phi}[-k(-2m+k)\nu_0^2+2[-nk-l(-m+k)]\nu_0f_0-l(2n+l)f_0^2]} \\
& + \frac{1}{16} \sum_{\substack{m,n,k,l \\ =-\infty \\ =-\infty}}^{\infty} J_m(\beta) J_n(m\psi) J_{m+k}(\beta) J_{n+l}([m+k]\psi) \cdot e^{j[k\gamma+l\delta]} \cdot e^{j[k\nu_0+lf_0](\phi+t)} \\
& \cdot (-1)^{2m+k+4n+2l} \cdot e^{j\frac{1}{2}\ddot{\phi}[k(-2m-k)\nu_0^2+2[-nk+l(-m-k)]\nu_0f_0+l(-2n-l)f_0^2]} \\
& + \frac{1}{16} \sum_{\substack{m,n,k,l \\ =-\infty \\ =-\infty}}^{\infty} J_m(\beta) J_n(m\psi) J_{m+k}(\beta) J_{n-l}([m+k]\psi) \cdot e^{j[k\gamma-l\delta]} \cdot e^{j[k\nu_0-lf_0](\phi+t)} \\
& \cdot (-1)^{2m+k+4n-2l} \cdot e^{j\frac{1}{2}\ddot{\phi}[k(-2m-k)\nu_0^2+2[-nk-l(-m-k)]\nu_0f_0-l(-2n+l)f_0^2]} \\
& + \frac{1}{16} \sum_{\substack{m,n,k,l \\ =-\infty \\ =-\infty}}^{\infty} J_m(\beta) J_n(m\psi) J_{m-k}(\beta) J_{n+l}([m-k]\psi) \cdot e^{j[-k\gamma+l\delta]} \cdot e^{j[-k\nu_0+lf_0](\phi+t)} \\
& \cdot (-1)^{2m-k+4n+2l} \cdot e^{j\frac{1}{2}\ddot{\phi}[-k(-2m+k)\nu_0^2+2[nk+l(-m+k)]\nu_0f_0+l(-2n-l)f_0^2]} \\
& + \frac{1}{16} \sum_{\substack{m,n,k,l \\ =-\infty \\ =-\infty}}^{\infty} J_m(\beta) J_n(m\psi) J_{m-k}(\beta) J_{n-l}([m-k]\psi) \cdot e^{j[-k\gamma-l\delta]} \cdot e^{j[-k\nu_0-lf_0](\phi+t)} \\
& \cdot (-1)^{2m-k+4n-2l} \cdot e^{j\frac{1}{2}\ddot{\phi}[-k(-2m+k)\nu_0^2+2[nk-l(-m+k)]\nu_0f_0-l(-2n+l)f_0^2]}
\end{aligned}$$

We need to distinguish in between the following cases

$$(-1)^{\pm l} = \begin{cases} 1 & l \text{ even} \\ -1 & l \text{ odd} \end{cases}$$

$$(-1)^{\pm k \pm l} = \begin{cases} 1 & k \text{ even, } l \text{ even} & \text{or} & k \text{ odd, } l \text{ odd} \\ -1 & k \text{ odd, } l \text{ even} & & k \text{ even, } l \text{ odd} \end{cases}$$

$$(-1)^{\pm k} = \begin{cases} 1 & k \text{ even} \\ -1 & k \text{ odd} \end{cases}$$

Therefore our discussion is now limited to the following cases

$$\left\{ \begin{array}{l} k \text{ even, } l \text{ even} \\ k \text{ even, } l \text{ odd} \\ k \text{ odd, } l \text{ even} \\ k \text{ odd, } l \text{ odd} \end{array} \right.$$

k even, l even case

$$\begin{aligned}
&= \frac{1}{16} \sum_{\substack{m,n,k,l \\ =-\infty}}^{\infty} J_m(\beta) J_n(m\psi) J_{m-k}(\beta) J_{n-l}([m-k]\psi) \cdot e^{j[k\gamma+l\delta]} \cdot e^{j[k\nu_0+lf_0](\phi+t)} \\
&\cdot e^{j\frac{1}{2}\phi[k(2m-k)\nu_0^2+2[nk+l(m-k)]\nu_0f_0+l(2n-l)f_0^2]} \\
&+ \frac{1}{16} \sum_{\substack{m,n,k,l \\ =-\infty}}^{\infty} J_m(\beta) J_n(m\psi) J_{m-k}(\beta) J_{n+l}([m-k]\psi) \cdot e^{j[k\gamma-l\delta]} \cdot e^{j[k\nu_0-lf_0](\phi+t)} \\
&\cdot e^{j\frac{1}{2}\phi[k(2m-k)\nu_0^2+2[nk-l(m-k)]\nu_0f_0-l(2n+l)f_0^2]} \\
&+ \frac{1}{16} \sum_{\substack{m,n,k,l \\ =-\infty}}^{\infty} J_m(\beta) J_n(m\psi) J_{m+k}(\beta) J_{n-l}([m+k]\psi) \cdot e^{j[-k\gamma+l\delta]} \cdot e^{j[-k\nu_0+lf_0](\phi+t)} \\
&\cdot e^{j\frac{1}{2}\phi[-k(2m+k)\nu_0^2+2[-nk+l(m+k)]\nu_0f_0+l(2n-l)f_0^2]} \\
&+ \frac{1}{16} \sum_{\substack{m,n,k,l \\ =-\infty}}^{\infty} J_m(\beta) J_n(m\psi) J_{m+k}(\beta) J_{n+l}([m+k]\psi) \cdot e^{j[-k\gamma-l\delta]} \cdot e^{j[-k\nu_0-lf_0](\phi+t)} \\
&\cdot e^{j\frac{1}{2}\phi[-k(2m+k)\nu_0^2+2[-nk-l(m+k)]\nu_0f_0-l(2n+l)f_0^2]} \\
&+ \frac{1}{16} \sum_{\substack{m,n,k,l \\ =-\infty}}^{\infty} J_m(\beta) J_n(m\psi) J_{m-k}(\beta) J_{n+l}([m-k]\psi) \cdot e^{j[k\gamma+l\delta]} \cdot e^{j[k\nu_0+lf_0](\phi+t)} \\
&\cdot e^{j\frac{1}{2}\phi[k(2m-k)\nu_0^2+2[-nk+l(m-k)]\nu_0f_0+l(-2n-l)f_0^2]} \\
&+ \frac{1}{16} \sum_{\substack{m,n,k,l \\ =-\infty}}^{\infty} J_m(\beta) J_n(m\psi) J_{m-k}(\beta) J_{n-l}([m-k]\psi) \cdot e^{j[k\gamma-l\delta]} \cdot e^{j[k\nu_0-lf_0](\phi+t)} \\
&\cdot e^{j\frac{1}{2}\phi[k(2m-k)\nu_0^2+2[-nk-l(m-k)]\nu_0f_0-l(-2n+l)f_0^2]} \\
&+ \frac{1}{16} \sum_{\substack{m,n,k,l \\ =-\infty}}^{\infty} J_m(\beta) J_n(m\psi) J_{m+k}(\beta) J_{n+l}([m+k]\psi) \cdot e^{j[-k\gamma+l\delta]} \cdot e^{j[-k\nu_0+lf_0](\phi+t)} \\
&\cdot e^{j\frac{1}{2}\phi[-k(2m+k)\nu_0^2+2[nk+l(m+k)]\nu_0f_0+l(-2n-l)f_0^2]} \\
&+ \frac{1}{16} \sum_{\substack{m,n,k,l \\ =-\infty}}^{\infty} J_m(\beta) J_n(m\psi) J_{m+k}(\beta) J_{n-l}([m+k]\psi) \cdot e^{j[-k\gamma-l\delta]} \cdot e^{j[-k\nu_0-lf_0](\phi+t)} \\
&\cdot e^{j\frac{1}{2}\phi[-k(2m+k)\nu_0^2+2[nk-l(m+k)]\nu_0f_0-l(-2n+l)f_0^2]} \\
&+ \frac{1}{16} \sum_{\substack{m,n,k,l \\ =-\infty}}^{\infty} J_m(\beta) J_n(m\psi) J_{m+k}(\beta) J_{n-l}([m+k]\psi) \cdot e^{j[k\gamma+l\delta]} \cdot e^{j[k\nu_0+lf_0](\phi+t)} \\
&\cdot e^{j\frac{1}{2}\phi[k(-2m-k)\nu_0^2+2[nk+l(-m-k)]\nu_0f_0+l(2n-l)f_0^2]} \\
&+ \frac{1}{16} \sum_{\substack{m,n,k,l \\ =-\infty}}^{\infty} J_m(\beta) J_n(m\psi) J_{m+k}(\beta) J_{n+l}([m+k]\psi) \cdot e^{j[k\gamma-l\delta]} \cdot e^{j[k\nu_0-lf_0](\phi+t)} \\
&\cdot e^{j\frac{1}{2}\phi[k(-2m-k)\nu_0^2+2[nk-l(-m-k)]\nu_0f_0-l(2n+l)f_0^2]} \\
&+ \frac{1}{16} \sum_{\substack{m,n,k,l \\ =-\infty}}^{\infty} J_m(\beta) J_n(m\psi) J_{m-k}(\beta) J_{n-l}([m-k]\psi) \cdot e^{j[-k\gamma+l\delta]} \cdot e^{j[-k\nu_0+lf_0](\phi+t)}
\end{aligned}$$

$$\begin{aligned}
& \cdot e^{j\frac{1}{2}\ddot{\phi}[-k(-2m+k)\nu_0^2+2[-nk+l(-m+k)]\nu_0f_0+l(2n-l)f_0^2]} \\
& + \frac{1}{16} \sum_{\substack{m,n,k,l \\ =-\infty}}^{\infty} J_m(\beta)J_n(m\psi)J_{m-k}(\beta)J_{n+l}([m-k]\psi) \cdot e^{j[-k\gamma-l\delta]} \cdot e^{j[-k\nu_0-lf_0](\phi+t)} \\
& \cdot e^{j\frac{1}{2}\ddot{\phi}[-k(-2m+k)\nu_0^2+2[-nk-l(-m+k)]\nu_0f_0-l(2n+l)f_0^2]} \\
& + \frac{1}{16} \sum_{\substack{m,n,k,l \\ =-\infty}}^{\infty} J_m(\beta)J_n(m\psi)J_{m+k}(\beta)J_{n+l}([m+k]\psi) \cdot e^{j[k\gamma+l\delta]} \cdot e^{j[k\nu_0+lf_0](\phi+t)} \\
& \cdot e^{j\frac{1}{2}\ddot{\phi}[k(-2m-k)\nu_0^2+2[-nk+l(-m-k)]\nu_0f_0+l(-2n-l)f_0^2]} \\
& + \frac{1}{16} \sum_{\substack{m,n,k,l \\ =-\infty}}^{\infty} J_m(\beta)J_n(m\psi)J_{m+k}(\beta)J_{n-l}([m+k]\psi) \cdot e^{j[k\gamma-l\delta]} \cdot e^{j[k\nu_0-lf_0](\phi+t)} \\
& \cdot e^{j\frac{1}{2}\ddot{\phi}[k(-2m-k)\nu_0^2+2[-nk-l(-m-k)]\nu_0f_0-l(-2n+l)f_0^2]} \\
& + \frac{1}{16} \sum_{\substack{m,n,k,l \\ =-\infty}}^{\infty} J_m(\beta)J_n(m\psi)J_{m-k}(\beta)J_{n+l}([m-k]\psi) \cdot e^{j[-k\gamma+l\delta]} \cdot e^{j[-k\nu_0+lf_0](\phi+t)} \\
& \cdot e^{j\frac{1}{2}\ddot{\phi}[-k(-2m+k)\nu_0^2+2[nk+l(-m+k)]\nu_0f_0+l(-2n-l)f_0^2]} \\
& + \frac{1}{16} \sum_{\substack{m,n,k,l \\ =-\infty}}^{\infty} J_m(\beta)J_n(m\psi)J_{m-k}(\beta)J_{n-l}([m-k]\psi) \cdot e^{j[-k\gamma-l\delta]} \cdot e^{j[-k\nu_0-lf_0](\phi+t)} \\
& \cdot e^{j\frac{1}{2}\ddot{\phi}[-k(-2m+k)\nu_0^2+2[nk-l(-m+k)]\nu_0f_0-l(-2n+l)f_0^2]} \\
& + \frac{1}{16} \sum_{\substack{m,n,k,l \\ =-\infty}}^{\infty} J_m(\beta)J_n(m\psi)J_{m-k}(\beta)J_{n-l}([m-k]\psi) \cdot e^{j[k\gamma+l\delta]} \cdot e^{j[k\nu_0+lf_0](\phi+t)} \\
& \cdot e^{j\frac{1}{2}\ddot{\phi}[k(2m-k)\nu_0^2+2[nk+l(m-k)]\nu_0f_0+l(2n-l)f_0^2]} \\
& + \frac{1}{16} \sum_{\substack{m,n,k,l \\ =-\infty}}^{\infty} J_m(\beta)J_n(m\psi)J_{m-k}(\beta)J_{n-l}([m-k]\psi) \cdot e^{j[-k\gamma-l\delta]} \cdot e^{j[-k\nu_0-lf_0](\phi+t)} \\
& \cdot e^{j\frac{1}{2}\ddot{\phi}[-k(-2m+k)\nu_0^2+2[nk-l(-m+k)]\nu_0f_0-l(-2n+l)f_0^2]} \\
& + \frac{1}{16} \sum_{\substack{m,n,k,l \\ =-\infty}}^{\infty} J_m(\beta)J_n(m\psi)J_{m-k}(\beta)J_{n-l}([m-k]\psi) \cdot e^{j[k\gamma-l\delta]} \cdot e^{j[k\nu_0-lf_0](\phi+t)} \\
& \cdot e^{j\frac{1}{2}\ddot{\phi}[k(2m-k)\nu_0^2+2[-nk-l(m-k)]\nu_0f_0-l(-2n+l)f_0^2]} \\
& + \frac{1}{16} \sum_{\substack{m,n,k,l \\ =-\infty}}^{\infty} J_m(\beta)J_n(m\psi)J_{m-k}(\beta)J_{n-l}([m-k]\psi) \cdot e^{j[-k\gamma+l\delta]} \cdot e^{j[-k\nu_0+lf_0](\phi+t)} \\
& \cdot e^{j\frac{1}{2}\ddot{\phi}[-k(-2m+k)\nu_0^2+2[-nk+l(-m+k)]\nu_0f_0+l(2n-l)f_0^2]} \\
& + \frac{1}{16} \sum_{\substack{m,n,k,l \\ =-\infty}}^{\infty} J_m(\beta)J_n(m\psi)J_{m-k}(\beta)J_{n+l}([m-k]\psi) \cdot e^{j[k\gamma-l\delta]} \cdot e^{j[k\nu_0-lf_0](\phi+t)} \\
& \cdot e^{j\frac{1}{2}\ddot{\phi}[k(2m-k)\nu_0^2+2[nk-l(m-k)]\nu_0f_0-l(2n+l)f_0^2]}
\end{aligned}$$

rearranging common RF fading terms (due to dispersion) in adjacent lines

$$\begin{aligned}
& = \frac{1}{16} \sum_{\substack{m,n,k,l \\ =-\infty}}^{\infty} J_m(\beta)J_n(m\psi)J_{m-k}(\beta)J_{n-l}([m-k]\psi) \cdot e^{j[k\gamma+l\delta]} \cdot e^{j[k\nu_0+lf_0](\phi+t)} \\
& \cdot e^{j\frac{1}{2}\ddot{\phi}[k(2m-k)\nu_0^2+2[nk+l(m-k)]\nu_0f_0+l(2n-l)f_0^2]} \\
& + \frac{1}{16} \sum_{\substack{m,n,k,l \\ =-\infty}}^{\infty} J_m(\beta)J_n(m\psi)J_{m-k}(\beta)J_{n-l}([m-k]\psi) \cdot e^{j[-k\gamma-l\delta]} \cdot e^{j[-k\nu_0-lf_0](\phi+t)} \\
& \cdot e^{j\frac{1}{2}\ddot{\phi}[-k(-2m+k)\nu_0^2+2[nk-l(-m+k)]\nu_0f_0-l(-2n+l)f_0^2]} \\
& + \frac{1}{16} \sum_{\substack{m,n,k,l \\ =-\infty}}^{\infty} J_m(\beta)J_n(m\psi)J_{m-k}(\beta)J_{n-l}([m-k]\psi) \cdot e^{j[k\gamma-l\delta]} \cdot e^{j[k\nu_0-lf_0](\phi+t)} \\
& \cdot e^{j\frac{1}{2}\ddot{\phi}[k(2m-k)\nu_0^2+2[-nk-l(m-k)]\nu_0f_0-l(-2n+l)f_0^2]} \\
& + \frac{1}{16} \sum_{\substack{m,n,k,l \\ =-\infty}}^{\infty} J_m(\beta)J_n(m\psi)J_{m-k}(\beta)J_{n-l}([m-k]\psi) \cdot e^{j[-k\gamma+l\delta]} \cdot e^{j[-k\nu_0+lf_0](\phi+t)} \\
& \cdot e^{j\frac{1}{2}\ddot{\phi}[-k(-2m+k)\nu_0^2+2[-nk+l(-m+k)]\nu_0f_0+l(2n-l)f_0^2]} \\
& + \frac{1}{16} \sum_{\substack{m,n,k,l \\ =-\infty}}^{\infty} J_m(\beta)J_n(m\psi)J_{m-k}(\beta)J_{n+l}([m-k]\psi) \cdot e^{j[k\gamma-l\delta]} \cdot e^{j[k\nu_0-lf_0](\phi+t)} \\
& \cdot e^{j\frac{1}{2}\ddot{\phi}[k(2m-k)\nu_0^2+2[nk-l(m-k)]\nu_0f_0-l(2n+l)f_0^2]}
\end{aligned}$$

$$\begin{aligned}
& + \frac{1}{16} \sum_{\substack{m,n,k,l \\ =-\infty}}^{\infty} J_m(\beta) J_n(m\psi) J_{m-k}(\beta) J_{n+l}([m-k]\psi) \cdot e^{j[-k\gamma+l\delta]} \cdot e^{j[-k\nu_0+lf_0](\phi+t)} \\
& \cdot e^{j\frac{1}{2}\phi[-k(-2m+k)\nu_0^2+2[nk+l(-m+k)]\nu_0f_0+l(-2n-l)f_0^2]} \\
& + \frac{1}{16} \sum_{\substack{m,n,k,l \\ =-\infty}}^{\infty} J_m(\beta) J_n(m\psi) J_{m-k}(\beta) J_{n+l}([m-k]\psi) \cdot e^{j[k\gamma+l\delta]} \cdot e^{j[k\nu_0+lf_0](\phi+t)} \\
& \cdot e^{j\frac{1}{2}\phi[k(2m-k)\nu_0^2+2[-nk+l(m-k)]\nu_0f_0+l(-2n-l)f_0^2]} \\
& + \frac{1}{16} \sum_{\substack{m,n,k,l \\ =-\infty}}^{\infty} J_m(\beta) J_n(m\psi) J_{m-k}(\beta) J_{n+l}([m-k]\psi) \cdot e^{j[-k\gamma-l\delta]} \cdot e^{j[-k\nu_0-lf_0](\phi+t)} \\
& \cdot e^{j\frac{1}{2}\phi[-k(-2m+k)\nu_0^2+2[-nk-l(-m+k)]\nu_0f_0-l(2n+l)f_0^2]} \\
& + \frac{1}{16} \sum_{\substack{m,n,k,l \\ =-\infty}}^{\infty} J_m(\beta) J_n(m\psi) J_{m+k}(\beta) J_{n-l}([m+k]\psi) \cdot e^{j[-k\gamma+l\delta]} \cdot e^{j[-k\nu_0+lf_0](\phi+t)} \\
& \cdot e^{j\frac{1}{2}\phi[-k(2m+k)\nu_0^2+2[-nk+l(m+k)]\nu_0f_0+l(2n-l)f_0^2]} \\
& + \frac{1}{16} \sum_{\substack{m,n,k,l \\ =-\infty}}^{\infty} J_m(\beta) J_n(m\psi) J_{m+k}(\beta) J_{n-l}([m+k]\psi) \cdot e^{j[k\gamma-l\delta]} \cdot e^{j[k\nu_0-lf_0](\phi+t)} \\
& \cdot e^{j\frac{1}{2}\phi[k(-2m-k)\nu_0^2+2[-nk-l(-m-k)]\nu_0f_0-l(-2n+l)f_0^2]} \\
& + \frac{1}{16} \sum_{\substack{m,n,k,l \\ =-\infty}}^{\infty} J_m(\beta) J_n(m\psi) J_{m+k}(\beta) J_{n-l}([m+k]\psi) \cdot e^{j[-k\gamma-l\delta]} \cdot e^{j[-k\nu_0-lf_0](\phi+t)} \\
& \cdot e^{j\frac{1}{2}\phi[-k(2m+k)\nu_0^2+2[nk-l(m+k)]\nu_0f_0-l(-2n+l)f_0^2]} \\
& + \frac{1}{16} \sum_{\substack{m,n,k,l \\ =-\infty}}^{\infty} J_m(\beta) J_n(m\psi) J_{m+k}(\beta) J_{n-l}([m+k]\psi) \cdot e^{j[k\gamma+l\delta]} \cdot e^{j[k\nu_0+lf_0](\phi+t)} \\
& \cdot e^{j\frac{1}{2}\phi[k(-2m-k)\nu_0^2+2[nk+l(-m-k)]\nu_0f_0+l(2n-l)f_0^2]} \\
& + \frac{1}{16} \sum_{\substack{m,n,k,l \\ =-\infty}}^{\infty} J_m(\beta) J_n(m\psi) J_{m+k}(\beta) J_{n+l}([m+k]\psi) \cdot e^{j[-k\gamma-l\delta]} \cdot e^{j[-k\nu_0-lf_0](\phi+t)} \\
& \cdot e^{j\frac{1}{2}\phi[-k(2m+k)\nu_0^2+2[-nk-l(m+k)]\nu_0f_0-l(2n+l)f_0^2]} \\
& + \frac{1}{16} \sum_{\substack{m,n,k,l \\ =-\infty}}^{\infty} J_m(\beta) J_n(m\psi) J_{m+k}(\beta) J_{n+l}([m+k]\psi) \cdot e^{j[k\gamma+l\delta]} \cdot e^{j[k\nu_0+lf_0](\phi+t)} \\
& \cdot e^{j\frac{1}{2}\phi[k(-2m-k)\nu_0^2+2[-nk+l(-m-k)]\nu_0f_0+l(-2n-l)f_0^2]} \\
& + \frac{1}{16} \sum_{\substack{m,n,k,l \\ =-\infty}}^{\infty} J_m(\beta) J_n(m\psi) J_{m+k}(\beta) J_{n+l}([m+k]\psi) \cdot e^{j[-k\gamma+l\delta]} \cdot e^{j[-k\nu_0+lf_0](\phi+t)} \\
& \cdot e^{j\frac{1}{2}\phi[-k(2m+k)\nu_0^2+2[nk+l(m+k)]\nu_0f_0+l(-2n-l)f_0^2]} \\
& + \frac{1}{16} \sum_{\substack{m,n,k,l \\ =-\infty}}^{\infty} J_m(\beta) J_n(m\psi) J_{m+k}(\beta) J_{n+l}([m+k]\psi) \cdot e^{j[k\gamma-l\delta]} \cdot e^{j[k\nu_0-lf_0](\phi+t)}
\end{aligned}$$

$$e^{j\frac{1}{2}\phi}[k(-2m-k)\nu_0^2+2[nk-l(-m-k)]\nu_0f_0-l(2n+l)f_0^2]$$

assembling trigonometric identities

$$\begin{aligned}
&= \frac{1}{8} \sum_{\substack{m,n,k,l \\ =-\infty}}^{\infty} J_m(\beta)J_n(m\psi)J_{m-k}(\beta)J_{n-l}([m-k]\psi) \cdot \cos[(k\nu_0+lf_0)(\dot{\phi}+t)+k\gamma+l\delta] \\
&\cdot e^{j\frac{1}{2}\phi}[k(2m-k)\nu_0^2+2[nk+l(m-k)]\nu_0f_0+l(2n-l)f_0^2] \\
&+ \frac{1}{8} \sum_{\substack{m,n,k,l \\ =-\infty}}^{\infty} J_m(\beta)J_n(m\psi)J_{m-k}(\beta)J_{n-l}([m-k]\psi) \cdot \cos[(k\nu_0-lf_0)(\dot{\phi}+t)+k\gamma-l\delta] \\
&\cdot e^{j\frac{1}{2}\phi}[-k(-2m+k)\nu_0^2+2[-nk+l(-m+k)]\nu_0f_0+l(2n-l)f_0^2] \\
&+ \frac{1}{8} \sum_{\substack{m,n,k,l \\ =-\infty}}^{\infty} J_m(\beta)J_n(m\psi)J_{m-k}(\beta)J_{n+l}([m-k]\psi) \cdot \cos[(k\nu_0-lf_0)(\dot{\phi}+t)+k\gamma-l\delta] \\
&\cdot e^{j\frac{1}{2}\phi}[k(2m-k)\nu_0^2+2[nk-l(m-k)]\nu_0f_0-l(2n+l)f_0^2] \\
&+ \frac{1}{8} \sum_{\substack{m,n,k,l \\ =-\infty}}^{\infty} J_m(\beta)J_n(m\psi)J_{m-k}(\beta)J_{n+l}([m-k]\psi) \cdot \cos[(k\nu_0+lf_0)(\dot{\phi}+t)+k\gamma+l\delta] \\
&\cdot e^{j\frac{1}{2}\phi}[k(2m-k)\nu_0^2+2[-nk+l(m-k)]\nu_0f_0+l(-2n-l)f_0^2] \\
&+ \frac{1}{8} \sum_{\substack{m,n,k,l \\ =-\infty}}^{\infty} J_m(\beta)J_n(m\psi)J_{m+k}(\beta)J_{n-l}([m+k]\psi) \cdot \cos[(k\nu_0-lf_0)(\dot{\phi}+t)+k\gamma-l\delta] \\
&\cdot e^{j\frac{1}{2}\phi}[-k(2m+k)\nu_0^2+2[-nk+l(m+k)]\nu_0f_0+l(2n-l)f_0^2] \\
&+ \frac{1}{8} \sum_{\substack{m,n,k,l \\ =-\infty}}^{\infty} J_m(\beta)J_n(m\psi)J_{m+k}(\beta)J_{n-l}([m+k]\psi) \cdot \cos[(k\nu_0+lf_0)(\dot{\phi}+t)+k\gamma+l\delta] \\
&\cdot e^{j\frac{1}{2}\phi}[k(-2m-k)\nu_0^2+2[nk+l(-m-k)]\nu_0f_0+l(2n-l)f_0^2] \\
&+ \frac{1}{8} \sum_{\substack{m,n,k,l \\ =-\infty}}^{\infty} J_m(\beta)J_n(m\psi)J_{m+k}(\beta)J_{n+l}([m+k]\psi) \cdot \cos[(k\nu_0+lf_0)(\dot{\phi}+t)+k\gamma+l\delta] \\
&\cdot e^{j\frac{1}{2}\phi}[-k(2m+k)\nu_0^2+2[-nk-l(m+k)]\nu_0f_0-l(2n+l)f_0^2] \\
&+ \frac{1}{8} \sum_{\substack{m,n,k,l \\ =-\infty}}^{\infty} J_m(\beta)J_n(m\psi)J_{m+k}(\beta)J_{n+l}([m+k]\psi) \cdot \cos[(k\nu_0-lf_0)(\dot{\phi}+t)+k\gamma-l\delta] \\
&\cdot e^{j\frac{1}{2}\phi}[-k(2m+k)\nu_0^2+2[nk+l(m+k)]\nu_0f_0+l(-2n-l)f_0^2]
\end{aligned}$$

after rearranging common expressions and substitute $l = -l$

$$\begin{aligned}
&= \frac{1}{8} \sum_{\substack{m,n,k,l \\ =-\infty}}^{\infty} J_m(\beta)J_n(m\psi)J_{m-k}(\beta)J_{n-l}([m-k]\psi) \cdot \cos[(k\nu_0+lf_0)(\dot{\phi}+t)+k\gamma+l\delta] \\
&\cdot e^{j\frac{1}{2}\phi}[k(2m-k)\nu_0^2+2[nk+l(m-k)]\nu_0f_0+l(2n-l)f_0^2] \\
&+ \frac{1}{8} \sum_{\substack{m,n,k,l \\ =-\infty}}^{\infty} J_m(\beta)J_n(m\psi)J_{m-k}(\beta)J_{n-l}([m-k]\psi) \cdot \cos[(k\nu_0+lf_0)(\dot{\phi}+t)+k\gamma+l\delta]
\end{aligned}$$

$$\begin{aligned}
& \cdot e^{j\frac{1}{2}\dot{\phi}[k(2m-k)\nu_0^2+2[nk+l(m-k)]\nu_0f_0+l(2n-l)f_0^2]} \\
& + \frac{1}{8} \sum_{\substack{m,n,k,l \\ =-\infty}}^{\infty} J_m(\beta)J_n(m\psi)J_{m-k}(\beta)J_{n+l}([m-k]\psi) \cdot \cos[(k\nu_0+lf_0)(\dot{\phi}+t)+k\gamma+l\delta] \\
& \cdot e^{j\frac{1}{2}\dot{\phi}[k(2m-k)\nu_0^2+2[-nk+l(m-k)]\nu_0f_0+l(-2n-l)f_0^2]} \\
& + \frac{1}{8} \sum_{\substack{m,n,k,l \\ =-\infty}}^{\infty} J_m(\beta)J_n(m\psi)J_{m-k}(\beta)J_{n+l}([m-k]\psi) \cdot \cos[(k\nu_0+lf_0)(\dot{\phi}+t)+k\gamma+l\delta] \\
& \cdot e^{j\frac{1}{2}\dot{\phi}[-k(-2m+k)\nu_0^2+2[-nk-l(-m+k)]\nu_0f_0-l(2n+l)f_0^2]} \\
& + \frac{1}{8} \sum_{\substack{m,n,k,l \\ =-\infty}}^{\infty} J_m(\beta)J_n(m\psi)J_{m+k}(\beta)J_{n-l}([m+k]\psi) \cdot \cos[(k\nu_0+lf_0)(\dot{\phi}+t)+k\gamma+l\delta] \\
& \cdot e^{j\frac{1}{2}\dot{\phi}[k(-2m-k)\nu_0^2+2[nk+l(-m-k)]\nu_0f_0+l(2n-l)f_0^2]} \\
& + \frac{1}{8} \sum_{\substack{m,n,k,l \\ =-\infty}}^{\infty} J_m(\beta)J_n(m\psi)J_{m+k}(\beta)J_{n-l}([m+k]\psi) \cdot \cos[(k\nu_0+lf_0)(\dot{\phi}+t)+k\gamma+l\delta] \\
& \cdot e^{j\frac{1}{2}\dot{\phi}[-k(2m+k)\nu_0^2+2[nk-l(m+k)]\nu_0f_0+l(2n-l)f_0^2]} \\
& + \frac{1}{8} \sum_{\substack{m,n,k,l \\ =-\infty}}^{\infty} J_m(\beta)J_n(m\psi)J_{m+k}(\beta)J_{n+l}([m+k]\psi) \cdot \cos[(k\nu_0+lf_0)(\dot{\phi}+t)+k\gamma+l\delta] \\
& \cdot e^{j\frac{1}{2}\dot{\phi}[-k(2m+k)\nu_0^2-2[nk+l(m+k)]\nu_0f_0-l(2n+l)f_0^2]} \\
& + \frac{1}{8} \sum_{\substack{m,n,k,l \\ =-\infty}}^{\infty} J_m(\beta)J_n(m\psi)J_{m+k}(\beta)J_{n+l}([m+k]\psi) \cdot \cos[(k\nu_0+lf_0)(\dot{\phi}+t)+k\gamma+l\delta] \\
& \cdot e^{j\frac{1}{2}\dot{\phi}[-k(2m+k)\nu_0^2-2[nk+l(m+k)]\nu_0f_0-l(2n+l)f_0^2]}
\end{aligned}$$

substitute $n = -n$

$$\begin{aligned}
& = \frac{1}{4} \sum_{\substack{m,n,k,l \\ =-\infty}}^{\infty} J_m(\beta)J_n(m\psi)J_{m-k}(\beta)J_{n-l}([m-k]\psi) \cdot \cos[(k\nu_0+lf_0)(\dot{\phi}+t)+k\gamma+l\delta] \\
& \cdot e^{j\frac{1}{2}\dot{\phi}[k(2m-k)\nu_0^2+2[nk+l(m-k)]\nu_0f_0+l(2n-l)f_0^2]} \\
& + \frac{1}{4} \sum_{\substack{m,n,k,l \\ =-\infty}}^{\infty} J_m(\beta)J_{-n}(m\psi)J_{m-k}(\beta)J_{-n+l}([m-k]\psi) \cdot \cos[(k\nu_0+lf_0)(\dot{\phi}+t)+k\gamma+l\delta] \\
& \cdot e^{j\frac{1}{2}\dot{\phi}[k(2m-k)\nu_0^2+2[nk+l(m-k)]\nu_0f_0+l(2n-l)f_0^2]} \\
& + \frac{1}{4} \sum_{\substack{m,n,k,l \\ =-\infty}}^{\infty} J_m(\beta)J_{-n}(m\psi)J_{m+k}(\beta)J_{-n-l}([m+k]\psi) \cdot \cos[(k\nu_0+lf_0)(\dot{\phi}+t)+k\gamma+l\delta] \\
& \cdot e^{j\frac{1}{2}\dot{\phi}[k(-2m-k)\nu_0^2+2[-nk+l(m+k)]\nu_0f_0-l(2n+l)f_0^2]} \\
& + \frac{1}{4} \sum_{\substack{m,n,k,l \\ =-\infty}}^{\infty} J_m(\beta)J_n(m\psi)J_{m+k}(\beta)J_{n+l}([m+k]\psi) \cdot \cos[(k\nu_0+lf_0)(\dot{\phi}+t)+k\gamma+l\delta] \\
& \cdot e^{j\frac{1}{2}\dot{\phi}[-k(2m+k)\nu_0^2-2[nk+l(m+k)]\nu_0f_0-l(2n+l)f_0^2]}
\end{aligned}$$

l even case

$$\begin{aligned}
&= \frac{1}{4} \sum_{\substack{m,n,k,l \\ =-\infty}}^{\infty} J_m(\beta) J_n(m\psi) J_{m-k}(\beta) J_{n-l}([m-k]\psi) \cdot \cos[(k\nu_0 + lf_0)(\dot{\phi} + t) + k\gamma + l\delta] \\
&\cdot e^{j\frac{1}{2}\dot{\phi}[k(2m-k)\nu_0^2 + 2[nk+l(m-k)]\nu_0 f_0 + l(2n-l)f_0^2]} \\
&+ \frac{1}{4} \sum_{\substack{m,n,k,l \\ =-\infty}}^{\infty} J_m(\beta) J_n(m\psi) J_{m-k}(\beta) J_{n-l}([m-k]\psi) \cdot \cos[(k\nu_0 + lf_0)(\dot{\phi} + t) + k\gamma + l\delta] \\
&\cdot e^{j\frac{1}{2}\dot{\phi}[k(2m-k)\nu_0^2 + 2[nk+l(m-k)]\nu_0 f_0 + l(2n-l)f_0^2]} \\
&+ \frac{1}{4} \sum_{\substack{m,n,k,l \\ =-\infty}}^{\infty} J_m(\beta) J_n(m\psi) J_{m+k}(\beta) J_{n+l}([m+k]\psi) \cdot \cos[(k\nu_0 + lf_0)(\dot{\phi} + t) + k\gamma + l\delta] \\
&\cdot e^{-j\frac{1}{2}\dot{\phi}[k(2m+k)\nu_0^2 + 2[nk+l(m+k)]\nu_0 f_0 + l(2n+l)f_0^2]} \\
&+ \frac{1}{4} \sum_{\substack{m,n,k,l \\ =-\infty}}^{\infty} J_m(\beta) J_n(m\psi) J_{m+k}(\beta) J_{n+l}([m+k]\psi) \cdot \cos[(k\nu_0 + lf_0)(\dot{\phi} + t) + k\gamma + l\delta] \\
&\cdot e^{-j\frac{1}{2}\dot{\phi}[k(2m+k)\nu_0^2 + 2[nk+l(m+k)]\nu_0 f_0 + l(2n+l)f_0^2]} \\
&= \frac{1}{2} \sum_{\substack{m,n,k,l \\ =-\infty}}^{\infty} J_m(\beta) J_n(m\psi) J_{m-k}(\beta) J_{n-l}([m-k]\psi) \cdot \cos[(k\nu_0 + lf_0)(\dot{\phi} + t) + k\gamma + l\delta] \\
&\cdot e^{j\frac{1}{2}\dot{\phi}[k(2m-k)\nu_0^2 + 2[nk+l(m-k)]\nu_0 f_0 + l(2n-l)f_0^2]} \\
&+ \frac{1}{2} \sum_{\substack{m,n,k,l \\ =-\infty}}^{\infty} J_m(\beta) J_n(m\psi) J_{m+k}(\beta) J_{n+l}([m+k]\psi) \cdot \cos[(k\nu_0 + lf_0)(\dot{\phi} + t) + k\gamma + l\delta] \\
&\cdot e^{-j\frac{1}{2}\dot{\phi}[k(2m+k)\nu_0^2 + 2[nk+l(m+k)]\nu_0 f_0 + l(2n+l)f_0^2]}
\end{aligned}$$

in 2nd equation substitute variable

$$m + k = \xi, \quad m = \xi - k, \quad 2m + k = 2\xi - 2k + k = 2\xi - k$$

$$\Rightarrow m + k \rightarrow m; \quad m \rightarrow m - k; \quad 2m + k \rightarrow 2m - k$$

$$n + l = \xi, \quad n = \xi - l, \quad 2n + l = 2\xi - 2l + l = 2\xi - l$$

$$\Rightarrow n + l \rightarrow n; \quad n \rightarrow n - l; \quad 2n + l \rightarrow 2n - l$$

$$\begin{aligned}
&= \frac{1}{2} \sum_{\substack{m,n,k,l \\ =-\infty}}^{\infty} J_m(\beta) J_n(m\psi) J_{m-k}(\beta) J_{n-l}([m-k]\psi) \cdot \cos[(k\nu_0 + lf_0)(\dot{\phi} + t) + k\gamma + l\delta] \\
&\cdot e^{j\frac{1}{2}\dot{\phi}[k(2m-k)\nu_0^2 + 2[nk+l(m-k)]\nu_0 f_0 + l(2n-l)f_0^2]} \\
&+ \frac{1}{2} \sum_{\substack{m,n,k,l \\ =-\infty}}^{\infty} J_{m-k}(\beta) J_{n-l}([m-k]\psi) J_m(\beta) J_n(m\psi) \cdot \cos[(k\nu_0 + lf_0)(\dot{\phi} + t) + k\gamma + l\delta] \\
&\cdot e^{-j\frac{1}{2}\dot{\phi}[k(2m-k)\nu_0^2 + 2[(n-l)k+lm]\nu_0 f_0 + l(2n-l)f_0^2]} \\
&= \sum_{\substack{m,n,k,l \\ =-\infty}}^{\infty} J_m(\beta) J_n(m\psi) J_{m-k}(\beta) J_{n-l}([m-k]\psi) \cdot \cos[(k\nu_0 + lf_0)(\dot{\phi} + t) + k\gamma + l\delta]
\end{aligned}$$

$$\cdot \cos\left(\frac{1}{2}\ddot{\phi} [k(2m-k)\nu_0^2 + 2[nk+l(m-k)]\nu_0 f_0 + l(2n-l)f_0^2]\right)$$

or (substitute $n \rightarrow n+l$, $m \rightarrow m+k$)

$$= \sum_{\substack{m,n,k,l \\ =-\infty}}^{\infty} J_m(\beta) J_n(m\psi) J_{m+k}(\beta) J_{n+l}([m+k]\psi) \cdot \cos[(k\nu_0 + lf_0)(\dot{\phi} + t) + k\gamma + l\delta]$$

$$\cdot \cos\left(\frac{1}{2}\ddot{\phi} [k(2m+k)\nu_0^2 + 2[nk+l(m+k)]\nu_0 f_0 + l(2n+l)f_0^2]\right).$$

k even, l odd case

$$\begin{aligned}
&= \frac{1}{16} \sum_{\substack{m,n,k,l \\ =-\infty}}^{\infty} J_m(\beta) J_n(m\psi) J_{m-k}(\beta) J_{n-l}([m-k]\psi) \cdot e^{j[k\gamma+l\delta]} \cdot e^{j[k\nu_0+lf_0](\phi+t)} \\
&\cdot e^{j\frac{1}{2}\phi[k(2m-k)\nu_0^2+2[nk+l(m-k)]\nu_0f_0+l(2n-l)f_0^2]} \\
&+ \frac{1}{16} \sum_{\substack{m,n,k,l \\ =-\infty}}^{\infty} J_m(\beta) J_n(m\psi) J_{m-k}(\beta) J_{n+l}([m-k]\psi) \cdot e^{j[k\gamma-l\delta]} \cdot e^{j[k\nu_0-lf_0](\phi+t)} \\
&\cdot e^{j\frac{1}{2}\phi[k(2m-k)\nu_0^2+2[nk-l(m-k)]\nu_0f_0-l(2n+l)f_0^2]} \\
&+ \frac{1}{16} \sum_{\substack{m,n,k,l \\ =-\infty}}^{\infty} J_m(\beta) J_n(m\psi) J_{m+k}(\beta) J_{n-l}([m+k]\psi) \cdot e^{j[-k\gamma+l\delta]} \cdot e^{j[-k\nu_0+lf_0](\phi+t)} \\
&\cdot e^{j\frac{1}{2}\phi[-k(2m+k)\nu_0^2+2[-nk+l(m+k)]\nu_0f_0+l(2n-l)f_0^2]} \\
&+ \frac{1}{16} \sum_{\substack{m,n,k,l \\ =-\infty}}^{\infty} J_m(\beta) J_n(m\psi) J_{m+k}(\beta) J_{n+l}([m+k]\psi) \cdot e^{j[-k\gamma-l\delta]} \cdot e^{j[-k\nu_0-lf_0](\phi+t)} \\
&\cdot e^{j\frac{1}{2}\phi[-k(2m+k)\nu_0^2+2[-nk-l(m+k)]\nu_0f_0-l(2n+l)f_0^2]} \\
&- \frac{1}{16} \sum_{\substack{m,n,k,l \\ =-\infty}}^{\infty} J_m(\beta) J_n(m\psi) J_{m-k}(\beta) J_{n+l}([m-k]\psi) \cdot e^{j[k\gamma+l\delta]} \cdot e^{j[k\nu_0+lf_0](\phi+t)} \\
&\cdot e^{j\frac{1}{2}\phi[k(2m-k)\nu_0^2+2[-nk+l(m-k)]\nu_0f_0+l(-2n-l)f_0^2]} \\
&- \frac{1}{16} \sum_{\substack{m,n,k,l \\ =-\infty}}^{\infty} J_m(\beta) J_n(m\psi) J_{m-k}(\beta) J_{n-l}([m-k]\psi) \cdot e^{j[k\gamma-l\delta]} \cdot e^{j[k\nu_0-lf_0](\phi+t)} \\
&\cdot e^{j\frac{1}{2}\phi[k(2m-k)\nu_0^2+2[-nk-l(m-k)]\nu_0f_0-l(-2n+l)f_0^2]} \\
&- \frac{1}{16} \sum_{\substack{m,n,k,l \\ =-\infty}}^{\infty} J_m(\beta) J_n(m\psi) J_{m+k}(\beta) J_{n+l}([m+k]\psi) \cdot e^{j[-k\gamma+l\delta]} \cdot e^{j[-k\nu_0+lf_0](\phi+t)} \\
&\cdot e^{j\frac{1}{2}\phi[-k(2m+k)\nu_0^2+2[nk+l(m+k)]\nu_0f_0+l(-2n-l)f_0^2]} \\
&- \frac{1}{16} \sum_{\substack{m,n,k,l \\ =-\infty}}^{\infty} J_m(\beta) J_n(m\psi) J_{m+k}(\beta) J_{n-l}([m+k]\psi) \cdot e^{j[-k\gamma-l\delta]} \cdot e^{j[-k\nu_0-lf_0](\phi+t)} \\
&\cdot e^{j\frac{1}{2}\phi[-k(2m+k)\nu_0^2+2[nk-l(m+k)]\nu_0f_0-l(-2n+l)f_0^2]} \\
&- \frac{1}{16} \sum_{\substack{m,n,k,l \\ =-\infty}}^{\infty} J_m(\beta) J_n(m\psi) J_{m+k}(\beta) J_{n-l}([m+k]\psi) \cdot e^{j[k\gamma+l\delta]} \cdot e^{j[k\nu_0+lf_0](\phi+t)} \\
&\cdot e^{j\frac{1}{2}\phi[k(-2m-k)\nu_0^2+2[nk+l(-m-k)]\nu_0f_0+l(2n-l)f_0^2]} \\
&- \frac{1}{16} \sum_{\substack{m,n,k,l \\ =-\infty}}^{\infty} J_m(\beta) J_n(m\psi) J_{m+k}(\beta) J_{n+l}([m+k]\psi) \cdot e^{j[k\gamma-l\delta]} \cdot e^{j[k\nu_0-lf_0](\phi+t)} \\
&\cdot e^{j\frac{1}{2}\phi[k(-2m-k)\nu_0^2+2[nk-l(-m-k)]\nu_0f_0-l(2n+l)f_0^2]} \\
&- \frac{1}{16} \sum_{\substack{m,n,k,l \\ =-\infty}}^{\infty} J_m(\beta) J_n(m\psi) J_{m-k}(\beta) J_{n-l}([m-k]\psi) \cdot e^{j[-k\gamma+l\delta]} \cdot e^{j[-k\nu_0+lf_0](\phi+t)}
\end{aligned}$$

$$\begin{aligned}
& \cdot e^{j\frac{1}{2}\phi[-k(-2m+k)\nu_0^2+2[-nk+l(-m+k)]\nu_0f_0+l(2n-l)f_0^2]} \\
& -\frac{1}{16} \sum_{\substack{m,n,k,l \\ =-\infty}}^{\infty} J_m(\beta)J_n(m\psi)J_{m-k}(\beta)J_{n+l}([m-k]\psi) \cdot e^{j[-k\gamma-l\delta]} \cdot e^{j[-k\nu_0-lf_0](\phi+t)} \\
& \cdot e^{j\frac{1}{2}\phi[-k(-2m+k)\nu_0^2+2[-nk-l(-m+k)]\nu_0f_0-l(2n+l)f_0^2]} \\
& +\frac{1}{16} \sum_{\substack{m,n,k,l \\ =-\infty}}^{\infty} J_m(\beta)J_n(m\psi)J_{m+k}(\beta)J_{n+l}([m+k]\psi) \cdot e^{j[k\gamma+l\delta]} \cdot e^{j[k\nu_0+lf_0](\phi+t)} \\
& \cdot e^{j\frac{1}{2}\phi[k(-2m-k)\nu_0^2+2[-nk+l(-m-k)]\nu_0f_0+l(-2n-l)f_0^2]} \\
& +\frac{1}{16} \sum_{\substack{m,n,k,l \\ =-\infty}}^{\infty} J_m(\beta)J_n(m\psi)J_{m+k}(\beta)J_{n-l}([m+k]\psi) \cdot e^{j[k\gamma-l\delta]} \cdot e^{j[k\nu_0-lf_0](\phi+t)} \\
& \cdot e^{j\frac{1}{2}\phi[k(-2m-k)\nu_0^2+2[-nk-l(-m-k)]\nu_0f_0-l(-2n+l)f_0^2]} \\
& +\frac{1}{16} \sum_{\substack{m,n,k,l \\ =-\infty}}^{\infty} J_m(\beta)J_n(m\psi)J_{m-k}(\beta)J_{n+l}([m-k]\psi) \cdot e^{j[-k\gamma+l\delta]} \cdot e^{j[-k\nu_0+lf_0](\phi+t)} \\
& \cdot e^{j\frac{1}{2}\phi[-k(-2m+k)\nu_0^2+2[nk+l(-m+k)]\nu_0f_0+l(-2n-l)f_0^2]} \\
& +\frac{1}{16} \sum_{\substack{m,n,k,l \\ =-\infty}}^{\infty} J_m(\beta)J_n(m\psi)J_{m-k}(\beta)J_{n-l}([m-k]\psi) \cdot e^{j[-k\gamma-l\delta]} \cdot e^{j[-k\nu_0-lf_0](\phi+t)} \\
& \cdot e^{j\frac{1}{2}\phi[-k(-2m+k)\nu_0^2+2[nk-l(-m+k)]\nu_0f_0-l(-2n+l)f_0^2]} \\
& +\frac{1}{16} \sum_{\substack{m,n,k,l \\ =-\infty}}^{\infty} J_m(\beta)J_n(m\psi)J_{m-k}(\beta)J_{n-l}([m-k]\psi) \cdot e^{j[-k\gamma-l\delta]} \cdot e^{j[-k\nu_0-lf_0](\phi+t)} \\
& \cdot e^{j\frac{1}{2}\phi[-k(-2m+k)\nu_0^2+2[nk+l(-m+k)]\nu_0f_0+l(-2n-l)f_0^2]} \\
& +\frac{1}{16} \sum_{\substack{m,n,k,l \\ =-\infty}}^{\infty} J_m(\beta)J_n(m\psi)J_{m-k}(\beta)J_{n-l}([m-k]\psi) \cdot e^{j[-k\gamma-l\delta]} \cdot e^{j[-k\nu_0-lf_0](\phi+t)} \\
& \cdot e^{j\frac{1}{2}\phi[k(2m-k)\nu_0^2+2[nk+l(m-k)]\nu_0f_0+l(2n-l)f_0^2]} \\
& +\frac{1}{16} \sum_{\substack{m,n,k,l \\ =-\infty}}^{\infty} J_m(\beta)J_n(m\psi)J_{m-k}(\beta)J_{n-l}([m-k]\psi) \cdot e^{j[-k\gamma-l\delta]} \cdot e^{j[-k\nu_0-lf_0](\phi+t)} \\
& \cdot e^{j\frac{1}{2}\phi[-k(-2m+k)\nu_0^2+2[nk-l(-m+k)]\nu_0f_0-l(-2n+l)f_0^2]} \\
& -\frac{1}{16} \sum_{\substack{m,n,k,l \\ =-\infty}}^{\infty} J_m(\beta)J_n(m\psi)J_{m-k}(\beta)J_{n-l}([m-k]\psi) \cdot e^{j[k\gamma-l\delta]} \cdot e^{j[k\nu_0-lf_0](\phi+t)} \\
& \cdot e^{j\frac{1}{2}\phi[k(2m-k)\nu_0^2+2[-nk-l(m-k)]\nu_0f_0-l(-2n+l)f_0^2]} \\
& -\frac{1}{16} \sum_{\substack{m,n,k,l \\ =-\infty}}^{\infty} J_m(\beta)J_n(m\psi)J_{m-k}(\beta)J_{n-l}([m-k]\psi) \cdot e^{j[-k\gamma+l\delta]} \cdot e^{j[-k\nu_0+lf_0](\phi+t)} \\
& \cdot e^{j\frac{1}{2}\phi[-k(-2m+k)\nu_0^2+2[-nk+l(-m+k)]\nu_0f_0+l(2n-l)f_0^2]} \\
& +\frac{1}{16} \sum_{\substack{m,n,k,l \\ =-\infty}}^{\infty} J_m(\beta)J_n(m\psi)J_{m-k}(\beta)J_{n+l}([m-k]\psi) \cdot e^{j[k\gamma-l\delta]} \cdot e^{j[k\nu_0-lf_0](\phi+t)} \\
& \cdot e^{j\frac{1}{2}\phi[k(2m-k)\nu_0^2+2[nk-l(m-k)]\nu_0f_0-l(2n+l)f_0^2]}
\end{aligned}$$

rearranging common RF fading terms (due to dispersion) in adjacent lines

$$\begin{aligned}
& = \frac{1}{16} \sum_{\substack{m,n,k,l \\ =-\infty}}^{\infty} J_m(\beta)J_n(m\psi)J_{m-k}(\beta)J_{n-l}([m-k]\psi) \cdot e^{j[k\gamma+l\delta]} \cdot e^{j[k\nu_0+lf_0](\phi+t)} \\
& \cdot e^{j\frac{1}{2}\phi[k(2m-k)\nu_0^2+2[nk+l(m-k)]\nu_0f_0+l(2n-l)f_0^2]} \\
& +\frac{1}{16} \sum_{\substack{m,n,k,l \\ =-\infty}}^{\infty} J_m(\beta)J_n(m\psi)J_{m-k}(\beta)J_{n-l}([m-k]\psi) \cdot e^{j[-k\gamma-l\delta]} \cdot e^{j[-k\nu_0-lf_0](\phi+t)} \\
& \cdot e^{j\frac{1}{2}\phi[-k(-2m+k)\nu_0^2+2[nk-l(-m+k)]\nu_0f_0-l(-2n+l)f_0^2]} \\
& -\frac{1}{16} \sum_{\substack{m,n,k,l \\ =-\infty}}^{\infty} J_m(\beta)J_n(m\psi)J_{m-k}(\beta)J_{n-l}([m-k]\psi) \cdot e^{j[k\gamma-l\delta]} \cdot e^{j[k\nu_0-lf_0](\phi+t)} \\
& \cdot e^{j\frac{1}{2}\phi[k(2m-k)\nu_0^2+2[-nk-l(m-k)]\nu_0f_0-l(-2n+l)f_0^2]} \\
& -\frac{1}{16} \sum_{\substack{m,n,k,l \\ =-\infty}}^{\infty} J_m(\beta)J_n(m\psi)J_{m-k}(\beta)J_{n-l}([m-k]\psi) \cdot e^{j[-k\gamma+l\delta]} \cdot e^{j[-k\nu_0+lf_0](\phi+t)} \\
& \cdot e^{j\frac{1}{2}\phi[-k(-2m+k)\nu_0^2+2[-nk+l(-m+k)]\nu_0f_0+l(2n-l)f_0^2]} \\
& +\frac{1}{16} \sum_{\substack{m,n,k,l \\ =-\infty}}^{\infty} J_m(\beta)J_n(m\psi)J_{m-k}(\beta)J_{n+l}([m-k]\psi) \cdot e^{j[k\gamma-l\delta]} \cdot e^{j[k\nu_0-lf_0](\phi+t)} \\
& \cdot e^{j\frac{1}{2}\phi[k(2m-k)\nu_0^2+2[nk-l(m-k)]\nu_0f_0-l(2n+l)f_0^2]}
\end{aligned}$$

$$\begin{aligned}
& + \frac{1}{16} \sum_{\substack{m,n,k,l \\ =-\infty}}^{\infty} J_m(\beta) J_n(m\psi) J_{m-k}(\beta) J_{n+l}([m-k]\psi) \cdot e^{j[-k\gamma+l\delta]} \cdot e^{j[-k\nu_0+lf_0](\phi+t)} \\
& \cdot e^{j\frac{1}{2}\phi[-k(-2m+k)\nu_0^2+2[nk+l(-m+k)]\nu_0f_0+l(-2n-l)f_0^2]} \\
& - \frac{1}{16} \sum_{\substack{m,n,k,l \\ =-\infty}}^{\infty} J_m(\beta) J_n(m\psi) J_{m-k}(\beta) J_{n+l}([m-k]\psi) \cdot e^{j[k\gamma+l\delta]} \cdot e^{j[k\nu_0+lf_0](\phi+t)} \\
& \cdot e^{j\frac{1}{2}\phi[k(2m-k)\nu_0^2+2[-nk+l(m-k)]\nu_0f_0+l(-2n-l)f_0^2]} \\
& - \frac{1}{16} \sum_{\substack{m,n,k,l \\ =-\infty}}^{\infty} J_m(\beta) J_n(m\psi) J_{m-k}(\beta) J_{n+l}([m-k]\psi) \cdot e^{j[-k\gamma-l\delta]} \cdot e^{j[-k\nu_0-lf_0](\phi+t)} \\
& \cdot e^{j\frac{1}{2}\phi[-k(-2m+k)\nu_0^2+2[-nk-l(-m+k)]\nu_0f_0-l(2n+l)f_0^2]} \\
& + \frac{1}{16} \sum_{\substack{m,n,k,l \\ =-\infty}}^{\infty} J_m(\beta) J_n(m\psi) J_{m+k}(\beta) J_{n-l}([m+k]\psi) \cdot e^{j[-k\gamma+l\delta]} \cdot e^{j[-k\nu_0+lf_0](\phi+t)} \\
& \cdot e^{j\frac{1}{2}\phi[-k(2m+k)\nu_0^2+2[-nk+l(m+k)]\nu_0f_0+l(2n-l)f_0^2]} \\
& + \frac{1}{16} \sum_{\substack{m,n,k,l \\ =-\infty}}^{\infty} J_m(\beta) J_n(m\psi) J_{m+k}(\beta) J_{n-l}([m+k]\psi) \cdot e^{j[k\gamma-l\delta]} \cdot e^{j[k\nu_0-lf_0](\phi+t)} \\
& \cdot e^{j\frac{1}{2}\phi[k(-2m-k)\nu_0^2+2[-nk-l(-m-k)]\nu_0f_0-l(-2n+l)f_0^2]} \\
& - \frac{1}{16} \sum_{\substack{m,n,k,l \\ =-\infty}}^{\infty} J_m(\beta) J_n(m\psi) J_{m+k}(\beta) J_{n-l}([m+k]\psi) \cdot e^{j[-k\gamma-l\delta]} \cdot e^{j[-k\nu_0-lf_0](\phi+t)} \\
& \cdot e^{j\frac{1}{2}\phi[-k(2m+k)\nu_0^2+2[nk-l(m+k)]\nu_0f_0-l(-2n+l)f_0^2]} \\
& - \frac{1}{16} \sum_{\substack{m,n,k,l \\ =-\infty}}^{\infty} J_m(\beta) J_n(m\psi) J_{m+k}(\beta) J_{n-l}([m+k]\psi) \cdot e^{j[k\gamma+l\delta]} \cdot e^{j[k\nu_0+lf_0](\phi+t)} \\
& \cdot e^{j\frac{1}{2}\phi[k(-2m-k)\nu_0^2+2[nk+l(-m-k)]\nu_0f_0+l(2n-l)f_0^2]} \\
& + \frac{1}{16} \sum_{\substack{m,n,k,l \\ =-\infty}}^{\infty} J_m(\beta) J_n(m\psi) J_{m+k}(\beta) J_{n+l}([m+k]\psi) \cdot e^{j[-k\gamma-l\delta]} \cdot e^{j[-k\nu_0-lf_0](\phi+t)} \\
& \cdot e^{j\frac{1}{2}\phi[-k(2m+k)\nu_0^2+2[-nk-l(m+k)]\nu_0f_0-l(2n+l)f_0^2]} \\
& + \frac{1}{16} \sum_{\substack{m,n,k,l \\ =-\infty}}^{\infty} J_m(\beta) J_n(m\psi) J_{m+k}(\beta) J_{n+l}([m+k]\psi) \cdot e^{j[k\gamma+l\delta]} \cdot e^{j[k\nu_0+lf_0](\phi+t)} \\
& \cdot e^{j\frac{1}{2}\phi[k(-2m-k)\nu_0^2+2[-nk+l(-m-k)]\nu_0f_0+l(-2n-l)f_0^2]} \\
& - \frac{1}{16} \sum_{\substack{m,n,k,l \\ =-\infty}}^{\infty} J_m(\beta) J_n(m\psi) J_{m+k}(\beta) J_{n+l}([m+k]\psi) \cdot e^{j[-k\gamma+l\delta]} \cdot e^{j[-k\nu_0+lf_0](\phi+t)} \\
& \cdot e^{j\frac{1}{2}\phi[-k(2m+k)\nu_0^2+2[nk+l(m+k)]\nu_0f_0+l(-2n-l)f_0^2]} \\
& - \frac{1}{16} \sum_{\substack{m,n,k,l \\ =-\infty}}^{\infty} J_m(\beta) J_n(m\psi) J_{m+k}(\beta) J_{n+l}([m+k]\psi) \cdot e^{j[k\gamma-l\delta]} \cdot e^{j[k\nu_0-lf_0](\phi+t)}
\end{aligned}$$

$$e^{j\frac{1}{2}\phi}[k(-2m-k)\nu_0^2+2[nk-l(-m-k)]\nu_0f_0-l(2n+l)f_0^2]$$

assembling trigonometric identities

$$\begin{aligned}
&= \frac{1}{8} \sum_{\substack{m,n,k,l \\ =-\infty}}^{\infty} J_m(\beta)J_n(m\psi)J_{m-k}(\beta)J_{n-l}([m-k]\psi) \cdot \cos[(k\nu_0+lf_0)(\dot{\phi}+t)+k\gamma+l\delta] \\
&\cdot e^{j\frac{1}{2}\phi}[k(2m-k)\nu_0^2+2[nk+l(m-k)]\nu_0f_0+l(2n-l)f_0^2] \\
&- \frac{1}{8} \sum_{\substack{m,n,k,l \\ =-\infty}}^{\infty} J_m(\beta)J_n(m\psi)J_{m-k}(\beta)J_{n-l}([m-k]\psi) \cdot \cos[(k\nu_0-lf_0)(\dot{\phi}+t)+k\gamma-l\delta] \\
&\cdot e^{j\frac{1}{2}\phi}[k(2m-k)\nu_0^2+2[-nk-l(m-k)]\nu_0f_0-l(-2n+l)f_0^2] \\
&+ \frac{1}{8} \sum_{\substack{m,n,k,l \\ =-\infty}}^{\infty} J_m(\beta)J_n(m\psi)J_{m-k}(\beta)J_{n+l}([m-k]\psi) \cdot \cos[(k\nu_0-lf_0)(\dot{\phi}+t)+k\gamma-l\delta] \\
&\cdot e^{j\frac{1}{2}\phi}[k(2m-k)\nu_0^2+2[nk-l(m-k)]\nu_0f_0-l(2n+l)f_0^2] \\
&- \frac{1}{8} \sum_{\substack{m,n,k,l \\ =-\infty}}^{\infty} J_m(\beta)J_n(m\psi)J_{m-k}(\beta)J_{n+l}([m-k]\psi) \cdot \cos[(k\nu_0+lf_0)(\dot{\phi}+t)+k\gamma+l\delta] \\
&\cdot e^{j\frac{1}{2}\phi}[k(2m-k)\nu_0^2+2[-nk+l(m-k)]\nu_0f_0+l(-2n-l)f_0^2] \\
&+ \frac{1}{8} \sum_{\substack{m,n,k,l \\ =-\infty}}^{\infty} J_m(\beta)J_n(m\psi)J_{m+k}(\beta)J_{n-l}([m+k]\psi) \cdot \cos[(k\nu_0-lf_0)(\dot{\phi}+t)+k\gamma-l\delta] \\
&\cdot e^{j\frac{1}{2}\phi}[-k(2m+k)\nu_0^2+2[-nk+l(m+k)]\nu_0f_0+l(2n-l)f_0^2] \\
&- \frac{1}{8} \sum_{\substack{m,n,k,l \\ =-\infty}}^{\infty} J_m(\beta)J_n(m\psi)J_{m+k}(\beta)J_{n-l}([m+k]\psi) \cdot \cos[(k\nu_0+lf_0)(\dot{\phi}+t)+k\gamma+l\delta] \\
&\cdot e^{j\frac{1}{2}\phi}[-k(2m+k)\nu_0^2+2[nk-l(m+k)]\nu_0f_0-l(-2n+l)f_0^2] \\
&+ \frac{1}{8} \sum_{\substack{m,n,k,l \\ =-\infty}}^{\infty} J_m(\beta)J_n(m\psi)J_{m+k}(\beta)J_{n+l}([m+k]\psi) \cdot \cos[(k\nu_0+lf_0)(\dot{\phi}+t)+k\gamma+l\delta] \\
&\cdot e^{j\frac{1}{2}\phi}[-k(2m+k)\nu_0^2+2[-nk-l(m+k)]\nu_0f_0-l(2n+l)f_0^2] \\
&- \frac{1}{8} \sum_{\substack{m,n,k,l \\ =-\infty}}^{\infty} J_m(\beta)J_n(m\psi)J_{m+k}(\beta)J_{n+l}([m+k]\psi) \cdot \cos[(k\nu_0-lf_0)(\dot{\phi}+t)+k\gamma-l\delta] \\
&\cdot e^{j\frac{1}{2}\phi}[-k(2m+k)\nu_0^2+2[nk+l(m+k)]\nu_0f_0+l(-2n-l)f_0^2]
\end{aligned}$$

after rearranging common expressions and substitute $l = -l$

$$\begin{aligned}
&= \frac{1}{8} \sum_{\substack{m,n,k,l \\ =-\infty}}^{\infty} J_m(\beta)J_n(m\psi)J_{m-k}(\beta)J_{n-l}([m-k]\psi) \cdot \cos[(k\nu_0+lf_0)(\dot{\phi}+t)+k\gamma+l\delta] \\
&\cdot e^{j\frac{1}{2}\phi}[k(2m-k)\nu_0^2+2[nk+l(m-k)]\nu_0f_0+l(2n-l)f_0^2] \\
&+ \frac{1}{8} \sum_{\substack{m,n,k,l \\ =-\infty}}^{\infty} J_m(\beta)J_n(m\psi)J_{m-k}(\beta)J_{n-l}([m-k]\psi) \cdot \cos[(k\nu_0+lf_0)(\dot{\phi}+t)+k\gamma+l\delta]
\end{aligned}$$

$$\begin{aligned}
& \cdot e^{j\frac{1}{2}\ddot{\phi}[k(2m-k)\nu_0^2+2[nk+l(m-k)]\nu_0f_0+l(2n-l)f_0^2]} \\
& -\frac{1}{8}\sum_{\substack{m,n,k,l \\ =-\infty}}^{\infty} J_m(\beta)J_n(m\psi)J_{m-k}(\beta)J_{n+l}([m-k]\psi) \cdot \cos[(k\nu_0+lf_0)(\dot{\phi}+t)+k\gamma+l\delta] \\
& \cdot e^{j\frac{1}{2}\ddot{\phi}[k(2m-k)\nu_0^2+2[-nk+l(m-k)]\nu_0f_0+l(-2n-l)f_0^2]} \\
& -\frac{1}{8}\sum_{\substack{m,n,k,l \\ =-\infty}}^{\infty} J_m(\beta)J_n(m\psi)J_{m-k}(\beta)J_{n+l}([m-k]\psi) \cdot \cos[(k\nu_0+lf_0)(\dot{\phi}+t)+k\gamma+l\delta] \\
& \cdot e^{j\frac{1}{2}\ddot{\phi}[k(2m-k)\nu_0^2+2[-nk+l(m-k)]\nu_0f_0-l(2n+l)f_0^2]} \\
& -\frac{1}{8}\sum_{\substack{m,n,k,l \\ =-\infty}}^{\infty} J_m(\beta)J_n(m\psi)J_{m+k}(\beta)J_{n-l}([m+k]\psi) \cdot \cos[(k\nu_0+lf_0)(\dot{\phi}+t)+k\gamma+l\delta] \\
& \cdot e^{j\frac{1}{2}\ddot{\phi}[-k(2m+k)\nu_0^2+2[nk-l(m+k)]\nu_0f_0+l(2n-l)f_0^2]} \\
& -\frac{1}{8}\sum_{\substack{m,n,k,l \\ =-\infty}}^{\infty} J_m(\beta)J_n(m\psi)J_{m+k}(\beta)J_{n-l}([m+k]\psi) \cdot \cos[(k\nu_0+lf_0)(\dot{\phi}+t)+k\gamma+l\delta] \\
& \cdot e^{j\frac{1}{2}\ddot{\phi}[-k(2m+k)\nu_0^2+2[nk-l(m+k)]\nu_0f_0+l(2n-l)f_0^2]} \\
& +\frac{1}{8}\sum_{\substack{m,n,k,l \\ =-\infty}}^{\infty} J_m(\beta)J_n(m\psi)J_{m+k}(\beta)J_{n+l}([m+k]\psi) \cdot \cos[(k\nu_0+lf_0)(\dot{\phi}+t)+k\gamma+l\delta] \\
& \cdot e^{-j\frac{1}{2}\ddot{\phi}[k(2m+k)\nu_0^2+2[nk+l(m+k)]\nu_0f_0+l(2n+l)f_0^2]} \\
& +\frac{1}{8}\sum_{\substack{m,n,k,l \\ =-\infty}}^{\infty} J_m(\beta)J_n(m\psi)J_{m+k}(\beta)J_{n+l}([m+k]\psi) \cdot \cos[(k\nu_0+lf_0)(\dot{\phi}+t)+k\gamma+l\delta] \\
& \cdot e^{-j\frac{1}{2}\ddot{\phi}[k(2m+k)\nu_0^2+2[nk+l(m+k)]\nu_0f_0+l(2n+l)f_0^2]}
\end{aligned}$$

substitute $n = -n$

$$\begin{aligned}
& = \frac{1}{4}\sum_{\substack{m,n,k,l \\ =-\infty}}^{\infty} J_m(\beta)J_n(m\psi)J_{m-k}(\beta)J_{n-l}([m-k]\psi) \cdot \cos[(k\nu_0+lf_0)(\dot{\phi}+t)+k\gamma+l\delta] \\
& \cdot e^{j\frac{1}{2}\ddot{\phi}[k(2m-k)\nu_0^2+2[nk+l(m-k)]\nu_0f_0+l(2n-l)f_0^2]} \\
& -\frac{1}{4}\sum_{\substack{m,n,k,l \\ =-\infty}}^{\infty} J_m(\beta)J_{-n}(m\psi)J_{m-k}(\beta)J_{-n+l}([m-k]\psi) \cdot \cos[(k\nu_0+lf_0)(\dot{\phi}+t)+k\gamma+l\delta] \\
& \cdot e^{j\frac{1}{2}\ddot{\phi}[k(2m-k)\nu_0^2+2[nk+l(m-k)]\nu_0f_0-l(-2n+l)f_0^2]} \\
& -\frac{1}{4}\sum_{\substack{m,n,k,l \\ =-\infty}}^{\infty} J_m(\beta)J_{-n}(m\psi)J_{m+k}(\beta)J_{-n-l}([m+k]\psi) \cdot \cos[(k\nu_0+lf_0)(\dot{\phi}+t)+k\gamma+l\delta] \\
& \cdot e^{-j\frac{1}{2}\ddot{\phi}[k(2m+k)\nu_0^2+2[nk+l(m+k)]\nu_0f_0+l(2n+l)f_0^2]} \\
& +\frac{1}{4}\sum_{\substack{m,n,k,l \\ =-\infty}}^{\infty} J_m(\beta)J_n(m\psi)J_{m+k}(\beta)J_{n+l}([m+k]\psi) \cdot \cos[(k\nu_0+lf_0)(\dot{\phi}+t)+k\gamma+l\delta] \\
& \cdot e^{-j\frac{1}{2}\ddot{\phi}[k(2m+k)\nu_0^2+2[nk+l(m+k)]\nu_0f_0+l(2n+l)f_0^2]}
\end{aligned}$$

l odd case

$$\begin{aligned}
&= \frac{1}{4} \sum_{\substack{m,n,k,l \\ =-\infty}}^{\infty} J_m(\beta) J_n(m\psi) J_{m-k}(\beta) J_{n-l}([m-k]\psi) \cdot \cos[(k\nu_0 + lf_0)(\dot{\phi} + t) + k\gamma + l\delta] \\
&\cdot e^{j\frac{1}{2}\ddot{\phi}[k(2m-k)\nu_0^2 + 2[nk+l(m-k)]\nu_0 f_0 + l(2n-l)f_0^2]} \\
&+ \frac{1}{4} \sum_{\substack{m,n,k,l \\ =-\infty}}^{\infty} J_m(\beta) J_n(m\psi) J_{m-k}(\beta) J_{n-l}([m-k]\psi) \cdot \cos[(k\nu_0 + lf_0)(\dot{\phi} + t) + k\gamma + l\delta] \\
&\cdot e^{j\frac{1}{2}\ddot{\phi}[k(2m-k)\nu_0^2 + 2[nk+l(m-k)]\nu_0 f_0 - l(-2n+l)f_0^2]} \\
&+ \frac{1}{4} \sum_{\substack{m,n,k,l \\ =-\infty}}^{\infty} J_m(\beta) J_n(m\psi) J_{m+k}(\beta) J_{n+l}([m+k]\psi) \cdot \cos[(k\nu_0 + lf_0)(\dot{\phi} + t) + k\gamma + l\delta] \\
&\cdot e^{-j\frac{1}{2}\ddot{\phi}[k(2m+k)\nu_0^2 + 2[nk+l(m+k)]\nu_0 f_0 + l(2n+l)f_0^2]} \\
&+ \frac{1}{4} \sum_{\substack{m,n,k,l \\ =-\infty}}^{\infty} J_m(\beta) J_n(m\psi) J_{m+k}(\beta) J_{n+l}([m+k]\psi) \cdot \cos[(k\nu_0 + lf_0)(\dot{\phi} + t) + k\gamma + l\delta] \\
&\cdot e^{-j\frac{1}{2}\ddot{\phi}[k(2m+k)\nu_0^2 + 2[nk+l(m+k)]\nu_0 f_0 + l(2n+l)f_0^2]}
\end{aligned}$$

identical to previous case i.e., independent of l polarity

$$\begin{aligned}
&= \sum_{\substack{m,n,k,l \\ =-\infty}}^{\infty} J_m(\beta) J_n(m\psi) J_{m-k}(\beta) J_{n-l}([m-k]\psi) \cdot \cos[(k\nu_0 + lf_0)(\dot{\phi} + t) + k\gamma + l\delta] \\
&\cdot \cos\left(\frac{1}{2}\ddot{\phi} [k(2m-k)\nu_0^2 + 2[nk+l(m-k)]\nu_0 f_0 + l(2n-l)f_0^2]\right)
\end{aligned}$$

or

$$\begin{aligned}
&\sum_{\substack{m,n,k,l \\ =-\infty}}^{\infty} J_m(\beta) J_n(m\psi) J_{m+k}(\beta) J_{n+l}([m+k]\psi) \cdot \cos[(k\nu_0 + lf_0)(\dot{\phi} + t) + k\gamma + l\delta] \\
&\cdot \cos\left(\frac{1}{2}\ddot{\phi} [k(2m+k)\nu_0^2 + 2[nk+l(m+k)]\nu_0 f_0 + l(2n+l)f_0^2]\right).
\end{aligned}$$

k odd, l even case

$$\begin{aligned}
&= \frac{1}{16} \sum_{\substack{m,n,k,l \\ =-\infty}}^{\infty} J_m(\beta) J_n(m\psi) J_{m-k}(\beta) J_{n-l}([m-k]\psi) \cdot e^{j[k\gamma+l\delta]} \cdot e^{j[k\nu_0+lf_0](\phi+t)} \\
&\cdot e^{j\frac{1}{2}\phi[k(2m-k)\nu_0^2+2[nk+l(m-k)]\nu_0f_0+l(2n-l)f_0^2]} \\
&+ \frac{1}{16} \sum_{\substack{m,n,k,l \\ =-\infty}}^{\infty} J_m(\beta) J_n(m\psi) J_{m-k}(\beta) J_{n+l}([m-k]\psi) \cdot e^{j[k\gamma-l\delta]} \cdot e^{j[k\nu_0-lf_0](\phi+t)} \\
&\cdot e^{j\frac{1}{2}\phi[k(2m-k)\nu_0^2+2[nk-l(m-k)]\nu_0f_0-l(2n+l)f_0^2]} \\
&+ \frac{1}{16} \sum_{\substack{m,n,k,l \\ =-\infty}}^{\infty} J_m(\beta) J_n(m\psi) J_{m+k}(\beta) J_{n-l}([m+k]\psi) \cdot e^{j[-k\gamma+l\delta]} \cdot e^{j[-k\nu_0+lf_0](\phi+t)} \\
&\cdot e^{j\frac{1}{2}\phi[-k(2m+k)\nu_0^2+2[-nk+l(m+k)]\nu_0f_0+l(2n-l)f_0^2]} \\
&+ \frac{1}{16} \sum_{\substack{m,n,k,l \\ =-\infty}}^{\infty} J_m(\beta) J_n(m\psi) J_{m+k}(\beta) J_{n+l}([m+k]\psi) \cdot e^{j[-k\gamma-l\delta]} \cdot e^{j[-k\nu_0-lf_0](\phi+t)} \\
&\cdot e^{j\frac{1}{2}\phi[-k(2m+k)\nu_0^2+2[-nk-l(m+k)]\nu_0f_0-l(2n+l)f_0^2]} \\
&+ \frac{1}{16} \sum_{\substack{m,n,k,l \\ =-\infty}}^{\infty} J_m(\beta) J_n(m\psi) J_{m-k}(\beta) J_{n+l}([m-k]\psi) \cdot e^{j[k\gamma+l\delta]} \cdot e^{j[k\nu_0+lf_0](\phi+t)} \\
&\cdot e^{j\frac{1}{2}\phi[k(2m-k)\nu_0^2+2[-nk+l(m-k)]\nu_0f_0+l(-2n-l)f_0^2]} \\
&+ \frac{1}{16} \sum_{\substack{m,n,k,l \\ =-\infty}}^{\infty} J_m(\beta) J_n(m\psi) J_{m-k}(\beta) J_{n-l}([m-k]\psi) \cdot e^{j[k\gamma-l\delta]} \cdot e^{j[k\nu_0-lf_0](\phi+t)} \\
&\cdot e^{j\frac{1}{2}\phi[k(2m-k)\nu_0^2+2[-nk-l(m-k)]\nu_0f_0-l(-2n+l)f_0^2]} \\
&+ \frac{1}{16} \sum_{\substack{m,n,k,l \\ =-\infty}}^{\infty} J_m(\beta) J_n(m\psi) J_{m+k}(\beta) J_{n+l}([m+k]\psi) \cdot e^{j[-k\gamma+l\delta]} \cdot e^{j[-k\nu_0+lf_0](\phi+t)} \\
&\cdot e^{j\frac{1}{2}\phi[-k(2m+k)\nu_0^2+2[nk+l(m+k)]\nu_0f_0+l(-2n-l)f_0^2]} \\
&+ \frac{1}{16} \sum_{\substack{m,n,k,l \\ =-\infty}}^{\infty} J_m(\beta) J_n(m\psi) J_{m+k}(\beta) J_{n-l}([m+k]\psi) \cdot e^{j[-k\gamma-l\delta]} \cdot e^{j[-k\nu_0-lf_0](\phi+t)} \\
&\cdot e^{j\frac{1}{2}\phi[-k(2m+k)\nu_0^2+2[nk-l(m+k)]\nu_0f_0-l(-2n+l)f_0^2]} \\
&- \frac{1}{16} \sum_{\substack{m,n,k,l \\ =-\infty}}^{\infty} J_m(\beta) J_n(m\psi) J_{m+k}(\beta) J_{n-l}([m+k]\psi) \cdot e^{j[k\gamma+l\delta]} \cdot e^{j[k\nu_0+lf_0](\phi+t)} \\
&\cdot e^{j\frac{1}{2}\phi[k(-2m-k)\nu_0^2+2[nk+l(-m-k)]\nu_0f_0+l(2n-l)f_0^2]} \\
&- \frac{1}{16} \sum_{\substack{m,n,k,l \\ =-\infty}}^{\infty} J_m(\beta) J_n(m\psi) J_{m+k}(\beta) J_{n+l}([m+k]\psi) \cdot e^{j[k\gamma-l\delta]} \cdot e^{j[k\nu_0-lf_0](\phi+t)} \\
&\cdot e^{j\frac{1}{2}\phi[k(-2m-k)\nu_0^2+2[nk-l(-m-k)]\nu_0f_0-l(2n+l)f_0^2]} \\
&- \frac{1}{16} \sum_{\substack{m,n,k,l \\ =-\infty}}^{\infty} J_m(\beta) J_n(m\psi) J_{m-k}(\beta) J_{n-l}([m-k]\psi) \cdot e^{j[-k\gamma+l\delta]} \cdot e^{j[-k\nu_0+lf_0](\phi+t)}
\end{aligned}$$

$$\begin{aligned}
& \cdot e^{j\frac{1}{2}\phi[-k(-2m+k)\nu_0^2+2[-nk+l(-m+k)]\nu_0f_0+l(2n-l)f_0^2]} \\
& -\frac{1}{16}\sum_{\substack{m,n,k,l \\ =-\infty}}^{\infty} J_m(\beta)J_n(m\psi)J_{m-k}(\beta)J_{n+l}([m-k]\psi) \cdot e^{j[-k\gamma-l\delta]} \cdot e^{j[-k\nu_0-lf_0](\phi+t)} \\
& \cdot e^{j\frac{1}{2}\phi[-k(-2m+k)\nu_0^2+2[-nk-l(-m+k)]\nu_0f_0-l(2n+l)f_0^2]} \\
& -\frac{1}{16}\sum_{\substack{m,n,k,l \\ =-\infty}}^{\infty} J_m(\beta)J_n(m\psi)J_{m+k}(\beta)J_{n+l}([m+k]\psi) \cdot e^{j[k\gamma+l\delta]} \cdot e^{j[k\nu_0+lf_0](\phi+t)} \\
& \cdot e^{j\frac{1}{2}\phi[k(-2m-k)\nu_0^2+2[-nk+l(-m-k)]\nu_0f_0+l(-2n-l)f_0^2]} \\
& -\frac{1}{16}\sum_{\substack{m,n,k,l \\ =-\infty}}^{\infty} J_m(\beta)J_n(m\psi)J_{m+k}(\beta)J_{n-l}([m+k]\psi) \cdot e^{j[k\gamma-l\delta]} \cdot e^{j[k\nu_0-lf_0](\phi+t)} \\
& \cdot e^{j\frac{1}{2}\phi[k(-2m-k)\nu_0^2+2[-nk-l(-m-k)]\nu_0f_0-l(-2n+l)f_0^2]} \\
& -\frac{1}{16}\sum_{\substack{m,n,k,l \\ =-\infty}}^{\infty} J_m(\beta)J_n(m\psi)J_{m-k}(\beta)J_{n+l}([m-k]\psi) \cdot e^{j[-k\gamma+l\delta]} \cdot e^{j[-k\nu_0+lf_0](\phi+t)} \\
& \cdot e^{j\frac{1}{2}\phi[-k(-2m+k)\nu_0^2+2[nk+l(-m+k)]\nu_0f_0+l(-2n-l)f_0^2]} \\
& -\frac{1}{16}\sum_{\substack{m,n,k,l \\ =-\infty}}^{\infty} J_m(\beta)J_n(m\psi)J_{m-k}(\beta)J_{n-l}([m-k]\psi) \cdot e^{j[-k\gamma-l\delta]} \cdot e^{j[-k\nu_0-lf_0](\phi+t)} \\
& \cdot e^{j\frac{1}{2}\phi[-k(-2m+k)\nu_0^2+2[nk-l(-m+k)]\nu_0f_0-l(-2n+l)f_0^2]} \\
& -\frac{1}{16}\sum_{\substack{m,n,k,l \\ =-\infty}}^{\infty} J_m(\beta)J_n(m\psi)J_{m-k}(\beta)J_{n-l}([m-k]\psi) \cdot e^{j[-k\gamma-l\delta]} \cdot e^{j[-k\nu_0-lf_0](\phi+t)} \\
& \cdot e^{j\frac{1}{2}\phi[k(2m-k)\nu_0^2+2[nk+l(m-k)]\nu_0f_0+l(2n-l)f_0^2]} \\
& -\frac{1}{16}\sum_{\substack{m,n,k,l \\ =-\infty}}^{\infty} J_m(\beta)J_n(m\psi)J_{m-k}(\beta)J_{n-l}([m-k]\psi) \cdot e^{j[-k\gamma-l\delta]} \cdot e^{j[-k\nu_0-lf_0](\phi+t)} \\
& \cdot e^{j\frac{1}{2}\phi[-k(-2m+k)\nu_0^2+2[nk-l(-m+k)]\nu_0f_0-l(-2n+l)f_0^2]} \\
& +\frac{1}{16}\sum_{\substack{m,n,k,l \\ =-\infty}}^{\infty} J_m(\beta)J_n(m\psi)J_{m-k}(\beta)J_{n-l}([m-k]\psi) \cdot e^{j[k\gamma-l\delta]} \cdot e^{j[k\nu_0-lf_0](\phi+t)} \\
& \cdot e^{j\frac{1}{2}\phi[k(2m-k)\nu_0^2+2[-nk-l(m-k)]\nu_0f_0-l(-2n+l)f_0^2]} \\
& -\frac{1}{16}\sum_{\substack{m,n,k,l \\ =-\infty}}^{\infty} J_m(\beta)J_n(m\psi)J_{m-k}(\beta)J_{n-l}([m-k]\psi) \cdot e^{j[-k\gamma+l\delta]} \cdot e^{j[-k\nu_0+lf_0](\phi+t)} \\
& \cdot e^{j\frac{1}{2}\phi[-k(-2m+k)\nu_0^2+2[-nk+l(-m+k)]\nu_0f_0+l(2n-l)f_0^2]} \\
& +\frac{1}{16}\sum_{\substack{m,n,k,l \\ =-\infty}}^{\infty} J_m(\beta)J_n(m\psi)J_{m-k}(\beta)J_{n+l}([m-k]\psi) \cdot e^{j[k\gamma-l\delta]} \cdot e^{j[k\nu_0-lf_0](\phi+t)} \\
& \cdot e^{j\frac{1}{2}\phi[k(2m-k)\nu_0^2+2[nk-l(m-k)]\nu_0f_0-l(2n+l)f_0^2]}
\end{aligned}$$

rearranging common RF fading terms (due to dispersion) in adjacent lines

$$\begin{aligned}
& =\frac{1}{16}\sum_{\substack{m,n,k,l \\ =-\infty}}^{\infty} J_m(\beta)J_n(m\psi)J_{m-k}(\beta)J_{n-l}([m-k]\psi) \cdot e^{j[k\gamma+l\delta]} \cdot e^{j[k\nu_0+lf_0](\phi+t)} \\
& \cdot e^{j\frac{1}{2}\phi[k(2m-k)\nu_0^2+2[nk+l(m-k)]\nu_0f_0+l(2n-l)f_0^2]} \\
& -\frac{1}{16}\sum_{\substack{m,n,k,l \\ =-\infty}}^{\infty} J_m(\beta)J_n(m\psi)J_{m-k}(\beta)J_{n-l}([m-k]\psi) \cdot e^{j[-k\gamma-l\delta]} \cdot e^{j[-k\nu_0-lf_0](\phi+t)} \\
& \cdot e^{j\frac{1}{2}\phi[-k(-2m+k)\nu_0^2+2[nk-l(-m+k)]\nu_0f_0-l(-2n+l)f_0^2]} \\
& +\frac{1}{16}\sum_{\substack{m,n,k,l \\ =-\infty}}^{\infty} J_m(\beta)J_n(m\psi)J_{m-k}(\beta)J_{n-l}([m-k]\psi) \cdot e^{j[k\gamma-l\delta]} \cdot e^{j[k\nu_0-lf_0](\phi+t)} \\
& \cdot e^{j\frac{1}{2}\phi[k(2m-k)\nu_0^2+2[-nk-l(m-k)]\nu_0f_0-l(-2n+l)f_0^2]} \\
& -\frac{1}{16}\sum_{\substack{m,n,k,l \\ =-\infty}}^{\infty} J_m(\beta)J_n(m\psi)J_{m-k}(\beta)J_{n-l}([m-k]\psi) \cdot e^{j[-k\gamma+l\delta]} \cdot e^{j[-k\nu_0+lf_0](\phi+t)} \\
& \cdot e^{j\frac{1}{2}\phi[-k(-2m+k)\nu_0^2+2[-nk+l(-m+k)]\nu_0f_0+l(2n-l)f_0^2]} \\
& +\frac{1}{16}\sum_{\substack{m,n,k,l \\ =-\infty}}^{\infty} J_m(\beta)J_n(m\psi)J_{m-k}(\beta)J_{n+l}([m-k]\psi) \cdot e^{j[k\gamma-l\delta]} \cdot e^{j[k\nu_0-lf_0](\phi+t)} \\
& \cdot e^{j\frac{1}{2}\phi[k(2m-k)\nu_0^2+2[nk-l(m-k)]\nu_0f_0-l(2n+l)f_0^2]}
\end{aligned}$$

$$\begin{aligned}
& -\frac{1}{16} \sum_{\substack{m,n,k,l \\ =-\infty}}^{\infty} J_m(\beta) J_n(m\psi) J_{m-k}(\beta) J_{n+l}([m-k]\psi) \cdot e^{j[-k\gamma+l\delta]} \cdot e^{j[-k\nu_0+lf_0](\phi+t)} \\
& \cdot e^{j\frac{1}{2}\phi[-k(-2m+k)\nu_0^2+2[nk+l(-m+k)]\nu_0f_0+l(-2n-l)f_0^2]} \\
& +\frac{1}{16} \sum_{\substack{m,n,k,l \\ =-\infty}}^{\infty} J_m(\beta) J_n(m\psi) J_{m-k}(\beta) J_{n+l}([m-k]\psi) \cdot e^{j[k\gamma+l\delta]} \cdot e^{j[k\nu_0+lf_0](\phi+t)} \\
& \cdot e^{j\frac{1}{2}\phi[k(2m-k)\nu_0^2+2[-nk+l(m-k)]\nu_0f_0+l(-2n-l)f_0^2]} \\
& -\frac{1}{16} \sum_{\substack{m,n,k,l \\ =-\infty}}^{\infty} J_m(\beta) J_n(m\psi) J_{m-k}(\beta) J_{n+l}([m-k]\psi) \cdot e^{j[-k\gamma-l\delta]} \cdot e^{j[-k\nu_0-lf_0](\phi+t)} \\
& \cdot e^{j\frac{1}{2}\phi[-k(-2m+k)\nu_0^2+2[-nk-l(-m+k)]\nu_0f_0-l(2n+l)f_0^2]} \\
& +\frac{1}{16} \sum_{\substack{m,n,k,l \\ =-\infty}}^{\infty} J_m(\beta) J_n(m\psi) J_{m+k}(\beta) J_{n-l}([m+k]\psi) \cdot e^{j[-k\gamma+l\delta]} \cdot e^{j[-k\nu_0+lf_0](\phi+t)} \\
& \cdot e^{j\frac{1}{2}\phi[-k(2m+k)\nu_0^2+2[-nk+l(m+k)]\nu_0f_0+l(2n-l)f_0^2]} \\
& -\frac{1}{16} \sum_{\substack{m,n,k,l \\ =-\infty}}^{\infty} J_m(\beta) J_n(m\psi) J_{m+k}(\beta) J_{n-l}([m+k]\psi) \cdot e^{j[k\gamma-l\delta]} \cdot e^{j[k\nu_0-lf_0](\phi+t)} \\
& \cdot e^{j\frac{1}{2}\phi[k(-2m-k)\nu_0^2+2[-nk-l(-m-k)]\nu_0f_0-l(-2n+l)f_0^2]} \\
& +\frac{1}{16} \sum_{\substack{m,n,k,l \\ =-\infty}}^{\infty} J_m(\beta) J_n(m\psi) J_{m+k}(\beta) J_{n-l}([m+k]\psi) \cdot e^{j[-k\gamma-l\delta]} \cdot e^{j[-k\nu_0-lf_0](\phi+t)} \\
& \cdot e^{j\frac{1}{2}\phi[-k(2m+k)\nu_0^2+2[nk-l(m+k)]\nu_0f_0-l(-2n+l)f_0^2]} \\
& -\frac{1}{16} \sum_{\substack{m,n,k,l \\ =-\infty}}^{\infty} J_m(\beta) J_n(m\psi) J_{m+k}(\beta) J_{n-l}([m+k]\psi) \cdot e^{j[k\gamma+l\delta]} \cdot e^{j[k\nu_0+lf_0](\phi+t)} \\
& \cdot e^{j\frac{1}{2}\phi[k(-2m-k)\nu_0^2+2[nk+l(-m-k)]\nu_0f_0+l(2n-l)f_0^2]} \\
& +\frac{1}{16} \sum_{\substack{m,n,k,l \\ =-\infty}}^{\infty} J_m(\beta) J_n(m\psi) J_{m+k}(\beta) J_{n+l}([m+k]\psi) \cdot e^{j[-k\gamma-l\delta]} \cdot e^{j[-k\nu_0-lf_0](\phi+t)} \\
& \cdot e^{j\frac{1}{2}\phi[-k(2m+k)\nu_0^2+2[-nk-l(m+k)]\nu_0f_0-l(2n+l)f_0^2]} \\
& -\frac{1}{16} \sum_{\substack{m,n,k,l \\ =-\infty}}^{\infty} J_m(\beta) J_n(m\psi) J_{m+k}(\beta) J_{n+l}([m+k]\psi) \cdot e^{j[k\gamma+l\delta]} \cdot e^{j[k\nu_0+lf_0](\phi+t)} \\
& \cdot e^{j\frac{1}{2}\phi[k(-2m-k)\nu_0^2+2[-nk+l(-m-k)]\nu_0f_0+l(-2n-l)f_0^2]} \\
& +\frac{1}{16} \sum_{\substack{m,n,k,l \\ =-\infty}}^{\infty} J_m(\beta) J_n(m\psi) J_{m+k}(\beta) J_{n+l}([m+k]\psi) \cdot e^{j[-k\gamma+l\delta]} \cdot e^{j[-k\nu_0+lf_0](\phi+t)} \\
& \cdot e^{j\frac{1}{2}\phi[-k(2m+k)\nu_0^2+2[nk+l(m+k)]\nu_0f_0+l(-2n-l)f_0^2]} \\
& -\frac{1}{16} \sum_{\substack{m,n,k,l \\ =-\infty}}^{\infty} J_m(\beta) J_n(m\psi) J_{m+k}(\beta) J_{n+l}([m+k]\psi) \cdot e^{j[k\gamma-l\delta]} \cdot e^{j[k\nu_0-lf_0](\phi+t)}
\end{aligned}$$

$$\cdot e^{j\frac{1}{2}\dot{\phi}[k(-2m-k)\nu_0^2+2[nk-l(-m-k)]\nu_0f_0-l(2n+l)f_0^2]}$$

assembling trigonometric identities

$$= \frac{j}{8} \sum_{\substack{m,n,k,l \\ =-\infty}}^{\infty} J_m(\beta)J_n(m\psi)J_{m-k}(\beta)J_{n-l}([m-k]\psi) \cdot \sin[(k\nu_0 + lf_0)(\dot{\phi} + t) + k\gamma + l\delta]$$

$$\cdot e^{j\frac{1}{2}\dot{\phi}[k(2m-k)\nu_0^2+2[nk+l(m-k)]\nu_0f_0+l(2n-l)f_0^2]}$$

$$+ \frac{j}{8} \sum_{\substack{m,n,k,l \\ =-\infty}}^{\infty} J_m(\beta)J_n(m\psi)J_{m-k}(\beta)J_{n-l}([m-k]\psi) \cdot \sin[(k\nu_0 - lf_0)(\dot{\phi} + t) + k\gamma - l\delta]$$

$$\cdot e^{j\frac{1}{2}\dot{\phi}[k(2m-k)\nu_0^2+2[-nk-l(m-k)]\nu_0f_0-l(-2n+l)f_0^2]}$$

$$+ \frac{j}{8} \sum_{\substack{m,n,k,l \\ =-\infty}}^{\infty} J_m(\beta)J_n(m\psi)J_{m-k}(\beta)J_{n+l}([m-k]\psi) \cdot \sin[(k\nu_0 - lf_0)(\dot{\phi} + t) + k\gamma - l\delta]$$

$$\cdot e^{j\frac{1}{2}\dot{\phi}[k(2m-k)\nu_0^2+2[nk-l(m-k)]\nu_0f_0-l(2n+l)f_0^2]}$$

$$+ \frac{j}{8} \sum_{\substack{m,n,k,l \\ =-\infty}}^{\infty} J_m(\beta)J_n(m\psi)J_{m-k}(\beta)J_{n+l}([m-k]\psi) \cdot \sin[(k\nu_0 + lf_0)(\dot{\phi} + t) + k\gamma + l\delta]$$

$$\cdot e^{j\frac{1}{2}\dot{\phi}[k(2m-k)\nu_0^2+2[-nk+l(m-k)]\nu_0f_0+l(-2n-l)f_0^2]}$$

$$- \frac{j}{8} \sum_{\substack{m,n,k,l \\ =-\infty}}^{\infty} J_m(\beta)J_n(m\psi)J_{m+k}(\beta)J_{n-l}([m+k]\psi) \cdot \sin[(k\nu_0 - lf_0)(\dot{\phi} + t) + k\gamma - l\delta]$$

$$\cdot e^{j\frac{1}{2}\dot{\phi}[-k(2m+k)\nu_0^2+2[-nk+l(m+k)]\nu_0f_0+l(2n-l)f_0^2]}$$

$$- \frac{j}{8} \sum_{\substack{m,n,k,l \\ =-\infty}}^{\infty} J_m(\beta)J_n(m\psi)J_{m+k}(\beta)J_{n-l}([m+k]\psi) \cdot \sin[(k\nu_0 + lf_0)(\dot{\phi} + t) + k\gamma + l\delta]$$

$$\cdot e^{j\frac{1}{2}\dot{\phi}[-k(2m+k)\nu_0^2+2[nk-l(m+k)]\nu_0f_0-l(-2n+l)f_0^2]}$$

$$- \frac{j}{8} \sum_{\substack{m,n,k,l \\ =-\infty}}^{\infty} J_m(\beta)J_n(m\psi)J_{m+k}(\beta)J_{n+l}([m+k]\psi) \cdot \sin[(k\nu_0 + lf_0)(\dot{\phi} + t) + k\gamma + l\delta]$$

$$\cdot e^{j\frac{1}{2}\dot{\phi}[-k(2m+k)\nu_0^2+2[-nk-l(m+k)]\nu_0f_0-l(2n+l)f_0^2]}$$

$$- \frac{j}{8} \sum_{\substack{m,n,k,l \\ =-\infty}}^{\infty} J_m(\beta)J_n(m\psi)J_{m+k}(\beta)J_{n+l}([m+k]\psi) \cdot \sin[(k\nu_0 - lf_0)(\dot{\phi} + t) + k\gamma - l\delta]$$

$$\cdot e^{j\frac{1}{2}\dot{\phi}[-k(2m+k)\nu_0^2+2[nk+l(m+k)]\nu_0f_0+l(-2n-l)f_0^2]}$$

after rearranging common expressions and substitute $l = -l$

$$= \frac{j}{8} \sum_{\substack{m,n,k,l \\ =-\infty}}^{\infty} J_m(\beta)J_n(m\psi)J_{m-k}(\beta)J_{n-l}([m-k]\psi) \cdot \sin[(k\nu_0 + lf_0)(\dot{\phi} + t) + k\gamma + l\delta]$$

$$\cdot e^{j\frac{1}{2}\dot{\phi}[k(2m-k)\nu_0^2+2[nk+l(m-k)]\nu_0f_0+l(2n-l)f_0^2]}$$

$$+ \frac{j}{8} \sum_{\substack{m,n,k,l \\ =-\infty}}^{\infty} J_m(\beta)J_n(m\psi)J_{m-k}(\beta)J_{n-l}([m-k]\psi) \cdot \sin[(k\nu_0 + lf_0)(\dot{\phi} + t) + k\gamma + l\delta]$$

$$\begin{aligned}
& \cdot e^{j\frac{1}{2}\ddot{\phi}[k(2m-k)\nu_0^2+2[nk+l(m-k)]\nu_0f_0+l(2n-l)f_0^2]} \\
& + \frac{j}{8} \sum_{\substack{m,n,k,l \\ =-\infty}}^{\infty} J_m(\beta)J_n(m\psi)J_{m-k}(\beta)J_{n+l}([m-k]\psi) \cdot \sin[(k\nu_0+lf_0)(\dot{\phi}+t)+k\gamma+l\delta] \\
& \cdot e^{j\frac{1}{2}\ddot{\phi}[k(2m-k)\nu_0^2+2[-nk+l(m-k)]\nu_0f_0-l(2n+l)f_0^2]} \\
& + \frac{j}{8} \sum_{\substack{m,n,k,l \\ =-\infty}}^{\infty} J_m(\beta)J_n(m\psi)J_{m-k}(\beta)J_{n+l}([m-k]\psi) \cdot \sin[(k\nu_0+lf_0)(\dot{\phi}+t)+k\gamma+l\delta] \\
& \cdot e^{j\frac{1}{2}\ddot{\phi}[k(2m-k)\nu_0^2+2[-nk+l(m-k)]\nu_0-l(2n+l)f_0^2]} \\
& - \frac{j}{8} \sum_{\substack{m,n,k,l \\ =-\infty}}^{\infty} J_m(\beta)J_n(m\psi)J_{m+k}(\beta)J_{n-l}([m+k]\psi) \cdot \sin[(k\nu_0+lf_0)(\dot{\phi}+t)+k\gamma+l\delta] \\
& \cdot e^{j\frac{1}{2}\ddot{\phi}[-k(2m+k)\nu_0^2+2[nk-l(m+k)]\nu_0f_0+l(2n-l)f_0^2]} \\
& - \frac{j}{8} \sum_{\substack{m,n,k,l \\ =-\infty}}^{\infty} J_m(\beta)J_n(m\psi)J_{m+k}(\beta)J_{n-l}([m+k]\psi) \cdot \sin[(k\nu_0+lf_0)(\dot{\phi}+t)+k\gamma+l\delta] \\
& \cdot e^{j\frac{1}{2}\ddot{\phi}[-k(2m+k)\nu_0^2+2[nk-l(m+k)]\nu_0f_0+l(2n-l)f_0^2]} \\
& - \frac{j}{8} \sum_{\substack{m,n,k,l \\ =-\infty}}^{\infty} J_m(\beta)J_n(m\psi)J_{m+k}(\beta)J_{n+l}([m+k]\psi) \cdot \sin[(k\nu_0+lf_0)(\dot{\phi}+t)+k\gamma+l\delta] \\
& \cdot e^{j\frac{1}{2}\ddot{\phi}[-k(2m+k)\nu_0^2+2[-nk-l(m+k)]\nu_0f_0-l(2n+l)f_0^2]} \\
& - \frac{j}{8} \sum_{\substack{m,n,k,l \\ =-\infty}}^{\infty} J_m(\beta)J_n(m\psi)J_{m+k}(\beta)J_{n+l}([m+k]\psi) \cdot \sin[(k\nu_0+lf_0)(\dot{\phi}+t)+k\gamma+l\delta] \\
& \cdot e^{j\frac{1}{2}\ddot{\phi}[-k(2m+k)\nu_0^2+2[-nk-l(m+k)]\nu_0f_0-l(2n+l)f_0^2]}
\end{aligned}$$

substitute $n = -n$

$$\begin{aligned}
& = \frac{j}{4} \sum_{\substack{m,n,k,l \\ =-\infty}}^{\infty} J_m(\beta)J_n(m\psi)J_{m-k}(\beta)J_{n-l}([m-k]\psi) \cdot \sin[(k\nu_0+lf_0)(\dot{\phi}+t)+k\gamma+l\delta] \\
& \cdot e^{j\frac{1}{2}\ddot{\phi}[k(2m-k)\nu_0^2+2[nk+l(m-k)]\nu_0f_0+l(2n-l)f_0^2]} \\
& + \frac{j}{4} \sum_{\substack{m,n,k,l \\ =-\infty}}^{\infty} J_m(\beta)J_{-n}(m\psi)J_{m-k}(\beta)J_{-n+l}([m-k]\psi) \cdot \sin[(k\nu_0+lf_0)(\dot{\phi}+t)+k\gamma+l\delta] \\
& \cdot e^{j\frac{1}{2}\ddot{\phi}[k(2m-k)\nu_0^2+2[nk+l(m-k)]\nu_0f_0+l(2n-l)f_0^2]} \\
& - \frac{j}{4} \sum_{\substack{m,n,k,l \\ =-\infty}}^{\infty} J_m(\beta)J_{-n}(m\psi)J_{m+k}(\beta)J_{-n-l}([m+k]\psi) \cdot \sin[(k\nu_0+lf_0)(\dot{\phi}+t)+k\gamma+l\delta] \\
& \cdot e^{j\frac{1}{2}\ddot{\phi}[-k(2m+k)\nu_0^2-2[nk+l(m+k)]\nu_0f_0-l(2n+l)f_0^2]} \\
& - \frac{j}{4} \sum_{\substack{m,n,k,l \\ =-\infty}}^{\infty} J_m(\beta)J_n(m\psi)J_{m+k}(\beta)J_{n+l}([m+k]\psi) \cdot \sin[(k\nu_0+lf_0)(\dot{\phi}+t)+k\gamma+l\delta] \\
& \cdot e^{j\frac{1}{2}\ddot{\phi}[-k(2m+k)\nu_0^2-2[nk+l(m+k)]\nu_0f_0-l(2n+l)f_0^2]}
\end{aligned}$$

l even case

$$\begin{aligned}
&= \frac{j}{4} \sum_{\substack{m,n,k,l \\ =-\infty}}^{\infty} J_m(\beta) J_n(m\psi) J_{m-k}(\beta) J_{n-l}([m-k]\psi) \cdot \sin[(k\nu_0 + lf_0)(\dot{\phi} + t) + k\gamma + l\delta] \\
&\cdot e^{j\frac{1}{2}\ddot{\phi}[k(2m-k)\nu_0^2 + 2[nk+l(m-k)]\nu_0 f_0 + l(2n-l)f_0^2]} \\
&+ \frac{j}{4} \sum_{\substack{m,n,k,l \\ =-\infty}}^{\infty} J_m(\beta) J_n(m\psi) J_{m-k}(\beta) J_{n-l}([m-k]\psi) \cdot \sin[(k\nu_0 + lf_0)(\dot{\phi} + t) + k\gamma + l\delta] \\
&\cdot e^{j\frac{1}{2}\ddot{\phi}[k(2m-k)\nu_0^2 + 2[nk+l(m-k)]\nu_0 f_0 + l(2n-l)f_0^2]} \\
&- \frac{j}{4} \sum_{\substack{m,n,k,l \\ =-\infty}}^{\infty} J_m(\beta) J_n(m\psi) J_{m+k}(\beta) J_{n+l}([m+k]\psi) \cdot \sin[(k\nu_0 + lf_0)(\dot{\phi} + t) + k\gamma + l\delta] \\
&\cdot e^{j\frac{1}{2}\ddot{\phi}[-k(2m+k)\nu_0^2 - 2[nk+l(m+k)]\nu_0 f_0 - l(2n+l)f_0^2]} \\
&- \frac{j}{4} \sum_{\substack{m,n,k,l \\ =-\infty}}^{\infty} J_m(\beta) J_n(m\psi) J_{m+k}(\beta) J_{n+l}([m+k]\psi) \cdot \sin[(k\nu_0 + lf_0)(\dot{\phi} + t) + k\gamma + l\delta] \\
&\cdot e^{j\frac{1}{2}\ddot{\phi}[-k(2m+k)\nu_0^2 - 2[nk+l(m+k)]\nu_0 f_0 - l(2n+l)f_0^2]} \\
&= \frac{j}{2} \sum_{\substack{m,n,k,l \\ =-\infty}}^{\infty} J_m(\beta) J_n(m\psi) J_{m-k}(\beta) J_{n-l}([m-k]\psi) \cdot \sin[(k\nu_0 + lf_0)(\dot{\phi} + t) + k\gamma + l\delta] \\
&\cdot e^{j\frac{1}{2}\ddot{\phi}[k(2m-k)\nu_0^2 + 2[nk+l(m-k)]\nu_0 f_0 + l(2n-l)f_0^2]} \\
&- \frac{j}{2} \sum_{\substack{m,n,k,l \\ =-\infty}}^{\infty} J_m(\beta) J_n(m\psi) J_{m+k}(\beta) J_{n+l}([m+k]\psi) \cdot \sin[(k\nu_0 + lf_0)(\dot{\phi} + t) + k\gamma + l\delta] \\
&\cdot e^{-j\frac{1}{2}\ddot{\phi}[k(2m+k)\nu_0^2 + 2[nk+l(m+k)]\nu_0 f_0 + l(2n+l)f_0^2]}
\end{aligned}$$

in 2nd equation substitute variable

$$\begin{aligned}
&\Rightarrow m+k \rightarrow m; \quad m \rightarrow m-k; \quad 2m+k \rightarrow 2m-k \\
&\Rightarrow n+l \rightarrow n; \quad n \rightarrow n-l; \quad 2n+l \rightarrow 2n-l \\
&= \frac{j}{2} \sum_{\substack{m,n,k,l \\ =-\infty}}^{\infty} J_m(\beta) J_n(m\psi) J_{m-k}(\beta) J_{n-l}([m-k]\psi) \cdot \sin[(k\nu_0 + lf_0)(\dot{\phi} + t) + k\gamma + l\delta] \\
&\cdot e^{j\frac{1}{2}\ddot{\phi}[k(2m-k)\nu_0^2 + 2[nk+l(m-k)]\nu_0 f_0 + l(2n-l)f_0^2]} \\
&- \frac{j}{2} \sum_{\substack{m,n,k,l \\ =-\infty}}^{\infty} J_{m-k}(\beta) J_{n-l}([m-k]\psi) J_m(\beta) J_n(m\psi) \cdot \sin[(k\nu_0 + lf_0)(\dot{\phi} + t) + k\gamma + l\delta] \\
&\cdot e^{-j\frac{1}{2}\ddot{\phi}[k(2m-k)\nu_0^2 + 2[(n-l)k+lm]\nu_0 f_0 + l(2n-l)f_0^2]} \\
&= - \sum_{\substack{m,n,k,l \\ =-\infty}}^{\infty} J_m(\beta) J_n(m\psi) J_{m-k}(\beta) J_{n-l}([m-k]\psi) \cdot \sin[(k\nu_0 + lf_0)(\dot{\phi} + t) + k\gamma + l\delta] \\
&\cdot \sin\left(\frac{1}{2}\ddot{\phi}[k(2m-k)\nu_0^2 + 2[nk+l(m-k)]\nu_0 f_0 + l(2n-l)f_0^2]\right)
\end{aligned}$$

or

$$\begin{aligned}
&= - \sum_{\substack{m,n,k,l \\ =-\infty}}^{\infty} J_m(\beta) J_n(m\psi) J_{m+k}(\beta) J_{n+l}([m+k]\psi) \cdot \sin[(k\nu_0 + lf_0)(\dot{\phi} + t) + k\gamma + l\delta] \\
&\cdot \sin\left(\frac{1}{2}\ddot{\phi}[k(2m+k)\nu_0^2 + 2[nk+l(m+k)]\nu_0 f_0 + l(2n+l)f_0^2]\right).
\end{aligned}$$

k odd, l odd case

$$\begin{aligned}
&= \frac{1}{16} \sum_{\substack{m,n,k,l \\ =-\infty}}^{\infty} J_m(\beta) J_n(m\psi) J_{m-k}(\beta) J_{n-l}([m-k]\psi) \cdot e^{j[k\gamma+l\delta]} \cdot e^{j[k\nu_0+lf_0](\phi+t)} \\
&\cdot e^{j\frac{1}{2}\phi[k(2m-k)\nu_0^2+2[nk+l(m-k)]\nu_0f_0+l(2n-l)f_0^2]} \\
&+ \frac{1}{16} \sum_{\substack{m,n,k,l \\ =-\infty}}^{\infty} J_m(\beta) J_n(m\psi) J_{m-k}(\beta) J_{n+l}([m-k]\psi) \cdot e^{j[k\gamma-l\delta]} \cdot e^{j[k\nu_0-lf_0](\phi+t)} \\
&\cdot e^{j\frac{1}{2}\phi[k(2m-k)\nu_0^2+2[nk-l(m-k)]\nu_0f_0-l(2n+l)f_0^2]} \\
&+ \frac{1}{16} \sum_{\substack{m,n,k,l \\ =-\infty}}^{\infty} J_m(\beta) J_n(m\psi) J_{m+k}(\beta) J_{n-l}([m+k]\psi) \cdot e^{j[-k\gamma+l\delta]} \cdot e^{j[-k\nu_0+lf_0](\phi+t)} \\
&\cdot e^{j\frac{1}{2}\phi[-k(2m+k)\nu_0^2+2[-nk+l(m+k)]\nu_0f_0+l(2n-l)f_0^2]} \\
&+ \frac{1}{16} \sum_{\substack{m,n,k,l \\ =-\infty}}^{\infty} J_m(\beta) J_n(m\psi) J_{m+k}(\beta) J_{n+l}([m+k]\psi) \cdot e^{j[-k\gamma-l\delta]} \cdot e^{j[-k\nu_0-lf_0](\phi+t)} \\
&\cdot e^{j\frac{1}{2}\phi[-k(2m+k)\nu_0^2+2[-nk-l(m+k)]\nu_0f_0-l(2n+l)f_0^2]} \\
&- \frac{1}{16} \sum_{\substack{m,n,k,l \\ =-\infty}}^{\infty} J_m(\beta) J_n(m\psi) J_{m-k}(\beta) J_{n+l}([m-k]\psi) \cdot e^{j[k\gamma+l\delta]} \cdot e^{j[k\nu_0+lf_0](\phi+t)} \\
&\cdot e^{j\frac{1}{2}\phi[k(2m-k)\nu_0^2+2[-nk+l(m-k)]\nu_0f_0+l(-2n-l)f_0^2]} \\
&- \frac{1}{16} \sum_{\substack{m,n,k,l \\ =-\infty}}^{\infty} J_m(\beta) J_n(m\psi) J_{m-k}(\beta) J_{n-l}([m-k]\psi) \cdot e^{j[k\gamma-l\delta]} \cdot e^{j[k\nu_0-lf_0](\phi+t)} \\
&\cdot e^{j\frac{1}{2}\phi[k(2m-k)\nu_0^2+2[-nk-l(m-k)]\nu_0f_0-l(-2n+l)f_0^2]} \\
&- \frac{1}{16} \sum_{\substack{m,n,k,l \\ =-\infty}}^{\infty} J_m(\beta) J_n(m\psi) J_{m+k}(\beta) J_{n+l}([m+k]\psi) \cdot e^{j[-k\gamma+l\delta]} \cdot e^{j[-k\nu_0+lf_0](\phi+t)} \\
&\cdot e^{j\frac{1}{2}\phi[-k(2m+k)\nu_0^2+2[nk+l(m+k)]\nu_0f_0+l(-2n-l)f_0^2]} \\
&- \frac{1}{16} \sum_{\substack{m,n,k,l \\ =-\infty}}^{\infty} J_m(\beta) J_n(m\psi) J_{m+k}(\beta) J_{n-l}([m+k]\psi) \cdot e^{j[-k\gamma-l\delta]} \cdot e^{j[-k\nu_0-lf_0](\phi+t)} \\
&\cdot e^{j\frac{1}{2}\phi[-k(2m+k)\nu_0^2+2[nk-l(m+k)]\nu_0f_0-l(-2n+l)f_0^2]} \\
&+ \frac{1}{16} \sum_{\substack{m,n,k,l \\ =-\infty}}^{\infty} J_m(\beta) J_n(m\psi) J_{m+k}(\beta) J_{n-l}([m+k]\psi) \cdot e^{j[k\gamma+l\delta]} \cdot e^{j[k\nu_0+lf_0](\phi+t)} \\
&\cdot e^{j\frac{1}{2}\phi[k(-2m-k)\nu_0^2+2[nk+l(-m-k)]\nu_0f_0+l(2n-l)f_0^2]} \\
&+ \frac{1}{16} \sum_{\substack{m,n,k,l \\ =-\infty}}^{\infty} J_m(\beta) J_n(m\psi) J_{m+k}(\beta) J_{n+l}([m+k]\psi) \cdot e^{j[k\gamma-l\delta]} \cdot e^{j[k\nu_0-lf_0](\phi+t)} \\
&\cdot e^{j\frac{1}{2}\phi[k(-2m-k)\nu_0^2+2[nk-l(-m-k)]\nu_0f_0-l(2n+l)f_0^2]} \\
&+ \frac{1}{16} \sum_{\substack{m,n,k,l \\ =-\infty}}^{\infty} J_m(\beta) J_n(m\psi) J_{m-k}(\beta) J_{n-l}([m-k]\psi) \cdot e^{j[-k\gamma+l\delta]} \cdot e^{j[-k\nu_0+lf_0](\phi+t)}
\end{aligned}$$

$$\begin{aligned}
& \cdot e^{j\frac{1}{2}\ddot{\phi}[-k(-2m+k)\nu_0^2+2[-nk+l(-m+k)]\nu_0f_0+l(2n-l)f_0^2]} \\
& + \frac{1}{16} \sum_{\substack{m,n,k,l \\ =-\infty}}^{\infty} J_m(\beta)J_n(m\psi)J_{m-k}(\beta)J_{n+l}([m-k]\psi) \cdot e^{j[-k\gamma-l\delta]} \cdot e^{j[-k\nu_0-lf_0](\phi+t)} \\
& \cdot e^{j\frac{1}{2}\ddot{\phi}[-k(-2m+k)\nu_0^2+2[-nk-l(-m+k)]\nu_0f_0-l(2n+l)f_0^2]} \\
& - \frac{1}{16} \sum_{\substack{m,n,k,l \\ =-\infty}}^{\infty} J_m(\beta)J_n(m\psi)J_{m+k}(\beta)J_{n+l}([m+k]\psi) \cdot e^{j[k\gamma+l\delta]} \cdot e^{j[k\nu_0+lf_0](\phi+t)} \\
& \cdot e^{j\frac{1}{2}\ddot{\phi}[k(-2m-k)\nu_0^2+2[-nk+l(-m-k)]\nu_0f_0+l(-2n-l)f_0^2]} \\
& - \frac{1}{16} \sum_{\substack{m,n,k,l \\ =-\infty}}^{\infty} J_m(\beta)J_n(m\psi)J_{m+k}(\beta)J_{n-l}([m+k]\psi) \cdot e^{j[k\gamma-l\delta]} \cdot e^{j[k\nu_0-lf_0](\phi+t)} \\
& \cdot e^{j\frac{1}{2}\ddot{\phi}[k(-2m-k)\nu_0^2+2[-nk-l(-m-k)]\nu_0f_0-l(-2n+l)f_0^2]} \\
& - \frac{1}{16} \sum_{\substack{m,n,k,l \\ =-\infty}}^{\infty} J_m(\beta)J_n(m\psi)J_{m-k}(\beta)J_{n+l}([m-k]\psi) \cdot e^{j[-k\gamma+l\delta]} \cdot e^{j[-k\nu_0+lf_0](\phi+t)} \\
& \cdot e^{j\frac{1}{2}\ddot{\phi}[-k(-2m+k)\nu_0^2+2[nk+l(-m+k)]\nu_0f_0+l(-2n-l)f_0^2]} \\
& - \frac{1}{16} \sum_{\substack{m,n,k,l \\ =-\infty}}^{\infty} J_m(\beta)J_n(m\psi)J_{m-k}(\beta)J_{n-l}([m-k]\psi) \cdot e^{j[-k\gamma-l\delta]} \cdot e^{j[-k\nu_0-lf_0](\phi+t)} \\
& \cdot e^{j\frac{1}{2}\ddot{\phi}[-k(-2m+k)\nu_0^2+2[nk-l(-m+k)]\nu_0f_0-l(-2n+l)f_0^2]} \\
& - \frac{1}{16} \sum_{\substack{m,n,k,l \\ =-\infty}}^{\infty} J_m(\beta)J_n(m\psi)J_{m-k}(\beta)J_{n-l}([m-k]\psi) \cdot e^{j[k\gamma+l\delta]} \cdot e^{j[k\nu_0+lf_0](\phi+t)} \\
& \cdot e^{j\frac{1}{2}\ddot{\phi}[k(2m-k)\nu_0^2+2[nk+l(m-k)]\nu_0f_0+l(2n-l)f_0^2]} \\
& - \frac{1}{16} \sum_{\substack{m,n,k,l \\ =-\infty}}^{\infty} J_m(\beta)J_n(m\psi)J_{m-k}(\beta)J_{n-l}([m-k]\psi) \cdot e^{j[-k\gamma-l\delta]} \cdot e^{j[-k\nu_0-lf_0](\phi+t)} \\
& \cdot e^{j\frac{1}{2}\ddot{\phi}[-k(-2m+k)\nu_0^2+2[nk-l(-m+k)]\nu_0f_0-l(-2n+l)f_0^2]} \\
& + \frac{1}{16} \sum_{\substack{m,n,k,l \\ =-\infty}}^{\infty} J_m(\beta)J_n(m\psi)J_{m-k}(\beta)J_{n-l}([m-k]\psi) \cdot e^{j[-k\gamma+l\delta]} \cdot e^{j[-k\nu_0+lf_0](\phi+t)} \\
& \cdot e^{j\frac{1}{2}\ddot{\phi}[-k(-2m+k)\nu_0^2+2[-nk+l(-m+k)]\nu_0f_0+l(2n-l)f_0^2]} \\
& - \frac{1}{16} \sum_{\substack{m,n,k,l \\ =-\infty}}^{\infty} J_m(\beta)J_n(m\psi)J_{m-k}(\beta)J_{n-l}([m-k]\psi) \cdot e^{j[k\gamma-l\delta]} \cdot e^{j[k\nu_0-lf_0](\phi+t)} \\
& \cdot e^{j\frac{1}{2}\ddot{\phi}[k(2m-k)\nu_0^2+2[-nk-l(m-k)]\nu_0f_0-l(-2n+l)f_0^2]} \\
& + \frac{1}{16} \sum_{\substack{m,n,k,l \\ =-\infty}}^{\infty} J_m(\beta)J_n(m\psi)J_{m-k}(\beta)J_{n+l}([m-k]\psi) \cdot e^{j[k\gamma-l\delta]} \cdot e^{j[k\nu_0-lf_0](\phi+t)} \\
& \cdot e^{j\frac{1}{2}\ddot{\phi}[k(2m-k)\nu_0^2+2[nk-l(m-k)]\nu_0f_0-l(2n+l)f_0^2]}
\end{aligned}$$

rearranging common RF fading terms (due to dispersion) in adjacent lines

$$\begin{aligned}
& = \frac{1}{16} \sum_{\substack{m,n,k,l \\ =-\infty}}^{\infty} J_m(\beta)J_n(m\psi)J_{m-k}(\beta)J_{n-l}([m-k]\psi) \cdot e^{j[k\gamma+l\delta]} \cdot e^{j[k\nu_0+lf_0](\phi+t)} \\
& \cdot e^{j\frac{1}{2}\ddot{\phi}[k(2m-k)\nu_0^2+2[nk+l(m-k)]\nu_0f_0+l(2n-l)f_0^2]} \\
& - \frac{1}{16} \sum_{\substack{m,n,k,l \\ =-\infty}}^{\infty} J_m(\beta)J_n(m\psi)J_{m-k}(\beta)J_{n-l}([m-k]\psi) \cdot e^{j[-k\gamma-l\delta]} \cdot e^{j[-k\nu_0-lf_0](\phi+t)} \\
& \cdot e^{j\frac{1}{2}\ddot{\phi}[-k(-2m+k)\nu_0^2+2[nk-l(-m+k)]\nu_0f_0-l(-2n+l)f_0^2]} \\
& + \frac{1}{16} \sum_{\substack{m,n,k,l \\ =-\infty}}^{\infty} J_m(\beta)J_n(m\psi)J_{m-k}(\beta)J_{n-l}([m-k]\psi) \cdot e^{j[-k\gamma+l\delta]} \cdot e^{j[-k\nu_0+lf_0](\phi+t)} \\
& \cdot e^{j\frac{1}{2}\ddot{\phi}[-k(-2m+k)\nu_0^2+2[-nk+l(-m+k)]\nu_0f_0+l(2n-l)f_0^2]} \\
& - \frac{1}{16} \sum_{\substack{m,n,k,l \\ =-\infty}}^{\infty} J_m(\beta)J_n(m\psi)J_{m-k}(\beta)J_{n-l}([m-k]\psi) \cdot e^{j[k\gamma-l\delta]} \cdot e^{j[k\nu_0-lf_0](\phi+t)} \\
& \cdot e^{j\frac{1}{2}\ddot{\phi}[k(2m-k)\nu_0^2+2[-nk-l(m-k)]\nu_0f_0-l(-2n+l)f_0^2]} \\
& + \frac{1}{16} \sum_{\substack{m,n,k,l \\ =-\infty}}^{\infty} J_m(\beta)J_n(m\psi)J_{m-k}(\beta)J_{n+l}([m-k]\psi) \cdot e^{j[k\gamma-l\delta]} \cdot e^{j[k\nu_0-lf_0](\phi+t)} \\
& \cdot e^{j\frac{1}{2}\ddot{\phi}[k(2m-k)\nu_0^2+2[nk-l(m-k)]\nu_0f_0-l(2n+l)f_0^2]}
\end{aligned}$$

$$\begin{aligned}
& -\frac{1}{16} \sum_{\substack{m,n,k,l \\ =-\infty}}^{\infty} J_m(\beta)J_n(m\psi)J_{m-k}(\beta)J_{n+l}([m-k]\psi) \cdot e^{j[-k\gamma+l\delta]} \cdot e^{j[-k\nu_0+lf_0](\phi+t)} \\
& \cdot e^{j\frac{1}{2}\phi[-k(-2m+k)\nu_0^2+2[nk+l(-m+k)]\nu_0f_0+l(-2n-l)f_0^2]} \\
& -\frac{1}{16} \sum_{\substack{m,n,k,l \\ =-\infty}}^{\infty} J_m(\beta)J_n(m\psi)J_{m-k}(\beta)J_{n+l}([m-k]\psi) \cdot e^{j[k\gamma+l\delta]} \cdot e^{j[k\nu_0+lf_0](\phi+t)} \\
& \cdot e^{j\frac{1}{2}\phi[k(2m-k)\nu_0^2+2[-nk+l(m-k)]\nu_0f_0+l(-2n-l)f_0^2]} \\
& +\frac{1}{16} \sum_{\substack{m,n,k,l \\ =-\infty}}^{\infty} J_m(\beta)J_n(m\psi)J_{m-k}(\beta)J_{n+l}([m-k]\psi) \cdot e^{j[-k\gamma-l\delta]} \cdot e^{j[-k\nu_0-lf_0](\phi+t)} \\
& \cdot e^{j\frac{1}{2}\phi[-k(-2m+k)\nu_0^2+2[-nk-l(-m+k)]\nu_0f_0-l(2n+l)f_0^2]} \\
& +\frac{1}{16} \sum_{\substack{m,n,k,l \\ =-\infty}}^{\infty} J_m(\beta)J_n(m\psi)J_{m+k}(\beta)J_{n-l}([m+k]\psi) \cdot e^{j[-k\gamma+l\delta]} \cdot e^{j[-k\nu_0+lf_0](\phi+t)} \\
& \cdot e^{j\frac{1}{2}\phi[-k(2m+k)\nu_0^2+2[-nk+l(m+k)]\nu_0f_0+l(2n-l)f_0^2]} \\
& -\frac{1}{16} \sum_{\substack{m,n,k,l \\ =-\infty}}^{\infty} J_m(\beta)J_n(m\psi)J_{m+k}(\beta)J_{n-l}([m+k]\psi) \cdot e^{j[k\gamma-l\delta]} \cdot e^{j[k\nu_0-lf_0](\phi+t)} \\
& \cdot e^{j\frac{1}{2}\phi[k(-2m-k)\nu_0^2+2[-nk-l(-m-k)]\nu_0f_0-l(-2n+l)f_0^2]} \\
& -\frac{1}{16} \sum_{\substack{m,n,k,l \\ =-\infty}}^{\infty} J_m(\beta)J_n(m\psi)J_{m+k}(\beta)J_{n-l}([m+k]\psi) \cdot e^{j[-k\gamma-l\delta]} \cdot e^{j[-k\nu_0-lf_0](\phi+t)} \\
& \cdot e^{j\frac{1}{2}\phi[-k(2m+k)\nu_0^2+2[nk-l(m+k)]\nu_0f_0-l(-2n+l)f_0^2]} \\
& +\frac{1}{16} \sum_{\substack{m,n,k,l \\ =-\infty}}^{\infty} J_m(\beta)J_n(m\psi)J_{m+k}(\beta)J_{n-l}([m+k]\psi) \cdot e^{j[k\gamma+l\delta]} \cdot e^{j[k\nu_0+lf_0](\phi+t)} \\
& \cdot e^{j\frac{1}{2}\phi[k(-2m-k)\nu_0^2+2[nk+l(-m-k)]\nu_0f_0+l(2n-l)f_0^2]} \\
& +\frac{1}{16} \sum_{\substack{m,n,k,l \\ =-\infty}}^{\infty} J_m(\beta)J_n(m\psi)J_{m+k}(\beta)J_{n+l}([m+k]\psi) \cdot e^{j[-k\gamma-l\delta]} \cdot e^{j[-k\nu_0-lf_0](\phi+t)} \\
& \cdot e^{j\frac{1}{2}\phi[-k(2m+k)\nu_0^2+2[-nk-l(m+k)]\nu_0f_0-l(2n+l)f_0^2]} \\
& -\frac{1}{16} \sum_{\substack{m,n,k,l \\ =-\infty}}^{\infty} J_m(\beta)J_n(m\psi)J_{m+k}(\beta)J_{n+l}([m+k]\psi) \cdot e^{j[k\gamma+l\delta]} \cdot e^{j[k\nu_0+lf_0](\phi+t)} \\
& \cdot e^{j\frac{1}{2}\phi[k(-2m-k)\nu_0^2+2[-nk+l(-m-k)]\nu_0f_0+l(-2n-l)f_0^2]} \\
& -\frac{1}{16} \sum_{\substack{m,n,k,l \\ =-\infty}}^{\infty} J_m(\beta)J_n(m\psi)J_{m+k}(\beta)J_{n+l}([m+k]\psi) \cdot e^{j[-k\gamma+l\delta]} \cdot e^{j[-k\nu_0+lf_0](\phi+t)} \\
& \cdot e^{j\frac{1}{2}\phi[-k(2m+k)\nu_0^2+2[nk+l(m+k)]\nu_0f_0+l(-2n-l)f_0^2]} \\
& +\frac{1}{16} \sum_{\substack{m,n,k,l \\ =-\infty}}^{\infty} J_m(\beta)J_n(m\psi)J_{m+k}(\beta)J_{n+l}([m+k]\psi) \cdot e^{j[k\gamma-l\delta]} \cdot e^{j[k\nu_0-lf_0](\phi+t)}
\end{aligned}$$

$$e^{j\frac{1}{2}\dot{\phi}[k(-2m-k)\nu_0^2+2[nk-l(-m-k)]\nu_0f_0-l(2n+l)f_0^2]}$$

assembling trigonometric identities

$$\begin{aligned}
&= \frac{j}{8} \sum_{\substack{m,n,k,l \\ =-\infty}}^{\infty} J_m(\beta)J_n(m\psi)J_{m-k}(\beta)J_{n-l}([m-k]\psi) \cdot \sin[(k\nu_0+lf_0)(\dot{\phi}+t)+k\gamma+l\delta] \\
&\cdot e^{j\frac{1}{2}\dot{\phi}[k(2m-k)\nu_0^2+2[nk+l(m-k)]\nu_0f_0+l(2n-l)f_0^2]} \\
&- \frac{j}{8} \sum_{\substack{m,n,k,l \\ =-\infty}}^{\infty} J_m(\beta)J_n(m\psi)J_{m-k}(\beta)J_{n-l}([m-k]\psi) \cdot \sin[(k\nu_0-lf_0)(\dot{\phi}+t)+k\gamma-l\delta] \\
&\cdot e^{j\frac{1}{2}\dot{\phi}[-k(-2m+k)\nu_0^2+2[-nk+l(-m+k)]\nu_0f_0+l(2n-l)f_0^2]} \\
&+ \frac{j}{8} \sum_{\substack{m,n,k,l \\ =-\infty}}^{\infty} J_m(\beta)J_n(m\psi)J_{m-k}(\beta)J_{n+l}([m-k]\psi) \cdot \sin[(k\nu_0-lf_0)(\dot{\phi}+t)+k\gamma-l\delta] \\
&\cdot e^{j\frac{1}{2}\dot{\phi}[k(2m-k)\nu_0^2+2[nk-l(m-k)]\nu_0f_0-l(2n+l)f_0^2]} \\
&- \frac{j}{8} \sum_{\substack{m,n,k,l \\ =-\infty}}^{\infty} J_m(\beta)J_n(m\psi)J_{m-k}(\beta)J_{n+l}([m-k]\psi) \cdot \sin[(k\nu_0+lf_0)(\dot{\phi}+t)+k\gamma+l\delta] \\
&\cdot e^{j\frac{1}{2}\dot{\phi}[k(2m-k)\nu_0^2+2[-nk+l(m-k)]\nu_0f_0+l(-2n-l)f_0^2]} \\
&- \frac{j}{8} \sum_{\substack{m,n,k,l \\ =-\infty}}^{\infty} J_m(\beta)J_n(m\psi)J_{m+k}(\beta)J_{n-l}([m+k]\psi) \cdot \sin[(k\nu_0-lf_0)(\dot{\phi}+t)+k\gamma-l\delta] \\
&\cdot e^{j\frac{1}{2}\dot{\phi}[-k(2m+k)\nu_0^2+2[-nk+l(m+k)]\nu_0f_0+l(2n-l)f_0^2]} \\
&+ \frac{j}{8} \sum_{\substack{m,n,k,l \\ =-\infty}}^{\infty} J_m(\beta)J_n(m\psi)J_{m+k}(\beta)J_{n-l}([m+k]\psi) \cdot \sin[(k\nu_0+lf_0)(\dot{\phi}+t)+k\gamma+l\delta] \\
&\cdot e^{j\frac{1}{2}\dot{\phi}[-k(2m+k)\nu_0^2+2[nk-l(m+k)]\nu_0f_0-l(-2n+l)f_0^2]} \\
&- \frac{j}{8} \sum_{\substack{m,n,k,l \\ =-\infty}}^{\infty} J_m(\beta)J_n(m\psi)J_{m+k}(\beta)J_{n+l}([m+k]\psi) \cdot \sin[(k\nu_0+lf_0)(\dot{\phi}+t)+k\gamma+l\delta] \\
&\cdot e^{j\frac{1}{2}\dot{\phi}[-k(2m+k)\nu_0^2+2[-nk-l(m+k)]\nu_0f_0-l(2n+l)f_0^2]} \\
&+ \frac{j}{8} \sum_{\substack{m,n,k,l \\ =-\infty}}^{\infty} J_m(\beta)J_n(m\psi)J_{m+k}(\beta)J_{n+l}([m+k]\psi) \cdot \sin[(k\nu_0-lf_0)(\dot{\phi}+t)+k\gamma-l\delta] \\
&\cdot e^{j\frac{1}{2}\dot{\phi}[-k(2m+k)\nu_0^2+2[nk+l(m+k)]\nu_0f_0+l(-2n-l)f_0^2]}
\end{aligned}$$

after rearranging common expressions and substitute $l = -l$

$$\begin{aligned}
&= \frac{j}{8} \sum_{\substack{m,n,k,l \\ =-\infty}}^{\infty} J_m(\beta)J_n(m\psi)J_{m-k}(\beta)J_{n-l}([m-k]\psi) \cdot \sin[(k\nu_0+lf_0)(\dot{\phi}+t)+k\gamma+l\delta] \\
&\cdot e^{j\frac{1}{2}\dot{\phi}[k(2m-k)\nu_0^2+2[nk+l(m-k)]\nu_0f_0+l(2n-l)f_0^2]} \\
&+ \frac{j}{8} \sum_{\substack{m,n,k,l \\ =-\infty}}^{\infty} J_m(\beta)J_n(m\psi)J_{m-k}(\beta)J_{n-l}([m-k]\psi) \cdot \sin[(k\nu_0+lf_0)(\dot{\phi}+t)+k\gamma+l\delta]
\end{aligned}$$

$$\begin{aligned}
& \cdot e^{j\frac{1}{2}\ddot{\phi}[k(2m-k)\nu_0^2+2[nk+l(m-k)]\nu_0f_0+l(2n-l)f_0^2]} \\
& -\frac{j}{8}\sum_{\substack{m,n,k,l \\ =-\infty}}^{\infty} J_m(\beta)J_n(m\psi)J_{m-k}(\beta)J_{n+l}([m-k]\psi) \cdot \sin[(k\nu_0+lf_0)(\dot{\phi}+t)+k\gamma+l\delta] \\
& \cdot e^{j\frac{1}{2}\ddot{\phi}[k(2m-k)\nu_0^2+2[-nk+l(m-k)]\nu_0f_0-l(2n+l)f_0^2]} \\
& -\frac{j}{8}\sum_{\substack{m,n,k,l \\ =-\infty}}^{\infty} J_m(\beta)J_n(m\psi)J_{m-k}(\beta)J_{n+l}([m-k]\psi) \cdot \sin[(k\nu_0+lf_0)(\dot{\phi}+t)+k\gamma+l\delta] \\
& \cdot e^{j\frac{1}{2}\ddot{\phi}[k(2m-k)\nu_0^2+2[-nk+l(m-k)]\nu_0-l(2n+l)f_0^2]} \\
& +\frac{j}{8}\sum_{\substack{m,n,k,l \\ =-\infty}}^{\infty} J_m(\beta)J_n(m\psi)J_{m+k}(\beta)J_{n-l}([m+k]\psi) \cdot \sin[(k\nu_0+lf_0)(\dot{\phi}+t)+k\gamma+l\delta] \\
& \cdot e^{j\frac{1}{2}\ddot{\phi}[-k(2m+k)\nu_0^2+2[nk-l(m+k)]\nu_0f_0+l(2n-l)f_0^2]} \\
& +\frac{j}{8}\sum_{\substack{m,n,k,l \\ =-\infty}}^{\infty} J_m(\beta)J_n(m\psi)J_{m+k}(\beta)J_{n-l}([m+k]\psi) \cdot \sin[(k\nu_0+lf_0)(\dot{\phi}+t)+k\gamma+l\delta] \\
& \cdot e^{j\frac{1}{2}\ddot{\phi}[-k(2m+k)\nu_0^2+2[nk-l(m+k)]\nu_0f_0+l(2n-l)f_0^2]} \\
& -\frac{j}{8}\sum_{\substack{m,n,k,l \\ =-\infty}}^{\infty} J_m(\beta)J_n(m\psi)J_{m+k}(\beta)J_{n+l}([m+k]\psi) \cdot \sin[(k\nu_0+lf_0)(\dot{\phi}+t)+k\gamma+l\delta] \\
& \cdot e^{j\frac{1}{2}\ddot{\phi}[-k(2m+k)\nu_0^2+2[-nk-l(m+k)]\nu_0f_0-l(2n+l)f_0^2]} \\
& -\frac{j}{8}\sum_{\substack{m,n,k,l \\ =-\infty}}^{\infty} J_m(\beta)J_n(m\psi)J_{m+k}(\beta)J_{n+l}([m+k]\psi) \cdot \sin[(k\nu_0+lf_0)(\dot{\phi}+t)+k\gamma+l\delta] \\
& \cdot e^{j\frac{1}{2}\ddot{\phi}[-k(2m+k)\nu_0^2+2[-nk-l(m+k)]\nu_0f_0-l(2n+l)f_0^2]}
\end{aligned}$$

substitute $n = -n$

$$\begin{aligned}
& =\frac{j}{4}\sum_{\substack{m,n,k,l \\ =-\infty}}^{\infty} J_m(\beta)J_n(m\psi)J_{m-k}(\beta)J_{n-l}([m-k]\psi) \cdot \sin[(k\nu_0+lf_0)(\dot{\phi}+t)+k\gamma+l\delta] \\
& \cdot e^{j\frac{1}{2}\ddot{\phi}[k(2m-k)\nu_0^2+2[nk+l(m-k)]\nu_0f_0+l(2n-l)f_0^2]} \\
& -\frac{j}{4}\sum_{\substack{m,n,k,l \\ =-\infty}}^{\infty} J_m(\beta)J_{-n}(m\psi)J_{m-k}(\beta)J_{-n+l}([m-k]\psi) \cdot \sin[(k\nu_0+lf_0)(\dot{\phi}+t)+k\gamma+l\delta] \\
& \cdot e^{j\frac{1}{2}\ddot{\phi}[k(2m-k)\nu_0^2+2[nk+l(m-k)]\nu_0f_0+l(2n-l)f_0^2]} \\
& +\frac{j}{4}\sum_{\substack{m,n,k,l \\ =-\infty}}^{\infty} J_m(\beta)J_{-n}(m\psi)J_{m+k}(\beta)J_{-n-l}([m+k]\psi) \cdot \sin[(k\nu_0+lf_0)(\dot{\phi}+t)+k\gamma+l\delta] \\
& \cdot e^{j\frac{1}{2}\ddot{\phi}[-k(2m+k)\nu_0^2-2[nk+l(m+k)]\nu_0f_0-l(2n+l)f_0^2]} \\
& -\frac{j}{4}\sum_{\substack{m,n,k,l \\ =-\infty}}^{\infty} J_m(\beta)J_n(m\psi)J_{m+k}(\beta)J_{n+l}([m+k]\psi) \cdot \sin[(k\nu_0+lf_0)(\dot{\phi}+t)+k\gamma+l\delta] \\
& \cdot e^{-j\frac{1}{2}\ddot{\phi}[k(2m+k)\nu_0^2+2[nk+l(m+k)]\nu_0f_0+l(2n+l)f_0^2]}
\end{aligned}$$

l odd case

$$\begin{aligned}
&= \frac{j}{4} \sum_{\substack{m,n,k,l \\ =-\infty}}^{\infty} J_m(\beta) J_n(m\psi) J_{m-k}(\beta) J_{n-l}([m-k]\psi) \cdot \sin[(k\nu_0 + lf_0)(\dot{\phi} + t) + k\gamma + l\delta] \\
&\cdot e^{j\frac{1}{2}\dot{\phi}[k(2m-k)\nu_0^2 + 2[nk+l(m-k)]\nu_0 f_0 + l(2n-l)f_0^2]} \\
&+ \frac{j}{4} \sum_{\substack{m,n,k,l \\ =-\infty}}^{\infty} J_m(\beta) J_n(m\psi) J_{m-k}(\beta) J_{n-l}([m-k]\psi) \cdot \sin[(k\nu_0 + lf_0)(\dot{\phi} + t) + k\gamma + l\delta] \\
&\cdot e^{j\frac{1}{2}\dot{\phi}[k(2m-k)\nu_0^2 + 2[nk+l(m-k)]\nu_0 f_0 + l(2n-l)f_0^2]} \\
&- \frac{j}{4} \sum_{\substack{m,n,k,l \\ =-\infty}}^{\infty} J_m(\beta) J_n(m\psi) J_{m+k}(\beta) J_{n+l}([m+k]\psi) \cdot \sin[(k\nu_0 + lf_0)(\dot{\phi} + t) + k\gamma + l\delta] \\
&\cdot e^{-j\frac{1}{2}\dot{\phi}[k(2m+k)\nu_0^2 + 2[nk+l(m+k)]\nu_0 f_0 + l(2n+l)f_0^2]} \\
&- \frac{j}{4} \sum_{\substack{m,n,k,l \\ =-\infty}}^{\infty} J_m(\beta) J_n(m\psi) J_{m+k}(\beta) J_{n+l}([m+k]\psi) \cdot \sin[(k\nu_0 + lf_0)(\dot{\phi} + t) + k\gamma + l\delta] \\
&\cdot e^{-j\frac{1}{2}\dot{\phi}[k(2m+k)\nu_0^2 + 2[nk+l(m+k)]\nu_0 f_0 + l(2n+l)f_0^2]} \\
&= \frac{j}{2} \sum_{\substack{m,n,k,l \\ =-\infty}}^{\infty} J_m(\beta) J_n(m\psi) J_{m-k}(\beta) J_{n-l}([m-k]\psi) \cdot \sin[(k\nu_0 + lf_0)(\dot{\phi} + t) + k\gamma + l\delta] \\
&\cdot e^{j\frac{1}{2}\dot{\phi}[k(2m-k)\nu_0^2 + 2[nk+l(m-k)]\nu_0 f_0 + l(2n-l)f_0^2]} \\
&- \frac{j}{2} \sum_{\substack{m,n,k,l \\ =-\infty}}^{\infty} J_m(\beta) J_n(m\psi) J_{m+k}(\beta) J_{n+l}([m+k]\psi) \cdot \sin[(k\nu_0 + lf_0)(\dot{\phi} + t) + k\gamma + l\delta] \\
&\cdot e^{-j\frac{1}{2}\dot{\phi}[k(2m+k)\nu_0^2 + 2[nk+l(m+k)]\nu_0 f_0 + l(2n+l)f_0^2]}
\end{aligned}$$

in 2nd equation substitute variable

$$\begin{aligned}
&\Rightarrow m+k \rightarrow m; m \rightarrow m-k; 2m+k \rightarrow 2m-k \\
&\Rightarrow n+l \rightarrow n; n \rightarrow n-l; 2n+l \rightarrow 2n-l \\
&= \frac{j}{2} \sum_{\substack{m,n,k,l \\ =-\infty}}^{\infty} J_m(\beta) J_n(m\psi) J_{m-k}(\beta) J_{n-l}([m-k]\psi) \cdot \sin[(k\nu_0 + lf_0)(\dot{\phi} + t) + k\gamma + l\delta] \\
&\cdot e^{j\frac{1}{2}\dot{\phi}[k(2m-k)\nu_0^2 + 2[nk+l(m-k)]\nu_0 f_0 + l(2n-l)f_0^2]} \\
&- \frac{j}{2} \sum_{\substack{m,n,k,l \\ =-\infty}}^{\infty} J_{m-k}(\beta) J_{n-l}([m-k]\psi) J_m(\beta) J_n(m\psi) \cdot \sin[(k\nu_0 + lf_0)(\dot{\phi} + t) + k\gamma + l\delta] \\
&\cdot e^{-j\frac{1}{2}\dot{\phi}[k(2m-k)\nu_0^2 + 2[(n-l)k+lm]\nu_0 f_0 + l(2n-l)f_0^2]}
\end{aligned}$$

identical to previous case i.e., independent of l polarity

$$= - \sum_{\substack{m,n,k,l \\ =-\infty}}^{\infty} J_m(\beta) J_n(m\psi) J_{m-k}(\beta) J_{n-l}([m-k]\psi) \cdot \sin[(k\nu_0 + lf_0)(\dot{\phi} + t) + k\gamma + l\delta]$$

$$\cdot \sin\left(\frac{1}{2}\ddot{\phi}\left[k(2m-k)\nu_0^2 + 2[nk+l(m-k)]\nu_0f_0 + l(2n-l)f_0^2\right]\right)$$

or

$$= - \sum_{\substack{m,n,k,l \\ =-\infty}}^{\infty} J_m(\beta)J_n(m\psi)J_{m+k}(\beta)J_{n+l}([m+k]\psi) \cdot \sin[(k\nu_0+lf_0)(\dot{\phi}+t) + k\gamma + l\delta]$$

$$\cdot \sin\left(\frac{1}{2}\ddot{\phi}\left[k(2m+k)\nu_0^2 + 2[nk+l(m+k)]\nu_0f_0 + l(2n+l)f_0^2\right]\right).$$

Finally we can summarize these calculations by noting that the expression :

$$\sum_{\substack{m,n,k,l \\ =-\infty}}^{\infty} J_m(\beta)J_n(m\psi)J_{m-k}(\beta)J_{n-l}([m-k]\psi) \cdot e^{j[k\gamma+l\delta]} \cdot e^{j[k\nu_0+lf_0](\dot{\phi}+t)}$$

$$\cdot e^{j\frac{1}{2}\ddot{\phi}[k(2m-k)\nu_0^2+2[nk+l(m-k)]\nu_0f_0+l(2n-l)f_0^2]}$$

is independent of l polarity, and can be represented in the equivalent form

$$= \sum_{m,n,k,l=-\infty}^{\infty} J_m(\beta)J_{m+k}(\beta)J_n(m\psi)J_{n+l}([m+k]\psi) \cdot$$

$$\cdot \left[\begin{array}{c} \cos[(k\nu_0+lf_0)(\dot{\phi}+t) + k\gamma + l\delta] \\ -\sin[(k\nu_0+lf_0)(\dot{\phi}+t) + k\gamma + l\delta] \end{array} \right]_k$$

$$\cdot \left[\begin{array}{c} \cos\left[\frac{1}{2}\ddot{\phi}\left(k(2m+k)\nu_0^2 + 2[nk+l(m+k)]\nu_0f_0 + l(2n+l)f_0^2\right)\right] \\ \sin\left[\frac{1}{2}\ddot{\phi}\left(k(2m+k)\nu_0^2 + 2[nk+l(m+k)]\nu_0f_0 + l(2n+l)f_0^2\right)\right] \end{array} \right]_k$$

where $\left[\begin{array}{c} \dots \\ \dots \end{array} \right]_k$ formalism formalism is introduced to denote that top element is chosen if k is even and bottom if k is odd.

8 Appendix B: Extended model for conventional MPS

We will examine the LTI signal analysis of the MPS in the most general case, especially treating the modulated signal in case of amplitude slopes. We drive the MZM with a voltage signal which has DC and AC terms (the DC term could also be a constant phase delay between the ports), such that

$$RF = \pi \frac{V_b + V \sin(\nu_0 t)}{V_\pi} \triangleq \alpha + \beta \cdot \sin(\nu_0 t)$$

where V_b is the bias voltage, V is the modulation voltage, V_π is the voltage applied to achieve a π phase shift and $\hat{\nu}_0$ is the RF driving frequency (we omit the 2π constant in the harmonic for brevity). The signal is more conveniently parametrized by $\hat{\alpha}$ and $\hat{\beta}$.

first we look at the optical field arriving to the DUT after passing the MZM in the bar port with the use of Jacobi-Anger identity. Which demonstrates that there is an entire comb spectrum generated with distributed powers dependent on $J_n(\beta)$ is the n-th j-Bessel function at β value

$$\begin{aligned} U(t) &= \frac{\sqrt{P_0}}{2} \cdot e^{j\Omega_0 t} \cdot (e^{j\alpha} \cdot e^{j\beta \cdot \sin(\nu_0 t)} - 1) \\ &= \frac{\sqrt{P_0}}{2} \cdot e^{j\Omega_0 t} \cdot \left(e^{j\alpha} \cdot \sum_{n=-\infty}^{\infty} J_n(\beta) \cdot e^{j \cdot n \cdot \nu_0 t} - 1 \right), \quad n \in \mathbb{N} \\ Y(t) &= \frac{\sqrt{P_0}}{2} \cdot e^{j\phi(\Omega_0)} e^{j\Omega_0 t} \cdot \left[e^{j\alpha} \cdot \sum_{n=-\infty}^{\infty} J_n(\beta) \cdot B(\Omega_0 + n\nu_0) \cdot e^{j(n\nu_0 \phi + \frac{n^2 \nu_0^2 \ddot{\phi}}{2})} \cdot e^{jn\nu_0 t} \right. \\ &\quad \left. - B(\Omega_0) \right] \end{aligned}$$

Since $n\nu_0 \ll \Omega_0$, we shall make the following approximations:

1. The typical assumption is that the attenuation experienced by all the tones is identical. However, in our approach the amplitude is developed using a Taylor series for the DUT response, assumption being that the amplitude can be expressed as a Taylor expansion up to 1st order about carrier frequency.

$$\Rightarrow B(\Omega_0 + n\nu_0) \cong B(\Omega_0) + \left. \frac{\partial B}{\partial \omega} \right|_{\Omega_0} n\nu_0 + \dots = B(\Omega_0) + \dot{B} \cdot n\nu_0 + \dots$$

2. The phase is developed using a Taylor series for the DUT response, assumption being that the phase can be expressed as a Taylor expansion up to 2nd order about carrier frequency.

$$\Rightarrow \phi(\Omega_0 + n\nu_0) \cong \phi(\Omega_0) + \left. \frac{\partial \phi}{\partial \omega} \right|_{\Omega_0} n\nu_0 + \left. \frac{1}{2} \frac{\partial^2 \phi}{\partial \omega^2} \right|_{\Omega_0} (n\nu_0)^2 + \dots$$

$$= \phi(\Omega_0) + \dot{\phi} \cdot n\nu_0 + \frac{1}{2} \ddot{\phi} \cdot (n\nu_0)^2 + \dots$$

$$\begin{aligned} Y(t) &= \frac{\sqrt{P_0}}{2} \cdot B(\Omega_0) \cdot e^{j\phi(\Omega_0)} e^{j\Omega_0 t} \cdot \left[e^{j\alpha} \cdot \sum_{n=-\infty}^{\infty} J_n(\beta) \cdot \left[1 + \frac{\dot{B} \cdot n\nu_0}{B(\Omega_0)} \right] \cdot e^{jn\nu_0(\phi+t)} \cdot e^{j \frac{n^2 \nu_0^2 \ddot{\phi}}{2}} \right. \\ &\quad \left. - 1 \right] \end{aligned}$$

$$Y^*(t) = \frac{\sqrt{P_0}}{2} \cdot B(\Omega_0) \cdot e^{-j\phi(\Omega_0)} e^{-j\Omega_0 t} \cdot \left[e^{-j\alpha} \cdot \sum_{m=-\infty}^{\infty} J_m(\beta) \cdot \left[1 + \frac{\dot{B} \cdot m \nu_0}{B(\Omega_0)} \right] \cdot e^{-jm\nu_0(\phi+t)} \right. \\ \left. \cdot e^{-j \frac{m^2 \nu_0^2 \dot{\phi}}{2}} - 1 \right]$$

the expression of the photocurrent

$$P(t) = Y(t) \cdot Y^*(t) = \frac{P_0}{4} \cdot B(\Omega_0)^2 \\ \cdot \left[e^{j\alpha} \cdot \sum_{n=-\infty}^{\infty} J_n(\beta) \cdot \left[1 + \frac{\dot{B} \cdot n \nu_0}{B(\Omega_0)} \right] \cdot e^{jn\nu_0(\phi+t)} \cdot e^{j \frac{n^2 \nu_0^2 \dot{\phi}}{2}} - 1 \right] \\ \cdot \left[e^{-j\alpha} \cdot \sum_{m=-\infty}^{\infty} J_m(\beta) \cdot \left[1 + \frac{\dot{B} \cdot m \nu_0}{B(\Omega_0)} \right] \cdot e^{-jm\nu_0(\phi+t)} \cdot e^{-j \frac{m^2 \nu_0^2 \dot{\phi}}{2}} - 1 \right] \\ = \frac{P_0}{4} \cdot B(\Omega_0)^2 \cdot \left\{ \sum_{n=-\infty}^{\infty} \sum_{m=-\infty}^{\infty} J_n(\beta) J_m(\beta) \cdot \left[1 + \frac{\dot{B} \cdot n \nu_0}{B(\Omega_0)} \right] \cdot \left[1 + \frac{\dot{B} \cdot m \nu_0}{B(\Omega_0)} \right] \right. \\ \cdot e^{j(n-m)\nu_0(\phi+t) + \frac{\dot{\phi}(n^2 - m^2)\nu_0^2}{2}} \\ - e^{j\alpha} \cdot \sum_{n=-\infty}^{\infty} J_n(\beta) \cdot \left[1 + \frac{\dot{B} \cdot n \nu_0}{B(\Omega_0)} \right] \cdot e^{jn\nu_0(\phi+t)} \cdot e^{j \frac{n^2 \nu_0^2 \dot{\phi}}{2}} \\ \left. - e^{-j\alpha} \cdot \sum_{m=-\infty}^{\infty} J_m(\beta) \cdot \left[1 + \frac{\dot{B} \cdot m \nu_0}{B(\Omega_0)} \right] \cdot e^{-jm\nu_0(\phi+t)} \cdot e^{-j \frac{m^2 \nu_0^2 \dot{\phi}}{2}} + 1 \right\}$$

in order to emphasis the harmonics we can define a index change $k = n - m \Rightarrow m = n - k$

$$n^2 - m^2 = (n - m)(n + m) = k \cdot (2n - k)$$

also for the harmonics appearing we can switch $n, m = k$

$$P(t) = \frac{P_0}{4} \cdot B(\Omega_0)^2 \cdot \left\{ \sum_{n=-\infty}^{\infty} \sum_{k=-\infty}^{\infty} J_n(\beta) J_{n-k}(\beta) \cdot \left[1 + \frac{\dot{B} \cdot n \nu_0}{B(\Omega_0)} \right] \cdot \left[1 + \frac{\dot{B} \cdot (n-k) \nu_0}{B(\Omega_0)} \right] \right. \\ \cdot e^{jk\nu_0(\phi+t)} \cdot e^{j \frac{\dot{\phi} k(2n-k)\nu_0^2}{2}} - e^{j\alpha} \cdot \sum_{k=-\infty}^{\infty} J_k(\beta) \cdot \left[1 + \frac{\dot{B} \cdot k \nu_0}{B(\Omega_0)} \right] \cdot e^{jk\nu_0(\phi+t)} \cdot e^{j \frac{k^2 \nu_0^2 \dot{\phi}}{2}} \\ \left. - e^{-j\alpha} \cdot \sum_{k=-\infty}^{\infty} J_k(\beta) \cdot \left[1 + \frac{\dot{B} \cdot k \nu_0}{B(\Omega_0)} \right] \cdot e^{-jk\nu_0(\phi+t)} \cdot e^{-j \frac{k^2 \nu_0^2 \dot{\phi}}{2}} + 1 \right\} \\ \sum_{n=-\infty}^{\infty} \sum_{k=-\infty}^{\infty} J_n(\beta) J_{n-k}(\beta) \cdot \left[1 + \frac{\dot{B} \cdot (2n-k) \nu_0}{B(\Omega_0)} + \frac{\dot{B}^2 \cdot n(n-k) \nu_0^2}{B(\Omega_0)^2} \right] \cdot e^{jk\nu_0(\phi+t)} \cdot e^{j \frac{\dot{\phi} k(2n-k)\nu_0^2}{2}}$$

the 1st term in the square brackets denotes the standard model for evaluation of MPS method, the 2nd and 3rd terms are arising cause of our extended model. We can use an approach that splits each infinite sum into plus/minus sign accordingly in order to simplify this expression

$$= \frac{1}{2} \sum_{n=-\infty}^{\infty} \sum_{k=-\infty}^{\infty} J_n(\beta) J_{n-k}(\beta) \cdot \left[1 + \frac{\dot{B} \cdot (2n-k) \nu_0}{B(\Omega_0)} + \frac{\dot{B}^2 \cdot n(n-k) \nu_0^2}{B(\Omega_0)^2} \right] \cdot e^{jk\nu_0(\phi+t)} \cdot e^{j \frac{\dot{\phi} k(2n-k)\nu_0^2}{2}} \\ + \frac{1}{2} \sum_{n=-\infty}^{\infty} \sum_{k=-\infty}^{\infty} J_{-n}(\beta) J_{-n-k}(\beta) \cdot \left[1 + \frac{\dot{B} \cdot (-2n-k) \nu_0}{B(\Omega_0)} + \frac{\dot{B}^2 \cdot (-n)(-n-k) \nu_0^2}{B(\Omega_0)^2} \right] \cdot e^{jk\nu_0(\phi+t)} \cdot e^{j \frac{\dot{\phi} k(-2n-k)\nu_0^2}{2}}$$

$$\begin{aligned}
&= \frac{1}{4} \sum_{n=-\infty}^{\infty} \sum_{k=-\infty}^{\infty} J_n(\beta) J_{n-k}(\beta) \cdot \left[1 + \frac{\dot{B} \cdot (2n-k) \nu_0}{B(\Omega_0)} + \frac{\dot{B}^2 \cdot n(n-k) \nu_0^2}{B(\Omega_0)^2} \right] \cdot e^{jk\nu_0(\dot{\phi}+t)} \cdot e^{j \frac{\dot{\phi}k(2n-k) \nu_0^2}{2}} \\
&+ \frac{1}{4} \sum_{n=-\infty}^{\infty} \sum_{k=-\infty}^{\infty} J_n(\beta) J_{n+k}(\beta) \cdot \left[1 + \frac{\dot{B} \cdot (2n+k) \nu_0}{B(\Omega_0)} + \frac{\dot{B}^2 \cdot n(n+k) \nu_0^2}{B(\Omega_0)^2} \right] \cdot e^{-jk\nu_0(\dot{\phi}+t)} \cdot e^{-j \frac{\dot{\phi}k(2n+k) \nu_0^2}{2}} \\
&+ \frac{1}{4} \sum_{n=-\infty}^{\infty} \sum_{k=-\infty}^{\infty} J_{-n}(\beta) J_{-n-k}(\beta) \cdot \left[1 - \frac{\dot{B} \cdot (2n+k) \nu_0}{B(\Omega_0)} + \frac{\dot{B}^2 \cdot n(n+k) \nu_0^2}{B(\Omega_0)^2} \right] \cdot e^{jk\nu_0(\dot{\phi}+t)} \cdot e^{-j \frac{\dot{\phi}k(2n+k) \nu_0^2}{2}} \\
&+ \frac{1}{4} \sum_{n=-\infty}^{\infty} \sum_{k=-\infty}^{\infty} J_{-n}(\beta) J_{-n+k}(\beta) \cdot \left[1 - \frac{\dot{B} \cdot (2n-k) \nu_0}{B(\Omega_0)} + \frac{\dot{B}^2 \cdot n(n-k) \nu_0^2}{B(\Omega_0)^2} \right] \cdot e^{-jk\nu_0(\dot{\phi}+t)} \cdot e^{j \frac{\dot{\phi}k(2n-k) \nu_0^2}{2}}
\end{aligned}$$

Using $J_{-n}(x) = (-1)^n \cdot J_n(x)$

$$\begin{aligned}
&= \frac{1}{4} \sum_{n=-\infty}^{\infty} \sum_{k=-\infty}^{\infty} J_n(\beta) J_{n-k}(\beta) \cdot \left[1 + \frac{\dot{B} \cdot (2n-k) \nu_0}{B(\Omega_0)} + \frac{\dot{B}^2 \cdot n(n-k) \nu_0^2}{B(\Omega_0)^2} \right] \cdot e^{jk\nu_0(\dot{\phi}+t)} \cdot e^{j \frac{\dot{\phi}k(2n-k) \nu_0^2}{2}} \\
&+ \frac{1}{4} \sum_{n=-\infty}^{\infty} \sum_{k=-\infty}^{\infty} J_n(\beta) J_{n+k}(\beta) \cdot \left[1 + \frac{\dot{B} \cdot (2n+k) \nu_0}{B(\Omega_0)} + \frac{\dot{B}^2 \cdot n(n+k) \nu_0^2}{B(\Omega_0)^2} \right] \cdot e^{-jk\nu_0(\dot{\phi}+t)} \cdot e^{-j \frac{\dot{\phi}k(2n+k) \nu_0^2}{2}} \\
&+ \frac{1}{4} \sum_{n=-\infty}^{\infty} \sum_{k=-\infty}^{\infty} (-1)^{2n+k} J_n(\beta) J_{n+k}(\beta) \cdot \left[1 - \frac{\dot{B} \cdot (2n+k) \nu_0}{B(\Omega_0)} + \frac{\dot{B}^2 \cdot n(n+k) \nu_0^2}{B(\Omega_0)^2} \right] \cdot e^{jk\nu_0(\dot{\phi}+t)} \cdot e^{-j \frac{\dot{\phi}k(2n+k) \nu_0^2}{2}} \\
&+ \frac{1}{4} \sum_{n=-\infty}^{\infty} \sum_{k=-\infty}^{\infty} (-1)^{2n-k} J_n(\beta) J_{n-k}(\beta) \cdot \left[1 - \frac{\dot{B} \cdot (2n-k) \nu_0}{B(\Omega_0)} + \frac{\dot{B}^2 \cdot n(n-k) \nu_0^2}{B(\Omega_0)^2} \right] \cdot e^{-jk\nu_0(\dot{\phi}+t)} \cdot e^{j \frac{\dot{\phi}k(2n-k) \nu_0^2}{2}}
\end{aligned}$$

rearranging these terms for harmonic identification

$$\begin{aligned}
&= \frac{1}{4} \sum_{n=-\infty}^{\infty} \sum_{k=-\infty}^{\infty} J_n(\beta) J_{n-k}(\beta) \cdot e^{j \frac{\dot{\phi}k(2n-k) \nu_0^2}{2}} \\
&\cdot \left[\left(e^{jk\nu_0(\dot{\phi}+t)} + (-1)^{2n-k} \cdot e^{-jk\nu_0(\dot{\phi}+t)} \right) \right. \\
&+ \frac{\dot{B} \cdot (2n-k) \nu_0}{B(\Omega_0)} \cdot \left(e^{jk\nu_0(\dot{\phi}+t)} - (-1)^{2n-k} \cdot e^{-jk\nu_0(\dot{\phi}+t)} \right) \\
&+ \left. \frac{\dot{B}^2 \cdot n(n-k) \nu_0^2}{B(\Omega_0)^2} \cdot \left(e^{jk\nu_0(\dot{\phi}+t)} + (-1)^{2n-k} \cdot e^{-jk\nu_0(\dot{\phi}+t)} \right) \right] \\
&+ \frac{1}{4} \sum_{n=-\infty}^{\infty} \sum_{k=-\infty}^{\infty} J_n(\beta) J_{n+k}(\beta) \cdot e^{-j \frac{\dot{\phi}k(2n+k) \nu_0^2}{2}} \\
&\cdot \left[\left(e^{-jk\nu_0(\dot{\phi}+t)} + (-1)^{2n+k} \cdot e^{jk\nu_0(\dot{\phi}+t)} \right) \right. \\
&+ \frac{\dot{B} \cdot (2n+k) \nu_0}{B(\Omega_0)} \cdot \left(e^{-jk\nu_0(\dot{\phi}+t)} - (-1)^{2n+k} \cdot e^{jk\nu_0(\dot{\phi}+t)} \right) \\
&+ \left. \frac{\dot{B}^2 \cdot n(n+k) \nu_0^2}{B(\Omega_0)^2} \cdot \left(e^{-jk\nu_0(\dot{\phi}+t)} + (-1)^{2n+k} \cdot e^{jk\nu_0(\dot{\phi}+t)} \right) \right]
\end{aligned}$$

We need to distinguish in between the following cases

$$(-1)^{2n \pm k} = (-1)^{\pm k} = \begin{cases} 1 & k \text{ even} \\ -1 & k \text{ odd} \end{cases}$$

case of k even

$$\begin{aligned}
&= \frac{1}{2} \sum_{n=-\infty}^{\infty} \sum_{k=-\infty}^{\infty} J_n(\beta) J_{n-k}(\beta) \cdot e^{j \frac{\ddot{\phi} k (2n-k) \nu_0^2}{2}} \\
&\cdot \left[\left(1 + \frac{\dot{B}^2 \cdot n(n-k) \nu_0^2}{B(\Omega_0)^2} \right) \cdot \cos[k\nu_0(\dot{\phi} + t)] \right. \\
&\left. + j \frac{\dot{B} \cdot (2n-k) \nu_0}{B(\Omega_0)} \cdot \sin[k\nu_0(\dot{\phi} + t)] \right] \\
&+ \frac{1}{2} \sum_{n=-\infty}^{\infty} \sum_{k=-\infty}^{\infty} J_n(\beta) J_{n+k}(\beta) \cdot e^{-j \frac{\ddot{\phi} k (2n+k) \nu_0^2}{2}} \\
&\cdot \left[\left(1 + \frac{\dot{B}^2 \cdot n(n+k) \nu_0^2}{B(\Omega_0)^2} \right) \cdot \cos[k\nu_0(\dot{\phi} + t)] \right. \\
&\left. - j \frac{\dot{B} \cdot (2n+k) \nu_0}{B(\Omega_0)} \cdot \sin[k\nu_0(\dot{\phi} + t)] \right]
\end{aligned}$$

we can substitute the indexes in the 2nd term $q = n + k \Rightarrow n = q - k$

$$\begin{aligned}
&= \frac{1}{2} \sum_{n=-\infty}^{\infty} \sum_{k=-\infty}^{\infty} J_n(\beta) J_{n-k}(\beta) \cdot e^{j \frac{\ddot{\phi} k (2n-k) \nu_0^2}{2}} \\
&\cdot \left[\left(1 + \frac{\dot{B}^2 \cdot n(n-k) \nu_0^2}{B(\Omega_0)^2} \right) \cdot \cos[k\nu_0(\dot{\phi} + t)] \right. \\
&\left. + j \frac{\dot{B} \cdot (2n-k) \nu_0}{B(\Omega_0)} \cdot \sin[k\nu_0(\dot{\phi} + t)] \right] \\
&+ \frac{1}{2} \sum_{n=-\infty}^{\infty} \sum_{k=-\infty}^{\infty} J_n(\beta) J_{n-k}(\beta) \cdot e^{-j \frac{\ddot{\phi} k (2n-k) \nu_0^2}{2}} \\
&\cdot \left[\left(1 + \frac{\dot{B}^2 \cdot n(n-k) \nu_0^2}{B(\Omega_0)^2} \right) \cdot \cos[k\nu_0(\dot{\phi} + t)] \right. \\
&\left. - j \frac{\dot{B} \cdot (2n-k) \nu_0}{B(\Omega_0)} \cdot \sin[k\nu_0(\dot{\phi} + t)] \right] \\
&= \frac{1}{2} \sum_{n=-\infty}^{\infty} \sum_{k=-\infty}^{\infty} J_n(\beta) J_{n-k}(\beta) \cdot e^{j \frac{\ddot{\phi} k (2n-k) \nu_0^2}{2}} \\
&\cdot \left[\left(1 + \frac{\dot{B}^2 \cdot n(n-k) \nu_0^2}{B(\Omega_0)^2} \right) \cdot \cos[k\nu_0(\dot{\phi} + t)] \cdot \left(e^{j \frac{\ddot{\phi} k (2n-k) \nu_0^2}{2}} + e^{-j \frac{\ddot{\phi} k (2n-k) \nu_0^2}{2}} \right) \right. \\
&\left. + j \frac{\dot{B} \cdot (2n-k) \nu_0}{B(\Omega_0)} \cdot \sin[k\nu_0(\dot{\phi} + t)] \cdot \left(e^{j \frac{\ddot{\phi} k (2n-k) \nu_0^2}{2}} - e^{-j \frac{\ddot{\phi} k (2n-k) \nu_0^2}{2}} \right) \right] \\
&= \sum_{n=-\infty}^{\infty} \sum_{k=-\infty}^{\infty} J_n(\beta) J_{n-k}(\beta) \\
&\cdot \left[\left(1 + \frac{\dot{B}^2 \cdot n(n-k) \nu_0^2}{B(\Omega_0)^2} \right) \cdot \cos\left[\frac{\ddot{\phi} k (2n-k) \nu_0^2}{2}\right] \cdot \cos[k\nu_0(\dot{\phi} + t)] \right. \\
&\left. - \frac{\dot{B} \cdot (2n-k) \nu_0}{B(\Omega_0)} \cdot \sin\left[\frac{\ddot{\phi} k (2n-k) \nu_0^2}{2}\right] \cdot \sin[k\nu_0(\dot{\phi} + t)] \right]
\end{aligned}$$

case of k odd

$$\begin{aligned}
&= \frac{1}{2} \sum_{n=-\infty}^{\infty} \sum_{k=-\infty}^{\infty} J_n(\beta) J_{n-k}(\beta) \cdot e^{j \frac{\ddot{\phi} k (2n-k) \nu_0^2}{2}} \\
&\cdot \left[j \left(1 + \frac{\dot{B}^2 \cdot n(n-k) \nu_0^2}{B(\Omega_0)^2} \right) \cdot \sin[k\nu_0(\dot{\phi} + t)] \right. \\
&+ \left. \frac{\dot{B} \cdot (2n-k) \nu_0}{B(\Omega_0)} \cdot \cos[k\nu_0(\dot{\phi} + t)] \right] \\
&+ \frac{1}{2} \sum_{n=-\infty}^{\infty} \sum_{k=-\infty}^{\infty} J_n(\beta) J_{n+k}(\beta) \cdot e^{-j \frac{\ddot{\phi} k (2n+k) \nu_0^2}{2}} \\
&\cdot \left[-j \left(1 + \frac{\dot{B}^2 \cdot n(n+k) \nu_0^2}{B(\Omega_0)^2} \right) \cdot \sin[k\nu_0(\dot{\phi} + t)] \right. \\
&+ \left. \frac{\dot{B} \cdot (2n+k) \nu_0}{B(\Omega_0)} \cdot \cos[k\nu_0(\dot{\phi} + t)] \right]
\end{aligned}$$

we can substitute the indexes in the 2nd term $q = n + k \Rightarrow n = q - k$

$$\begin{aligned}
&= \frac{1}{2} \sum_{n=-\infty}^{\infty} \sum_{k=-\infty}^{\infty} J_n(\beta) J_{n-k}(\beta) \cdot e^{j \frac{\ddot{\phi} k (2n-k) \nu_0^2}{2}} \\
&\cdot \left[j \left(1 + \frac{\dot{B}^2 \cdot n(n-k) \nu_0^2}{B(\Omega_0)^2} \right) \cdot \sin[k\nu_0(\dot{\phi} + t)] \right. \\
&+ \left. \frac{\dot{B} \cdot (2n-k) \nu_0}{B(\Omega_0)} \cdot \cos[k\nu_0(\dot{\phi} + t)] \right] \\
&+ \frac{1}{2} \sum_{n=-\infty}^{\infty} \sum_{k=-\infty}^{\infty} J_n(\beta) J_{n-k}(\beta) \cdot e^{-j \frac{\ddot{\phi} k (2n-k) \nu_0^2}{2}} \\
&\cdot \left[-j \left(1 + \frac{\dot{B}^2 \cdot n(n-k) \nu_0^2}{B(\Omega_0)^2} \right) \cdot \sin[k\nu_0(\dot{\phi} + t)] \right. \\
&+ \left. \frac{\dot{B} \cdot (2n-k) \nu_0}{B(\Omega_0)} \cdot \cos[k\nu_0(\dot{\phi} + t)] \right] \\
&= \frac{1}{2} \sum_{n=-\infty}^{\infty} \sum_{k=-\infty}^{\infty} J_n(\beta) J_{n-k}(\beta) \\
&\cdot \left[j \left(1 + \frac{\dot{B}^2 \cdot n(n-k) \nu_0^2}{B(\Omega_0)^2} \right) \cdot \sin[k\nu_0(\dot{\phi} + t)] \cdot \left(e^{j \frac{\ddot{\phi} k (2n-k) \nu_0^2}{2}} - e^{-j \frac{\ddot{\phi} k (2n-k) \nu_0^2}{2}} \right) \right. \\
&+ \left. \frac{\dot{B} \cdot (2n-k) \nu_0}{B(\Omega_0)} \cdot \cos[k\nu_0(\dot{\phi} + t)] \cdot \left(e^{j \frac{\ddot{\phi} k (2n-k) \nu_0^2}{2}} + e^{-j \frac{\ddot{\phi} k (2n-k) \nu_0^2}{2}} \right) \right] \\
&= \sum_{n=-\infty}^{\infty} \sum_{k=-\infty}^{\infty} J_n(\beta) J_{n-k}(\beta) \\
&\cdot \left[- \left(1 + \frac{\dot{B}^2 \cdot n(n-k) \nu_0^2}{B(\Omega_0)^2} \right) \cdot \sin\left[\frac{\ddot{\phi} k (2n-k) \nu_0^2}{2}\right] \cdot \sin[k\nu_0(\dot{\phi} + t)] \right. \\
&+ \left. \frac{\dot{B} \cdot (2n-k) \nu_0}{B(\Omega_0)} \cdot \cos\left[\frac{\ddot{\phi} k (2n-k) \nu_0^2}{2}\right] \cdot \cos[k\nu_0(\dot{\phi} + t)] \right]
\end{aligned}$$

Now we will deal with the harmonic terms involving the MZM bias point α

$$-e^{j\alpha} \cdot \sum_{k=-\infty}^{\infty} J_k(\beta) \cdot \left[1 + \frac{\dot{B} \cdot k\nu_0}{B(\Omega_0)}\right] \cdot e^{jk\nu_0(\dot{\phi}+t)} \cdot e^{j\frac{k^2\nu_0^2\ddot{\phi}}{2}}$$

$$-e^{-j\alpha} \cdot \sum_{k=-\infty}^{\infty} J_k(\beta) \cdot \left[1 + \frac{\dot{B} \cdot k\nu_0}{B(\Omega_0)}\right] \cdot e^{-jk\nu_0(\dot{\phi}+t)} \cdot e^{-j\frac{k^2\nu_0^2\ddot{\phi}}{2}}$$

separating this expression into two segments, the regular calculation without amplitude variation (case of '1' term), and the amplitude variation term.

$$= -\frac{e^{j\alpha}}{2} \cdot \sum_{k=-\infty}^{\infty} e^{j\frac{k^2\nu_0^2\ddot{\phi}}{2}} \cdot [J_k(\beta)e^{jk\nu_0(\dot{\phi}+t)} + J_{-k}(\beta)e^{-jk\nu_0(\dot{\phi}+t)}]$$

$$-\frac{e^{-j\alpha}}{2} \cdot \sum_{k=-\infty}^{\infty} e^{-j\frac{k^2\nu_0^2\ddot{\phi}}{2}} \cdot [J_k(\beta)e^{-jk\nu_0(\dot{\phi}+t)} + J_{-k}(\beta)e^{jk\nu_0(\dot{\phi}+t)}]$$

Using $J_{-n}(x) = (-1)^n \cdot J_n(x)$

$$= -\frac{e^{j\alpha}}{2} \cdot \sum_{k=-\infty}^{\infty} e^{j\frac{k^2\nu_0^2\ddot{\phi}}{2}} J_k(\beta) \cdot [e^{jk\nu_0(\dot{\phi}+t)} + (-1)^k e^{-jk\nu_0(\dot{\phi}+t)}]$$

$$-\frac{e^{-j\alpha}}{2} \cdot \sum_{k=-\infty}^{\infty} e^{-j\frac{k^2\nu_0^2\ddot{\phi}}{2}} J_k(\beta) \cdot [e^{-jk\nu_0(\dot{\phi}+t)} + (-1)^k e^{jk\nu_0(\dot{\phi}+t)}]$$

We need to distinguish in between the following cases

$$(-1)^{\pm k} = \begin{cases} 1 & k \text{ even} \\ -1 & k \text{ odd} \end{cases}$$

case of k even

$$= -\sum_{k=-\infty}^{\infty} e^{j[\alpha + \frac{k^2\nu_0^2\ddot{\phi}}{2}]} J_k(\beta) \cdot \cos[k\nu_0(\dot{\phi} + t)]$$

$$-\sum_{k=-\infty}^{\infty} e^{-j[\alpha + \frac{k^2\nu_0^2\ddot{\phi}}{2}]} J_k(\beta) \cdot \cos[k\nu_0(\dot{\phi} + t)]$$

$$= -2 \sum_{k=-\infty}^{\infty} J_k(\beta) \cdot \cos[\alpha + \frac{k^2\nu_0^2\ddot{\phi}}{2}] \cdot \cos[k\nu_0(\dot{\phi} + t)]$$

case of k odd

$$= -j \cdot \sum_{k=-\infty}^{\infty} e^{j[\alpha + \frac{k^2\nu_0^2\ddot{\phi}}{2}]} J_k(\beta) \cdot \sin[k\nu_0(\dot{\phi} + t)]$$

$$+j \cdot \sum_{k=-\infty}^{\infty} e^{-j[\alpha + \frac{k^2\nu_0^2\ddot{\phi}}{2}]} J_k(\beta) \cdot \sin[k\nu_0(\dot{\phi} + t)]$$

$$= 2 \cdot \sum_{k=-\infty}^{\infty} J_k(\beta) \cdot \sin[\alpha + \frac{k^2\nu_0^2\ddot{\phi}}{2}] \cdot \sin[k\nu_0(\dot{\phi} + t)]$$

now we will treat the amplitude variation correction according to a Taylor expansion

$$-e^{j\alpha} \cdot \sum_{k=-\infty}^{\infty} J_k(\beta) \cdot \frac{\dot{B} \cdot k\nu_0}{B(\Omega_0)} \cdot e^{jk\nu_0(\dot{\phi}+t)} \cdot e^{j\frac{k^2\nu_0^2\ddot{\phi}}{2}}$$

$$\begin{aligned}
& -e^{-j\alpha} \cdot \sum_{k=-\infty}^{\infty} J_k(\beta) \cdot \frac{\dot{B} \cdot k\nu_0}{B(\Omega_0)} \cdot e^{-jk\nu_0(\dot{\phi}+t)} \cdot e^{-j\frac{k^2\nu_0^2\ddot{\phi}}{2}} \\
& = -\frac{e^{j\alpha}}{2} \sum_{k=-\infty}^{\infty} e^{j\frac{k^2\nu_0^2\ddot{\phi}}{2}} \frac{\dot{B} \cdot k\nu_0}{B(\Omega_0)} \left[J_k(\beta) e^{jk\nu_0(\dot{\phi}+t)} - J_{-k}(\beta) e^{-jk\nu_0(\dot{\phi}+t)} \right] \\
& -\frac{e^{-j\alpha}}{2} \sum_{k=-\infty}^{\infty} e^{-j\frac{k^2\nu_0^2\ddot{\phi}}{2}} \frac{\dot{B} \cdot k\nu_0}{B(\Omega_0)} \left[J_k(\beta) e^{-jk\nu_0(\dot{\phi}+t)} - J_{-k}(\beta) e^{jk\nu_0(\dot{\phi}+t)} \right]
\end{aligned}$$

Using $J_{-n}(x) = (-1)^n \cdot J_n(x)$

$$\begin{aligned}
& = -\frac{e^{j\alpha}}{2} \sum_{k=-\infty}^{\infty} e^{j\frac{k^2\nu_0^2\ddot{\phi}}{2}} J_k(\beta) \frac{\dot{B} \cdot k\nu_0}{B(\Omega_0)} \left[e^{jk\nu_0(\dot{\phi}+t)} - (-1)^k e^{-jk\nu_0(\dot{\phi}+t)} \right] \\
& -\frac{e^{-j\alpha}}{2} \sum_{k=-\infty}^{\infty} e^{-j\frac{k^2\nu_0^2\ddot{\phi}}{2}} J_k(\beta) \frac{\dot{B} \cdot k\nu_0}{B(\Omega_0)} \left[e^{-jk\nu_0(\dot{\phi}+t)} - (-1)^k e^{jk\nu_0(\dot{\phi}+t)} \right]
\end{aligned}$$

We need to distinguish in between the following cases

$$(-1)^{\pm k} = \begin{cases} 1 & k \text{ even} \\ -1 & k \text{ odd} \end{cases}$$

case of k even

$$\begin{aligned}
& = -j \sum_{k=-\infty}^{\infty} e^{j[\alpha + \frac{k^2\nu_0^2\ddot{\phi}}{2}]} J_k(\beta) \frac{\dot{B} \cdot k\nu_0}{B(\Omega_0)} \cdot \sin[k\nu_0(\dot{\phi} + t)] \\
& + j \sum_{k=-\infty}^{\infty} e^{-j[\alpha + \frac{k^2\nu_0^2\ddot{\phi}}{2}]} J_k(\beta) \frac{\dot{B} \cdot k\nu_0}{B(\Omega_0)} \cdot \sin[k\nu_0(\dot{\phi} + t)] \\
& = 2 \sum_{k=-\infty}^{\infty} J_k(\beta) \frac{\dot{B} \cdot k\nu_0}{B(\Omega_0)} \cdot \sin[\alpha + \frac{k^2\nu_0^2\ddot{\phi}}{2}] \cdot \sin[k\nu_0(\dot{\phi} + t)]
\end{aligned}$$

case of k odd

$$\begin{aligned}
& = - \sum_{k=-\infty}^{\infty} e^{j[\alpha + \frac{k^2\nu_0^2\ddot{\phi}}{2}]} J_k(\beta) \frac{\dot{B} \cdot k\nu_0}{B(\Omega_0)} \cdot \cos[k\nu_0(\dot{\phi} + t)] \\
& - \sum_{k=-\infty}^{\infty} e^{-j[\alpha + \frac{k^2\nu_0^2\ddot{\phi}}{2}]} J_k(\beta) \frac{\dot{B} \cdot k\nu_0}{B(\Omega_0)} \cdot \cos[k\nu_0(\dot{\phi} + t)] \\
& = -2 \sum_{k=-\infty}^{\infty} J_k(\beta) \frac{\dot{B} \cdot k\nu_0}{B(\Omega_0)} \cdot \cos[\alpha + \frac{k^2\nu_0^2\ddot{\phi}}{2}] \cdot \cos[k\nu_0(\dot{\phi} + t)]
\end{aligned}$$

Therefore we can note that the generated photocurrent expression:

$$P(t) = \frac{P_0}{4} \cdot B(\Omega_0)^2 \cdot \left\{ \sum_{n=-\infty}^{\infty} \sum_{k=-\infty}^{\infty} J_n(\beta) J_{n-k}(\beta) \cdot \left[1 + \frac{\dot{B} \cdot n \nu_0}{B(\Omega_0)} \right] \cdot \left[1 + \frac{\dot{B} \cdot (n-k) \nu_0}{B(\Omega_0)} \right] \right. \\ \cdot e^{jk\nu_0(\dot{\phi}+t)} \cdot e^{j\frac{\ddot{\phi}k(2n-k)\nu_0^2}{2}} - e^{j\alpha} \cdot \sum_{k=-\infty}^{\infty} J_k(\beta) \cdot \left[1 + \frac{\dot{B} \cdot k \nu_0}{B(\Omega_0)} \right] \cdot e^{jk\nu_0(\dot{\phi}+t)} \cdot e^{j\frac{k^2\nu_0^2\ddot{\phi}}{2}} \\ \left. - e^{-j\alpha} \cdot \sum_{k=-\infty}^{\infty} J_k(\beta) \cdot \left[1 + \frac{\dot{B} \cdot k \nu_0}{B(\Omega_0)} \right] \cdot e^{-jk\nu_0(\dot{\phi}+t)} \cdot e^{-j\frac{k^2\nu_0^2\ddot{\phi}}{2}} + 1 \right\}$$

is identical according to these calculations to the following expression

$$P(t) = \frac{P_0}{4} \cdot B(\Omega_0)^2 \cdot \left\{ 1 + \sum_{n=-\infty}^{\infty} \sum_{k=-\infty}^{\infty} J_n(\beta) J_{n-k}(\beta) \right. \\ \left[\begin{array}{l} - \left(1 + \frac{\dot{B}^2 \cdot n(n-k)\nu_0^2}{B(\Omega_0)^2} \right) \sin\left[\frac{\ddot{\phi}k(2n-k)\nu_0^2}{2}\right] \sin[k\nu_0(\dot{\phi}+t)] + \frac{\dot{B} \cdot (2n-k)\nu_0}{B(\Omega_0)} \cos\left[\frac{\ddot{\phi}k(2n-k)\nu_0^2}{2}\right] \cos[k\nu_0(\dot{\phi}+t)] \\ \left(1 + \frac{\dot{B}^2 \cdot n(n-k)\nu_0^2}{B(\Omega_0)^2} \right) \cos\left[\frac{\ddot{\phi}k(2n-k)\nu_0^2}{2}\right] \cos[k\nu_0(\dot{\phi}+t)] - \frac{\dot{B} \cdot (2n-k)\nu_0}{B(\Omega_0)} \sin\left[\frac{\ddot{\phi}k(2n-k)\nu_0^2}{2}\right] \sin[k\nu_0(\dot{\phi}+t)] \end{array} \right]_k \\ \left. + 2 \sum_{k=-\infty}^{\infty} J_k(\beta) \cdot \left[\begin{array}{l} \sin\left[\alpha + \frac{k^2\nu_0^2\ddot{\phi}}{2}\right] \sin[k\nu_0(\dot{\phi}+t)] - \frac{\dot{B} \cdot k\nu_0}{B(\Omega_0)} \cos\left[\alpha + \frac{k^2\nu_0^2\ddot{\phi}}{2}\right] \cos[k\nu_0(\dot{\phi}+t)] \\ - \cos\left[\alpha + \frac{k^2\nu_0^2\ddot{\phi}}{2}\right] \cos[k\nu_0(\dot{\phi}+t)] + \frac{\dot{B} \cdot k\nu_0}{B(\Omega_0)} \sin\left[\alpha + \frac{k^2\nu_0^2\ddot{\phi}}{2}\right] \sin[k\nu_0(\dot{\phi}+t)] \end{array} \right]_k \right\}$$

where $\left[\begin{array}{c} \dots \\ \dots \end{array} \right]_k$ formalism is introduced to denote that top element is chosen if k is odd and bottom is k is even.

Let's look at the previous model DC response (without amplitude variation) (k=0)

$$\tilde{P}_0 = \frac{P_0}{4} \cdot B(\Omega_0)^2 \cdot \left[\sum_{n=-\infty}^{\infty} J_n(\beta)^2 - 2J_0(\beta)\cos(\alpha) + 1 \right].$$

We can see that each generated sidetone, $J_n(\beta)$, contributes to the DC response dependent on β , the contribution of the optical carrier, $J_0(\beta)$, is dependent upon MZM bias point α .

Let's look at the current model DC response (k=0)

$$\bar{P}_0 = \frac{P_0}{4} \cdot B(\Omega_0)^2 \cdot \left[\sum_{n=-\infty}^{\infty} J_n(\beta)^2 \left(1 + \frac{\dot{B}^2 \cdot n^2 \nu_0^2}{B(\Omega_0)^2} \right) - 2J_0(\beta)\cos(\alpha) + 1 \right].$$

We can see that each generated sidetone, $J_n(\beta)$, contributes to the DC response dependent on β , with a small correction compared with MPS standard model dependent on $\left(\dot{B}n\nu_0 \right)^2$, as in standard MPS model the contribution of the optical carrier, $J_0(\beta)$, is dependent upon MZM bias point α .

Let's look at the response at first harmonics on the previous model ($k = \pm 1$)

$$\tilde{P}_1 = \frac{P_0}{4} \cdot B(\Omega_0)^2 \cdot \left\{ 4J_1(\beta)\sin\left[\alpha + \frac{\ddot{\phi}\nu_0^2}{2}\right]\sin[\nu_0(\dot{\phi}+t)] - 2 \sum_{n=-\infty}^{\infty} J_n(\beta)J_{n-1}(\beta) \right. \\ \left. \sin\left[\frac{\ddot{\phi}(2n-1)\nu_0^2}{2}\right]\sin[\nu_0(\dot{\phi}+t)] \right\}$$

Response at first harmonic ($k = \pm 1$)

$$\begin{aligned}\bar{P}_1 &= \frac{P_0}{4} \cdot B(\Omega_0)^2 \cdot \left\{ 2 \sum_{n=-\infty}^{\infty} J_n(\beta) J_{n-1}(\beta) \cdot \left[- \left(1 + \frac{\dot{B}^2 \cdot n(n-1) \nu_0^2}{B(\Omega_0)^2} \right) \sin \left[\frac{\ddot{\phi}(2n-1) \nu_0^2}{2} \right] \right. \right. \\ &\cdot \sin[\nu_0(\dot{\phi} + t)] + \frac{\dot{B} \cdot (2n-1) \nu_0}{B(\Omega_0)} \cos \left[\frac{\ddot{\phi}(2n-1) \nu_0^2}{2} \right] \cos[\nu_0(\dot{\phi} + t)] \left. \right] \\ &+ 4J_1(\beta) \cdot \left(\sin \left[\alpha + \frac{\nu_0^2 \ddot{\phi}}{2} \right] \sin[\nu_0(\dot{\phi} + t)] - \frac{\dot{B} \cdot \nu_0}{B(\Omega_0)} \cos \left[\alpha + \frac{\nu_0^2 \ddot{\phi}}{2} \right] \cos[\nu_0(\dot{\phi} + t)] \right) \left. \right\}\end{aligned}$$

We can note that the extended model represents that for each desired signal there might be a distortion that arises from amplitude slope experienced by the different sidetones. It is imparent that a larger amplitude slope value, the stronger these distortions will be.

Let's look at the response at first harmonics on the previous model ($k = \pm 2$)

$$\begin{aligned}\tilde{P}_2 &= \frac{P_0}{4} \cdot B(\Omega_0)^2 \cdot \left\{ 2 \sum_{n=-\infty}^{\infty} J_n(\beta) J_{n-2}(\beta) \cos[\ddot{\phi}(2n-2) \nu_0^2] \cos[2\nu_0(\dot{\phi} + t)] \right. \\ &\left. - 4J_2(\beta) \cos \left[\alpha + \ddot{\phi} 2 \nu_0^2 \right] \cos[2\nu_0(\dot{\phi} + t)] \right\}\end{aligned}$$

Response at second harmonics ($k = \pm 2$) {more detailed to show how I came to these final answers}

$$\begin{aligned}\bar{P}_2 &= \frac{P_0}{4} \cdot B(\Omega_0)^2 \cdot \left\{ \sum_{n=-\infty}^{\infty} J_n(\beta) J_{n-2}(\beta) \cdot \right. \\ &\left[\left(1 + \frac{\dot{B}^2 \cdot n(n-2) \nu_0^2}{B(\Omega_0)^2} \right) \cos \left[\frac{\ddot{\phi} 2(2n-2) \nu_0^2}{2} \right] \cos[2\nu_0(\dot{\phi} + t)] - \frac{\dot{B} \cdot (2n-2) \nu_0}{B(\Omega_0)} \sin \left[\frac{\ddot{\phi} 2(2n-2) \nu_0^2}{2} \right] \sin[2\nu_0(\dot{\phi} + t)] \right] \\ &+ \sum_{n=-\infty}^{\infty} J_n(\beta) J_{n+2}(\beta) \cdot \\ &\left[\left(1 + \frac{\dot{B}^2 \cdot n(n+2) \nu_0^2}{B(\Omega_0)^2} \right) \cos \left[-\frac{\ddot{\phi} 2(2n+2) \nu_0^2}{2} \right] \cos[-2\nu_0(\dot{\phi} + t)] - \frac{\dot{B} \cdot (2n+2) \nu_0}{B(\Omega_0)} \sin \left[-\frac{\ddot{\phi} 2(2n+2) \nu_0^2}{2} \right] \sin[-2\nu_0(\dot{\phi} + t)] \right] \\ &+ 2J_2(\beta) \cdot \\ &\left[-\cos \left[\alpha + \frac{2^2 \nu_0^2 \ddot{\phi}}{2} \right] \cos[2\nu_0(\dot{\phi} + t)] + \frac{\dot{B} \cdot 2 \nu_0}{B(\Omega_0)} \sin \left[\alpha + \frac{2^2 \nu_0^2 \ddot{\phi}}{2} \right] \sin[2\nu_0(\dot{\phi} + t)] \right] \\ &+ 2J_{-2}(\beta) \cdot \\ &\left. \left[-\cos \left[\alpha + \frac{2^2 \nu_0^2 \ddot{\phi}}{2} \right] \cos[-2\nu_0(\dot{\phi} + t)] - \frac{\dot{B} \cdot 2 \nu_0}{B(\Omega_0)} \sin \left[\alpha + \frac{2^2 \nu_0^2 \ddot{\phi}}{2} \right] \sin[-2\nu_0(\dot{\phi} + t)] \right] \right\}\end{aligned}$$

substitute index $q = n + k \Rightarrow n = q - k$ and using $J_{-n}(x) = (-1)^n \cdot J_n(x)$

$$\begin{aligned}&= \frac{P_0}{4} \cdot B(\Omega_0)^2 \cdot \left\{ \sum_{n=-\infty}^{\infty} J_n(\beta) J_{n-2}(\beta) \cdot \right. \\ &\left[\left(1 + \frac{\dot{B}^2 \cdot n(n-2) \nu_0^2}{B(\Omega_0)^2} \right) \cos \left[\frac{\ddot{\phi} 2(2n-2) \nu_0^2}{2} \right] \cos[2\nu_0(\dot{\phi} + t)] - \frac{\dot{B} \cdot (2n-2) \nu_0}{B(\Omega_0)} \sin \left[\frac{\ddot{\phi} 2(2n-2) \nu_0^2}{2} \right] \sin[2\nu_0(\dot{\phi} + t)] \right] \\ &+ \sum_{n=-\infty}^{\infty} J_n(\beta) J_{n-2}(\beta) \cdot \\ &\left. \left[\left(1 + \frac{\dot{B}^2 \cdot n(n-2) \nu_0^2}{B(\Omega_0)^2} \right) \cos \left[\frac{\ddot{\phi} 2(2n-2) \nu_0^2}{2} \right] \cos[2\nu_0(\dot{\phi} + t)] - \frac{\dot{B} \cdot (2n-2) \nu_0}{B(\Omega_0)} \sin \left[\frac{\ddot{\phi} 2(2n-2) \nu_0^2}{2} \right] \sin[2\nu_0(\dot{\phi} + t)] \right] \right\}\end{aligned}$$

$$\begin{aligned}
& +2J_2(\beta) \cdot \\
& \left[-\cos\left[\alpha + \frac{2^2\nu_0^2\ddot{\phi}}{2}\right] \cos[2\nu_0(\dot{\phi} + t)] + \frac{\dot{B} \cdot 2\nu_0}{B(\Omega_0)} \sin\left[\alpha + \frac{2^2\nu_0^2\ddot{\phi}}{2}\right] \sin[2\nu_0(\dot{\phi} + t)] \right] \\
& +2J_2(\beta) \cdot \\
& \left[-\cos\left[\alpha + \frac{2^2\nu_0^2\ddot{\phi}}{2}\right] \cos[2\nu_0(\dot{\phi} + t)] + \frac{\dot{B} \cdot 2\nu_0}{B(\Omega_0)} \sin\left[\alpha + \frac{2^2\nu_0^2\ddot{\phi}}{2}\right] \sin[2\nu_0(\dot{\phi} + t)] \right] \Big\} \\
\Rightarrow \bar{P}_2 = \frac{P_0}{4} \cdot B(\Omega_0)^2 \cdot \left\{ 2 \sum_{n=-\infty}^{\infty} J_n(\beta) J_{n-2}(\beta) \cdot \left[\left(1 + \frac{\dot{B}^2 \cdot n(n-2)\nu_0^2}{B(\Omega_0)^2} \right) \cos\left[\frac{\dot{\phi} 2(2n-2)\nu_0^2}{2}\right] \right. \right. \\
\cdot \cos[2\nu_0(\dot{\phi} + t)] - \frac{\dot{B} \cdot (2n-2)\nu_0}{B(\Omega_0)} \sin\left[\frac{\dot{\phi} 2(2n-2)\nu_0^2}{2}\right] \sin[2\nu_0(\dot{\phi} + t)] \Big] \\
& \left. +4J_2(\beta) \cdot \left[-\cos\left[\alpha + \frac{2^2\nu_0^2\ddot{\phi}}{2}\right] \cos[2\nu_0(\dot{\phi} + t)] + \frac{\dot{B} \cdot 2\nu_0}{B(\Omega_0)} \sin\left[\alpha + \frac{2^2\nu_0^2\ddot{\phi}}{2}\right] \sin[2\nu_0(\dot{\phi} + t)] \right] \right\}
\end{aligned}$$

Finally, we can estimate the contribution of the amplitude change to the phase measurement in the standard MPS method. The photocurrent is multiplied with a local oscillator signal oscillating at the ν_0 frequency, $LO(t) = \sin[\nu_0 t]$, using the following trigonometric identities

$$\cos \alpha \cdot \sin \beta = \frac{1}{2} [\sin(\alpha + \beta) - \sin(\alpha - \beta)]$$

$$\sin \alpha \cdot \sin \beta = \frac{1}{2} [\cos(\alpha - \beta) - \cos(\alpha + \beta)]$$

The photocurrent is composed of these expressions $\bar{P} = \bar{P}_0 + \bar{P}_1 + \bar{P}_2$. We will focus on the contribution to the DC signal, caused by the down converting to DC with the local oscillator signal. There is no need to multiply \bar{P}_0 or \bar{P}_2 since any harmonic contribution will be filtered out using the low pass filter.

Therefore the contributions to the signal are as following:

$$\begin{aligned} \bar{P}_1 &= \frac{P_0}{4} \cdot B(\Omega_0)^2 \cdot \left\{ 2 \sum_{n=-\infty}^{\infty} J_n(\beta) J_{n-1}(\beta) \cdot \left[- \left(1 + \frac{\dot{B}^2 \cdot n(n-1) \nu_0^2}{B(\Omega_0)^2} \right) \sin\left[\frac{\ddot{\phi}(2n-1) \nu_0^2}{2}\right] \right. \right. \\ &\quad \cdot \sin[\nu_0(\dot{\phi} + t)] + \frac{\dot{B} \cdot (2n-1) \nu_0}{B(\Omega_0)} \cos\left[\frac{\ddot{\phi}(2n-1) \nu_0^2}{2}\right] \cos[\nu_0(\dot{\phi} + t)] \left. \right] \\ &\quad + 4J_1(\beta) \cdot \left(\sin\left[\alpha + \frac{\nu_0^2 \ddot{\phi}}{2}\right] \sin[\nu_0(\dot{\phi} + t)] - \frac{\dot{B} \cdot \nu_0}{B(\Omega_0)} \cos\left[\alpha + \frac{\nu_0^2 \ddot{\phi}}{2}\right] \cos[k\nu(\dot{\phi} + t)] \right) \left. \right\} \\ V_1(t)_{\text{LPF}} &= [\bar{P}_1 \cdot \sin[\nu_0 t]]_{\text{LPF}} = \frac{P_0}{4} \cdot B(\Omega_0)^2 \cdot \left\{ \sum_{n=-\infty}^{\infty} J_n(\beta) J_{n-1}(\beta) \left[- \left(1 + \frac{\dot{B}^2 \cdot n(n-1) \nu_0^2}{B(\Omega_0)^2} \right) \right. \right. \\ &\quad \cdot \sin\left[\frac{\ddot{\phi}(2n-1) \nu_0^2}{2}\right] \cos[\nu_0 \dot{\phi}] - \frac{\dot{B} \cdot (2n-1) \nu_0}{B(\Omega_0)} \cos\left[\frac{\ddot{\phi}(2n-1) \nu_0^2}{2}\right] \sin[\nu_0 \dot{\phi}] \left. \right] \\ &\quad + 2J_1(\beta) \cdot \left(\sin\left[\alpha + \frac{\nu_0^2 \ddot{\phi}}{2}\right] \cos[\nu_0 \dot{\phi}] + \frac{\dot{B} \cdot \nu_0}{B(\Omega_0)} \cos\left[\alpha + \frac{\nu_0^2 \ddot{\phi}}{2}\right] \sin[\nu_0 \dot{\phi}] \right) \left. \right\} \end{aligned}$$

We can conclude that the deviation from desired signal in the standard MPS depends on proper selection of MZM bias point α , and a proper selection of RF driving frequency to avoid RF fading due to dispersion. In the case of stronger amplitude slope, \dot{B} , the distortion of the desired signal will be more dominant. Since our RF driving $\beta \sim \pi \frac{1.5}{4.5} = 1.0472 \sim 1.05$. The assumption standing behind this is that our electrical circuit transfers the oscillating RF power through a perfect 50 ohms impedance network, which is usually not true, especially when treating a wide range of RF frequencies. According to Bessel-J function of the first kind, we should anticipate arising of approximately tones up to the second order, thus we will calculate the cases containing $n \in [-1, 2]$.

$$\begin{aligned} V_1(t)_{\text{LPF}} &= \frac{P_0}{4} \cdot B(\Omega_0)^2 \cdot \left\{ \sum_{n=-1}^2 J_n(\beta) J_{n-1}(\beta) \left[- \left(1 + \frac{\dot{B}^2 \cdot n(n-1) \nu_0^2}{B(\Omega_0)^2} \right) \right. \right. \\ &\quad \cdot \sin\left[\frac{\ddot{\phi}(2n-1) \nu_0^2}{2}\right] \cos[\nu_0 \dot{\phi}] - \frac{\dot{B} \cdot (2n-1) \nu_0}{B(\Omega_0)} \cos\left[\frac{\ddot{\phi}(2n-1) \nu_0^2}{2}\right] \sin[\nu_0 \dot{\phi}] \left. \right] \\ &\quad + 2J_1(\beta) \cdot \left(\sin\left[\alpha + \frac{\nu_0^2 \ddot{\phi}}{2}\right] \cos[\nu_0 \dot{\phi}] + \frac{\dot{B} \cdot \nu_0}{B(\Omega_0)} \cos\left[\alpha + \frac{\nu_0^2 \ddot{\phi}}{2}\right] \sin[\nu_0 \dot{\phi}] \right) \left. \right\} \\ &= \frac{P_0}{4} \cdot B(\Omega_0)^2 \cdot \left\{ 2J_1(\beta) \cdot \left(\sin\left[\alpha + \frac{\nu_0^2 \ddot{\phi}}{2}\right] \cos[\nu_0 \dot{\phi}] + \frac{\dot{B} \cdot \nu_0}{B(\Omega_0)} \cos\left[\alpha + \frac{\nu_0^2 \ddot{\phi}}{2}\right] \sin[\nu_0 \dot{\phi}] \right) \right. \end{aligned}$$

$$\begin{aligned}
& +J_{-1}(\beta)J_{-2}(\beta) \left[\left(1 + \frac{\dot{B}^2 \cdot 2\nu_0^2}{B(\Omega_0)^2}\right) \sin\left[\frac{\ddot{\phi}3\nu_0^2}{2}\right] \cos[\nu_0\dot{\phi}] + \frac{\dot{B} \cdot 3\nu_0}{B(\Omega_0)} \cos\left[\frac{\ddot{\phi}3\nu_0^2}{2}\right] \sin[\nu_0\dot{\phi}] \right] \\
& +J_0(\beta)J_{-1}(\beta) \left[\sin\left[\frac{\ddot{\phi}\nu_0^2}{2}\right] \cos[\nu_0\dot{\phi}] + \frac{\dot{B} \cdot \nu_0}{B(\Omega_0)} \cos\left[\frac{\ddot{\phi}\nu_0^2}{2}\right] \sin[\nu_0\dot{\phi}] \right] \\
& +J_1(\beta)J_0(\beta) \left[-\sin\left[\frac{\ddot{\phi}\nu_0^2}{2}\right] \cos[\nu_0\dot{\phi}] - \frac{\dot{B} \cdot \nu_0}{B(\Omega_0)} \cos\left[\frac{\ddot{\phi}\nu_0^2}{2}\right] \sin[\nu_0\dot{\phi}] \right] \\
& +J_2(\beta)J_1(\beta) \left[-\left(1 + \frac{\dot{B}^2 \cdot 2\nu_0^2}{B(\Omega_0)^2}\right) \sin\left[\frac{\ddot{\phi}3\nu_0^2}{2}\right] \cos[\nu_0\dot{\phi}] - \frac{\dot{B} \cdot 3\nu_0}{B(\Omega_0)} \cos\left[\frac{\ddot{\phi}3\nu_0^2}{2}\right] \sin[\nu_0\dot{\phi}] \right] \}
\end{aligned}$$

using $J_{-n}(x) = (-1)^n \cdot J_n(x)$

$$\begin{aligned}
& = \frac{P_0}{4} \cdot B(\Omega_0)^2 \cdot \left\{ 2J_1(\beta) \cdot \left(\sin\left[\alpha + \frac{\nu_0^2 \ddot{\phi}}{2}\right] \cos[\nu_0\dot{\phi}] + \frac{\dot{B} \cdot \nu_0}{B(\Omega_0)} \cos\left[\alpha + \frac{\nu_0^2 \ddot{\phi}}{2}\right] \sin[\nu_0\dot{\phi}] \right) \right. \\
& - J_1(\beta)J_2(\beta) \left[\left(1 + \frac{\dot{B}^2 \cdot 2\nu_0^2}{B(\Omega_0)^2}\right) \sin\left[\frac{\ddot{\phi}3\nu_0^2}{2}\right] \cos[\nu_0\dot{\phi}] + \frac{\dot{B} \cdot 3\nu_0}{B(\Omega_0)} \cos\left[\frac{\ddot{\phi}3\nu_0^2}{2}\right] \sin[\nu_0\dot{\phi}] \right] \\
& - J_0(\beta)J_1(\beta) \left[\sin\left[\frac{\ddot{\phi}\nu_0^2}{2}\right] \cos[\nu_0\dot{\phi}] + \frac{\dot{B} \cdot \nu_0}{B(\Omega_0)} \cos\left[\frac{\ddot{\phi}\nu_0^2}{2}\right] \sin[\nu_0\dot{\phi}] \right] \\
& - J_1(\beta)J_0(\beta) \left[\sin\left[\frac{\ddot{\phi}\nu_0^2}{2}\right] \cos[\nu_0\dot{\phi}] + \frac{\dot{B} \cdot \nu_0}{B(\Omega_0)} \cos\left[\frac{\ddot{\phi}\nu_0^2}{2}\right] \sin[\nu_0\dot{\phi}] \right] \\
& - J_2(\beta)J_1(\beta) \left[\left(1 + \frac{\dot{B}^2 \cdot 2\nu_0^2}{B(\Omega_0)^2}\right) \sin\left[\frac{\ddot{\phi}3\nu_0^2}{2}\right] \cos[\nu_0\dot{\phi}] + \frac{\dot{B} \cdot 3\nu_0}{B(\Omega_0)} \cos\left[\frac{\ddot{\phi}3\nu_0^2}{2}\right] \sin[\nu_0\dot{\phi}] \right] \} \\
& = \frac{P_0}{4} \cdot B(\Omega_0)^2 \cdot \left\{ 2J_1(\beta) \cdot \left(\sin\left[\alpha + \frac{\nu_0^2 \ddot{\phi}}{2}\right] \cos[\nu_0\dot{\phi}] + \frac{\dot{B} \cdot \nu_0}{B(\Omega_0)} \cos\left[\alpha + \frac{\nu_0^2 \ddot{\phi}}{2}\right] \sin[\nu_0\dot{\phi}] \right) \right. \\
& - 2J_0(\beta)J_1(\beta) \left[\sin\left[\frac{\ddot{\phi}\nu_0^2}{2}\right] \cos[\nu_0\dot{\phi}] + \frac{\dot{B} \cdot \nu_0}{B(\Omega_0)} \cos\left[\frac{\ddot{\phi}\nu_0^2}{2}\right] \sin[\nu_0\dot{\phi}] \right] \\
& - 2J_1(\beta)J_2(\beta) \left[\left(1 + \frac{\dot{B}^2 \cdot 2\nu_0^2}{B(\Omega_0)^2}\right) \sin\left[\frac{\ddot{\phi}3\nu_0^2}{2}\right] \cos[\nu_0\dot{\phi}] + \frac{\dot{B} \cdot 3\nu_0}{B(\Omega_0)} \cos\left[\frac{\ddot{\phi}3\nu_0^2}{2}\right] \sin[\nu_0\dot{\phi}] \right] \} \\
& = \frac{P_0}{2} \cdot B(\Omega_0)^2 \cdot \left\{ J_1(\beta) \cdot \left(\sin\left[\alpha + \frac{\nu_0^2 \ddot{\phi}}{2}\right] \cos[\nu_0\dot{\phi}] + \frac{\dot{B} \cdot \nu_0}{B(\Omega_0)} \cos\left[\alpha + \frac{\nu_0^2 \ddot{\phi}}{2}\right] \sin[\nu_0\dot{\phi}] \right) \right. \\
& - \left[J_0(\beta)J_1(\beta) \sin\left[\frac{\ddot{\phi}\nu_0^2}{2}\right] \cos[\nu_0\dot{\phi}] + J_0(\beta)J_1(\beta) \frac{\dot{B} \cdot \nu_0}{B(\Omega_0)} \cos\left[\frac{\ddot{\phi}\nu_0^2}{2}\right] \sin[\nu_0\dot{\phi}] \right] \\
& - \left[J_1(\beta)J_2(\beta) \left(1 + \frac{\dot{B}^2 \cdot 2\nu_0^2}{B(\Omega_0)^2}\right) \sin\left[\frac{\ddot{\phi}3\nu_0^2}{2}\right] \cos[\nu_0\dot{\phi}] + J_1(\beta)J_2(\beta) \frac{\dot{B} \cdot 3\nu_0}{B(\Omega_0)} \cos\left[\frac{\ddot{\phi}3\nu_0^2}{2}\right] \sin[\nu_0\dot{\phi}] \right] \}
\end{aligned}$$

In order to emphasize the extended model for MPS, we will arrange the signal according to the perturbations

$$\begin{aligned}
\Rightarrow V_1(t)_{\text{LPF}} & = \frac{P_0}{2} \cdot B(\Omega_0)^2 \cdot \left\{ \cos[\nu_0\dot{\phi}] \left[J_1(\beta) \left(\sin\left[\alpha + \frac{\nu_0^2 \ddot{\phi}}{2}\right] - J_0(\beta) \sin\left[\frac{\ddot{\phi}\nu_0^2}{2}\right] - J_2(\beta) \sin\left[\frac{\ddot{\phi}3\nu_0^2}{2}\right] \right) \right. \right. \\
& + \frac{\dot{B} \cdot \nu_0}{B(\Omega_0)} \sin[\nu_0\dot{\phi}] \left[J_1(\beta) \left(\cos\left[\alpha + \frac{\nu_0^2 \ddot{\phi}}{2}\right] - J_0(\beta) \cos\left[\frac{\ddot{\phi}\nu_0^2}{2}\right] - 3J_2(\beta) \cos\left[\frac{\ddot{\phi}3\nu_0^2}{2}\right] \right) \right] \\
& \left. - \frac{\dot{B}^2 \cdot \nu_0^2}{B(\Omega_0)^2} \cos[\nu_0\dot{\phi}] \left[2J_1(\beta)J_2(\beta) \sin\left[\frac{\ddot{\phi}3\nu_0^2}{2}\right] \right] \right\}
\end{aligned}$$

Finally, we can estimate the contribution of the amplitude change to the phase measurement in the 2nd order MPS with Audio method. The photocurrent is multiplied with a local oscillator signal oscillating at the ν_0 frequency, $LO(t) = \sin[2\nu_0 t]$, using the following trigonometric identities

$$\cos \alpha \cdot \sin \beta = \frac{1}{2} [\sin(\alpha + \beta) - \sin(\alpha - \beta)]$$

$$\sin \alpha \cdot \sin \beta = \frac{1}{2} [\cos(\alpha - \beta) - \cos(\alpha + \beta)]$$

The photocurrent is composed of these expressions $\bar{P} = \bar{P}_0 + \bar{P}_1 + \bar{P}_2$. We will focus on the contribution to the DC signal, caused by the down converting to DC with the local oscillator signal. There is no need to multiply \bar{P}_0 or \bar{P}_1 since any harmonic contribution will be filtered out using the low pass filter.

Therefore the contributions to the signal are as following:

$$\begin{aligned} \bar{P}_2 &= \frac{P_0}{4} \cdot B(\Omega_0)^2 \cdot \left\{ 2 \sum_{n=-\infty}^{\infty} J_n(\beta) J_{n-2}(\beta) \cdot \left[\left(1 + \frac{\dot{B}^2 \cdot n(n-2) \nu_0^2}{B(\Omega_0)^2} \right) \cos\left[\frac{\ddot{\phi} 2(2n-2) \nu_0^2}{2}\right] \right. \right. \\ &\cdot \cos[2\nu_0(\dot{\phi} + t)] - \frac{\dot{B} \cdot (2n-2) \nu_0}{B(\Omega_0)} \sin\left[\frac{\ddot{\phi} 2(2n-2) \nu_0^2}{2}\right] \sin[2\nu_0(\dot{\phi} + t)] \left. \right] \\ &+ 4J_2(\beta) \cdot \left[-\cos\left[\alpha + \frac{2^2 \nu_0^2 \ddot{\phi}}{2}\right] \cos[2\nu_0(\dot{\phi} + t)] + \frac{\dot{B} \cdot 2\nu_0}{B(\Omega_0)} \sin\left[\alpha + \frac{2^2 \nu_0^2 \ddot{\phi}}{2}\right] \sin[2\nu_0(\dot{\phi} + t)] \right] \left. \right\} \\ V_2(t)_{\text{LPF}} &= [\bar{P}_2 \cdot \sin[2\nu_0 t]]_{\text{HPF}} = \frac{P_0}{4} \cdot B(\Omega_0)^2 \cdot \left\{ \sum_{n=-\infty}^{\infty} J_n(\beta) J_{n-2}(\beta) \cdot \left[- \left(1 + \frac{\dot{B}^2 \cdot n(n-2) \nu_0^2}{B(\Omega_0)^2} \right) \right. \right. \\ &\cos[\ddot{\phi}(2n-2) \nu_0^2] \cdot \sin[2\nu_0 \dot{\phi}] - \frac{\dot{B} \cdot (2n-2) \nu_0}{B(\Omega_0)} \sin[\ddot{\phi}(2n-2) \nu_0^2] \cos[2\nu_0 \dot{\phi}] \left. \right] \\ &+ 2J_2(\beta) \cdot \left[\cos\left[\alpha + 2\nu_0^2 \ddot{\phi}\right] \sin[2\nu_0 \dot{\phi}] + \frac{\dot{B} \cdot 2\nu_0}{B(\Omega_0)} \sin\left[\alpha + 2\nu_0^2 \ddot{\phi}\right] \cos[2\nu_0 \dot{\phi}] \right] \left. \right\} \end{aligned}$$

Since our RF driving $\beta \sim \pi \frac{1.5}{4.5} = 1.0472 \sim 1.05$. The assumption standing behind this is that our electrical circuit transfers the oscillating RF power through a perfect 50 ohms impedance network, which is usually not true, especially when treating a wide range of RF frequencies. According to Bessel-J function of the first kind, we should anticipate arising of approximately tones up to the second order, thus we will calculate the cases containing $n \in [0, 2]$.

$$\begin{aligned} V_2(t)_{\text{LPF}} &= \frac{P_0}{4} \cdot B(\Omega_0)^2 \cdot \left\{ \sum_{n=0}^2 J_n(\beta) J_{n-2}(\beta) \cdot \left[- \left(1 + \frac{\dot{B}^2 \cdot n(n-2) \nu_0^2}{B(\Omega_0)^2} \right) \right. \right. \\ &\cos[\ddot{\phi}(2n-2) \nu_0^2] \cdot \sin[2\nu_0 \dot{\phi}] - \frac{\dot{B} \cdot (2n-2) \nu_0}{B(\Omega_0)} \sin[\ddot{\phi}(2n-2) \nu_0^2] \cos[2\nu_0 \dot{\phi}] \left. \right] \\ &+ 2J_2(\beta) \cdot \left[\cos\left[\alpha + 2\nu_0^2 \ddot{\phi}\right] \sin[2\nu_0 \dot{\phi}] + \frac{\dot{B} \cdot 2\nu_0}{B(\Omega_0)} \sin\left[\alpha + 2\nu_0^2 \ddot{\phi}\right] \cos[2\nu_0 \dot{\phi}] \right] \left. \right\} \\ &= \frac{P_0}{4} \cdot B(\Omega_0)^2 \cdot \left\{ 2J_2(\beta) \cdot \left[\cos\left[\alpha + 2\nu_0^2 \ddot{\phi}\right] \sin[2\nu_0 \dot{\phi}] + \frac{\dot{B} \cdot 2\nu_0}{B(\Omega_0)} \sin\left[\alpha + 2\nu_0^2 \ddot{\phi}\right] \cos[2\nu_0 \dot{\phi}] \right] \right. \\ &+ J_2(\beta) J_0(\beta) \cdot \left[-\cos[\ddot{\phi} 2\nu_0^2] \cdot \sin[2\nu_0 \dot{\phi}] - \frac{\dot{B} \cdot 2\nu_0}{B(\Omega_0)} \sin[\ddot{\phi} 2\nu_0^2] \cos[2\nu_0 \dot{\phi}] \right] \left. \right\} \end{aligned}$$

$$\begin{aligned}
& + J_1(\beta) J_{-1}(\beta) \cdot \left[- \left(1 - \frac{\dot{B}^2 \cdot 1\nu_0^2}{B(\Omega_0)^2} \right) \cdot \sin[2\nu_0\dot{\phi}] \right] \\
& + J_0(\beta) J_{-2}(\beta) \cdot \left[-\cos[\ddot{\phi}2\nu_0^2] \cdot \sin[2\nu_0\dot{\phi}] - \frac{\dot{B} \cdot 2\nu_0}{B(\Omega_0)} \sin[\ddot{\phi}2\nu_0^2] \cos[2\nu_0\dot{\phi}] \right] \Big\} \\
& \text{using } J_{-n}(x) = (-1)^n \cdot J_n(x) \\
& = \frac{P_0}{4} \cdot B(\Omega_0)^2 \cdot \left\{ 2J_2(\beta) \cdot \left[\cos[\alpha + 2\nu_0^2\ddot{\phi}] \sin[2\nu_0\dot{\phi}] + \frac{\dot{B} \cdot 2\nu_0}{B(\Omega_0)} \sin[\alpha + 2\nu_0^2\ddot{\phi}] \cos[2\nu_0\dot{\phi}] \right] \right. \\
& + J_2(\beta) J_0(\beta) \cdot \left[-\cos[\ddot{\phi}2\nu_0^2] \cdot \sin[2\nu_0\dot{\phi}] - \frac{\dot{B} \cdot 2\nu_0}{B(\Omega_0)} \sin[\ddot{\phi}2\nu_0^2] \cos[2\nu_0\dot{\phi}] \right] \\
& + J_1(\beta) J_1(\beta) \cdot \left[\left(1 - \frac{\dot{B}^2 \cdot 1\nu_0^2}{B(\Omega_0)^2} \right) \cdot \sin[2\nu_0\dot{\phi}] \right] \\
& \left. + J_0(\beta) J_2(\beta) \cdot \left[-\cos[\ddot{\phi}2\nu_0^2] \cdot \sin[2\nu_0\dot{\phi}] - \frac{\dot{B} \cdot 2\nu_0}{B(\Omega_0)} \sin[\ddot{\phi}2\nu_0^2] \cos[2\nu_0\dot{\phi}] \right] \right\} \\
& = \frac{P_0}{4} \cdot B(\Omega_0)^2 \cdot \left\{ 2J_2(\beta) \cdot \left[\cos[\alpha + 2\nu_0^2\ddot{\phi}] \sin[2\nu_0\dot{\phi}] + \frac{\dot{B} \cdot 2\nu_0}{B(\Omega_0)} \sin[\alpha + 2\nu_0^2\ddot{\phi}] \cos[2\nu_0\dot{\phi}] \right] \right. \\
& + J_1(\beta) J_1(\beta) \cdot \left[\left(1 - \frac{\dot{B}^2 \cdot 1\nu_0^2}{B(\Omega_0)^2} \right) \cdot \sin[2\nu_0\dot{\phi}] \right] \\
& \left. + 2J_0(\beta) J_2(\beta) \cdot \left[-\cos[\ddot{\phi}2\nu_0^2] \cdot \sin[2\nu_0\dot{\phi}] - \frac{\dot{B} \cdot 2\nu_0}{B(\Omega_0)} \sin[\ddot{\phi}2\nu_0^2] \cos[2\nu_0\dot{\phi}] \right] \right\}.
\end{aligned}$$

In order to emphasize the extended model for MPS, we will arrange the signal according to the perturbations

$$\begin{aligned}
\Rightarrow V_2(t)_{\text{LPF}} & = \frac{P_0}{2} \cdot B(\Omega_0)^2 \cdot \left\{ \sin[2\nu_0\dot{\phi}] \left[J_2(\beta) \left(\cos[\alpha + 2\nu_0^2\ddot{\phi}] - J_0(\beta) \cos[2\nu_0^2\ddot{\phi}] \right) + \frac{1}{2} J_1^2(\beta) \right] \right. \\
& + \frac{\dot{B} \cdot \nu_0}{B(\Omega_0)} \cos[2\nu_0\dot{\phi}] \left[2J_2(\beta) \left(\sin[\alpha + 2\nu_0^2\ddot{\phi}] - J_0(\beta) \sin[2\nu_0^2\ddot{\phi}] \right) \right] \\
& \left. - \frac{\dot{B}^2 \cdot \nu_0^2}{B(\Omega_0)^2} \sin[2\nu_0\dot{\phi}] \left[\frac{1}{2} J_1^2(\beta) \right] \right\}
\end{aligned}$$

תחום התקשורת האופטית התפתח מאד בעשור האחרון. העברת מידע ברוחב סרט גדול יותר מושגת בדרך כלל על ידי הקטנת המרווח בין הערוצים האופטיים או לחילופין על ידי העלאת קצב המידע המועבר בערוץ האופטי. אפיון רכיבים אופטיים וכן ניטור פעיל של רשת התקשורת דורשים שיטות מדידה מדויקות. פונקצית ההעברה המרוכבת של רכיבים אופטיים משפיעה על ביצועי מערכות התקשורת. לפיכך, ניתוח ומדידות מדויקות של פונקצית ההעברה המרוכבת הינם חיוניים על מנת לבצע אופטימיזציה בביצועים של מערכות התקשורת האופטית.

מרחק נשיאת המידע וקצב ההעברה מוגבלים על ידי הנפיצה הכרומטית בסיב האופטי וכן על ידי שינוי התדר הזמני של משדרי הלייזר. נהוג לבצע מדידה של נפיצה כרומטית על ידי טכניקת אפנון הסחת המופע Modulation Phase Shift (MPS). רזולוציית מדידה גבוהה מושגת על ידי שימוש בתדר רדיו גבוה, אולם המופע עלול לחזור על עצמו וכתוצאה מכך תיגרם שגיאה בקריאת הסחת המופע. במחקר הנוכחי אנו מציגים מערכת מדידה לאפיון ספקטראלי מרוכב של רכיבים וסיבים אופטיים. בהתבסס על שינוי של טכניקת ה-MPS הסטנדרטית, אנו מכניסים אפנון לתדר הרדיו, המאפשר לנו לגלות שינויי מופע קטנים ועל ידי כך להתגבר על מגבלות טכניקת ה-MPS. תכונתה העיקרית של המערכת היא גילוי שינויי מופע ברגישות גבוהה, המאפשר לנו שימוש בתדר רדיו נמוך הנדרש במדידות מדויקות של רכיבים המכילים שינויים ספקטראליים עדינים כגון מיקרו-מתנדנים (micro-resonators) וכן רכיבים המאטים את מהירות האור (slow light devices).

אנו מנתחים את השיפור בטכניקת ה-MPS ע"י שימוש בקירובי אותות קטנים ומשווים את התוצאות לניתוח האנליטי המלא של היגב טכניקת ה-MPS. הניתוח האנליטי המלא משמש לאופטימיזציה של הטכניקה המוצעת. מערכת המדידה הורכבה במעבדה שלנו באמצעות רכיבים מסחריים זמינים אופטיים וחשמליים. אפיינו את האותות העוברים במערכת המדידה. ניתנה חשיבות למניעת אותות רדיו גבוהים (כלומר הגבוהים מסדר ראשון) במוצא השדה האלקטרומגנטי של המאפן האופטי (Mach-Zehnder Modulator), אשר עלולים להפריע למדידה הרצויה. בנוסף, ניתנה חשיבות למניעת זליגות אותות במעגל החשמלי, דבר שעשוי להפריע למדידת אותות קטנים. הצגנו את מערכת המדידה בשתי אפשרויות פעולה, כאשר גילוי האות מתבצע ע"י שימוש בתדר רדיו בודד או כפול. מדדנו מספר קטגוריות של רכיבים וסיבים אופטיים על מנת להדגים את טכניקת המדידה. סיימנו בדיון על יתרונות וחסרונות של הטכניקה המוצעת.

האוניברסיטה העברית בירושלים, הפקולטה למתמטיקה ולמדעי הטבע

בית הספר להנדסה ומדעי המחשב, המחלקה לפיסיקה יישומית

עבודת גמר לתואר מוסמך במדעי הטבע

אפיון פונקצית המעבר המרוכבת

(אמפליטודה ופאזה)

של רכיבים אופטיים

מוגש על ידי יורם פלטי

מספר תלמיד 04017529-1

העבודה הוכנה בהדרכת ד"ר דן מרום

22 נובמבר, 2009

ה' בכסלו תש"ע